Imperial College London

The Consequences of Life without Sex

An Examination into Taxonomy and Evolution of the Anciently Asexual Bdelloid Rotifers

Cuong Quoc Tang

A thesis submitted for the degree of Doctor of Philosophy

from the Department of Life Sciences,

Imperial College London

July 2014

Abstract

The anciently asexual bdelloid rotifers are a ubiquitous and ecologically important group coined "evolutionary scandals" owing to their diversification and persistence over evolutionary time despite the pressures of obligate parthenogenesis. Understanding the biodiversity of rotifers, in the context of reproductive mode, will aid in the understanding of how differences in sex and ecology drive biodiversity patterns.

Given that resolved taxonomy is a prerequisite to investigating larger scale macroevolutionary patterns, and that rotifer taxonomy is confounded by morphostasis, cryptic diversity, and a dearth of expert taxonomists, this thesis first deals with the use of DNA taxonomy as a tool to alleviate the taxonomic crisis so prevalent in the group. Results from multiple meta-analyses exploring the effects of choice in gene, phylogenetic reconstruction methods, and species delimitation metrics, provide better guidelines for DNA taxonomy. The analyses suggest that coalescent-based DNA taxonomy using the Generalised Mixed Yule Coalescent model in conjunction with the cytochrome oxidase 1 subunit *c* gene analysed in a Bayesian inference phylogenetic framework using BEAST, provides realistic and tangible species clusters (evolutionarily significant units; ESU) in both asexual and sexual organisms.

Using these ESUs, the efficacy of DNA barcoding for identifying rotifer species is examined. These analyses suggest that the sexual monogonont rotifers are more readily identifiable than the asexual bdelloid rotifers. Explicit comparison of genetic discreteness of asexual and sexual rotifers indicates that sexual rotifers are separated by larger genetic and phylogenetic gaps than asexual rotifers and thus are more discrete. Combined, these analyses indicate that sex, specifically reproductive isolation, is the predominant factor in explaining why species form discrete clusters rather than a continuum of forms.

Finally, a dated multilocus molecular phylogeny of Bdelloidea is reconstructed. The phylogeny suggests that bdelloid rotifers have persisted for at least 40 million years, but that bdelloid higher taxa are typically polyphyletic.

Acknowledgements

I would like to thank Diego and Tim for their support all the way through the PhD. From you I've learnt what it is to be a scientist, and your example is an inspiration and something I want to emulate. Of all of the candidates, I'm glad you picked me. I hope that through all this work I've been a valuable addition to your groups. Thanks for never saying *no*, irrespective of how odd things sounded. Everything I've done for this PhD is down to you both.

Years in the Barralab and the ever expanding BLAB family have been a huge privilege. Thanks for all of the help and for being such a pleasure to work alongside. Your support has been a massive pick me up. In particular, Aelys Humphreys, Isobel Eyres, and Chris Wilson for their discussions on all things evolutionary and bdelloid, and Alejandra, Diane, Francesca, Chris, Matt, Shorok, Damian, Drew, and Laura, for making, sometimes, gruelling days much more enjoyable.

Life at Silwood wouldn't have been the same had it not been for the friends that I've been fortunate enough to make on the way, you are too numerous to name, but you know who you are. Thanks to ~~nearly~~ all of my housemates over the years, especially Shorok who has been looking after me and feeding me for the last few months. You've all given me respite from work and stopped me going really peculiar towards the end.

Yet all of this wouldn't have been possible without the support of my family. I dedicate this thesis to them. Your enthusiasm and pride for my academic career is only matched by the bemused expressions you have when I try to explain what it is I do. *Cảm ơn bố và mẹ*.

To Elle, you make me a happier person. Always.

And to Charlie, who would have been a better academic than me.

This thesis was funded by a NERC studentship.

Declaration of originality

I hereby declare that this thesis includes some work that has been the result of joint work. In all cases, the key ideas, primary contributions, experimental designs, data analysis, interpretation, and writing were performed by myself under the supervision of both Tim Barraclough and Diego Fontaneto, but specific chapters have been made possible by certain collaborators providing data.

Chapter 2 has been published in a slightly modified form in: *Tang CQ, Leasi F, Obertegger U, Kieneke A, Barraclough TG, Fontaneto D. (2012) The widely used small subunit 18S rDNA molecule greatly underestimates true diversity in biodiversity surveys of the meiofauna. Proceedings of the National Academy of Sciences of the United States of America, 109, 16208–16212*. Three of the 55 alignments used were generated by Francesca Leasi (*Testudinella* spp.), Ulrike Obertegger (*Synchaeta* spp.), and Alex Kieneke (*Turbanella* spp.). The rest of the datasets were generated either by myself, or collated by myself from GenBank.

Chapter 3 is in press at *Methods in Ecology and Evolution* as: *Tang, CQ, Humphreys, AM, Fontaneto, D, Barraclough, TG (2014) Effects of phylogenetic reconstruction method on the robustness of species delimitation using single-locus data. Methods in Ecology and Evolution*. All of the data was either downloaded from GenBank or provided by Chris Meyer (cowries dataset). The analyses and the manuscript was performed and written principally by myself, with helpful comments from Aelys Humphries.

Chapter 5 is in press at *Evolution* as: *Tang, C. Q., Obertegger, U., Fontaneto, D., & Barraclough, T. G. (2014). Sexual species are separated by larger genetic gaps than asexual species in rotifers. Evolution, 68(10), 2901–2916.* The data were mostly downloaded from GenBank, but additional targeted sequencing was obtained by Ulrike Obertegger. Other than these targeted sequences, all of the data collection and analyses were performed by myself.

Chapter 6 uses samples collected by myself, Nataliia Iakovenko, Chris G. Wilson, Carl W. Birky Jr, and Diego Fontaneto. Nuclear primers were designed using transcriptomic alignments provided by Isobel Eyres and Tim Barraclough. All of the subsequent lab work and analyses were performed by myself.

Permission to reprint chapters 2, 3, and 5 can be found at the back of the thesis (pp208-210).

Table of contents

Figures and tables

Data accessibility

Chapter 2: The GenBank accession numbers and the GenBank search terms used to find them are shown in Dataset 1 and Table GenBank, respectively (both found on the repository CD). All of the sequences generated for this study are deposited on GenBank (accession number: JX494729-JX494746). All of the alignments (full and haplotype) and trees used for Chapter 2 are deposited on figshare under http://dx.doi.org/10.6084/m9.figshare.1177954.

Chapter 3: The GenBank accession numbers and the GenBank search terms used to find them are shown in Table S3.2 and Table GenBank, respectively (both found on the repository CD). All of the haplotype alignments used to make the trees are found on TreeBASE under the study ID 14643. The trees are deposited on Dryad under doi:10.5061/dryad.8rv46.

Chapter 4: The GenBank accession numbers and the GenBank search terms used to find them are shown in Table S3.2 and Table GenBank, respectively (both found on the repository CD). All of the alignments, RAxML trees, and BEAST trees are available on figshare under the http://dx.doi.org/10.6084/m9.figshare.1177969, http://dx.doi.org/10.6084/m9.figshare.1177970, http://dx.doi.org/10.6084/m9.figshare.1177971, respectively.

Chapter 5: The GenBank accession numbers and the GenBank search terms used to find them are shown in Table S3.2 and Table GenBank, respectively (both found on the repository CD). The new sequences generated for this chapter have been deposited on GenBank under the accession numbers shown in Table S5.1. All of the haplotype alignments and the trees are found on TreeBASE under the study ID 14643.

Chapter 6: The sequences generated for this study are deposited on GenBank (accession number: KM043131 - KM043271). All of the alignments and trees are deposited on the repository CD and on figshare under http://dx.doi.org/10.6084/m9.figshare.1177992 and http://dx.doi.org/10.6084/m9.figshare.1178002, respectively.

Abbreviations

% var.	% variance
ABGD	Automated Barcode Gap Discovery
AIC	Akaike Information Criterion
ANOVA	Analysis of Variance
BCM	Best Close Match
BEAST	Bayesian Evolutionary Analysis by Sampling Trees
BEAUti	Bayesian Evolutionary Analysis Utility
BI	Bayesian Inference
BIC	Bayesian Information Criterion
BP&P	Bayesian Phylogenetics and Phylogeography
BSC	Biological Species Concept
CBOL	Consortium for the Barcode of Life
COI	Cytochrome *c* oxidase subunit I
DNA	Deoxyribonucleic acid
eDNA	Environmental DNA
EGSC	Evolutionary Genetic Species Concept
ESC	Evolutionary Species Concept
ESS	Effective Sample Size
ESU	Evolutionarily Significant Unit
$ESU_{expected}$	Expected diversity
ESU_{mean}	Average number of ESUs
ESU_{morph}	Expected diversity based on morphology
ESU_{X}	Observed ESU
GARLI	Genetic Algorithm for Rapid Likelihood Inference
GLM	Generalised Linear Model
GLMM	Generalized Linear Mixed Models
GMYC	Generalised Mixed Yule Coalescent
GTR+Γ+I	Generalised Time-Reversible Model + Gamma + Inverse Proportion
HPD	Highest Posterior Density
ITS	Internal Transcribed Spacer
K2P	Kimura two parameter model
LMEM	Linear Mixed Effect Models
MCCR	Monte Carlo constant rates
MCMC	Markov chain Monte Carlo
ML	Maximum Likelihood
MM-GMYC	Multimodel GMYC
MOTU	Molecular Operational Taxonomic Unit
mtDNA	Mitochondrial DNA
MT-GMYC	Multiple threshold GMYC
MYA	Million years ago
MYR	Million years
N	Census population size
N_e	Effective population size
NA	Not Applicable
NDT	Nucleotide Divergence Threshold
NGS	Next Generation Sequencing
NJ	Neighbour Joining
NN	Nearest Neighbour
NNI	Nearest Neighbour Interchange
NS	Not Significant
nuDNA	Nuclear DNA
OTU	Operational Taxonomic Unit

PCR	Polymerase Chain Reaction
PhyML	Phylogenetic estimation using Maximum Likelihood
PSC	Phylogenetic Species Concept
PTP	Poisson Tree Process
PTP-all	PTP of all available trees
PTP-raw	PTP of trees without *post hoc* branch smoothing
RAxML	Randomized Accelerated Maximum Likelihood
rDNA	Ribosomal DNA
SPR	Subtree Pruning
ST-GMYC	Single threshold GMYC
Tax.	Taxonomic rank
TI	Optimised Threshold ID
TMRCA	Time to Most Recent Common Ancestor
Tukey HSD	Tukey Honest Significant Difference
UPGMA	Unweighted Pair Group Method with Arithmetic Mean
BOLD	Barcode of Life Data Systems

Chapter 1: Introduction

Sex is the predominant reproductive mode throughout the animal kingdom (Williams 1975; Maynard Smith 1978; Bell 1982; Michod and Levin 1988); despite theorised costs, more than 99% of animal life reproduces sexually (White 1978; Ashman et al. 2014). These costs comprise lower population growth rate with males contributing nothing but genes to the next generation (two-fold cost of males; Maynard Smith 1978), the energy costs and the potential burden of sexually transmitted diseases and predators associated with finding a suitable mate (Bell 1982), and the disruption of favourable genetic combinations (Bell 1982; Kondrashov 1993). The benefits of sex must exceed the associated costs and are the subject of more than 20 non-mutually exclusive theories (West et al. 1999; Butlin 2002). These theories fall into two categories (Hurst and Peck 1996): (1) the increased rate of adaptive evolution to changing environments and the various benefits these underlie (Weismann 1889; Burt 2000; Otto and Lenormand 2002; Goddard et al. 2005), a special case of which would include adapting to the relentless pressure of rapidly coevolving parasites and pathogens (Red Queen hypothesis; Jaenike 1978; Hamilton et al. 1990); and (2) the removal of deleterious mutations through recombination (Muller 1932; including transposable elements; Arkhipova and Meselson 2005; Schurko et al. 2009). Despite decades of academic pursuit, the question *why sex* is still regarded as one of the biggest unexplained evolutionary conundrums.

By corollary, asexual lineages are prone to extinction because they are unable to quickly adapt in the face of change (Fisher-Muller advantage of sex; Fisher 1930; Muller 1932), or because they are prone to extinction resulting from an insurmountable mutation load (Muller's ratchet; Muller 1932; Maynard Smith and Száthmary 1995). As such, asexually reproducing groups are short lived, peripherally distributed across the tree of life (Butlin 2002), and foreshadowed as an evolutionary dead-end with a swift ticket to extinction (Maynard Smith 1978). Contrary to this general pattern, however, ancient asexual organisms exist that have persisted over evolutionary timescales (Judson and Normark 1996; although what constitutes being "ancient" is debatable - Neiman et al. 2009) and diversified into ecological, morphological, and genetic clusters akin to sexual species (Schön and Martens 2003; Birky et al. 2005; Fontaneto et al. 2007d; Heethoff et al. 2009; Bode et al. 2010; Danchin et al. 2011; Schwander et al. 2011; Schön et al. 2012). These so called ancient asexuals present a significant challenge to evolutionary theory, and as such have been coined evolutionary scandals (Maynard Smith 1986; Judson and Normark 1996). Studying these ancient asexual scandals and how they cope with the consequences of asexuality gives insight into the ubiquity of sex and how important sex, or the lack of sex, is in shaping biodiversity (Coyne and Orr 2004; Neiman et al. 2009).

Bdelloid rotifers are widely accepted as the best supported case for ancient asexuality (Poinar and Ricci 1992; Birky 2010; Danchin et al. 2011; Flot et al. 2013). Bdelloidea is a class of meiofaunal microinvertebrates belonging to the phylum Rotifera (Wallace et al. 2006), which comprises a highly

diverse (Segers 2007), ubiquitous (Fontaneto et al. 2008a), euryoecious (Wallace et al. 2006), and ecologically important group (Hutchinson 1967). As well as their ancient asexual status (recently strengthened by genomic analyses, Flot et al. 2013, reviewed in detail below), this group is unique among other Metazoa given their incredible tolerance to various stresses such as desiccation (Ricci et al. 2007; Gladyshev 2008), and high prevalence and functionalisation of horizontally transferred genes (Pouchkina-Stantcheva et al. 2007; Gladyshev et al. 2008; Boschetti et al. 2012), and therefore, have been studied for a diverse catalogue of ecological and evolutionary novelties. Indeed their ancient asexuality, when framed with the variety of reproductive modes in the Rotifera phylum, makes the study system a rare opportunity to test hypotheses regarding the consequences of asexuality.

Rotifera

Rotifers were first discovered by Anton van Leeuwenhoek in the late 1600s (Wallace and Smith 2013). Rotifers, Latin for *wheel bearer*, are named after the cephalic appendages (trochi) they use to beat detritus into their digestive tracts, which resemble rotating wheels. Rotifera is a phylum of miniscule (ca. 50-2,000μm), unsegmented, bilaterally symmetrical metazoans that are ubiquitous in aquatic environments worldwide (Segers 2008); these include fresh-, brackish and marine waters, in soil, lichen, mosses, and other ephemeral environments (Wallace and Smith 2013; Walsh et al. 2014). Rotifers are commonly dominant in terms of species richness and abundance in many habitats as plankton, interstitial sediments, and periphyton (Wallace et al. 2006). They are typically primary consumers (Ricci et al. 2001) and detritivores (Wallace 2002), although some groups have a diverse array of dietary habits (Melone et al. 1998a; Ricci et al. 2001), and are considered as “the most important soft-bodied invertebrates in the fresh-water plankton” (Hutchinson 1967). Despite their wide distribution, they have a very uniform morphology, which has led some to suggest that natural selection has had little effect on their morphological characteristics (Ricci 1987).

Rotifera diversity is split into three classes: the Seisonacea (four species), the Monogononta (1,570 species), and the Bdelloidea (461 species), and these differ in their reproductive mode (Segers 2007). Seisonids are sexual and monogononts are cyclically parthenogenetic, both have a sexual stage in their life cycle with meiosis, pairing of chromosomes, chiasmata, the reduction in ploidy, the subsequent formation of gametes, and the restoration of the full ploidy level upon fertilisation (Gilbert 1988). The parthenogenetic phase of monogononts is apomictic (consult Fig. 1.1 for full life cycles). Bdelloid rotifers are obligate parthenogens (more precisely apomictic thelytoky; Hsu 1956) whereby a female produces daughters from unfertilised eggs; explicitly, there is no meiosis, chromosomes do not pair, and the oocyte undergoes a single “mitotic” cell division, thereby passing on a perfect clone of their genotype to the offspring (Gilbert 1993). Some studies also place Acanthocephala, macroscopic parasitic worms, within the same clade as rotifers (Garey and Near 1996; Garey et al. 1998; García-

Varela and León 2000; Min and Park 2009; Lasek-Nesselquist 2012), although the relationships remain controversial (Fontaneto and Jondelius 2011). Acanthocephala are obligate sexuals.

Conclusions from comparative studies looking into differences in biodiversity patterns with respect to reproductive mode can be used reflectively to postulate the predominance of sex despite its costs and to answer questions such as *why do species exist as discrete entities* (Tang et al. 2014b)? The disordered rotifer taxonomy throughout its hierarchy, however, threatens their use in evolutionary studies.

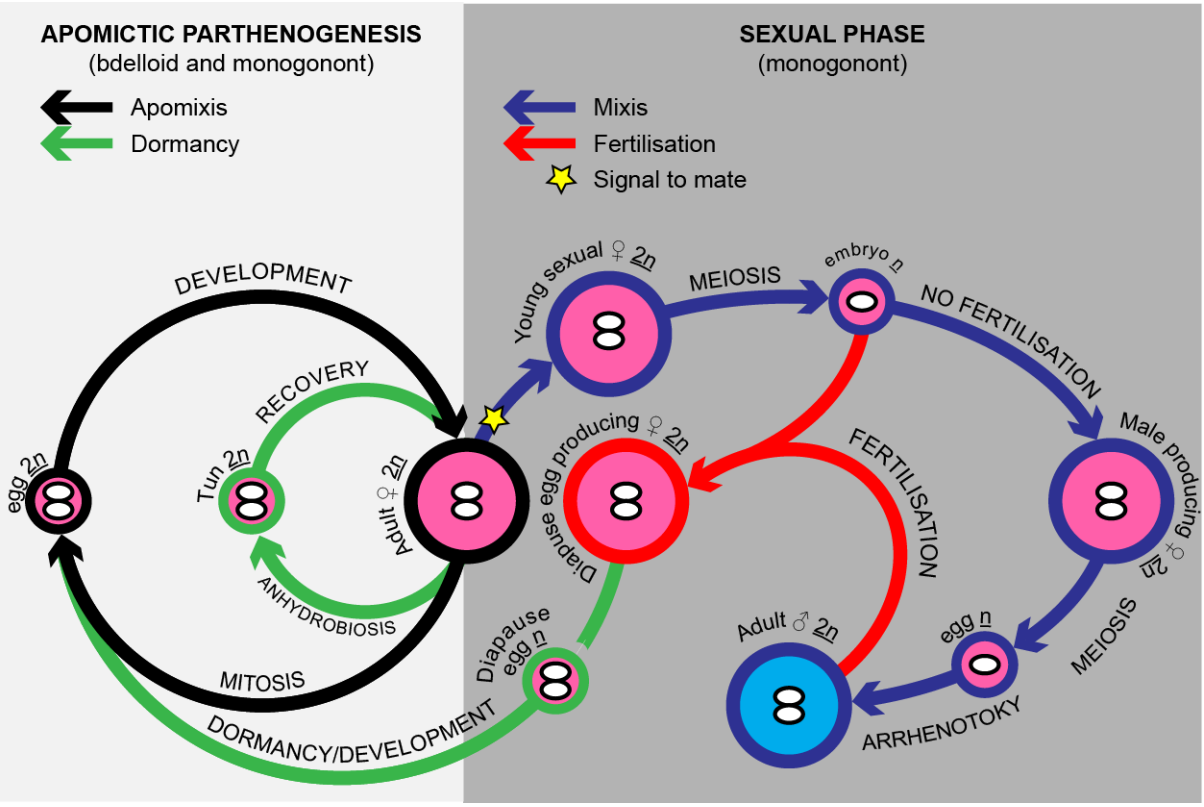

Figure 1.1 The typical rotifer life cycle.
Bdelloid rotifers reproduce exclusively via apomictic parthenogenesis, while monogononts have a sexual phase induced by density dependent environmental cues. This figure is adapted from information in Serra and Snell (2009).

Defining asexual species

The existence of asexual species is controversial (Dobzhansky and Dobzhansky 1937; Dobzhansky 1950; Hull 1980; Coyne and Orr 2004). Most asexual lineages do not persist for long enough to diversify, and those that do form entities that are incompatible with certain criteria of the biological species concept (i.e. they are never "potentially interbreeding" - Mayr 1942; de Queiroz 2005a). A naïve view, borne out of the idea that gene flow is the only force that unites populations into lineages (e.g. Dobzhansky and Dobzhansky 1937), is that clonal organisms are expected to form a continuum of genetic variation, instead of discrete species (e.g. Sepp and Paal 1998). Assuming that birth and

death are equally probable throughout the population, and that there is no carrying capacity, the accumulation of independent mutations from parent to the *n*th generation will manifest as a continuous distribution of genetic variation. This scenario, however, is unrealistic (Barraclough et al. 2003).

Barraclough et al. (2003) formulated a general theory of speciation for both asexual and sexual organisms. Briefly, populations are limited by finite resources, and owing to either stochastic effects or natural selection, birth and death rates for each member of a population are not equally probable, such that random extinction and unequal birth rates act to form transient clusters separated by shallow gaps. However, allopatric speciation by physical isolation or sympatric speciation by divergent selection for adaptation to different niches can result in the formation independent arenas for the evolutionary processes of mutation, selection, and drift. Given enough time, physical isolation or divergent selection result in the formation of discernable clusters akin to species. Allopatric speciation in asexuals occurs in much the same way as for sexual organisms, but sympatric speciation might be easier because it is unencumbered by gene flow breaking down independent evolutionary histories.

Asexual clusters formed in this way have characteristics that match the criteria of several species concepts: they form independently evolving, reciprocally monophyletic (after a sufficiently long divergence time) genotypic clusters (Evolutionary - Simpson 1951; Phylogenetic - Rosen 1979; Evolutionary Genetic species concept Birky et al. 2010), they might accrue phenotypic differences under neutrality (Phenetic species concept - Sokal and Crovello 1970) or ecological and phenotypic differences by divergent selection (Ecological species concept - Van Valen 1976), and clusters that form by divergent selection in sympatry are unlikely to merge again (encapsulating some of the criteria of the biological species concept - Mayr 1942 - although without reference to gene exchange). These species are observable as clusters separated by long gaps and diagnosable by species delimitation methods (Birky and Barraclough 2009) such as the Generalised Mixed Yule Coalescent model (GMYC - Pons et al. 2006; Fontaneto et al. 2007d; Fujisawa and Barraclough 2013) or the K/θ model (Birky et al. 2005), both discussed further below. Whether these gaps are equivalent in asexual and sexual organisms (i.e. how discrete species are) is only recently known (Tang et al. 2014b).

Ancient asexuality

Bdelloid rotifers

The ancient asexual status of bdelloid rotifers is supported by multiple lines of evidence (Judson and Normark 1996; Mark Welch and Meselson 2000; Danchin et al. 2011). Despite much study since the eighteenth century (Danchin et al. 2011), amounting to nearly half a million observed individuals (Birky 2010), not a single male has been found. Genomic evidence suggests that the chromosomal structure of bdelloids (at least in *Adineta vaga*) is incompatible with meiosis (Flot et al. 2013), such

that allelic regions have been rearranged, on occasion into palindromic sequences on the same chromosome. The accumulation of deleterious mutations in the absence of meiosis (Barraclough et al. 2007) and the absence of deleterious transposable elements, that would otherwise drive asexual lineages to extinction, is consistent with bdelloids being asexual (Arkhipova and Meselson 2000; Schurko et al. 2009). Fossil evidence (Poinar and Ricci 1992) suggest that bdelloid rotifers have gone without sex for at least 40 million years, a figure congruent with phylogenetic analyses (Tang et al. 2014b) and in this time bdelloid rotifers have diversified into a rich array of species (Donner 1965; Barraclough et al. 2003; Fontaneto et al. 2007d, 2009; Birky et al. 2011; Iakovenko et al. 2013).

Other putatively ancient asexual systems other than bdelloid rotifers exist (e.g. oribatid mites - Heethoff et al. 2009; darwinulid ostracods - Schön et al. 2009; *Timema* stick insects - Schwander et al. 2011; see Danchin et al. 2011) but none are as conclusive or accessible as the Rotifera system (as described below but also reviewed in Judson and Normark 1996; Normark et al. 2003; Schurko et al. 2009; Danchin et al. 2011).

Oribatid mites (Acari: Arthropoda)

High genetic divergences between clades of exclusively parthenogenetic oribatid mites and their sexual siblings, indicate that asexuality has evolved multiple times (Maraun et al. 2003) up to 100 million (Heethoff et al. 2007) or 200 million years ago (Hammer and Wallwork 1979). The ancient asexual status of oribatid mites is debatable owing to the discovery of rare sterile males (Palmer and Norton 1991), and the re-evolution of sexuality from parthenogenetic ancestors (Domes et al. 2007; although this may be an artefact of improper statistics, see Goldberg and Igić 2008). Whether or not all of these rare non-functional spanandric males are functional at a population level is debatable (Palmer and Norton 1992).

Darwinulid ostracods (Ostracoda: Arthropoda)

Ostracod crustaceans are of particular interest for the study of sex because the group has a high incidence of transitions from sex to asex (Bell 1982; Chaplin et al. 1994) and one of the best fossil records (Moore 1961). Prior to 2006, no living darwinulid ostracod males had been observed (Schön et al. 2009), although two putative males fossils had been proposed (Brady and Robertson 1870; Turner 1895). The legitimacy of ancient asexuality in the group has been cast into doubt with the discovery of three living males of the *Vestalenula* genus (Smith et al. 2006), which have sexually dimorphic antennae and fifth limb morphologies but misleadingly similar carapace shape and size to juvenile females. Proponents of the darwinulid ancient asexuality argue that these rare males are probably non-functional atavisms with no evidence of copulation or sperm (Martens and Schön 2008; Schön et al. 2009), and that even if rare functional males existed, they would be ineffective at a population level (Birky 2010). It could be argued that maintaining the ability to produce morphological males for many millions of years without the production of sperm seems implausible.

Timema stick insects (Pterygota: Arthropoda)

Timema stick insects are a relatively species poor genus of at least five species. Molecular evidence, namely high intraspecific divergence of mitochondrial sequence and nuclear allele divergence patterns (Meselson effect accredited to Mark Welch and Meselson 2001; although see White 1945), and accumulation of deleterious mutations (Schwander et al. 2011; Henry et al. 2012), indicates that *Timema* stick insects have persisted for a relatively recent time of up to 2 million years without sex.

Root knot nematodes (Secernentea: Nematoda)

Root knot nematodes (*Meloidogyne*) comprise a genus of at least 97 species (Hunt and Handoo 2009) and has independently evolved obligate asexuality twice (Holterman et al. 2009; although likely 3-4 times - D. Lunt pers. comm.). The ancient asexual status of root knot nematodes is not primarily based on the lack of males (for which males are usually very rare in the wild, but can be environmentally induced; Castagnone-Sereno 2006; Snyder et al. 2006), but on genomic characteristics such as high levels of aneuploidy and variable chromosome numbers within species (Sasser and Carter 1985; Castagnone-Sereno 2006), allelic sequence divergence, and paralogous allele effects (Lunt 2008). Molecular analyses of the mitochondrial DNA indicates that parthenogenesis in the group could be upto 80 million years (Hugall et al. 1997), although Lunt (2008) suggests a recent origin by interspecific hybridisation.

Comparing patterns of biodiversity between asexual and sexual lineages, in a group with enough diversity, and of sufficient age, provides insights into how sex acts in forming them. This thesis makes comparisons between bdelloid and monogonont rotifers, the Eurotatoria, a group of high diversity, with large bank of available genetic data, and where evidence contradicting the ancient asexual status of bdelloid rotifers is yet to surface.

Taxonomy

The meiofauna, rotifers included, are among the last frontiers of undiscovered biodiversity (Creer et al. 2010; Curini-Galletti et al. 2012). This polyphyletic group of microinvertebrates (defined as animals that can pass through a 500µm mesh) harbours unprecedented levels of diversity (Creer et al. 2010; Fonseca et al. 2010), a high degree of morphostasis and taxonomic crypsis (e.g. Fontaneto et al. 2009; Tang et al. 2012), and include representatives from approximately 60% of animal phyla (Creer and Sinniger 2012). Blaxter et al. (2004) described the description of rare novelty in meiofaunal groups as a “Herculean task”, this is perhaps reflected in the waning number of new descriptions since a peak in the 1930s (Fig. 1.2), the growing number of ecologists using molecular operational taxonomic units (MOTUs, described below) detached form their corresponding “species” names (Blaxter et al. 2005), and the wider adoption of next generation sequencing technologies (Bik et al. 2012b; e.g. Creer and Sinniger 2012).

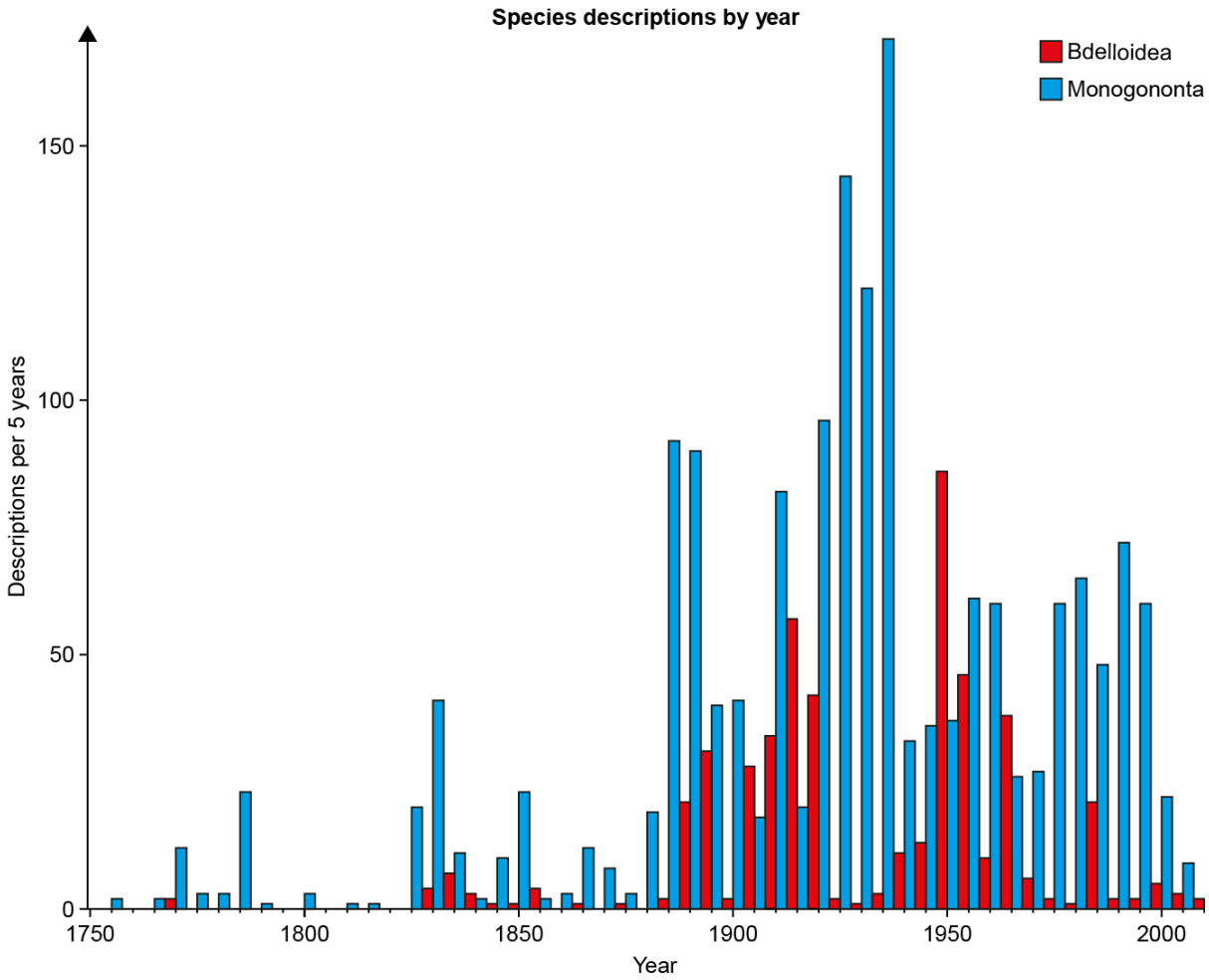

Figure 1.2 Description of new bdelloid (red) and monogonont (blue) rotifer species from 1750 to present day. Records extracted from Segers (2007).

Good, resolved taxonomy is central to biodiversity studies, unfortunately Bdelloidea and its phylum Rotifera are problematic taxonomic groups (Fontaneto 2014). Bdelloidea is a relatively diverse class consisting of three orders (Adinetida, Philodinavida, and Philodinida), four families (Adinetidea, Habrotrochidae, Philodinavidea, and Philodinidea), and approximately 460 species split over 19 genera (Donner 1965; Melone and Ricci 1995; Melone et al. 1998b; Segers 2007). Some morphological characters (e.g. spine presence, spine length, lorica constriction) historically used to diagnose species are plastic and hold inconsistent taxonomic validity (Zhang et al. 2010; Leasi et al. 2013; Fontaneto 2014). The poor taxonomy in the group is only exacerbated by the taxonomic crisis (Blaxter 2003, 2004; Agnarsson and Kuntner 2007), with too much unknown diversity (Fontaneto et al. 2009; Kaya et al. 2009) and too few expert "rotiferologists" (Wallace 2002; Fontaneto et al. 2012a) and modern keys (species level identification rely heavily on Donner 1965). It seems as though what we know about rotifers is heavily influenced by where the few rotiferologists are or were (Fontaneto et al. 2012a), while much of the world (especially the tropics) remain *aqua incognita* (Wallace 2002). Indeed the 2,000 described Rotifera morphospecies (Segers 2007) represent a huge underestimate of

the actual diversity (e.g. Suatoni et al. 2006; Fontaneto et al. 2009; Kaya et al. 2009; Tang et al. 2012).

The occurrence of cryptic species in Rotifera is well documented in both bdelloids (e.g. Fontaneto et al. 2008b, 2009, 2011; Kaya et al. 2009) and monogononts (e.g. Gómez et al. 2002; Leasi et al. 2013). Take the monogonont species *Brachionus plicatilis*, for example, which is an important for modern aquaculture morphospecies (e.g. Baer et al. 2008). It was originally described by Otto Friedrich Müller in 1786, and through various iterative analyses of morphology, karyology, genetics, and reproductive behaviour, one species became two (Segers 1995), then three (Ciros-Perez 2001), then nine (Gómez et al. 2002), then 15 (Suatoni et al. 2006), and now at least 26 species (Tang et al. 2012). To date only four of these MOTUs have been described formally (Ciros-Perez 2001; Fontaneto et al. 2007a), although a consortium in the near future is being setup to formally describe the remaining MOTUs based on molecular and morphometric evidence (Fontaneto, pers. comm.). Even though there is some effort going into rectifying this gaping deficit in *Brachionus plicatilis*, there is no such promise for many other 38 species complexes compiled by Fontaneto (2014). At worst, there are dustbin taxa such as *Rotaria rotatoria* (Bdelloidea: Rotifera), which is a morphospecies consisting of at least 70 potential cryptic species (Fontaneto et al. 2007d, 2009, 2012b; Tang et al. 2012).

Molecular techniques and their limitations: Issues with using one locus instead of many

Molecular techniques have revolutionised how biodiversity is investigated (Gómez 2005; Birky 2007; Taberlet et al. 2012; Yu et al. 2012) and are especially useful where traditional taxonomic characteristics (morphologies, ecologies, behaviours) are either uninformative or difficult to measure (Blaxter 2003, 2004; Fontaneto 2014). These techniques fall into two distinct applications that have advantages and limitations in their own right (Vogler and Monaghan 2007; Collins and Cruickshank 2012): (1) DNA barcoding *sensu stricto* (Hebert et al. 2003a) provides a large scale, repeatable, and rapid means to identify already known species against a DNA sequence database (Puillandre et al. 2012b), and (2) species discovery (Sites and Marshall 2003; Camargo and Sites 2013) is the delimitation of new diversity using DNA barcodes. While the former is widely accepted when the sequences match exactly those on a database (Desalle 2006), the latter is relatively more controversial (DeSalle et al. 2005; Matz and Nielsen 2005; Vogler and Monaghan 2007).

DNA barcoding

DNA barcodes are analogous to retail barcodes in that a species' genetic code at a standardised locus can be used as an species identifier (Hebert et al. 2003a). The process of DNA barcoding involves the amplification of a standard genetic region (COI for animals - Hebert et al. 2003b; matK and rbcL for plants - CBOL Plant Working Group 2009; Schoch et al. 2012), the comparison of this sequence to a database (e.g. Ratnasingham and Hebert 2007), and some degree of clustering based on nucleotide similarity (Hebert et al. 2003b).

The idea of identifying animal species using a universal stretch of DNA (DNA barcode) has developed over time. The exact phrase "DNA barcoding" is *probably* attributable to Paul D. N. Hebert (2003b), although Mark Blaxter was using the term "molecular barcoding" for exactly the same purpose a little earlier (i.e. the use of 18S to identify soil nematodes - Floyd et al. 2002; and as a personal communication in Ritz and Trudgill 1999). The actual practice of identifying biodiversity using molecular characters (albeit not always COI) has earlier origins and likely lies with practitioners like Norman R. Pace, who used short standardized 16S sequences to identify microbial diversity (Pace 1997), although with more of an environmental survey focus. These techniques have been used much earlier for forensics (e.g. Higuchi et al. 1988), for other groups using different loci (e.g. Yeast - Kurtzman 1994; Bacteria - Wilson 1995), and even for animals (e.g. Baker and Palumbi 1994; Gómez et al. 2002). The identification of species relies on the idea that their sequences will cluster so that intraspecific divergences will always be less than interspecific divergences (the barcode gap), and that this gap is consistent and diagnosable across all animal species (this is not always true, discussed below). DNA barcoding has been used for the rapid assessment of diversity (e.g. Ward et al. 2005; Yu et al. 2012), to identify larval stages (e.g. Webb et al. 2006), and for forensics (e.g. Dawnay et al. 2007).

Other than the concerns regarding the encroachment of DNA taxonomy on traditional taxonomy and the purported waning funding for traditional taxonomy (Ebach and Holdrege 2005; but see Gregory 2005), and the bias against traditional taxonomy in higher impact journals (Krell 2002), several practical limitations have been suggested that reduce the efficacy of COI-based DNA barcoding. Co-amplification and sequencing of pseudogenes (nuclear mitochondrial pseudogenes [NUMTS] - Thalmann et al. 2004; Song et al. 2008) can lead to misrepresentative focal barcodes. Similarly, introgressive hybridisation between species, the movement of whole genes, can also lead to misrepresentative focal barcodes (Chase et al. 2005). Incomplete lineage sorting (Funk and Omland 2003) resulting in a barcode overlap (i.e. the distinction between intra- and interspecific variation; Meyer and Paulay 2005) can lead to lumping of otherwise distinct species. Diagnosable morphological differences that develop due to divergent selection are likely to manifest much sooner than a neutral gene, therefore species can be detected much sooner than variation at neutral markers becomes completely sorted (Will and Rubinoff 2004). Furthermore, if a barcode gap exists, it is unlikely to be equivalent between lineages of different ecologies, evolutionary histories, and stresses. For example Hebert et al. (2003a) recommended a 3% divergence as a threshold for species based on divergences between known species, while Vences et al. (2005) found intraspecific variation in COI in amphibians of up to 18%. Studies suggest that the lack of a barcode gap might be due to restricted geographical, intra- and interspecific sampling (Meyer and Paulay 2005; Wiemers and Fiedler 2007; Bergsten et al. 2012). While the potential incongruency of COI (particularly with regard to genetic saturation) with other loci and the species phylogeny (Sota and Vogler 2001; Rubinoff 2006; Rubinoff

et al. 2006) and the idea that "one gene fits all" (Moritz and Cicero 2004) might lead to unrepresentative biodiversity patterns. Some of these issues are easily dealt with (e.g. non-functional NUMTs are characterised by stop codons or frame-shift mutations that are observable by eye or overcome with better primer design; Robeson et al. 2009), others need re-evaluation (e.g. lack of a barcode gap - Meyer 2003; Chapter 4).

DNA taxonomy

DNA taxonomy is a useful tool for assessing the taxonomic diversity within challenging groups (Blaxter 2004; Blaxter et al. 2004) where morphostasis and cryptic diversity (Fontaneto et al. 2008b, 2011; Leasi et al. 2013), and a dwindling pool of taxonomists (Hebert et al. 2003a; Blaxter et al. 2004) confound the traditional approach. The general idea is to use some criterion based on patterns of DNA sequence variation to delimit and count taxa (e.g. species, operational taxonomic units). The simplest criterion is nucleotide sequence divergence, such that species are defined by a percentage cut-off based on observed divergence in better known clades (e.g. Hebert et al. 2003a). Alternatively, algorithmic metrics founded in evolutionary theory have been developed to delimit species with no *a priori* species hypotheses (Vogler and Monaghan 2007) using single locus (e.g. K/θ - Birky et al. 2005; GMYC - Pons et al. 2006; PTP - Zhang et al. 2013) and multilocus datasets (e.g. BP&P - Yang and Rannala 2010). These methods use a range of inputs (nucleotide alignments and phylogenies) to assess different signatures of the species boundary. These metrics form putative, primary species hypotheses (Puillandre et al. 2012b) that can be tested if other data are available (e.g. morphometric, geographical locality data).

Three used in this thesis include: K/θ (Birky et al. 2005, 2010), the GMYC (Pons et al. 2006; Fontaneto et al. 2007d; Fujisawa and Barraclough 2013), and the PTP (Zhang et al. 2013). Briefly (but discussed in greater detail in Chapters 2 and 3) these methods rely on the expectation that species will form as distinct clusters on a gene tree separated by long branches (Birky and Barraclough 2009; Birky 2013; Fig. 5.1 in Chapter 5). These species clusters (ESUs) are detectable as monophyletic populations that have either four times as much interclade variation than intraclade variation (K/θ based on population genetic theory - Birky et al. 2005), significantly faster intraspecific relative to interspecific branching rates (GMYC based on coalescent theory - Pons et al. 2006), or significantly more intraspecific relative to interspecific substitutions (PTP based on coalescent theory - Zhang et al. 2013).

In rotifers, where taxonomic characters are sometimes plastic and uninformative (Fontaneto et al. 2007a; Zhang et al. 2010; Leasi et al. 2013; Fontaneto 2014), molecular techniques have been especially useful for the generation of, at least, putative species hypotheses (e.g. Birky et al. 2011). Furthermore, DNA taxonomy can be used to delimit species under a single species concept (i.e. the evolutionary species concept; Simpson 1951 and its derivatives). This is particularly important when

investigating asexual taxa for which the biological species concept, which requires that species are members of a population that actually or potentially interbreed in nature, is not compatible.

DNA taxonomy is not a substitute for traditional taxonomy, ideally there would exist an abundance of rotiferologists supplementing rigorous traditional taxonomic methods with molecular techniques in an integrative and iterative manner (e.g. Birky et al. 2011; or the planned integrative taxonomy workshop disentangling the *Brachionus plicatilis* species complex). To better understand the processes that form rotifer biodiversity, it is essential that we have comparable units of diversity devoid of misidentifications and incompatible species concepts, which is achievable using DNA taxonomy (Fig. 1.3). Despite the concerns raised about DNA taxonomy, particularly the use of a single locus, the method has been used to with rotifers to delimit species that are morphologically (Birky et al. 2011; Malekzadeh-Viayeh et al. 2014), ecologically (Fontaneto et al. 2007d), and reproductively isolated (Schröder and Walsh 2007).

Thesis structure

Using rotifers as a model organism, I will investigate the implications of asexuality on rotifer biodiversity. The thesis has three overarching themes summarised by these questions (Fig. 1.4): (1) how can molecular techniques be adopted to better assess rotifer biodiversity, (2) why do species exist as discrete entities as opposed to a continuum of forms, and (3) are named bdelloid higher taxa monophyletic?

Firstly, I evaluate DNA-based species delimitation methods and identify how these are affected by marker choice (Chapter 2 – *The widely used small subunit 18S rDNA greatly underestimates true diversity in biodiversity surveys of the meiofauna – PNAS 2012, 109, 16208-16212*) and delimitation method choice (Chapter 2 and Chapter 3 – *Effects of phylogenetic reconstruction on the robustness of species delimitation methods using single-locus data – Methods in Ecology and Evolution, in press*). In Chapter 3 I examine the effect of phylogenetic reconstruction method on coalescent-based species delimitation methods, which is widely neglected and rarely justified. In Chapter 4 I determine how biodiversity delimited by molecular and traditional morphological methods compare with respect to identification by DNA barcoding (*DNA barcoding of rotifers*).

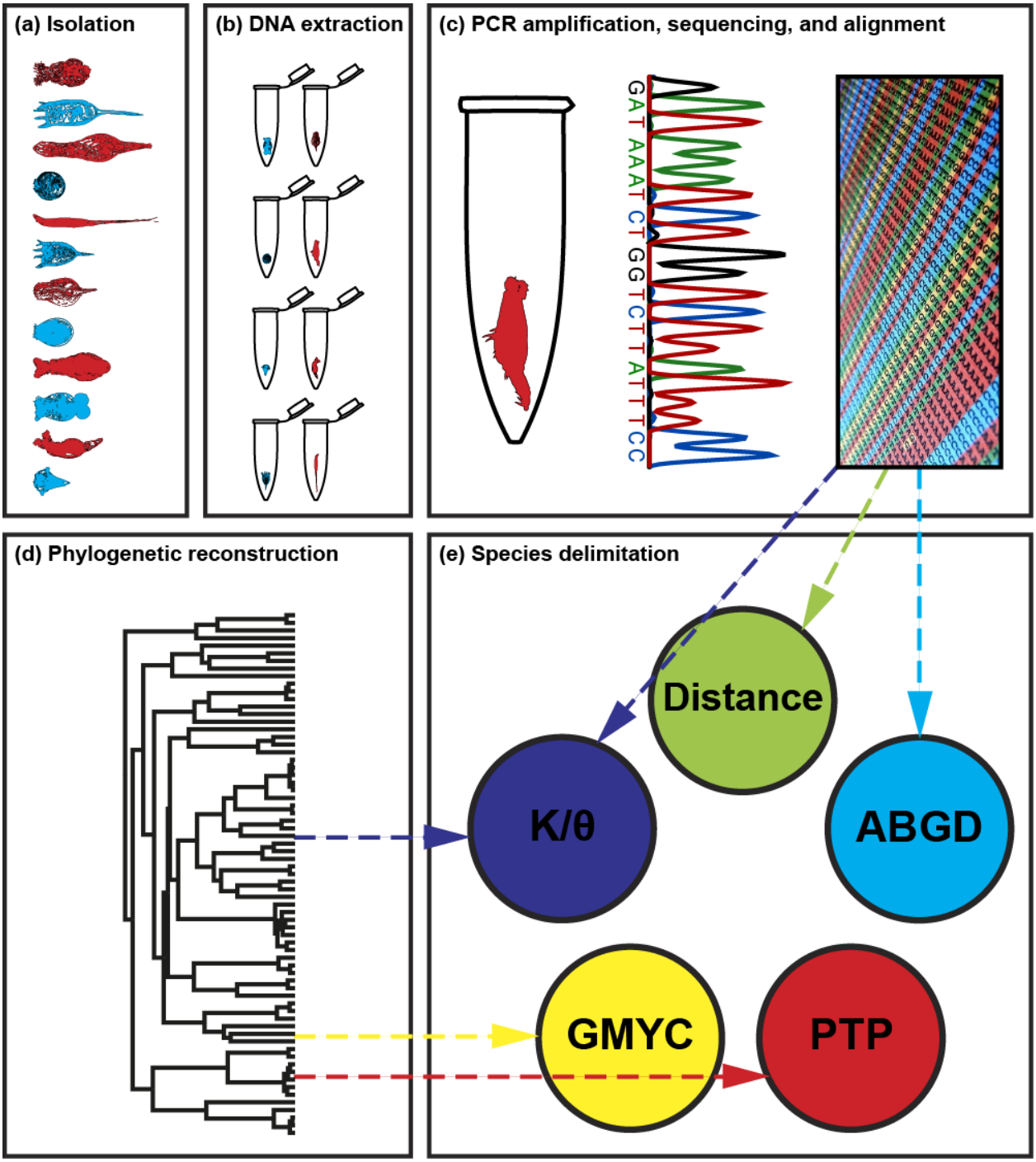

Figure 1.3 Typical DNA taxonomy workflow used for rotifers.
(**a**) Animals are isolated in the wild and identified to morphospecies level under light microscopy. (**b**) These animals are washed in ddH_20 and transferred to individual tubes in which the DNA is extracted. (**c**) Specific genetic loci are amplified, Sanger sequenced, and aligned. (**d**) The alignment is used to reconstruct a phylogeny. (**e**) The alignment (**c**) and/or the phylogeny (**d**) are used as input for various species delimitation metrics. Various stages of the DNA taxonomy process can be altered, and these alterations have implications on the final estimated species count. Different genetic loci (e.g. COI mtDNA vs. 18S rDNA; **c**), different phylogenetic reconstructions methods (e.g. maximum likelihood vs. Bayesian inference; **d**), or different species delimitation metrics can be used (e.g. GMYC vs. PTP; **e**).

Chapters 2, 3, and 4 are species delimitation method evaluations, which ultimately justify the use of the COI, BEAST, and the GMYC method for species delimitation for sexual as well as asexual lineages. In Chapter 5 I investigate one of the most neglected, yet important questions in speciation biology: "Why do species form discrete entities rather than a continuum of forms?" (*Sexual Species are separated by larger Genetic Gaps than Asexual Species in Rotifers – Evolution, online early*). I compare the discreteness of asexual bdelloid rotifer and sexual monogonont rotifer ESUs and provide a thorough examination of how bdelloid and monogonont diversification rates differ.

Finally, in Chapter 6 (*Dated Molecular Phylogeny of Bdelloid Rotifers*) I examine the evolutionary relationships within Bdelloidea using 5 genes (COI mtDNA, 18S rDNA, 28S rDNA, and two nuclear genes designed using the transcriptome alignments from Eyres 2013) and a genus-level sampling to by reconstruct a molecular phylogeny.

Summary of aims

- To provide a set of guidelines for DNA taxonomy based on gene, species delimitation metric, and phylogenetic reconstruction choice.
- To test whether asexual species clusters are as discrete as sexual species.
- To generate a multilocus molecular phylogeny of Bdelloidea.

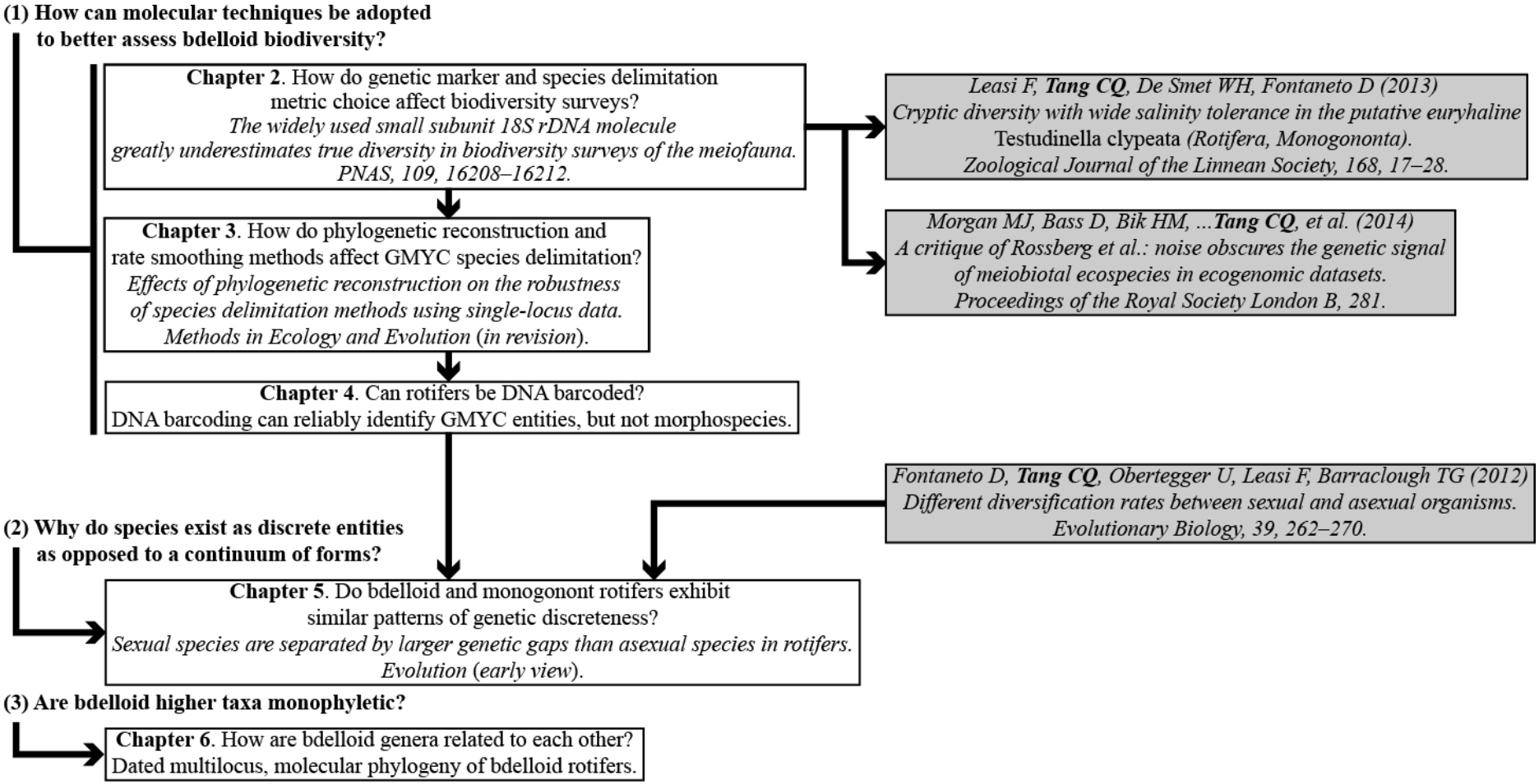

Figure 1.4 Workflow of the thesis split into the three main questions investigated: (1) How can molecular techniques be adopted to better assess bdelloid biodiversity, (2) Why do species exist as discrete entities as opposed to a continuum of forms, and (3) Do bdelloid higher taxa exist?
Arrows indicate where work done in previous chapters influences the work in subsequent chapters. Collaborations (grey boxes) and how they relate to the chapters is shown.

Chapter 2: The widely used small subunit 18S rDNA molecule greatly underestimates true diversity in biodiversity surveys of the meiofauna

Published as:

Tang, C. Q., Leasi, F., Obertegger, U., Kieneke, A., Barraclough, T. G., & Fontaneto, D. (2012). The widely used small subunit 18S rDNA molecule greatly underestimates true diversity in biodiversity surveys of the meiofauna. Proceedings of the National Academy of Sciences of the United States of America, 109, 16208–16212.

Abstract

Molecular tools have revolutionised the exploration of biodiversity, especially in organisms for which traditional taxonomy is difficult, such as for microscopic animals (meiofauna). Environmental (eDNA) surveys of extracellular DNA extracted from sediment samples or metabarcode surveys of DNA extracted from bulk DNA samples, using next generation sequencing technology (NGS), are increasingly popular for assessing biodiversity. Most of these surveys use the nuclear gene encoding small-subunit rDNA (18S) as a marker; however, different markers and metrics used for delimiting species have not yet been evaluated against each other or against morphologically defined species (morphospecies). We assessed more than 12,000 meiofaunal sequences of 18S and of the main alternatively used marker (COI mtDNA) belonging to 55 datasets covering three taxonomic ranks. Our results show that 18S reduced diversity estimates by a factor of 0.4 relative to morphospecies, whereas COI increased diversity estimates by a factor of 7.6. Moreover, estimates of species richness using COI were robust among three of four commonly used delimitation metrics, whereas estimates using 18S varied widely with the different metrics. We show that meiofaunal diversity has been greatly underestimated by 18S NGS surveys and that the use of COI provides a better estimate of diversity. The suitability of COI is supported by cross-mating experiments in the literature and evolutionary analyses of discreteness in patterns of genetic variation. Furthermore its splitting of morphospecies is expected from documented levels of cryptic taxa in exemplar meiofauna. We recommend against using 18S as a marker for biodiversity surveys and suggest that use of COI for NGS surveys could provide more accurate estimates of species richness in the future.

Introduction

Species are a fundamental unit of biological diversity and their delimitation is central in ecology and evolution. Species delimitation using DNA (DNA taxonomy) has the potential to bypass many of the difficulties associated with traditional morphological taxonomy (Hebert et al. 2003a). With developments in high-throughput sequencing technologies and bioinformatic pipelines, it is now possible to sequence a single genetic locus *en masse* from extracellular DNA in the environment (eDNA surveys; Bik et al. 2012b; Taberlet et al. 2012) or bulk DNA samples (metabarcoding; Yu et al. 2012) and delimit species on a large scale. Such surveys have been used to describe the diversity of microorganisms (Robeson et al. 2009), macrofauna (Ficetola et al. 2008), fungi (Blaalid et al. 2012), and plants (Yoccoz et al. 2012) in previously understudied habitats such as the soil biota (Wu et al. 2011), sediments (Chariton et al. 2010), and water (Ficetola et al. 2008; Bik et al. 2012c). Faced with these technological advances, it is now more important than ever to evaluate the reliability of the genetic loci used for DNA taxonomy, and to assess the congruence of their results with morphological taxonomy. Without such an assessment, biodiversity analyses may be misleading.

Given this potential, there have been surprisingly few broad-scale attempts to calibrate the use of different markers and metrics in next generation sequencing (NGS) surveys. Here, we use a clade-targeted sampling regime to test different loci and metrics used in NGS surveys, relative to morphologically defined species (morphospecies). Our study is, taxonomically, one of the broadest surveys to date. By identifying diversity from systematic samples of clades, we provide guidelines that can be used with NGS surveys to better understand the evolution and ecology of animal diversity, using the example of meiofauna, a major reservoir of biodiversity that contains most of the animal phyla (Giere 2009).

Meiofaunal organisms (defined as animals that can pass through a 500µm mesh) cannot be reliably treated using traditional taxonomic methods due to their size (<2mm), morphological homogeneity (Fontaneto et al. 2009), non-informative species descriptions (Godfray 2002), and lack of expert taxonomists (Curini-Galletti et al. 2012). It is therefore expected that morphospecies will underestimate the true diversity of these organisms (Fontaneto et al. 2009). The use of NGS surveys can potentially make species delimitation more efficient and cost effective (Bik et al. 2012b). Current meiofaunal NGS surveys rely mainly on the nuclear small subunit 18S rDNA gene (Creer et al. 2010; Fonseca et al. 2010; Bik et al. 2012c). Cytochrome *c* oxidase subunit I (COI) mtDNA, while used for global barcoding initiatives (i.e. Consortium for the Barcode of Life, www.barcodeoflife.org and the International Barcode of Life project, www. ibol.org), is less widely used for NGS surveys. One of the main reasons is that high variability of COI can necessitate the use of taxon specific amplification and sequencing primers (e.g. Robeson et al. 2009; Sanna et al. 2009), although universal primer sets for

next generation sequencing (NGS) have been designed and successfully implemented recently (Meusnier et al. 2008).

Here, we compare putative species counts obtained using either COI or 18S across 55 meiofaunal datasets comprising three taxonomic ranks (15 species complexes, 26 genera, and 14 higher taxa above the genus level, including orders, classes, and phyla) and totalling more than 12,000 sequences. A number of analytical metrics exist for delimiting species (Hebert et al. 2003a; Sites and Marshall 2003; Pons et al. 2006; Wiens 2007; Birky et al. 2010; Puillandre et al. 2012a), which focus on different biological properties, require different data types (DNA, morphology, *etc*.), and have different minimal sampling requirements (Hebert et al. 2003a; Sites and Marshall 2003; Pons et al. 2006; Birky et al. 2010; Puillandre et al. 2012a). The relative performance of these different metrics has not yet been fully evaluated. Estimates are therefore compared between the two genes using four different delimitation metrics: the nucleotide divergence threshold (NDT; Hebert et al. 2003a), the automatic barcode gap discovery (ABGD; Puillandre et al. 2012a), the K/θ method (Birky et al. 2010), and the Generalized Mixed Yule Coalescent model (GMYC; Pons et al. 2006). These metrics were chosen because they can be implemented when DNA sequence data is the sole information available, as is the case in NGS surveys.

Materials and Methods

Data collection

We concentrated on meiofaunal species complexes, genera, and higher taxa for which a rich collection of sequences was available. Datasets were compiled if a minimum of 10 different sequences per taxon were available. In some cases (e.g. for some groups of nematodes, nemerteans, and flatworms), even organisms that are not strictly meiofauna have been included (e.g. larger or parasitic), if the majority of the taxa of the group belonged to meiofauna.

We obtained sequences of a fragment of COI (on average 623bp, Dataset S1) from 8,576 individuals (6,834 downloaded from GenBank; 1,742 generated for this study according to the protocol presented in the Supplementary Materials), and sequences of 18S rDNA (on average 1,647bp, Dataset S2.1) from 3,668 individuals (3,321 obtained from GenBank and 347 sequenced *de novo*). 18S sequences were amplified and sequenced directly only for each unique COI haplotype, as it became apparent from initial data collection that individuals with the same COI haplotype invariably had identical 18S sequences. A list of unique type specimens used in the analyses can be found in Dataset S2.1.

Overall, 12,244 sequences (of which 4,877 were unique) forming 55 datasets were analysed. In total 1,484 morphospecies were included; these were identified before sequencing using the most recent morphological revisions for the groups (listed in Curini-Galletti et al. 2012), or by using their GenBank accession identifier. Ambiguous names were conservatively excluded from the morphospecies count. Phylogenetic analyses were obtained using standard procedures (Supplementary Materials).

Nucleotide divergence threshold (NDT)

We applied a nucleotide divergence threshold (Hebert et al. 2003a) with a *friends of friends* approach (i.e. if divergence between taxa A-B and B-C is more than 3%, but divergence between A-C is less than 3%, then we consider taxa A, B and C to be a single cluster). The divergence threshold is based on empirically observed gaps and 97% is the most commonly used threshold for COI (e.g. Hebert et al. 2003b). We used a script written in R that clusters sequences from an alignment based on a user-defined divergence threshold, using an uncorrected distance matrix as input (available in Supplementary Materials).

Automatic barcode gap discovery (ABGD)

ABGD uses a range of prior intraspecific divergences to infer from the data a model-based one-sided confidence limit for interspecific divergence (Puillandre et al. 2012a). The ‘barcode gap’ is identified as the first significant gap beyond this limit. Genetic clusters were inferred using the ABGD online tool and the default settings (available at http://wwwabi.snv.jussieu.fr/public/abgd/abgdweb.html).

The correct species estimate was selected, as suggested by Puillandre et al. (2012a), using gene specific priors for maximum divergence of intraspecific diversity (0.01 for COI and 0.001 for 18S).

K/θ method (formerly known as the 4X rule)

The K/θ method uses population genetic theory to identify sister clades that are too divergent to arise solely by neutral genetic drift within a single population (Birky et al. 2010). A neighbour joining tree was constructed for each mtDNA dataset from uncorrected distance matrices using Geneious Pro 5.4.2. (Drummond et al. 2006). Starting from the tips of the tree, the maximum pairwise distance was recorded for each clade (θ). For each pair of sister clades, the maximum value of θ was then compared to K (minimum pairwise distance between clades). Clades that have a ratio of K/θ≥4 are considered to be reciprocally monophyletic entities with ≥95% probability (Birky et al. 2010).

Generalized Mixed Yule Coalescent (GMYC) method

The GMYC method (Pons et al. 2006) tests for a significant shift in the branching rate in an ultrametric tree. Such a shift is indicative of the switch from between-species to within-species processes, expected if a sample comprises multiple individuals from a set of independently evolving species. The outgroups were removed from the ultrametric trees and the GMYC method was implemented using the *splits* 1.0–11 (Ezard et al. 2009) package in R (available at http://r-forge.r-project.org/projects/splits/). Species were identified by a single threshold defined by a significant shift in branching rate.

Assessment of reliability

A linear model was used with a log transformed DNA/morph ratio as the response variable and gene identity, species delimitation metric, and taxonomic rank as fixed effects. The initial linear models included all the possible explanatory variables and their interactions. These were subsequently simplified using the *step* function in R to obtain the minimum adequate model. Model outputs were given as ANOVA tables and post-hoc Tukey HSD tests were performed to determine which factors were significantly different from each other.

To quantify the effect of sampling effort (per taxon sampling) we used the number of sequences per dataset. As an index for degree of undersampling (unsampled diversity), we used the ratio of observed entities to expected number of entities (determined using a Chao estimator, Chao 1984). Chao 1 estimator was used when both singlets and doublets were present in the dataset, Chao 2 estimator was used when either singlets or doublets were absent. These proxies for sampling effort and undersampling were included into a linear model as fixed effects along with gene, metric, and taxonomic rank.

Differing degrees of geographic coverage could inflate the congruency of delimitation metrics if genetic distance increases with geographical distance. We determined whether there was a significant

difference in geographical coverage of each of the genes and used a linear model to test whether congruency of delimitation metric species estimates could be explained by geographical coverage, gene, and taxonomic rank. The coefficient of variation among species estimates of different metrics was used as a proxy for their congruence, and number of countries within each dataset as a proxy for geographical coverage.

Misidentification of organisms by the authors submitting sequences to GenBank could underestimate the biodiversity already present in the samples. To address this concern, we identified all authors involved in submitting the sequences and determined whether they were taxonomists based on whether they had published a species description. This is a crude but true measure of taxonomist integrity but is likely to underestimate the capabilities of many authors. This subset of data was reanalysed as described previously.

Results

Choice of marker

Diversity estimates in meiofauna were significantly different between the two markers (COI and 18S) and between morphospecies and both genes in turn (Fig. 2.1, Table 2.1). COI yielded increased estimates of diversity relative to morphospecies, whereas 18S yielded decreased estimates of diversity (Fig. 2.1).

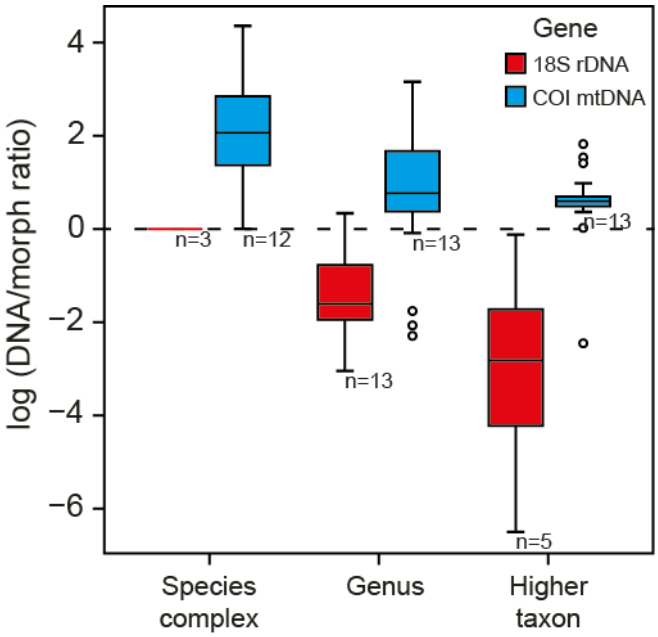

Figure 2.1 Ratio of species diversity estimated using DNA taxonomy compared to morphological taxonomy (dotted line) using either COI mtDNA (blue) or 18S rDNA (red) over three taxonomic ranks (species complex, genus and higher taxon).
DNA/morph ratios were averaged across both datasets and delimitation metric and log transformed. Open circles represent outlier values. The number of datasets (n) is shown under the boxes.

Sampling effort differed between the two genes, being greater for COI, but this did not account for the differences in the ratio of the species count based on DNA relative to the species count for morphology (referred to as the DNA/morph ratio) between the genes (Table 2.1). Furthermore, the number of datasets was balanced between COI and 18S, with 31 and 24 datasets, respectively (Table S2.1) and geographic coverage for each dataset did not differ significantly between the genes (Table S2.1).

The average number of taxa estimated for COI and 18S using the different metrics was 7.6 (±2.1 standard errors) and 0.4 (±0.1) times the morphological species estimate, respectively. Cryptic taxa were identified in all COI datasets (Fig. 2.2) across all taxonomic ranks. A higher number of taxa was expected from the COI dataset than the 18S dataset because most of the sequences come from investigations into cryptic species. Nevertheless, the estimated number of taxa using 18S was even

lower than the number indicated by morphological taxonomy (Fig. 2.2). Thus, 18S was not able to reach the level and detail of identification of diversity that taxonomists can reach with morphology alone.

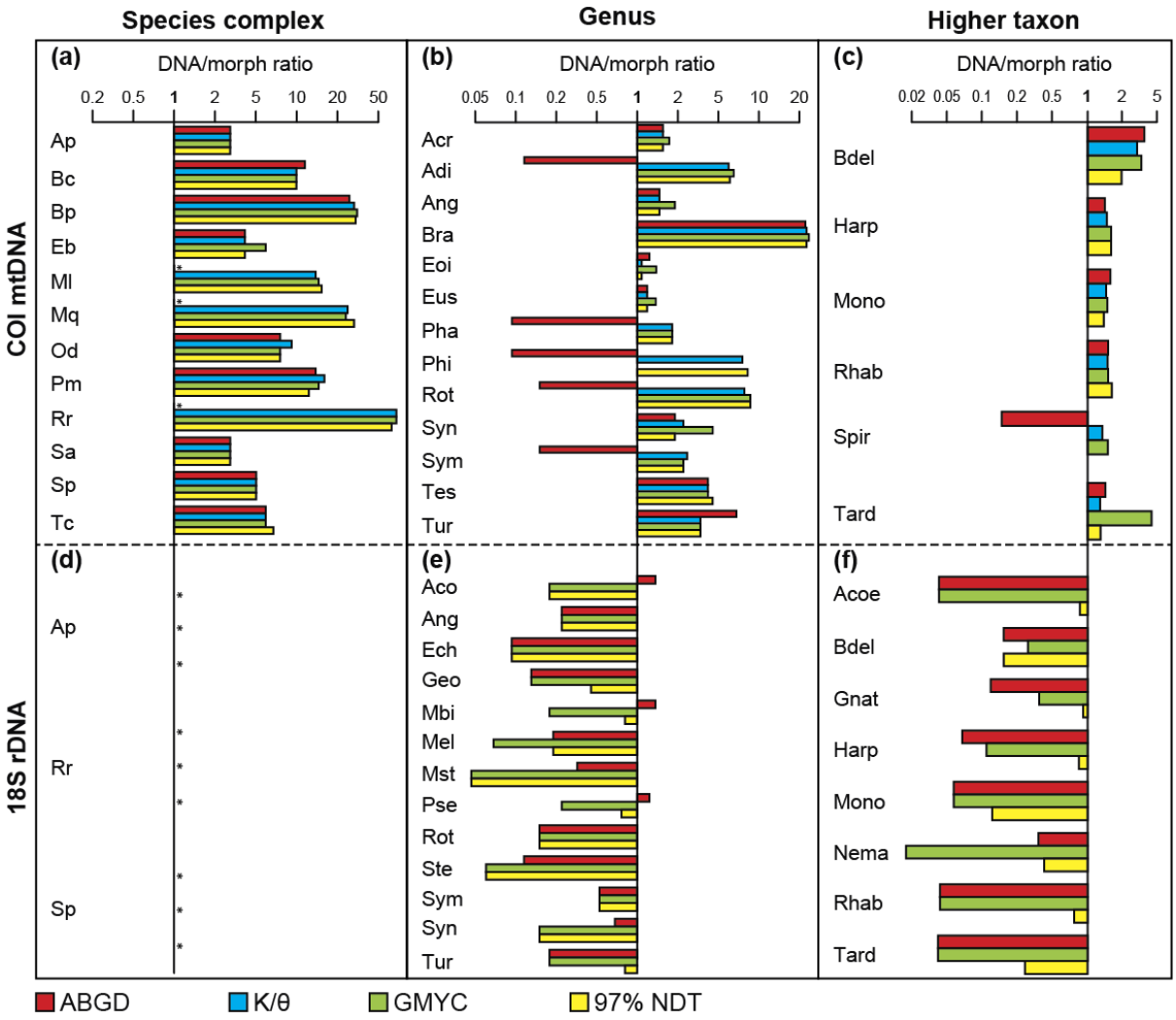

Figure 2.2 The ratio numbers of entities estimated using DNA taxonomy compared to morphological taxonomy (the y axis intersecting the x axis at 1) using different delimitation metrics and taxonomic ranks.
Four different delimitation metrics (ABGD = red, K/θ method = blue, GMYC = green, 97% nucleotide divergence threshold (NDT) = yellow) were used to compare DNA estimates to morphospecies, inferred from two different genes: COI (**a**, **b**, **c**) and 18S (**d**, **e**, **f**) and across three taxonomic ranks: species complexes (**a**, **d**), genera (**b**, **e**) and higher taxa (**c**, **f**). The x axis is log transformed for ease of comparison. The K/θ method can be used in conjunction with mtDNA only, and is absent from the plots using 18S. Species estimates and full names are shown in Table S2.1. Acronyms have two letters for species complexes, three for genera and four for higher taxa. Asterisks (*) specify instances where no additional species are estimated by DNA taxonomy compared to morphological taxonomy.

Controlling for potential confounding effects of differing sampling, by using datasets with COI and 18S sequenced from the same organisms, confirmed the general trend, with an average of 3.2 (±1.0) and 0.4 (±0.1) times the morphological species estimate for COI and 18S, respectively (Fig. S2.1).

Taxonomic rank

Taxonomic rank had a strong influence on the DNA/morph ratio for both COI and 18S (Table 2.2); with larger ratios for species complexes (15.3±2.7 and 1.0±0.0 times more entities for COI and 18S, respectively) than for genera (4.4±0.8 and 0.3±0.1, respectively) and higher taxa (2.2±0.3 and 0.2±0.1, respectively; Fig. 2.1).

Table 2.1 ANOVA used to explain differences in DNA/morph ratios.

Factor	Sum Sq.	D.F.	F value	*P*	% var.
Gene	428.7	1	352.79	$<2.2e^{-16}$	53.10
Metric	21.0	3	5.76	0.00087	2.60
Tax.	110.0	2	45.26	$<2.2e^{-16}$	13.62
Sampling	0.1	1	0.07	0.79	0.01
Metric x Tax.	11.2	6	1.53	0.17	1.38
Metric x Sampling	18.8	3	5.16	0.0019	2.33
Residuals	217.5	179			

% var. = amount of the variance explained by the factor,
Tax. = taxonomic rank, Sampling = sampling (number of sequences).

Delimitation metrics

Congruence among the different delimitation metrics was greater using COI than 18S (Fig. 2.2, Table S2.2). In COI, this pattern was not correlated to number of countries or taxonomic rank. Only species estimates from ABGD (4.4±1.2 times the morphological estimate) were significantly different from the others (9.5±1.5; Table S2.3; Fig. S2.2). The ABGD metric failed to delimit additional taxa in 26% of the datasets (Table S2.1). The DNA/morph ratio was influenced by the interaction between delimitation metric and degree of undersampling (i.e. the observed diversity compared to the expected diversity as determined using Chao estimators; Table 2.2), and so the small differences in diversity estimates among the metrics may be a function of how they behave with undersampling.

For 18S, there was very little congruence among results using different delimitation metrics (Fig. 2.2, Table S2.2). The GMYC estimated significantly fewer taxa (0.2±0.1 times the morphological estimate) than did both the nucleotide divergence 97% threshold (0.5±0.1) and ABGD metrics (0.4±0.1; Fig. S2.2). The estimates from the nucleotide divergence threshold became increasingly disparate from the other metrics with increasing threshold values. A 99% or a 99.5% threshold produced species estimates that were closer to the morphological estimate (average estimates were 0.8±0.1 and 1.1±0.2 times the morphological estimate, respectively).

Misidentification of morphospecies

To test whether misidentification of sequenced organisms (i.e. errors in morphospecies counts) could explain these patterns, we identified the subset of sequences generated by studies including a co-author who has published a taxonomic paper describing a new species (86.3% of COI and 55.1% of 18S sequences, Table S2.1). Our reasoning is that morphological identifications in those studies should be correct. Reanalysis using only those data confirmed the same scenario that 18S yields lower

diversity estimates and COI yields higher diversity estimates than morphospecies (Table S2.4). Furthermore, choice of metric, taxonomic rank, and sampling effect still affect the magnitude of estimates as identified for the entire dataset (Table S2.5).

Table 2.2 ANOVA used to explain DNA/morph ratio (COI and 18S analysed separately).

Factor	**Sum Sq.**	**D.F.**	**F value**	***P***	**% var.**
COI mtDNA					
Metric	27.8	3	12.03	<0.0001	13.5
Tax.	54.4	2	35.27	<0.0001	26.4
Country	14.8	1	19.14	<0.0001	7.2
Undersampling	0.2	1	0.26	0.61	0.1
Metric x Tax.	2.0	6	0.44	0.85	1.0
Tax. x Country	2.2	2	1.40	0.25	1.1
Metric x Undersampling	9.5	3	4.11	0.0088	4.6
Tax. x Undersampling	4.1	2	2.68	0.074	2.0
Country x Undersampling	0.1	1	0.12	0.73	0.04
Metric x Tax. x Undersampling	15.4	6	3.33	0.0052	7.5
Tax. x country x Undersampling	5.8	2	3.76	0.027	2.8
Residuals	69.4	90			
18S rDNA					
Metric	16.6	2	11.63	<0.0001	9.8
Tax.	64.8	2	45.42	<0.0001	38.2
Country	15.3	1	21.38	<0.0001	9.0
Metric x Tax.	24.2	4	8.47	<0.0001	14.3
Metric x Country	5.9	2	4.10	0.021	3.5
Residuals	42.8	60			

% var. = amount of the total variance explained by the factor, Tax. = taxonomic rank.

Discussion

A key limitation inherent to most biodiversity studies is the arduous task of identifying organisms in the wild. Reliance upon good taxonomy and species identification goes beyond biodiversity surveys because it has wide implications for a number of ecological and evolutionary studies (for a perspective see Yoccoz 2012). Here we demonstrate that biodiversity surveys of meiofaunal taxa will be greatly impacted by the choice of molecular marker. Using data covering a broad diversity of meiofaunal taxa, sampled across multiple taxonomic ranks, and applying four widely used delimitation metrics, we have shown that both 18S and morphology underestimate species diversity relative to COI (Fig. 2.1), independently of degree of undersampling. Further, the disparity in congruence among metrics for both genes was not driven by differences in the discreteness of geographical sampling (Table 2.2) or by errors in morphospecies identification.

Although COI leads to higher species counts than morphology, COI provides a better indicator of the true diversity than morphology for several reasons. First, cryptic taxa have previously been documented in many of the morphospecies assessed here (e.g. Suatoni et al. 2006; Fontaneto et al. 2009), and species boundaries have been confirmed within an integrative taxonomic framework (i.e. DNA taxonomy with cross-mating or additional morphological assessment; e.g. Schröder and Walsh 2007; Fonseca et al. 2008). Second, increased diversity based on COI is not simply due to higher variability, but associated with a sharp distinction in genetic distance within versus between evolutionary species (Table S2.1), which is indeed the signature that the evolutionary methods of K/θ and GMYC use to delimit species entities. There exist genetic clusters separated by larger 'gaps' in genetic variation than expected if all individuals belonged to a single interacting population. In sexual lineages, these clusters reflect reproductively isolated species. In asexual lineages, they are caused by geographical isolation or specialisation on distinct ecological niches (Birky and Barraclough 2009), as demonstrated by studies of exemplar clades (e.g. Fontaneto et al. 2007d, 2009; Schön et al. 2012). Patterns of genetic variation and differences between COI and 18S apply equally to asexual (i.e. bdelloid rotifers) and related sexual lineages (i.e. monogonont rotifers) in our sample (Table S2.6, Table SS.7).

We conclude that 18S, using these species delimitation metrics and the evolutionary species concept, is not powerful enough to delineate species-level diversity. Only a fixed threshold of 99.5% based on 18S (approaching the rate of potential PCR errors) can produce NGS estimates comparable to morphological estimates, but these are known to be underestimates due to the prevalence of cryptic species. The use of 18S might be appropriate to compare levels of relative diversity at higher taxonomic scales, but species-level patterns such as ecological distributions and geographical turnover should not be inferred from these data. Furthermore, the degree of lumping per morphospecies

estimated from 18S varies among different taxonomic groups (Fig. S2.1) and thus diversity might be very different depending on the composition of taxonomic groups present in an NGS sample.

The four metrics used require a different minimum number of sequences per entity to detect putative species, and thus in principle intraspecific undersampling might affect the metrics in different ways (Sites and Marshall 2003). Intraspecific undersampling did not affect our results, however, we observed a high degree of congruence for COI in terms of both species number and identity, particularly among the nucleotide divergence 97% threshold, K/θ, and GMYC methods (Fig. 2.2). Interestingly, the simple rule of pairwise similarity (Hebert et al. 2003a) gave results congruent to those provided by the two methods detecting signatures of independent evolution predicted by population genetic theory (Pons et al. 2006; Birky et al. 2010). The consistency among different delimitation metrics was much lower for 18S than for COI (Fig. 2.2; Table S2.3).

While these results provide strong reasons against using 18S for species delimitation, there are also difficulties associated with COI, which include high substitution rates, excessive saturation, biased substitution patterns, high AT content, and poorly conserved priming sites (Sanna et al. 2009; Creer et al. 2010). These issues are known to reduce the efficacy of COI in certain meiofauna (e.g. nematodes - Bhadury et al. 2006; and proseriates - Sanna et al. 2009) and this may be one of the main reasons why COI has rarely been used for meiofaunal NGS surveys (but see Robeson et al. 2009). Nonetheless, COI has been successfully used in an integrative taxonomic framework to delimit nematode cryptic species (e.g. Derycke et al. 2005; Fonseca et al. 2008). Here we included 11 nematode datasets and in each case diversity was split using COI and lumped using 18S, relative to morphological species, indicating that COI can be used to survey nematode diversity more reliably than with 18S.

An increasing number of next generation DNA metabarcoding surveys aim to quantify biodiversity (Taberlet et al. 2012), but this is a field in its infancy, which is expanding largely in tandem with evolving sequencing technologies and the wider integration into bioinformatic pipelines (Bik et al. 2012b). Use of COI with NGS is not yet popular. However, it has already been shown that a short mini-barcode fragment of COI can be amplified *en masse* with 454 pyrosequencing (Meusnier et al. 2008) and used to identify individual species with high accuracy across many eukaryotic groups. Combining the variability of COI with NGS technologies and a reference database of genetic sequences identified to a species level could massively enhance the taxonomic resolution and rate of diversity exploration in our changing world.

Chapter 3: Effects of phylogenetic reconstruction method on the robustness of species delimitation using single-locus data

In press:

Tang, C. Q., Humphreys, A. M., Fontaneto, D., & Barraclough, T. G. (2014). Effects of phylogenetic reconstruction method on the robustness of species delimitation using single locus data. Methods in Ecology and Evolution, in press.

Abstract

Coalescent-based species delimitation methods combine population genetic and phylogenetic theory to provide an objective means for delineating evolutionarily significant units of diversity. The Generalized Mixed Yule Coalescent (GMYC) and the Poisson Tree Process (PTP) are methods that use ultrametric (GMYC or PTP) or non-ultrametric (PTP) gene trees as input, intended for use mostly with single-locus data such as DNA barcodes. Here we assess how robust the GMYC and PTP are to different phylogenetic reconstruction and branch smoothing methods. We reconstruct over 400 ultrametric trees using up to 30 different combinations of phylogenetic and smoothing methods and perform over 2,000 separate species delimitation analyses across 16 empirical datasets. We then assess how variable diversity estimates are, in terms of richness and identity, with respect to species delimitation, phylogenetic, and smoothing methods. The PTP method generally generates diversity estimates that are more robust to different phylogenetic methods. The GMYC is more sensitive, but provides consistent estimates for BEAST trees. The lower consistency of GMYC estimates is likely a result of differences among gene trees introduced by the smoothing step. Unresolved nodes (real anomalies or methodological artefacts) affect both GMYC and PTP estimates, but have a greater effect on GMYC estimates. Branch smoothing is a difficult step and perhaps an underappreciated source of bias that may be widespread among studies of diversity and diversification. Nevertheless, careful choice of phylogenetic method does produce equivalent PTP and GMYC diversity estimates. We recommend simultaneous use of the PTP model with any model-based gene tree (e.g. RAxML) and GMYC approaches with BEAST trees for obtaining species hypotheses.

Introduction

Species are a fundamental unit for many fields of biology, yet their identification and delimitation are rarely straightforward (Hebert et al. 2003a). Molecular techniques allow for rapid and broad assessment of diversity of poorly known groups or where traditional techniques are difficult (e.g. Blaxter 2003; Tang et al. 2012; Fontaneto 2014). Well established metrics for species delimitation exist (see Sites and Marshall 2003; e.g. Birky et al. 2005; Flot et al. 2010; Puillandre et al. 2012a) but only a few are grounded in evolutionary theory and do not require *a priori* hypotheses regarding species entities (e.g. O'Meara 2010; Yang and Rannala 2010). Fewer still are designed for large-scale single-locus marker surveys (e.g. Fujisawa and Barraclough 2013; Zhang et al. 2013). With the increased frequency of DNA taxonomy studies and their potential marriage with next generation sequencing technologies (NGS - e.g. Creer et al. 2010), there is a need to determine potential sources of bias on diversity estimates. Here we evaluate robustness of the Generalized Mixed Yule Coalescent model (GMYC) and the Poisson Tree Process (PTP) species delimitation methods to different approaches of phylogenetic reconstruction of the gene trees. Robustness was assessed by how topological and branch length variation introduced by phylogenetic method influences delimitation estimates in terms of species richness and identity.

A special branch of phylogenetic species delimitation (see Sites and Marshall 2003) are coalescent-based species delimitation methods (e.g. Pons et al. 2006; Fontaneto et al. 2007d; Zhang et al. 2013), which combine coalescent theory with diversification models to infer the transition point between population and species-level processes on a gene tree. These approaches provide objective, clade-specific threshold(s) with which to delimit evolutionarily significant units (ESUs) of diversity (akin to species, as defined by the Evolutionary Species Concept - Simpson 1951). These methods provide an alternative to operational taxonomic unit (OTU) picking methods, which rely on arbitrary, clade-specific sequence similarity thresholds (Barraclough et al. 2009).

The GMYC is one of the most popular coalescent-based species delimitation methods and is designed for single-locus data (Fujisawa & Barraclough 2013; although it can be used with concatenated-loci data, e.g. Pons et al. 2006; Fontaneto et al. 2007) and has been used to describe new species (e.g. Birky et al. 2011). The method separately models the fit of Yule (pure birth; Yule 1925) and coalescent processes (Hudson 1990) to an ultrametric tree to define the transition from species-level to population-level processes, used to delimit ESUs. The PTP (Zhang et al. 2013) is a recently developed method that models speciation and coalescent events relative to numbers of substitutions rather than time, and uses heuristic algorithms to identify the most likely classification of branches into population and species-level processes, used to delimit ESUs. This approach assumes either that substitutions are clocklike or, if substitution rates vary across the tree, that coalescent and speciation

events occur at a constant rate per substitution event, rather than per unit of time. The key advantage of the PTP, however, is that it is devised for non-ultrametric trees.

Several studies have evaluated factors that could bias accuracy of the GMYC and PTP. For the GMYC, simulation studies have addressed the effects of various aspects of sampling (Papadopoulou et al. 2008; Bergsten et al. 2012; Reid and Carstens 2012; Talavera et al. 2013), population size, and speciation rates (Esselstyn et al. 2012; Fujisawa and Barraclough 2013). For the PTP, simulations have been used to evaluate the effect of birth rates (i.e. evolutionary distances between species) and sampling unevenness (Zhang et al. 2013). Less attention has been paid to the influence of different phylogenetic methods for reconstructing the underlying gene tree. For coalescent-based species delimitation, phylogenetic and branch smoothing (defined as methods that correct rate heterogeneity to make ultrametric, clocklike trees) methodology are potentially large sources of bias if branch length and topological variation is introduced by different phylogenetic methods, for example by different treatment of unresolved nodes and rate heterogeneity. Zero-length branches introduce infinite (logarithmic) branching rate artefacts that might bias species delimitation and underestimate (early placement of the threshold) or overestimate (recent placement) species diversity (GMYC), and heterogeneity in the rate of molecular evolution among lineages would violate the assumption that branching events can be modelled against substitutions directly (PTP). It is well known that different methods of rate smoothing introduce variability in branch lengths (Drummond and Suchard 2010) that can ultimately affect inferences made from the tree (Rutschmann 2006); artificially variable branch lengths might therefore result in variable diversity estimates with the GMYC. A previous assessment of the effect of phylogenetic method on GMYC ESU estimates showed that certain method combinations perform poorly (Talavera et al. 2013), but is not clear whether this is generally true.

The GMYC, in combination with at least 11 different phylogenetic and 9 smoothing methods (Table S1), has been used in over 150 studies. BEAST (Drummond and Rambaut 2007) is the most popular software for obtaining gene trees (48.9%), followed by MrBayes (25% - Ronquist et al. 2012) and RAxML (8.3% - Stamatakis 2006). BEAST is also the most popular software for rate-smoothing (53.3%), followed by r8s (28.5% - Sanderson 2003), PATHd8 (6.7% - Britton et al. 2007), and *chronopl* (5.5% - Paradis et al. 2004). It is not clear from the literature why one particular phylogenetic method is favoured. Is BEAST chosen (1) due to historical preference, (2) because a posterior sample of trees is desired, (3) because it does not require a *post hoc* rate-smoothing step, or (4) because it provides more accurate species hypotheses than other methods? We address the latter issue for both the GMYC and PTP by systematically evaluating their performance given different phylogenetic methods across several datasets.

We evaluate the GMYC and PTP methods using cytochrome *c* oxidase subunit 1 (COI) datasets, firstly, where the species boundaries and diversity are relatively well known: cowries (Meyer and

Paulay 2005), *Drosophila* spp., and Romanian butterflies (Dinca et al. 2011). Secondly, we compare the methods using 13 COI datasets of Rotifera, a phylum where the taxonomy is much less resolved, the sampling not as comprehensive, and where the benefit of DNA taxonomy is expected to be the greatest. We provide guidelines for maximising the robustness of species hypotheses based on single-locus data with respect to phylogenetic method.

Materials and Methods

Datasets and gene trees

We compiled over 12,000 COI sequences forming 16 datasets (Table S3.2), corresponding mostly to genera (Rotifera + *Drosophila*) but also a family (Cypraeidae [cowries]; Meyer and Paulay 2005) and a comprehensive geographical sample comprising several families (99% of Romanian butterfly species; Dinca et al. 2011). Tree reconstruction followed standard protocols (Supplementary Materials and Methods; Fig. S3.1): (1) align sequences with outgroups (Table S3.3) using MAFFT v6.814b (Katoh et al. 2009), (2) remove non-unique haplotypes (for comparability the same matrix was used for all analyses, although this step is not necessary prior to generation of BEAST trees, see Talavera et al. 2013), (3) reconstruct gene trees, and (4) make gene trees ultrametric. Gene trees were generated using distance (UPGMA - Sokal and Michener 1958; neighbour joining - Saitou and Nei 1987), maximum likelihood (RAxML - Stamatakis 2006; GARLI - Zwickl 2006; PhyML - Guindon et al. 2010), and Bayesian inference (MrBayes - Huelsenbeck and Ronquist 2001; BEAST - Drummond and Rambaut 2007). *Post hoc* branch smoothing (not necessary for BEAST and UPGMA trees) was performed using the R 2.15.2 (R Core Team 2014) package *ape* 3.0.7 functions (*chronopl* and *chronos* - Paradis et al. 2004), PATHd8 (Britton et al. 2007), and r8s (Sanderson 2003). More specific details can be found in the Supplementary Materials and Methods.

Unresolved nodes and rate heterogeneity

The presence of unresolved nodes and rate heterogeneity was measured directly from the trees. For each non-ultrametric gene tree, rate heterogeneity was measured as the standard deviation of the root to tip distances, where a greater standard deviation signifies greater rate heterogeneity. Analysis of BEAST trees was used to quantify whether the different species delimitation methods lead to different diversity estimates also where there are no unresolved nodes.

Species delimitation

The GMYC method with a single threshold (ST-GMYC), multiple thresholds (MT-GMYC; Monaghan et al. 2009; Fujisawa and Barraclough 2013), and a multimodel approach (MM-GMYC; Powell 2012; Fujisawa and Barraclough 2013), was applied to each ultrametric gene tree using the *splits* 1.0–11 (Ezard et al. 2009) R package. Reid and Carstens (2012) described a Bayesian implementation of the GMYC with flexible prior distribution, which samples the parameter space via Markov Chain Monte Carlo (MCMC) to account for phylogenetic model and parameter uncertainty. This method however was not used here because it was unfeasibly slow for the number of assessed here, but would make for an interesting extension. PTP analyses were performed using its webserver (http://species.h-its.org/). For each clade, up to 25 different GMYC and 30 PTP estimates were made. Primarily, the PTP analysis was used with non-ultrametric gene trees (PTP-raw: trees without *post*

hoc smoothing, as intended by Zhang et al. 2013), but smoothed trees were also used (PTP-all: all trees) for a direct comparison with the GMYC input trees.

Performance variation among methods – Species richness

The deviance of each ESU estimate from the expected diversity was gauged using the absolute difference between observed (ESU_X) and expected ($ESU_{expected}$) diversity, standardised among datasets by dividing by the average diversity of the focal dataset (ESU_{meanA}: including the focal ESU estimate). $ESU_{expected}$ was either obtained from the morphological species count (ESU_{morph}) or the average of the species counts from across all trees (ESU_{meanB}: excluding the focal ESU estimate). For the three datasets where the species boundaries have been better evaluated, the morphological species count was determined using either the GenBank species name (*Drosophila* and Romanian butterflies) or expert advice (cowries; C. Meyer pers. comm.). In the absence of a reliable taxonomic species count for the 13 Rotifera clades, ESU_{meanB} was used as a conservative estimate of species richness. The use of ESU_{meanB} as a proxy for $ESU_{expected}$ was validated by the relationship between the residual variation derived from ESU_{morph} and from ESU_{mean} for the non-Rotifera datasets (Supplementary File S3.1).

The performance measure, defined as residual variation, is therefore

$$|ESU_X - ESU_{expected}| \div ESU_{meanA}$$

and takes into account the overall variation in diversity estimate while remaining comparable among datasets with different diversity levels. Residual variation was determined for each gene tree and species delimitation method (see Supplementary File S3.2 for examples of the calculations).

Performance variation among methods – Species identity

Correspondence between ESUs and ESU_{morph}, in terms of species identity, was evaluated for the three non-Rotifera datasets. For each species delimitation estimate, the number of morphospecies that were split, lumped, or an exact match to an ESU_{morph} were counted. Exact matches are where an ESU contains all species from a single morphospecies and no other. Morphospecies are split if they are found in more than one ESU and lumped if multiple morphospecies are present within a single ESU. These counts were performed for ST-GMYC, MT-GMYC, PTP-all, and PTP-raw but not for MM-GMYC because the method returns non-integers.

Factors influencing residual variation of species richness and lumping and splitting of morphospecies

Generalised Linear Mixed Models (GLMM; Bates et al. 2014) with a Poisson error structure were used to ascertain how residual variation varies with species delimitation method, combination of phylogenetic and smoothing method, rate heterogeneity, and presence of unresolved nodes. Three GLMMs were used to ask: For (1) all trees and (2) BEAST trees, how does residual variation vary

with species delimitation and phylogenetic method? (3) For trees with *post hoc* smoothing, how does residual variation vary with species delimitation and phylogenetic method, presence of unresolved nodes and rate heterogeneity? For each of the models, residual variation was used as the response variable and clade was blocked out as a random effect.

A Generalised Linear Model (GLM) with a quasibinomial error structure was used to assess if the proportion of morphospecies that are an exact match to an ESU (response variable) differed among species delimitation method, clade, and combination of phylogenetic and smoothing method (explanatory variables).

For each of the models, significant differences among the levels were identified using *post hoc* Tukey HSD tests (*multcomp* 1.3-1 R package - Hothorn et al. 2008). All analyses were performed in R.

Results

For each of the 16 clades, ten gene trees (4x BEAST, MrBayes, GARLI, PhyML, RAxML, NJ, and UPGMA) and 25 ultrametric trees were generated. MrBayes analysis of the cowrie dataset (1,459 tips) failed to converge, leading to a total of 159 gene trees and 396 ultrametric trees. These were analysed using the ST-GMYC (396 analyses), MT-GMYC (374 analyses), and MM-GMYC (286 analyses). For the cowries, only the ST-GMYC was performed owing to computational demands; MT-GMYC ran for over a week on a 3GHz processor with 8GB RAM without reaching a local likelihood optimum. The reduced number of analyses for the MM-GMYC is due to the method not accommodating trees with unresolved nodes without manual input (the logarithm of zero length branches produces an infinite branching rate), which would not have been achievable within the realm of the present study. In total, 475 PTP and 1,056 GMYC analyses were performed (Table S3.3).

Species richness

For each dataset, the number of ESUs estimated (non-Rotifera, Fig. 1a-c; Rotifera, Fig. S2) and their residual variation (Table 3.1; Fig. 3.1d-g) varied among species delimitation methods. For all datasets, the PTP estimates, especially PTP-raw, best matched the expected diversity (Table 3.1; Fig. 3.1d-g). GMYC estimates varied depending on whether one or multiple thresholds or a multimodel approach was used (non-Rotifera, Fig. 3.1a-c; Rotifera, Fig. S3.2); the MM-GMYC and MT-GMYC inferences were the most consistent (Fig. 3.1d-g; Table 3.1). The ST-GMYC estimates were more variable (non-Rotifera, Fig. 3.1a-c; Rotifera, Fig. S3.2) and differed more from the expected diversity (Fig. 3.1d-g; Table 3.1). Reanalysis of these data without BEAST and UPGMA trees removes some of the significant differences associated with delimitation method (Table 3.1). For the non-Rotifera dataset, there are no differences among the species delimitation methods. For the Rotifera dataset, ST-GMYC is the only significantly different method (Table 3.1). When only BEAST trees were analysed, there were no significant differences in residual variation among delimitation methods (Fig. 3.2d-e; Table S3.4).

Different combinations of phylogenetic and smoothing method resulted in varied ESU estimates (non-Rotifera, Fig. S3.3; Rotifera, Fig. S3.2) and residual variation (Fig. 3.3; Fig. S3.4; Table S3.5). The tendency to under- or overestimate diversity relative to the mean varied randomly among trees smoothed with different methods (Table S3.6). Gene trees smoothed with the *chronopl* and *chronos* functions typically led to highly variable ESU estimates (non-Rotifera, Fig. S3.3; Rotifera, Fig. S3.2) that differed from the expected diversity (Fig. 3.3; Fig. S3.4; Table S3.6).

Table 3.1 Simultaneous pairwise Tukey HSD tests for General Linear Hypotheses. Differences in residual variation of ESU estimates between each delimitation method (Species richness) analysed separately for the non-Rotifera and Rotifera datasets and the proportion of exact matches to the traditional species (Species identity) analysed for non-Rotifera datasets.
ST-GMYC, MT-GMYC, and MM-GMYC refer to GMYC using a single-, multiple-threshold, and multimodel approach. PTP-all and PTP-raw refer to species delimitation analyses where either all of the trees were used, or only the trees that were not rate smoothed *post hoc*. Analyses were for (1) all of the trees and (2) the reduced dataset without BEAST or UPGMA trees (for which unresolved nodes were absent).

		Species richness non-Rotifera				**Rotifera**				**Species identity non-Rotifera**			
Comparison		**Estimate**	**Std. Error**	***Z***	***P***	**Estimate**	**Std. Error**	***Z***	***P***	**Estimate**	**Std. Error**	***Z***	***P***
All trees													
ST-GMYC	MT-GMYC	-0.023	0.07	-0.33	1	0.10	0.017	5.92	< 0.001	0.084	0.1	0.8	0.85
ST-GMYC	MM-GMYC	0.16	0.08	2.07	0.22	0.13	0.019	6.8	< 0.001	-	-	-	-
ST-GMYC	PTP	0.28	0.1	-4.80	<0.001	0.18	0.017	-10.4	< 0.001	-0.18	0.081	-2.16	0.13
ST-GMYC	PTP-raw	0.25	0.09	-2.71	0.05	0.19	0.03	-7.10	< 0.001	-0.12	0.12	-1.03	0.72
MT-GMYC	MM-GMYC	0.18	0.08	-2.26	0.15	0.024	0.019	-1.30	0.69	-	-	-	-
MT-GMYC	PTP	0.31	0.07	-4.54	<0.001	0.075	0.017	-4.41	< 0.001	-0.26	0.1	2.55	0.05
MT-GMYC	PTP-raw	0.28	0.10	-2.77	0.042	0.09	0.03	-3.31	0.0078	-0.21	0.14	1.52	0.41
MM-GMYC	PTP	0.13	0.07	-1.70	0.42	0.051	0.018	-2.77	0.042	-	-	-	-
MM-GMYC	PTP-raw	0.097	0.10	-0.93	0.88	0.066	0.03	-2.4	0.12	-	-	-	-
PTP	PTP-raw	-0.03	0.09	0.35	1	0.014	0.02	-0.58	0.98	0.051	0.11	-0.46	0.97
Reduced dataset with no BEAST or UPGMA trees													
ST-GMYC	MT-GMYC	0.16	0.25	0.63	0.97	0.18	0.038	4.74	< 0.001				
ST-GMYC	MM-GMYC	-0.15	0.3	-0.43	0.99	0.17	0.04	4.22	< 0.001				
ST-GMYC	PTP	0.045	0.18	-0.25	0.99	0.26	0.036	-7.162	< 0.001				
ST-GMYC	PTP-raw	0.11	0.40	-0.27	0.99	0.25	0.07	-3.52	0.0034				
MT-GMYC	MM-GMYC	-0.31	0.38	0.81	0.92	-0.0033	0.041	0.08	0.99				
MT-GMYC	PTP	-0.11	0.26	0.45	0.99	0.083	0.036	-2.28	0.14				
MT-GMYC	PTP-raw	-0.052	0	0.1	1	0.07	0.07	-1.00	0.85				
MM-GMYC	PTP	0.19	0.35	-0.56	0.98	0.086	0.040	-2.14	0.19				
MM-GMYC	PTP-raw	0.26	0.50	-0.52	0.98	0.074	0.07	-1.02	0.84				
PTP-raw	PTP	0.062	0.36	-0.18	1	-0.013	0.07	0.20	0.99				
Unresolved nodes absent	Unresolved nodes present	$2.95e^{-5}$	0.36	0	1	0.23	0.039	5.92	<0.001				

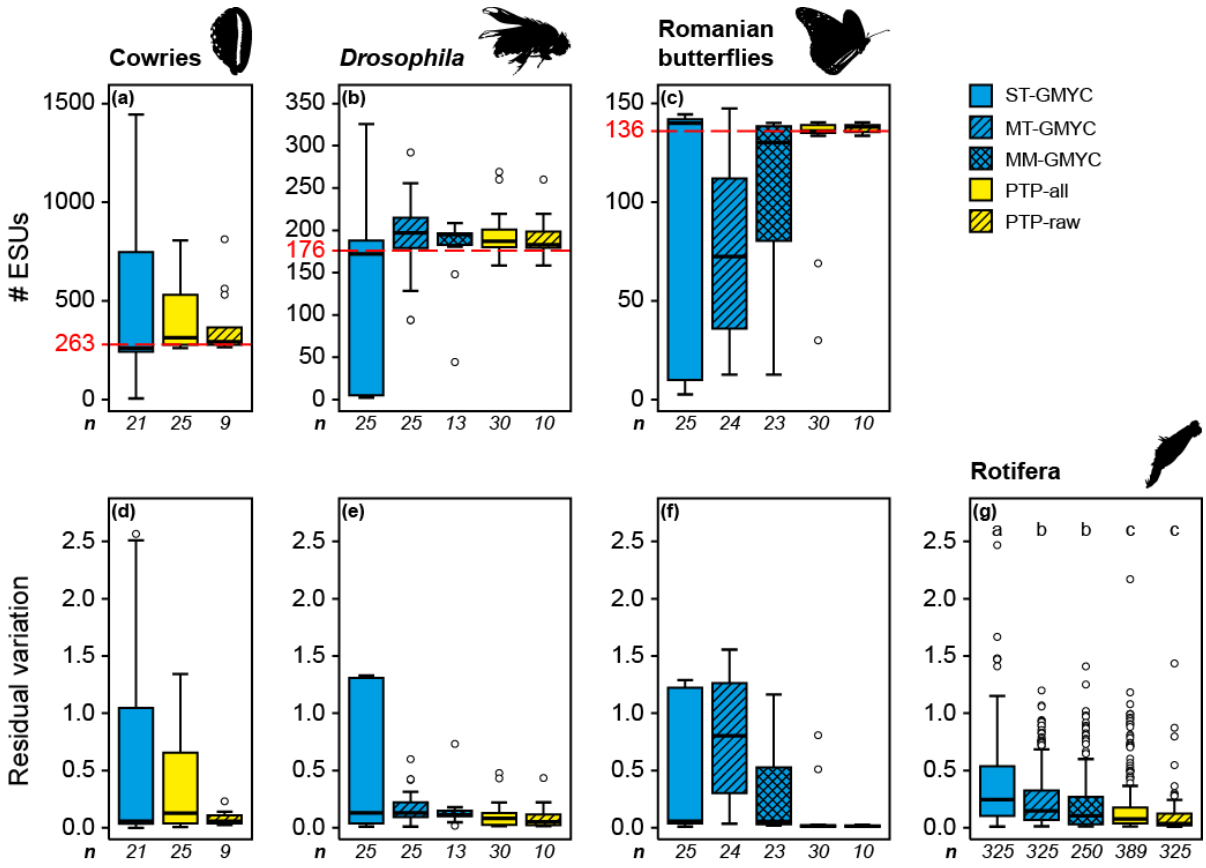

Figure 3.1 Distribution of ESU estimates (**a**-**c**) and residual variation around the expected diversity (either the traditional species count [ESU_{morph}; **d**-**f**] or the average ESU estimate for that clade [ESU_{meanB}; **g**]) per species delimitation method.
Cowries (**a**, **d**), *Drosophila* (**b**, **e**), Romanian butterflies (**c**, **f**), and Rotifera (**g**), and the five species delimitation methods for each clade (ST-GMYC = single threshold, MT-GMYC = multiple thresholds, MM-GMYC = multimodel, PTP-all = all trees, and PTP-raw = trees without post hoc smoothing) are shown separately. The traditional species count (red, dashed line), median (thick, black lines), first and third quartiles (box), 1.5 times the interquartile range (whiskers), and outliers (circles) are shown. Letters above the boxes represent significantly different comparisons.

Unresolved nodes and rate heterogeneity

The proportion of unresolved nodes differed among gene trees (Fig. 3.2c), from none for BEAST trees to 24% for NJ and 43.8% for MrBayes trees. Increased residual variation is related to the presence of unresolved nodes for Rotifera (GLMM: t=5.92, d.f.=1,046, P<0.0001; Fig. 3.2b) but not non-Rotifera (GLMM: t=0, d.f.=81, P=0.16; Fig. 3.2a) clades, and interacts with rate heterogeneity for both Rotifera (GLMM: t=-3.27, d.f.=1,046, P=0.0011) and non-Rotifera (GLMM: t=-3.28, d.f.=81, P=0.0015) datasets.

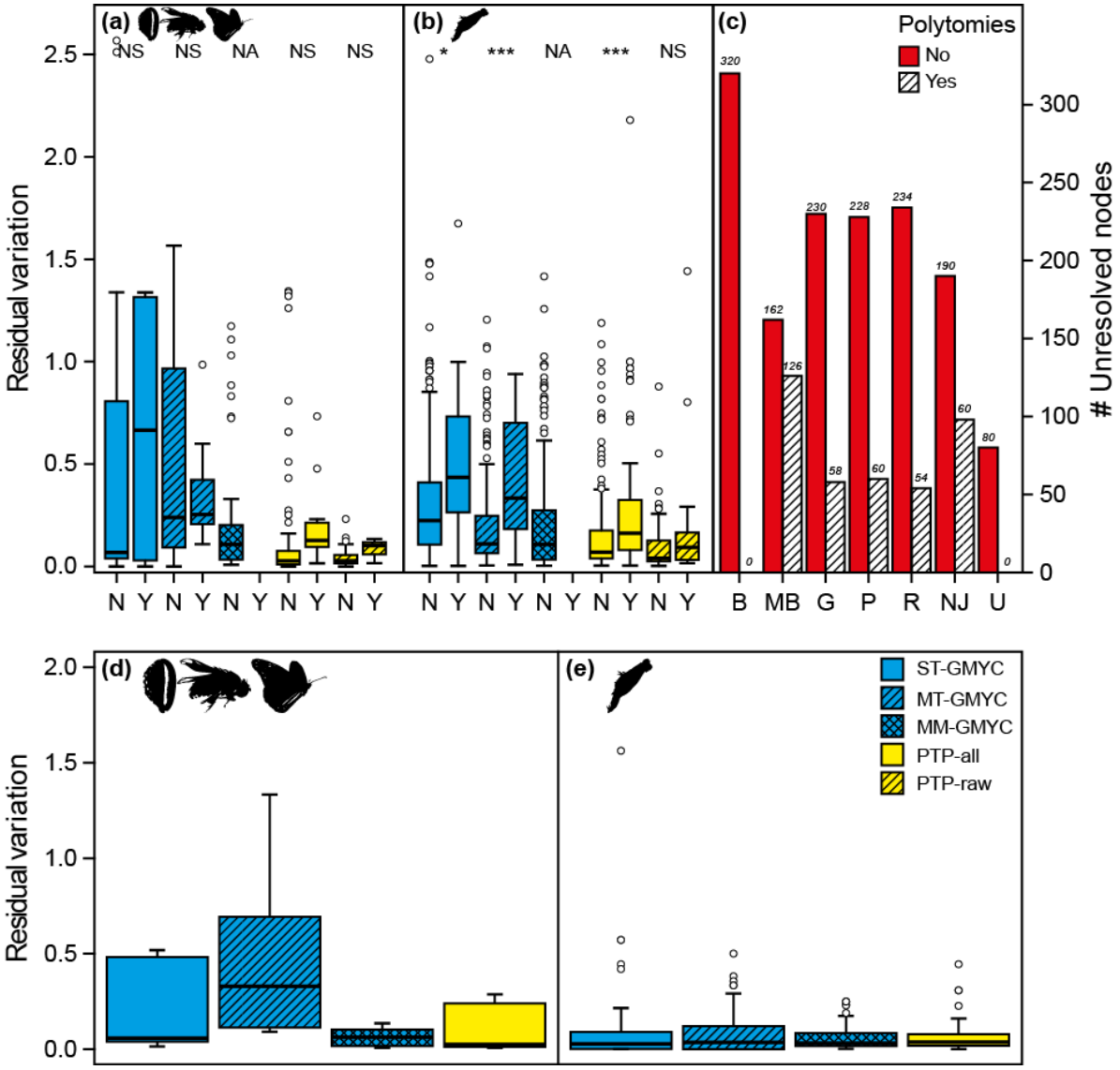

Figure 3.2 The relationship between residual variation of ESU estimates and species delimitation method when unresolved nodes are absent or present (non-Rotifera [**a**] and Rotifera [**b**]), and the number of unresolved nodes for each of the phylogenetic methods (**c**).
Analysis of BEAST trees on their own, where nodes are completely resolved, results in lower residual variation in both non-Rotifera (**d**) and Rotifera (**e**) datasets, compared to Fig. 3.1**d-f** and Fig. 3.1**g**, respectively. The five species delimitation methods are analysed separately. Signs above the boxes denote significant differences at $P < 0.05$ (*) and $P < 0.001$ (***). NA = not applicable, NS = not significant, N = unresolved nodes are absent, Y = unresolved nodes are present, B = BEAST, MB = MrBayes, G = GARLI, P = PhyML, R = RAxML, NJ = neighbour joining, and U = UPGMA.

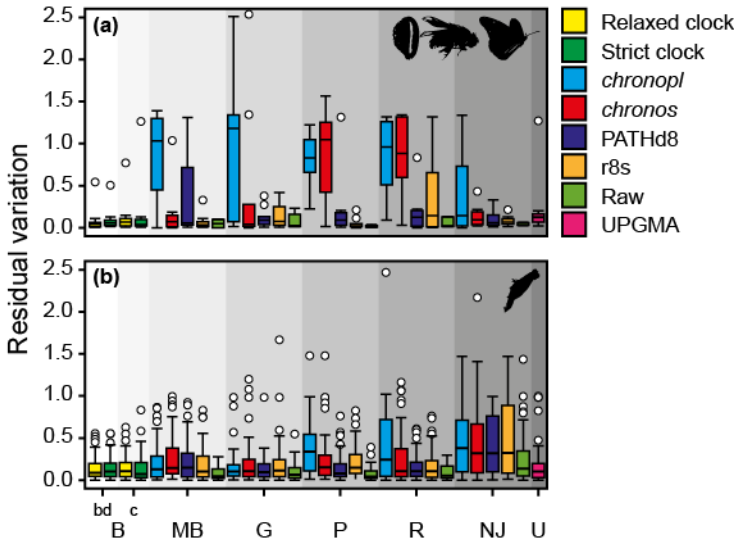

Figure 3.3 The relationship between residual variation of non-Rotifera (**a**) and Rotifera (**b**) ESU estimations pooled for all the delimitation methods with respect to the different combinations of phylogenetic and smoothing methods.
Each dataset was analysed using eight different phylogenetic methods (grey shaded areas). Median (thick black lines), first and third quartiles (box), 1.5 times the interquartile range (whiskers), and outliers (circles) are shown. bd = birthdeath, c = coalescent.

Species identity

The proportion of morphospecies that were inferred as an ESU did not differ significantly among the different species delimitation methods (Fig. 3.4; Table 3.1). Most of the combinations of phylogenetic and smoothing methods produced similar proportions of exact matches (Table S3.6; Fig. 3.4), but those smoothed with *chronopl* or *chronos* produced significantly lower proportions of exact matches, resulting from either higher levels of lumping or splitting. Differences were the largest among the datasets, with a significantly higher proportion of exact matches for the Romanian butterflies than for the cowries ($GLM_{binomial}$: $Z = 3.39$, $P < 0.001$; Fig. 3.4), but no differences when compared to the *Drosophila*. The proportion of exact matches was on average 63±2% and was highest for the Romanian butterflies (70.4±3.5%), followed by *Drosophila* (59.1±2.6), and cowries (58±4.4%; Fig. 3.4; Fig. S3.5). The type of mismatches differed in proportion between the three datasets (Fig. S3.5): cowries were typically split, *Drosophila* were lumped (ST-GMYC, PTP) and split (MT-GMYC), and the Romanian butterflies were lumped.

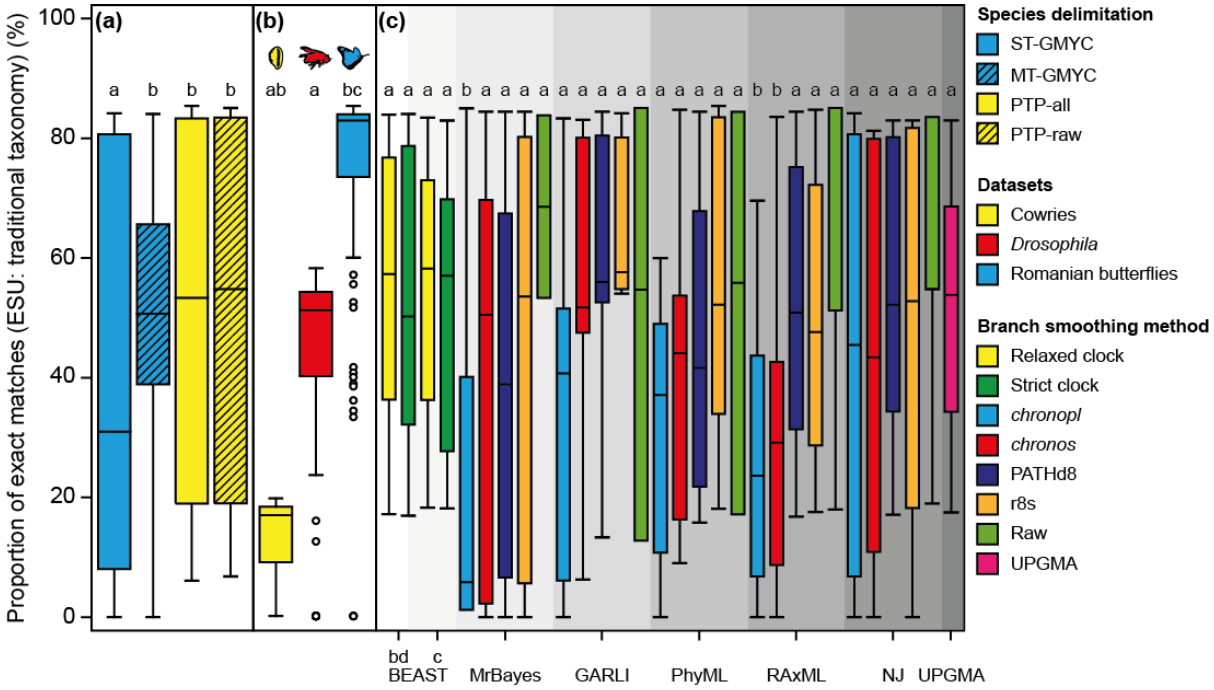

Figure 3.4 The relationship between the proportion of exact matches (morphospecies = ESU) and (**a**) species delimitation metric, (**b**) dataset, and (**c**) combination of phylogenetic and smoothing method.
Each dataset was analysed using eight different phylogenetic methods (grey shaded areas). Median (thick black lines), first and third quartiles (box), 1.5 times the interquartile range (whiskers), and outliers (circles) are shown. Letters above the boxes represent significantly different comparisons.

Discussion

Good taxonomy is central to any discipline using species as a fundamental unit. Coalescent-based, phylogenetic species delimitation clusters sequences into evolutionarily significant units. This approach relies heavily on the underlying tree and is affected by the choice of phylogenetic method (Talavera et al. 2013). Our results indicate that the PTP method produces ESU estimates that are more robust to phylogenetic reconstruction method than the GMYC method, except when BEAST trees are used.

Specifically, residual variation in ESU estimates was lowest for PTP-raw. The three implementations of the GMYC method differed in how robust they were to phylogenetic method (MM-GMYC > MT-GMYC > ST-GMYC). As expected, the MM-GMYC produced ESU estimates that were more robust to different phylogenetic methods, although the MM-GMYC estimate is typically an average. Species delimitation using both the PTP and GMYC methods was consistent (lower residual variation) for BEAST trees, possibly because they require no *post hoc* smoothing step and contain no unresolved nodes. In contrast, analysis of NJ trees resulted in particularly large deviations in ESU estimates, irrespective of smoothing method. This is not surprising given that NJ is a clustering method that does not rely on an evolutionary model (Saitou and Nei 1987), known to underperform if the distance measure is not a correct estimate of nucleotide substitutions (Tateno et al. 1994; although more recent simulations have shown that NJ is a good approximation for minimum evolution - Gascuel and Steel 2006). There is also a large increase in residual variation associated with *chronopl* and *chronos* branch smoothing, which are particularly prone to haphazard lumping and splitting ESUs irrespective of the degree of between-branch smoothing (λ) chosen (Supplementary File S3.3). This finding concurs with that of Talavera et al. (2013) who found that GMYC analyses of NJ trees smoothed with PATHd8, *chronopl*, or *chronos* produced aberrant ESU counts.

To quantify parameters that differ among trees and may affect ESU estimates, we analysed the effect of rate heterogeneity and unresolved nodes, which are either characteristics of poor tree reconstruction (methodological or sample issues) or real features of the data. We found a significant effect of both these parameters on the GMYC and PTP output: diversity estimates for trees with highly variable rates and/or unresolved nodes deviated more widely from the expected diversity than clocklike, resolved trees (e.g. BEAST trees). Branch smoothing of trees with highly variable substitution rates can lead to exaggerated stretching of branches (Drummond and Suchard 2010), which will detriment all coalescent-based species delimitation methods that use branch lengths as an input. Unresolved nodes in the tree impinge on correct diversity estimates because their resolution can lead to artefacts in the branch length data (e.g. infinite branching rates) that could result in misplaced coalescent thresholds used for delimitation. For the GMYC, splitting might occur if infinite branching rates are found closer to the tips, while for the PTP, it might result from increased average, observed

intraspecific cohesiveness resulting from no increase in branch lengths with more tips. Contrarily, the diversity could be underestimated if the unresolved nodes are closer to the root for the reciprocal reasons. Whether unresolved nodes and rate heterogeneity in the data are correlates or causes of incorrect diversity estimates remains to be tested. Encouragingly, their effect is alleviated when BEAST trees are used as input.

As a measure of how species identity differed among the methods, we assessed the proportion of ESUs that were exact matches to traditional species (morphospecies). We found similar levels of species richness to the traditional taxonomy but varying levels of discordance in identity between the traditional and DNA taxonomy. The proportion of exact matches was on average 63%, and variation in this was associated primarily with combination of phylogenetic and smoothing method and taxonomic group but less with species delimitation method. We found no significant differences in the proportion of exact matches between the species delimitation methods, although the PTP method was qualitatively higher. The largest differences were between the three clades, and potentially points to the varying levels of taxonomic work in these groups. These differences seem to be driven by aberrantly deviant ESU estimates (in terms of richness and identity) associated with the use of *chronopl* and *chronos* smoothing methods, which typically split the cowrie morphospecies and lumped the *Drosophila* and Romanian butterfly species.

Traditional species of the Romanian butterflies appear to be supported by DNA taxonomy perhaps because the dataset represents a geographical (rather than taxonomic) sample. Species are expected to appear more distinct in such a sample because the closest relatives of most sampled species will not be sampled (Bergsten et al. 2012). Although, the proportion of morphospecies that were lumped, relative to split, indicates that lower intraspecific sampling in this clade is overrepresenting the Yule process in the tree and thus missing some of the ESUs. The higher intraspecific sampling for the cowries and *Drosophila*, indicates that the splitting of these species could be associated with unresolved taxonomy (Packer et al. 2009) or overlapping intra- and interspecific variation (Meyer and Paulay 2005; Wiemers and Fiedler 2007). While efforts have been made to resolve the taxonomy of these groups (e.g. Meyer and Paulay 2005; O'Grady and Markow 2009), a more concerted effort is required to address the gap between DNA and traditional taxonomy across the entirety of these clades (C. Meyer pers. comm).

By assessing ESU counts across 16 datasets with over 1,500 separate species delimitation analyses, we have shown that the PTP-raw model with any robust gene tree and the GMYC used on BEAST trees produce consistently robust and, on average, accurate species estimates. These findings can probably be extrapolated to other genetic markers: COI and 18S are typically used for animals (e.g. Tang et al. 2012, 2014b), multiple markers (e.g. 16S) for bacteria (e.g. Barraclough et al. 2009; Morlon et al. 2012), ITS for fungi (Powell et al. 2011) and multiple markers (e.g. matK and rbcL) for

plants (e.g. CBOL Plant Working Group 2009). Although the variability of these markers will likely yield different degrees of coalescent clustering and species separation (e.g. Tang et al. 2012) that warrants a more thorough evaluation.

Coalescent-based species delimitation is likely to gain in popularity: either to facilitate the description of biodiversity in an integrative, iterative way as a tool to tackle the burgeoning taxonomic crisis (Puillandre et al. 2012b), or to cluster sequences from NGS studies (e.g. Creer et al. 2010; Chariton et al. 2014). The latter would benefit from evolutionary approaches that provide a deeper understanding of the nature and extent of diversity (Barraclough et al. 2009). Applying coalescent-based species delimitation to NGS is currently limited by the amount of variability, the short (but ever increasing) read lengths, the amplification success of the markers used, and the computational expense of the coalescent-based metrics. As with all DNA taxonomy studies, primers need to be designed to combat the low amplification success of certain primers (Zhan et al. 2014), robust bioinformatics pipelines need to be developed (S. Creer pers. comm.), and sampling regimes that are representative of intra- and interspecific variability and geographic range should be considered (Papadopoulou et al. 2008; Lohse 2009; Bergsten et al. 2012; Talavera et al. 2013).

The PTP method is appealing when speed is of the essence because ultrametric trees are not required (Zhang et al. 2013), meaning that some of the problems encountered and the additional computation required with branch smoothing may be circumvented. However, the PTP makes the assumption that branching events scale with substitutions rather than time, which might be violated when substitution rates are heterogeneous. The GMYC with a BEAST tree provided equally consistent estimates but obtaining BEAST trees is computationally expensive. However, when rate heterogeneity is high and can be adjusted across the tree estimation using models, perhaps by use of well-informed internal calibration priors, then diversity estimation might benefit from sophisticated dating and diversity estimation procedures. We feel that the GMYC is more true to the speciation process, in that speciation and coalescence happen over time and not necessarily in relation to how many substitutions occur in marker genes. While the transition between speciation- and coalescent-processes, used to delimit species, might be mirrored by differences in the number of species- and population-level substitutions (PTP), time is a more direct expression of the process, therefore methods that separately model this transition (time; GMYC) and phylogenetic methods that formally correct for substitution rate variation among species (e.g. BEAST) are conceptually more appropriate. We recommend use of both PTP and GMYC methods with the appropriate phylogenetic tree or choosing between them on a case-by-case basis, bearing in mind the differences in speed and underlying theory inherent in the two methods. The PTP method with non-ultrametric trees is currently quicker to implement than the GMYC, especially the MM-GMYC, although the speed of the GMYC could be increased with parallelisation. Both the phylogenetic and species delimitation steps become computationally demanding for larger datasets (e.g. NGS studies). Such datasets, which are often taxonomically broad,

are likely to violate use of a single substitution rate and so increased parameterisation and prior information is more likely to yield trees that better reflect the data and thus provide more realistic diversity estimates. We envisage that better phylogenetic handling of substitution rate heterogeneity within the samples, irrespective of delimitation method, and the use of ESU nodal support as a proxy for species identity confidence, would further improve the delimitation of primary species hypotheses from single-locus marker surveys.

Chapter 4: Factors affecting the successful DNA barcoding of neglected biodiversity: insights from the taxonomically unresolved Rotifera

Abstract

DNA barcoding is a technique proposed for the accelerated identification of biodiversity, but it is unreliable if the base taxonomic unit used is unresolved. Criticisms of DNA barcoding rely on the assumption that diversity is split into discrete groups separated by a distinct "barcode gap". Here we assess whether this barcode gap exists in the taxonomically neglected group of Rotifera using DNA taxonomy as a tool to circumvent their unresolved taxonomy. We assess the success of identification through DNA barcoding and highlight factors that correlate with this success and the ability to find a barcode gap. DNA barcode identification success is based on whether taxa can be re-identified based on three criteria (nearest neighbour, thresholds, and best close match). We show that taxa can be identified with high success rates but that flawless results are unlikely given the lack of an unequivocal barcode gap. Our results benefit from the simultaneous analysis of 12 different Rotifera datasets (>4,000 sequences) that differ in their sampling regimes and diversity, allowing us to show that finding a barcode gap is correlated with incomplete sampling and the prevalence of singletons. DNA barcode identification success is positively correlated with high numbers of sequences and greater sampling of expected diversity, contrastingly, the prevalence of singletons is a limiting factor. Interestingly we find that sexual monogonont rotifer species are identified with typically higher success than bdelloid rotifer species, indicating that perhaps discreteness of species might be related to reproductive mode, although more investigation is required. We anticipate that these results will be used to justify intensive breadth and depth of taxonomic sampling for DNA barcode identification success, but also that additional sources of evidence will be necessary to identify taxa without error.

Introduction

There is an overwhelming taxonomic crisis; the expected global biodiversity cannot feasibly be described by traditional means (Blaxter 2003; Carbayo and Marques 2011), especially with a paucity of specialised taxonomists (Meier et al. 2006). Consistent identification of species, a fundamental unit for most biodiversity studies, is quintessential for the understanding of their ecology and evolution (Creer et al. 2010). Meiofaunal groups (i.e. animals that can pass unharmed through a 500µm mesh), despite being abundant, diverse, and ecologically important (Giere 2009), are particularly unpopular among taxonomists (Kennedy and Jacoby 1999; Blaxter et al. 2004; Fontaneto et al. 2009), and thus relatively little is known about their true diversity and functioning (Blaxter 2003; Tautz et al. 2003; Blaxter et al. 2005; Curini-Galletti et al. 2012). Identification of meiofauna is difficult due to their small size, the reliance on live specimens, variable spatial and temporal distribution, cost in terms of both time and effort, limited taxonomic literature that is accessible to non-specialist workers, abundance of cryptic taxa, and limited curation of type specimens (Fontaneto et al. 2009; Curini-Galletti et al. 2012). The ubiquity of meiofauna and the difficulty with which they are traditionally identified combine to highlight an important yet neglected component of biodiversity.

DNA barcoding is the standardised use of a genetic loci (typically cytochrome oxidase *c* subunit I [COI] in animals – Hebert et al. 2003b, but also 18S – Floyd et al. 2002) as an effective and efficient means of rapidly identifying species (Hebert et al. 2003a; Vogler and Monaghan 2007). Variation in COI is used as a diagnostic measure to distinguish between species where perhaps traditional characteristics are unreliable or more difficult to measure (Zhang et al. 2010; Leasi et al. 2013; Fontaneto 2014). This approach for the identification of biodiversity has gained a lot of support, with the Consortium for the Barcode of Life (CBOL) and data systems (BOLD - Ratnasingham and Hebert 2007) being set up to tag and identify every organism on Earth. This approach is particularly attractive in groups where traditional taxonomy is challenging (Blaxter 2003; Blaxter et al. 2004; Pawlowski et al. 2012; Powell 2012).

DNA barcoding is difficult in taxonomically understudied groups (Meyer and Paulay 2005) as poor taxonomy and incompatible species criteria invalidate one of the key assumptions of DNA barcoding; namely that diversity is split into discrete groups with non-overlapping intra- and interspecific variation (i.e. the 'barcode gap'). Incorrect morphological assignment of species may lead to misinterpretation of results obtained by DNA barcoding. Unresolved taxonomy is common (Funk and Omland 2003), particularly in meiofauna (Tang et al. 2012), and this can artificially inflate the overlap between intra- and interspecific variation, thus shrouding any barcode gap (Astrin et al. 2012).

Rotifera is typical of meiofaunal groups in that it has unresolved taxonomy rife with cryptic taxa (e.g. Suatoni et al. 2006; Fontaneto et al. 2009). The unsettled taxonomy of rotifers is a major limitation to

their DNA barcode-based identification (although see García-Morales and Elías-Gutiérrez 2013), however, the wider adoption of DNA taxonomy (i.e. discovery of species via molecular techniques) has helped to clarify taxonomic issues as well as elucidate evolutionary and ecological patterns (see Fontaneto 2014 and references therein).

In the absence of a fully resolved taxonomy, an issue very apparent for the vast majority of meiofaunal groups (Tang et al. 2012), biologically relevant comparable units of diversity (evolutionarily significant units; ESUs) can be obtained by adopting methods such as the Generalized Mixed Yule Coalescent (GMYC) model for species delimitation (Pons et al. 2006; Fontaneto et al. 2007d; Birky and Barraclough 2009; Fujisawa and Barraclough 2013). Here I assess identification of Rotifera diversity through DNA barcoding of both traditionally defined morphospecies and ESUs. Specifically: (1) I ascertain whether a DNA barcode gap exists in a sample of 12 rotifer genera (>4,000 sequences), (2) whether three typically used DNA barcoding metrics (nearest neighbour, threshold ID, best close match) can consistently identify rotifer taxa, and (3) what factors correlate with its success and failure. By highlighting DNA barcode identification correlates of success, I provide a set of guidelines for DNA barcoding studies.

Materials and Methods

Data collection

Cytochrome oxidase *c* subunit I (COI) sequences were obtained from GenBank. This gene was chosen as it has been championed as the barcoding gene (Hebert et al. 2003a) as it is variable enough to delimit species (Tang et al. 2012) and as such has been the gene of choice for Rotifera. In total 4,250 sequences (of which 1,143 were unique) from a total of 95 morphospecies were analysed. The final dataset consisted of 12 genera, five of which were bdelloid rotifers with the remaining seven being monogonont rotifers.

Generalized Mixed Yule Coalescent model (GMYC)

The morphological assessment of meiofauna and the inferred species boundaries are often blurry and incomparable. The GMYC model (Pons et al. 2006; Fujisawa and Barraclough 2013) was implemented to define comparable units of biodiversity under the Evolutionary Genetic Species Concept (EGSC: Birky et al. 2010). The GMYC model tests for significant shifts in branching rate in an ultrametric tree indicative of a switch from between-species evolutionary processes (Yule) to within-species population level processes (coalescent). This is expected if the dataset comprises of multiple individuals from a set of independently evolving entities (Birky and Barraclough 2009; Fujisawa and Barraclough 2013). It then fits a model encompassing two different branching rates and calculates the fit of that model to the data, a X^2 test is performed to gauge the significance of the application of the GMYC model against the null hypothesis (i.e. a single coalescent with one branching rate). The threshold between population and species-level processes identified by the model is used to delimit taxa grounded in evolutionary theory (i.e. ESUs). This analysis were performed in R v2.15.2 (The R Development Core Team 2014) with the *splits* v1.0–11 package (Ezard et al. 2009 - available from https://r-forge.r-project.org/ projects/splits).

Phylogenetic analyses

The GMYC model requires fully dichotomous ultrametric gene trees as an input. DnaSP v5.10.01 (Librado and Rozas 2009) was used to collapse the sequences into unique haplotypes. These haplotypes were aligned with a suitable outgroup using MAFFT v7.017 (Katoh et al. 2009) with the default settings and were checked and edited in Geneious Pro v5.4.2 (Drummond et al. 2006).

Both maximum likelihood (ML) and Bayesian inferred (BI) trees were obtained for each dataset. Maximum likelihood trees were reconstructed using RAxML (Stamatakis et al. 2008) with a gamma model of rate heterogeneity. Each tree was made ultrametric using penalised likelihood in r8s v1.71 (Sanderson 2003) where cross-validation analyses were performed to determine the best rate of smoothing. In some cases multichotomies were collapsed in R using the *ape* 3.0.7 package (Paradis et al. 2004). Bayesian rooted, time-measured phylogenies were reconstructed using BEAST v1.6.1

(Drummond and Rambaut 2007). Both RAxML (and r8s) and BEAST methods for producing ultrametric trees are recommended for the GMYC method (Talavera et al. 2013; Chapter 3 - Tang et al. 2014a), and both were used to identify whether the results are comparable.

Barcode gap

We define a barcode gap in two ways: (1) using the morphospecies or ESU groupings to identify a lack of an overlap between minimum interspecific variation and maximum intraspecific variation (Meier et al. 2008) or (2) without *a priori* species groupings using the automatic barcode gap discovery method (ABGD; Puillandre et al. 2011).

(1) For each set of ESUs, we calculated intra- and interspecific pairwise distance under the Kimura two parameter (K2P) distance model (Kimura 1980) in R using the *spider* v1.1.3 package (Brown et al. 2012). To justify the use of K2P distances over other evolution models, we generated distance matrices for all of the datasets using the nine evolution models available in the *ape* (F81, F84, GG95, JC69, K80, K81, raw, T92, TN93) and calculated the minimum, mean, and maximum intra- and interspecific distances for each dataset. The effect of model choice was assessed by linear mixed effect models (LMEM; see below). We show that the K2P model is not significantly different to most other models of evolution and so we use the K2P model as is typical of DNA barcoding studies.

(2) Using the ABGD method, a barcode gap can be defined without any *a priori* species groupings. The ABGD uses a range of prior intraspecific divergences to infer from the data (sequence alignment) a model-based one-sided confidence limit for interspecific divergence (Puillandre et al. 2012a). The barcode gap is identified as the first significant increase in ranked distances beyond this limit; this ABGD barcode gap allows some overlap between intra- and interspecific distance. The presence of a barcode gap was determined using the ABGD online tool with a K2P model of evolution but otherwise default settings (available at http://wwwabi.snv.jussieu.fr/public/abgd/abgdweb.html). The correct species estimate (i.e. barcode gap threshold) was selected, as suggested by Puillandre et al. (2012a), using gene specific priors for maximum divergence of intraspecific diversity (0.01 for COI).

DNA barcoding summary statistics

Sequences in the haplotype alignments used to generate the GMYC entities were tagged according to either their morphospecies name or their GMYC entity number. Non-unique haplotypes removed in the previous step were replaced and given the same tag as the other sequences within the same haplotype. These sequences were analysed using the *spider* v1.1.3 package (Brown et al. 2012) in R, which was designed specifically for DNA barcoding analyses and provides summary statistics for a host of DNA barcoding statistics including: nearest neighbour (Hebert et al. 2003a), best close match (Meier et al. 2006), and optimized threshold IDs (Meyer and Paulay 2005). Each sequence in the datasets has a name vector (i.e. morphospecies or ESU name), the metrics take each sequence in turn

(with replacement) and assess whether that focal sequence can be identified based on the other sequences within that dataset. Each metric identifies the focal sequences measuring different aspects of the data. Specifically:

Nearest neighbour (NN) – This metric places the focal sequence into a neighbour joining distance tree and finds the closest individual to the target. The method is deemed a success if the nearest neighbour name matches the original focal sequence name.

Optimized threshold ID (TI) – This metric uses a distance matrix and highlights all of the sequences within a user defined threshold of the focal sequence. For the optimized threshold and the best close match metric (see below), this user defined threshold is optimized from the data by choosing the threshold that minimises the cumulative identification error. All of the species names within this distance threshold are returned. The success of this identification is based on the species names of those highlighted sequences. There are four possible outcomes for each identification query: "correct", "incorrect", "ambiguous", and "no ID". If all the sequences within the threshold have the same species name as the query, then it is considered "correct". If all the sequences within the threshold are different to the query, then the query is considered "incorrect". If both incorrect and correct sequences are within the threshold then the query name is considered "ambiguous". If there is no match within the threshold then the query is considered to have "no ID", this is typical of singleton taxa.

Best close match (BCM) – This method is similar to the nearest neighbour metric, but in addition it incorporates a threshold so that a "nearest neighbour" above an untenably large threshold would be considered unidentified (no ID). Similar to the optimized threshold ID, the same four outcomes ("correct", "incorrect", "ambiguous" and "no ID") are given, but differs from the threshold ID method in how it deals with ambiguous queries. As long as the closest match to the sequence within the threshold has the same species name, then it does not matter if other sequences within the threshold are incorrect. Ambiguous identification comes about when there is more than one equally close match of different species including the "correct" one.

To ascertain the effect of rare taxa, we conducted separate analyses on the same datasets but with singletons removed.

Data analysis

The analysis was split up into three parts: (1) Does choice of model of evolution affect the identification of a barcode gap, (2) What parameters correlate with ABGD success, and (3) What parameters correlate with ESU DNA barcoding success?

(1) Srivathsan and Meier (2012) suggested that choice of evolutionary model could affect the magnitude of a barcode gap. We used two different LMEMs in R using the *nlme* 3.1.105 package (Pinheiro et al. 2013) to determine whether choice of evolutionary model affects the magnitude of a barcode gap or an overlap. The response variables for these models were either the ratio of mean interspecific to intraspecific variation (Inter. mean / Intra. mean) or the overlap between the minimum interspecific and maximum intraspecific variation (Inter. min - Intra. max), evolutionary model and phylogenetic reconstruction method (BI or ML) were the explanatory variables, and dataset (12 in total) was blocked out as a random effect. A generalised linear model (GLM) is not used here because the Poisson family of error structure does not accommodate negative values.

(2) A GLM with a quasiPoisson error structure was used to identify which parameters correlated with the number of OTUs identified by the ABGD method. A maximal model was made with the number of ABGD OTUs as a response variable and the number of sequences, haplotypes, GMYC ESUs, group (Bdelloidea vs. Monogononta), and the proportion of expected diversity sampled as explanatory variables. The maximal model included all of the possible explanatory variables and their interactions. A minimum adequate model was produced by sequentially removing non-significant parameters (Crawley 2007) and assessing unacceptable increases in model deviance.

(3) The summary statistics for the DNA barcoding were collated for the different datasets; these included the distribution of NN, TI, and BCM scores. First we used a GLM with a quasibinomial error structure to ascertain whether the metric of identification (explanatory) predicted DNA barcode identification success (response). Secondly, to ascertain which parameters correlate with DNA barcoding success, a GLM with a binomial error structure was used with the DNA barcoding success value as the response variable and number of sequences, haplotypes, ESUs, group, and the proportion of expected diversity sampled as explanatory variables. The minimum adequate model was obtained from the maximal model and repeated for each of the three identification metrics.

Results

Phylogenetic analyses

We obtained 4,250 COI sequences from GenBank, 3,962 of which were identified to species level (95 morphospecies; Table S4.1). Most morphospecies (81 out of 95) were represented by multiple specimens, with an average of 42 sequences per morphospecies. The average sequence length was 624bp. No indels, NUMTs, or stop codons were found in any of the alignments.

Generalized Mixed Yule Coalescent model (GMYC)

GMYC analysis of the gene trees produced using the different phylogenetic methods resulted in little difference in ESU number (GLM: $t = 0.094$, D.F. = 46, $P = 0.93$) and identity. In total, the GMYC identified 509 BEAST and 498 RAxML ESUs. The ratio of ESU: morphospecies (DNA: traditional taxonomy) based on either BEAST or RAxML gene trees ranges from 2:1 (*Synchaeta*) to 11:1 (*Rotaria*). ESU counts were on average five times higher than morphospecies counts (Table S4.1). On average, each ESU has 2.26 (±0.21) unique haplotypes with a minority being singleton taxa (24.62%).

Finding the barcode gap

When generating distance matrices among the GMYC ESUs, all models of evolution (except the GG95 model) were not significantly different to K2P distances (Table 4.1). Based on K2P distances, none of the morphospecies groupings had a barcode gap. In all but three of these datasets (*Keratella*, *Lecane* and *Synchaeta*) the mean interspecific variation was actually less than the mean intraspecific variation (Table S4.1; Fig. 4.1). When groupings were based on ESUs instead of morphospecies, five (out of 12) of the ESU datasets had a barcode gap (Table S4.1) whereby the minimum interspecific distances were larger than the maximum intraspecific distances (Meier et al. 2008). When all sequences are pooled together, no distinct barcode gap exists (Fig. 4.1). The number of OTUs defined by the ABGD method is negatively correlated with the proportion of expected diversity sampled, and positively with the prevalence of singletons and the number of ESUs delimited using the GMYC method (Table 4.2; Fig. 4.2). The ABGD method was able to discover a barcode gap for eight datasets (Table S4.1). Of these eight datasets, four were found to have a barcode gap as defined by Meier, with only *Lecane* having a Meier barcode gap but not an ABGD barcode gap (Table S4.1). The ABGD method was able to find a barcode gap in *Ascomorpha*, *Brachionus*, *Philodina*, and *Rotaria* where no Meier barcode gap could be found.

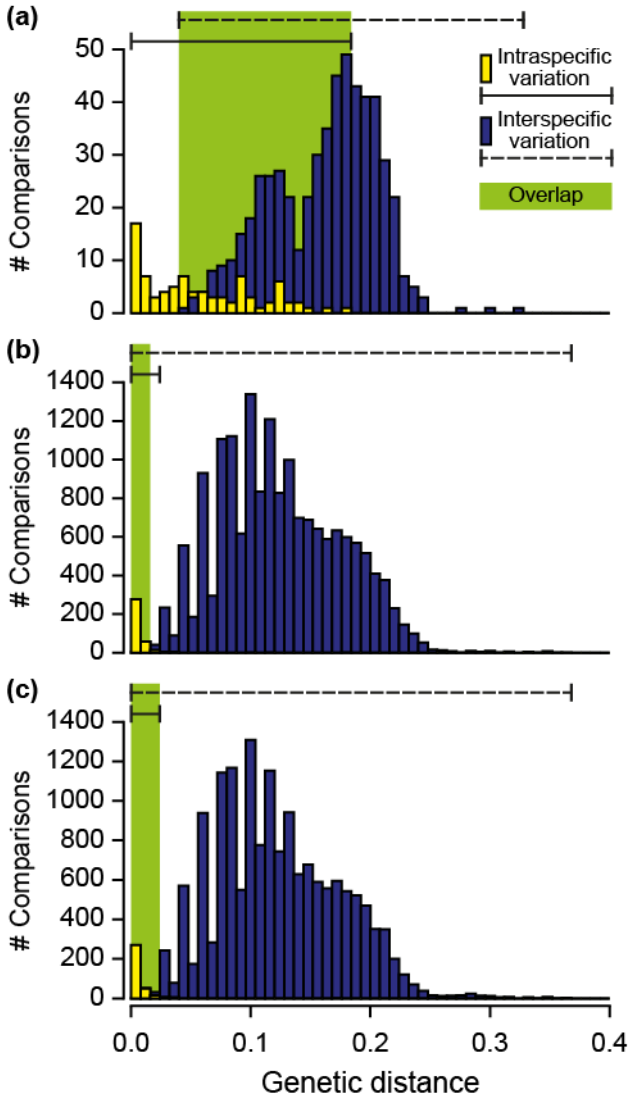

Figure 4.1 Distribution of pairwise intraspecific and interspecific variation for morphospecies (**a**), BEAST ESUs (**b**) and RAxML ESUs (**c**).
The ESUs were delimited using a single-threshold GMYC method.

DNA barcode based identification

Failure to identify ESUs via DNA barcoding is significantly and negatively correlated with the number of sequences, number of unique haplotypes, and the proportion of the expected diversity sampled, while being positively correlated with the number of singleton taxa (Table 4.3, Fig. 4.3). DNA barcode identification success was typically higher in monogonont compared to bdelloid rotifers (Table 4.3, Fig. 4.3). Successful identification of ESUs through DNA barcoding ranged from 63.16% to 100%. Removing the singletons from the analyses results in a significant improvement in identification success (Table 4.3; Fig. 4.4); success rates typically increase by 5.64% (±1.61) of the failure rate.

Table 4.1 LMEMs used to explain variation in barcode gap size with regard to model of evolution and gene tree choice. Two measures of barcode gap (or overlap) were analysed separately.

Response	**Model**	**Estimate**	**S.E.**	***t***	***P***
Inter. min - Intra. max	K2P | BEAST (intercept)	-5.67	2.84	-2	0.047
	F81	-0.06	0.61	-0.098	0.92
	F84	-0.084	0.61	-0.14	0.89
	GG95	-2.96	0.61	-4.83	0
	JC69	-0.0068	0.61	-0.011	0.99
	K81	-0.015	0.61	-0.024	0.98
	raw	0.52	0.61	0.85	0.4
	T92	-0.047	0.61	-0.077	0.94
	TN93	-0.19	0.61	-0.31	0.76
	RAxML	0.86	0.29	2.97	0.0034
Inter. mean / Intra. mean	K2P | BEAST (intercept)	5.56	0.69	8.05	0
	F81	0.0016	0.28	0.0058	0.995
	F84	0.037	0.28	0.13	0.89
	GG95	1.29	0.28	4.63	0
	JC69	-0.026	0.28	-0.094	0.93
	K81	0.0076	0.28	0.028	0.98
	raw	-0.37	0.28	-1.33	0.19
	T92	0.023	0.28	0.082	0.93
	TN93	0.048	0.28	0.17	0.86
	RAxML	0.056	0.13	0.43	0.67

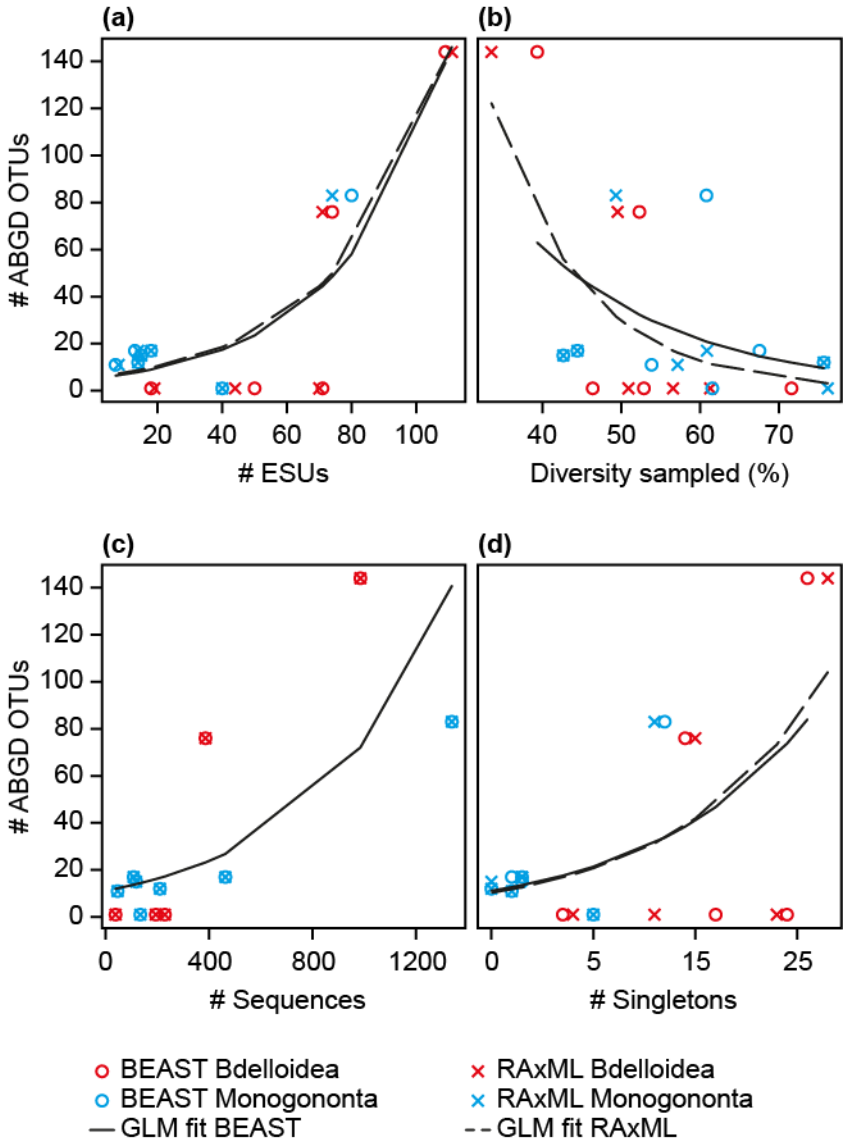

Figure 4.2 Predictors of ABGD success: (**a**) #ESUs, (**b**) diversity sampled (%),(**c**) # sequences, and (**d**) # singletons.
Bdelloid (red) and monogonont (blue) rotifers are split by colour, while BEAST (open circles) and RAxML (crosses) phylogenetic reconstruction methods are split by symbol. GLM model fits are shown for each pairwise comparison, again the BEAST (solid line) and RAxML (dotted line) fits are shown individually. Note that a single GLM fit is shown in (**c**) as the data for each GLM is the same. All of these GLM fits (except the # sequences comparison) are significant.

The difference in identification success rates between bdelloid and monogonont datasets is significant across the BEAST gene trees but only qualitative for the RAxML trees (Table 4.3; Fig. 4.5). The removal of singletons resulted in a 9.99% (±1.7) improvement in bdelloid DNA barcode identification success, but only a 2.54% (±0.69) improvement in monogononts. DNA barcode identification success did not differ between morphospecies or ESUs delimited from either RAxML or BEAST trees (Table S4.3; Fig. 4.4), while differences associated with metric choice were non-significant (Table S4.4) but consistent with regard to stringency (NN<BCM<TI) and therefore success (NN>BCM>TI). However, high accuracy of DNA barcoding using morphospecies groupings is inflated by the poor taxonomy of

dustbin taxa, as most tips are para- or polyphyletic (singletons = monophyletic: 19.8±10.5%; Table S4.1). For example, *Brachionus* morphospecies can be identified with more than 99% accuracy, but less than 5% of the sequences form monophyletic clades with conspecific sequences. In contrast, *Brachionus* ESUs are >98% monophyletic while still having high barcoding success rates (>99%).

Table 4.2 GLM used to explain the number of OTUs delimited using the ABGD method.

	Estimate	**S.E.**	***t***	***P***
(Intercept)	3.62	0.69	5.25	$4.58e^{-5}$
Diversity sampled (%)	-0.038	0.011	-3.35	0.0034
# Singletons	-0.27	0.056	-4.82	0.00012
# Sequences	-0.00082	0.00043	-1.93	0.069
# ESUs	0.11	0.02	5.52	$2.55e^{-5}$

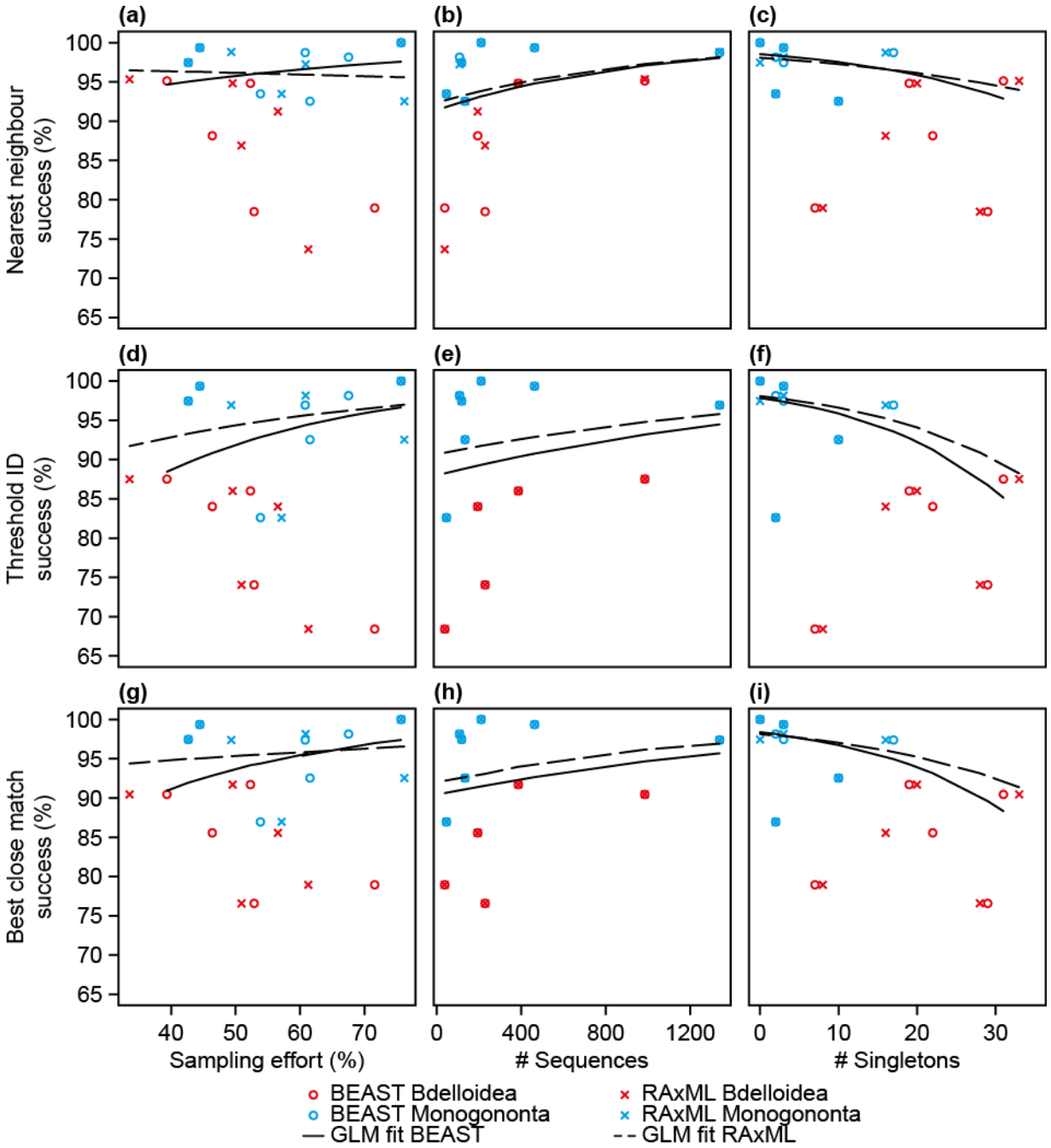

Figure 4.3 Barcode identification accuracy using nearest neighbour (**a**-**c**), threshold ID (**d**-**f**) and best close match (**g**-**i**) and its association with group (monogonont [grey] and bdelloid [black]), level of sampling (**a**, **d**, **g**), number of sequences (**b**, **e**, **h**) and prevalence of singleton taxa (**c**, **f**, **i**). GLM fits are shown for both BEAST (solid line) and RAxML datasets (dotted line).

Table 4.3 GLMs used to explain the DNA barcoding identification success rates, with metrics and gene trees analysed separately.

DNA barcoding metric	Phylogenetic reconstruction		Estimate	S.E.	*Z*	*P*
Nearest neighbour success (%)	BEAST	(Intercept)	6.3	1.57	4.01	$6.19e^{-5}$
		Diversity (%)	-0.12	0.035	-3.35	$8.08e^{-4}$
		# singletons	0.2	0.15	1.38	0.16736
		# sequences	-0.1	0.044	-2.28	0.022
		# haplotypes	-0.24	0.11	-2.25	0.025
		# ESUs	0.31	0.13	2.45	0.014
		Monogononta	1.57	0.68	2.3	0.022
		Diversity (%) x # sequences	0.0027	0.0012	2.3	0.021
		# singletons x # haplotypes	-0.0028	0.0012	-2.31	0.021
	RAxML	(Intercept)	9.18	2.22	4.14	$3.41e^{-5}$
		Diversity (%)	-0.12	0.041	-2.87	0.0042
		# singletons	0.93	0.27	3.42	$6.23e^{-4}$
		# sequences	-0.027	0.0094	-2.91	0.0036
		# haplotypes	-0.16	0.035	-4.59	$4.39e^{-6}$
		Diversity (%) x # singletons	-0.019	0.0053	-3.53	0.00042
		Diversity (%) x # sequences	0.00076	0.00024	3.13	0.0018
		Diversity (%) x # haplotypes	0.0026	0.00072	3.66	0.00026
Threshold ID success (%)	BEAST	(Intercept)	8.97	0.31	28.9	0.0012
		Diversity (%)	-0.29	0.0093	-30.55	0.0011
		# singletons	0.92	0.029	32.07	$9.71e^{-4}$
		# sequences	-0.33	0.011	-29.55	0.0011
		# haplotypes	-0.71	0.023	-30.55	0.0011
		# ESUs	0.88	0.029	30.86	0.001
		Monogononta	4.81	0.12	40.18	$6.49e^{-4}$
		Diversity (%) x # sequences	0.0085	0.00028	30.3	0.0011
		# singletons x # sequences	0.00037	0.000021	17.46	0.0033
		# singletons x # haplotypes	-0.0094	0.00029	-31.87	$9.83e^{-4}$
	RAxML	(Intercept)	6.93	2.08	3.33	$8.6e^{-4}$
		Diversity (%)	-0.093	0.037	-2.52	0.012
		# singletons	1.5	0.24	6.32	$2.58e^{-10}$
		# sequences	0.0077	0.0025	3.12	0.0018
		# haplotypes	-0.21	0.033	-6.41	$1.41e^{-10}$
		Diversity (%) x # singletons	-0.03	0.0046	-6.38	$1.77e^{-10}$
		# singletons x # sequences	-0.00053	0.000098	-5.4	$6.54e^{-8}$
		Diversity (%) x # haplotypes	0.0044	0.00068	6.44	$1.16e^{-10}$
Best close match success (%)	BEAST	(Intercept)	5.15	1.41	3.65	$2.66e^{-4}$
		Diversity (%)	-0.13	0.034	-3.79	$1.51e^{-4}$
		# singletons	0.38	0.14	2.74	0.0061
		# sequences	-0.14	0.043	-3.28	0.001
		# haplotypes	-0.33	0.1	-3.21	0.0013
		# ESUs	0.42	0.12	3.41	$6.59e^{-4}$
		Monogononta	2.37	0.67	3.53	$4.2e^{-4}$
		Diversity (%) x # sequences	0.0038	0.0012	3.3	$9.7e^{-4}$
		# singletons x # haplotypes	-0.0042	0.0012	-3.55	$3.81e^{-4}$
	RAxML	(Intercept)	7.67	2.46	3.12	0.0018
		Diversity (%)	-0.09	0.041	-2.17	0.03
		# singletons	1.43	0.31	4.63	$3.62e^{-6}$
		# sequences	0.0077	0.0024	3.14	0.0017
		# haplotypes	-0.21	0.047	-4.51	$6.51e^{-6}$
		Monogononta	-0.8	0.52	-1.54	0.12
		Diversity (%) x # singletons	-0.029	0.0063	-4.58	$4.71e^{-6}$
		# singletons x # sequences	-0.00048	0.0001	-4.63	$3.7e^{-6}$
		Diversity (%) x # haplotypes	0.0044	0.001	4.39	$1.12e^{-5}$

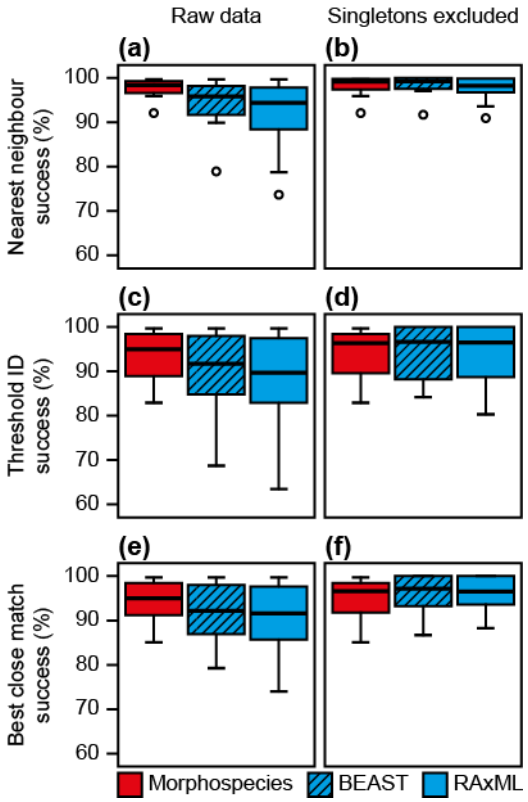

Figure 4.4 Barcode identification accuracy using nearest neighbour (**a**, **b**), threshold ID (**c**, **d**) and best close match (**e**, **d**) criteria of morphospecies (red), BEAST (blue hatched) and RAxML ESUs (blue solid).
The effect of excluding singletons is also shown (**b**, **d**, **f**). ESUs were delimited using a single-threshold GMYC method. Open circles represent data points outside the 75% quartile range.

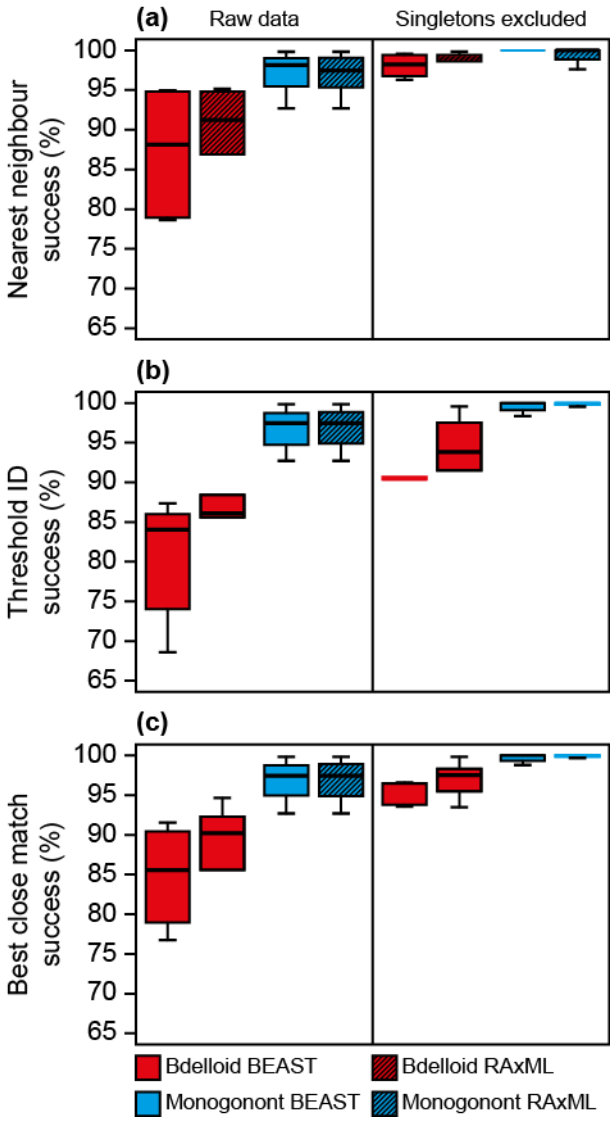

Figure 4.5 Barcode accuracy using nearest neighbour (**a**), threshold ID (**b**) and best close match (**c**) criteria of Bdelloidea (red) and Monogononta (blue) ESUs delimited using the GMYC method on BEAST (solid) and RAxML (hatched) trees.
The effect of excluding singletons is also shown.

Discussion

The initial promise of DNA barcoding was separated into the accelerated identification and description of taxa (Hebert et al. 2003a; Vogler and Monaghan 2007) *in lieu* of a dwindling community of traditional taxonomists and encroaching extinction rates (Wiens 2007). DNA barcoding is particularly attractive for groups such as Rotifera where the extreme level of undescribed, cryptic diversity directly contrasts the paucity of taxonomists examining them (e.g. Suatoni et al. 2006; Fontaneto et al. 2009). We have shown that in this sample of Rotifera, successful identification via DNA barcoding is possible with taxa delimited using the GMYC model (a proxy for resolved taxonomy), but that flawless identification is unlikely given the lack of an explicit barcode gap. Here, any failure in identification is associated with the presence of singletons, level of sampling (taxonomic or physical), amount of standing diversity, clade, and overlap between intra- and interspecific variation.

We report the absence of an unequivocal barcode gap, and concur with others (e.g. Meyer and Paulay 2005; Meier et al. 2006; Wiemers and Fiedler 2007) that its existence is contentious and unlikely. An overlap between intra- and interspecific variation is observed in most of the ESU datasets (58%) irrespective of which evolutionary model is used to generate the distance matrices. This overlap can exist for numerous reasons: (1) poor taxonomy that inflates the species boundaries and thus the intraspecific variation (Meyer and Paulay 2005; Astrin et al. 2012), (2) unsorted ancestral polymorphisms that give rise to non-monophyletic species with overestimated intraspecific variation and reduced interspecific variation (Meier et al. 2006), (3) increased sampling (geographic or taxonomic scale) that better encompass the extent of total intraspecific variation (Bergsten et al. 2012), and (4) heterogeneity in the rate of evolution that results in discrepancies in the amount of intra- and interspecific variation across the sample. In our datasets, the overlap among the GMYC delimited ESUs is likely a result of sampling and heterogeneity in the rate of evolution across the taxa.

It is widely known that incomplete sampling can affect the likelihood of finding a barcode gap (Papadopoulou et al. 2008; Bergsten et al. 2012), the range of sampling regimes apparent from the Rotifera data opportunistically sampled from GenBank allow us to empirically identify aspects of sampling that contribute to DNA barcode failure. Specifically, the prevalence of singletons is the biggest determinant of DNA barcode failure, this is because by definition there is no reference point in the database with which to identify them (Lim et al. 2012). Singletons and rare specimens are common in biodiversity surveys (Lim et al. 2012), and additional sampling scarcely helps in eliminating their rarity. This aspect is impossible to change without a concerted effort to increase the coverage of available, annotated, and taxonomically certified sequences.

Without *a priori* groupings, the ABGD method was unable to detect a barcode gap in a third of the datasets. Our analyses suggest that the success of the ABGD method is associated with the level of taxonomic sampling and the incidence of singleton taxa. Increasing the taxonomic coverage of sampling reduces the number of ABGD OTUs and we expect this is due to the increased intraspecific variation associated with additional sampling and the increased likelihood of encompassing more rate heterogeneity. Furthermore, there is a positive correlation between the number of ABGD OTUs and number of singletons present. Regardless of whether these singleton taxa are real rare taxa or artefacts associated with sequencing (Lim et al. 2012), their presence in the datasets acts to increase interspecific variation while lowering the mean intraspecific variation, thus increasing the chances of observing a barcode gap.

DNA barcode identification success is correlated with the proportion of expected diversity sampled (sampling extent), number of available sequences, and number of singletons (both proxies of sampling intensity). The effects of available sequence number and singletons are two counterbalanced proxies of sampling intensity. Sequences in a DNA barcode library are essentially reference points with which identification can happen, therefore more sequences equates to more reference points and therefore improved success rates. Singletons on the other hand will limit success. As DNA barcode identification success is inherently tied to distinctiveness of clusters (with regard to genetic space), and distinctiveness of clusters is inherently aligned with intra- and interspecific variation. It follows that sampling a higher proportion of expected diversity (i.e. sampling extent) will likely increase the interspecific variation and thus, if intraspecific variation is constant, the distinctiveness of clusters will increase. Therefore, increased taxonomic or geographic sampling will increase DNA barcode identification success because they act to increase species distinctiveness (Bergsten et al. 2012). On the other hand, if sampling acts to fill in gaps in the interspecific sample, rather than extending it, barcode gaps will become more nebulous and thus identification using DNA barcodes will suffer (Meyer and Paulay 2005).

Difference between bdelloids and monogononts

Specific to Rotifera, our analyses indicate that asexual bdelloid rotifers are less readily identifiable by DNA barcoding. This is likely due to the asexual bdelloid ESUs being less genetically discrete (Chapter 5; Tang et al. 2014b) whereby no reproductive isolation and genetic cohesiveness associated with sex acts to reduce genetic gaps between species. Bdelloid datasets have typically more singletons, but also a smaller proportion of their expected diversity sampled. We hypothesise that prevalence of singleton taxa and lower taxonomic coverage is related to a higher propensity for asexuals to form isolated clonal populations (exacerbated here by the higher dispersal capabilities of bdelloids) and not a difference in sampling effort between bdelloids and monogononts; this is evidenced by the facts that further sampling of bdelloids continues the discovery of additional

divergent haplotypes (e.g. Swanstrom et al. 2011) and while reducing the strength of genetic clustering (Tang et al. 2014b). Therefore for asexual study systems, the minimum sampling regime required for a successful DNA barcode survey likely needs to be more comprehensive than for sexual organisms.

Conclusion

The incorrect identification of species is not uncommon and undermines any ecological or evolutionary investigation. The unknown biosphere is large and only with the advancement of taxonomic databases through integrated taxonomy will we be able to consistently and confidently identify organisms. Promisingly, the identification via DNA barcoding of evolutionary genetic species (Birky and Barraclough 2009), otherwise known as molecular operational taxonomic units (MOTUs: Blaxter et al. 2005) or ESUs, yields high success rates. Defining taxa in this way facilitates access to taxonomically difficult groups (Blaxter et al. 2005) and provides a foundation that if used in conjunction with traditional taxonomy, within an iterative and integrative framework, will produce identifiable taxonomic units (Puillandre et al. 2012b). This integrative taxonomy, with molecular and traditional taxonomy reciprocally underpinning each other (e.g. Birky et al. 2011; Puillandre et al. 2012b), is the best way in which we can consistently describe diversity in groups where each tool on its own is unreliable. Even still, the nonexistence of an unequivocal barcode gap will limit the success of such studies and will warrant additional sources of taxonomic information for infallibility.

Chapter 5: Sexual species are separated by larger genetic gaps than asexual species in rotifers

Published as:

Tang, C. Q., Obertegger, U., Fontaneto, D., & Barraclough, T. G. (2014). Sexual species are separated by larger genetic gaps than asexual species in rotifers. Evolution, 68(10), 2901–2916.

Abstract

Why organisms diversify into discrete species instead of showing a continuum of genotypic and phenotypic forms is an important yet rarely studied question in speciation biology. Does species discreteness come from adaptation to fill discrete niches or from interspecific gaps generated by reproductive isolation? We investigate the importance of reproductive isolation by comparing genetic discreteness, in terms of intra- and interspecific variation, between facultatively sexual monogonont rotifers and obligately asexual bdelloid rotifers. We calculated the age (phylogenetic distance) and average pairwise genetic distance (raw distance) within and among evolutionary significant units of diversity in 6 bdelloid clades and 7 monogonont clades sampled for 4,211 individuals in total. We find that monogonont species are more discrete than bdelloid species with respect to divergence between species but exhibit similar levels of intraspecific variation (species cohesiveness). This pattern arises because bdelloids have diversified into discrete genetic clusters at a faster net rate than monogononts. Although sampling biases or differences in ecology that are independent of sexuality might also affect these patterns, the results are consistent with the hypothesis that bdelloids diversified at a faster rate into less discrete species because their diversification does not depend on the evolution of reproductive isolation.

Introduction

Genetic, morphological, and behavioural evidence have accumulated to show that species are real entities maintained by ecological differences and reproductive isolation (Schluter 2001; Coyne and Orr 2004; Puritz et al. 2012). Species are a fundamental unit of biology, and the existence of discontinuous groups of organisms, as opposed to a continuum of genotypes and phenotypes, is regarded as a ubiquitous phenomenon of life (Rieseberg et al. 2006). Why this discreteness exists at all is a neglected question and "perhaps the most important question about speciation" (Coyne and Orr 2004, p. 49).

Maynard Smith and Száthmary (1995) proposed two non-mutually exclusive hypotheses regarding the existence of discrete species: (1) Species exist because they fill distinct ecological niches. Differences in resource use impose divergent selection pressures on organisms and therefore distinct genotypic and phenotypic solutions evolve (reviewed in Schluter 2001). Organisms adapting to one niche are less suited to a second, and intermediate genotypes are poorly adapted to either niche. (2) Species exist as a consequence of sexual reproduction. Given enough time, reproductive isolation is an inevitable by-product of genetic divergence through selection or drift (Fisher 1930; Dobzhansky 1937; Rice and Hostert 1993). Reproductive isolation breaks up the continuum of genotypic and phenotypic diversity, and prevents the formation of hybrid forms (i.e. hybrid inferiority - Burke and Arnold 2001), whereas sexual reproduction maintains genetic coherence within species.

In sexual organisms, the predictions of these two hypotheses are closely entwined (Schluter 2001) because divergent adaptation to disparate niches (1) may result in the formation of isolating barriers (2). In asexual organisms, adaptation to different niches and genetic drift in geographic isolation can occur (1), but reproductive isolation plays no role above the level of individuals because reproductive barriers are already in place. Comparing diversification patterns between the two reproductive modes will enable us to test the two hypotheses regarding why diversity is discontinuous (Maynard Smith and Száthmary 1995; Barraclough and Nee 2001; Barraclough and Herniou 2003; Coyne and Orr 2004).

The two existing comparisons of species discreteness between asexual and sexual clades (i.e. Holman 1987; Fontaneto et al. 2007a) focused on morphological traits. These studies could not satisfactorily determine why discrete entities exist in nature: they lacked a broad sampling regime (Coyne and Orr 2004), they adopted incomparable species concepts historically used for sexual and asexual taxa (de Queiroz 2005), they were qualitative, and they were confounded by different amounts of taxonomic effort between the groups (Fontaneto et al. 2007a). We suggest that a quantitative comparison of patterns of discreteness in genotypes among comparable units of asexual and sexual diversity would make for a more powerful assessment of species discreteness (Barraclough et al. 2003).

Irrespective of their reproductive mode, organisms are expected to diverge into genetic clusters when faced with forces such as geographical isolation or divergent selection, that promote independent evolution between sub-populations (Barraclough et al. 2003). Across a clade, this should result in clusters of closely related individuals separated by longer stem branches (Fig. 5.1). In asexuals, independent evolution occurs because new mutant genotypes in one sub-population cannot spread and outcompete those in other sub-populations (Templeton 1989; Cohan 2001). By corollary, discrete genetic clusters within a higher clade can be used as a comparable measure of independently evolving groups that represent separate arenas for mutation, selection, and drift (Fisher 1930). These genetic clusters are broadly equivalent to species as defined by the evolutionary (Simpson 1951) or general lineage species concepts (De Queiroz 2007), and constitute entities for which the degree of clustering can be compared between sexual and asexual clades. While these genetic clusters have been invoked as species in a range of organisms (including asexuals, e.g. Birky et al. 2005; Heethoff et al. 2009; Schön et al. 2012), there has been no statistical comparison of patterns of clustering between related sexual and asexual clades.

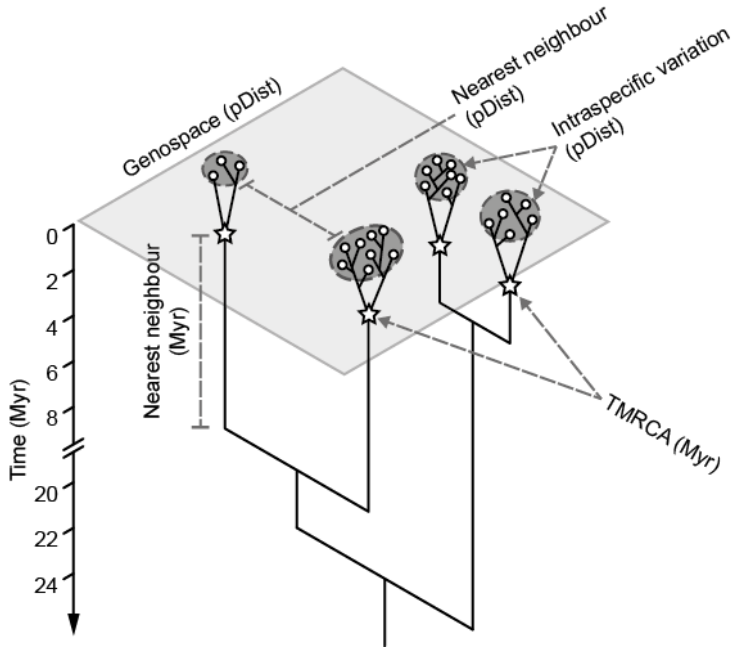

Figure 5.1 Schematic representation of genospace and how genetic variation corresponds to gene trees.
Intraspecific variation can be measured by genetic distance, as delineated by the dark grey dotted ellipses, or time to the most recent common ancestor (TMRCA), as indicated by the stars. Similarly, interspecific variation can be measured using raw genetic distances or phylogenetic distances (long branches). The size of the dotted circle and branch length is relative to the size of the intra- and interspecific variation, respectively. Here phylogenetic distance corresponds to time (MYR) as the trees are chronograms.

Here, we use a densely sampled dataset to survey clustering of a mitochondrial barcoding marker, cytochrome *c* oxidase subunit I (COI), in representative sexual and asexual clades of Rotifera. We

delimit genetic clusters, which we refer to as 'species' as defined above, using the Generalized Mixed Yule Coalescent model (GMYC - Pons et al. 2006; Fujisawa and Barraclough 2013 - see Barraclough et al. 2003 and Fontaneto et al. 2007b for a discussion of whether clusters should be regarded as populations, species, or some other unit of diversity). The method delimits statistically significant genetic clusters indicative of independently evolving lineages (Birky and Barraclough 2009) and provides comparable units that circumvent taxonomic issues that confound Rotifera taxonomy (e.g. Suatoni et al. 2006; Fontaneto et al. 2009). Putative rotifer species delimited using this method have been shown to be both morphologically and ecologically divergent (e.g. Birky et al. 2005; Fontaneto et al. 2007b).

The discreteness of species depends both on intra- and interspecific variation. These in turn are affected by population genetic mechanisms and patterns of net diversification (speciation [λ] minus extinction [μ]), respectively, as well as by sampling. We separate out the following questions:

(1) *Are species in asexual clades more or less cohesive than those in sexual clades?* Intraspecific variation, measured as average pairwise genetic distances (π) or the time to most recent common ancestor (TMRCA), reflects the cohesiveness of species. Cohesiveness will depend on the effective population size (N_e) as well as the demographic and selective history of the marker gene (Rosenberg and Nordborg 2002; Charlesworth et al. 2003). Several processes could cause systematic differences in intraspecific variation, potentially in different directions, between sexuals and asexuals. Even if census population sizes (N) were similar in sexuals and asexuals, and all other confounding factors were equal, asexual species should have double the effective population size for a mitochondrial marker (mtDNA). This is because all parents in the asexual species pass on mtDNA rather than just half the parents (Lynch and Hill 1986); therefore for asexuals, species clusters will be less genetically cohesive. However, selection might oppose this prediction. In asexual populations the entire genome is inherited as a single unit unaffected by recombination. Any selective sweep should reduce variation across the entire genome, while in sexuals selective sweeps only reduce variation in loci linked to beneficial mutations (Barraclough et al. 2007; Rice and Friberg 2009; Swanstrom et al. 2011). If asexual populations are afflicted by recurring selective sweeps, one would expect lower average genetic variation at marker genes than in sexual populations, even at neutral loci and sites. The balance of these different processes would determine any systematic differences in mtDNA variation between sexuals and asexuals. Finally, as well as these direct effects of reproductive mode, there might be other systematic differences in demography or ecology that could lead to differences in average levels of intraspecific genetic variation (Barraclough et al. 2007).

(2) *Are species in asexual clades more or less divergent from their closest related species than in sexual clades?* Average levels of interspecific divergence depend on the net rate of diversification. Somewhat paradoxically, faster net rates of diversification will tend to reduce the discreteness of

species because species will be on average less divergent from their nearest related species. A clade with greater species richness will tend to have shorter distances between species than a clade with fewer species of the same crown age. Reproductive mode could affect diversification in either direction: if speciation is limited by the rate at which reproductive isolation evolves (Felsenstein 1981; Rice and Hostert 1993), then one might expect asexuals to diversify more than sexuals because their diversification does not depend on the evolution of reproductive isolation (Barraclough and Herniou 2003). In contrast, if the rate of adaptation to new ecological niches limits speciation, then one might expect sexuals to diversify more because the greater efficiency of natural selection attributed to recombination (Weismann 1889; Burt 2000; Becks and Agrawal 2012) should allow them to adapt faster to new niches. Preliminary findings from Fontaneto et al. (2012) indicate that asexual bdelloid rotifers have a faster net diversification rate than their sexual sister clade. Here we extend their analyses: we include four additional genera, more sequences, provide better age estimates, and compare net diversification rates statistically with likelihood ratio tests.

(3) *Do confounding factors affect the comparison of sexuals and asexuals?* The pattern of discreteness in gene trees might be affected by other factors affecting the level of both intra- and interspecific sampling. For example, if sexual and asexual clades differ in their geographical distributions (i.e. more local endemics in sexuals compared to asexuals), then differences in genetic patterns might reflect sampling bias associated with dispersal ability, dormancy, or generation time independent from their reproductive mode.

Rotifera is an ideal phylum to address these questions because it encompasses clades (classes) with a variety of reproductive modes that have survived long enough for speciation (Coyne and Orr 1998; Burt 2000; Butlin 2002). Bdelloid rotifers are obligate asexuals (Mark Welch and Meselson 2000; Birky 2010; Flot et al. 2013), which fossil evidence suggests have persisted without sex for at least 35 million years (Poinar and Ricci 1992). Monogonont rotifers, their potential sister clade (Fontaneto and Jondelius 2011), are cyclical parthenogens with a frequency of recombination high enough to treat them as effectively sexual for macroevolutionary purposes (c.f. Tsai et al. 2008).

One complication for the study of diversification patterns is that the two classes vary in their ecology as well as in their sexuality. Differences in dispersal ability, for example, might affect their observed genetic patterns. Bdelloids are aquatic limnoterrestrial micro-invertebrates (i.e. inhabit terrestrial environments with an aqueous matrix), and most species can survive desiccation by contracting into a tun; this characteristic attributes them a high capacity for dispersal and subsequent colonisation and establishment in novel ephemeral environments (Jenkins and Underwood 1998; Wilson and Sherman 2013). Monogononts occupy a variety of aquatic habitats encompassing a range of salinity but, compared to bdelloids, are less likely to inhabit ephemeral environments as they are less tolerant of desiccation (Ricci 2001). Nonetheless, in bdelloids there is a range in desiccation tolerance (Ricci

1998) with several species restricted to the same habitats as monogononts: by including habitat type as a covariate in our comparisons we can attempt to disentangle the effect of ecology from reproductive mode (although we cannot rule out other ecological characteristics that might differ between the clades and influence diversification patterns).

We tested for differences in species discreteness between asexual bdelloid and sexual monogonont rotifers, in terms of intra- and interspecific variation (Fig. 5.1), using GMYC species delimited from COI sequence data. We also performed macroevolutionary analyses to compare the net rate of diversification and changes in rate over time (Nee et al. 1994; McPeek 2008). Conclusions from this system will add empirical genetic evidence to existing theoretical (Maynard Smith and Száthmary 1995; Coyne and Orr 2004) and morphological studies (Holman 1987; Fontaneto et al. 2007a) concerning why species are discrete.

Materials and Methods

Obtaining comparable units of diversity

Comparable units of diversity were delimited using the GMYC model with ultrametric phylogenies as input. Because downstream processes required estimates of divergence times, phylogenies were time-calibrated and anchored by substitution rate among the 13 datasets (described in more detail below). In the absence of fossil data and accepted calibration points or substitution rates for Rotifera, a backbone phylogeny was generated to obtain internal calibration nodes. The backbone phylogeny was generated using a concatenated alignment of 18S rDNA and COI mtDNA sequences from a subset of taxa representative of the sampled genera. Using this backbone phylogeny, a combined time-calibrated phylogeny of the specimens was reconstructed using COI and subsequently separated into individual gene trees for each of the 13 species complexes and genera. Detailed methods are as follows:

Data collection

COI sequence data were mined from GenBank and supplemented with targeted sequencing. A total of 4,211 COI sequences (3,659 GenBank; 552 sequenced [Table S5.1]) were collated from 13 monophyletic groups (herein referred to as datasets, each of which had a minimum 38 sequences) corresponding to genera or complexes of cryptic species (six bdelloid and seven monogonont species complexes or genera; Table S5.2). The sequences were split into these datasets because we are interested in processes acting at lower taxonomic levels and we lack comprehensive sampling at higher levels or in other genera/species complexes. Additional populations of the genera *Ascomorpha*, *Keratella*, and *Polyarthra* were sequenced following protocols similar to Obertegger et al. (2012). For the backbone phylogeny, 19 18S sequences were downloaded from GenBank and paired with, where possible, COI sequences from the same individual, but otherwise the same species or genera (Table S5.2). Most of these 18S sequences were produced for a previous study (Tang et al. 2012), the details of which are reported in the Supplementary Materials. Though these data came from multiple studies, the sampling regime used is standard among rotiferologists (DF was involved in the collection of 74.5% of the samples; Table S5.3). Further details of the methods used for specimen collection, sequencing, and concatenation can be found in the Supplementary Materials.

Differences in dispersal ability associated with habitat preferences might affect the genetic structure of the dataset and, subsequently, measures of discreteness and population genetics. This was factored into the analyses by annotating the sequences by habitat type - limnoterrestrial (limited to bdelloids) or aquatic habitats (typical of monogononts but also of several bdelloid clades; Table S5.3).

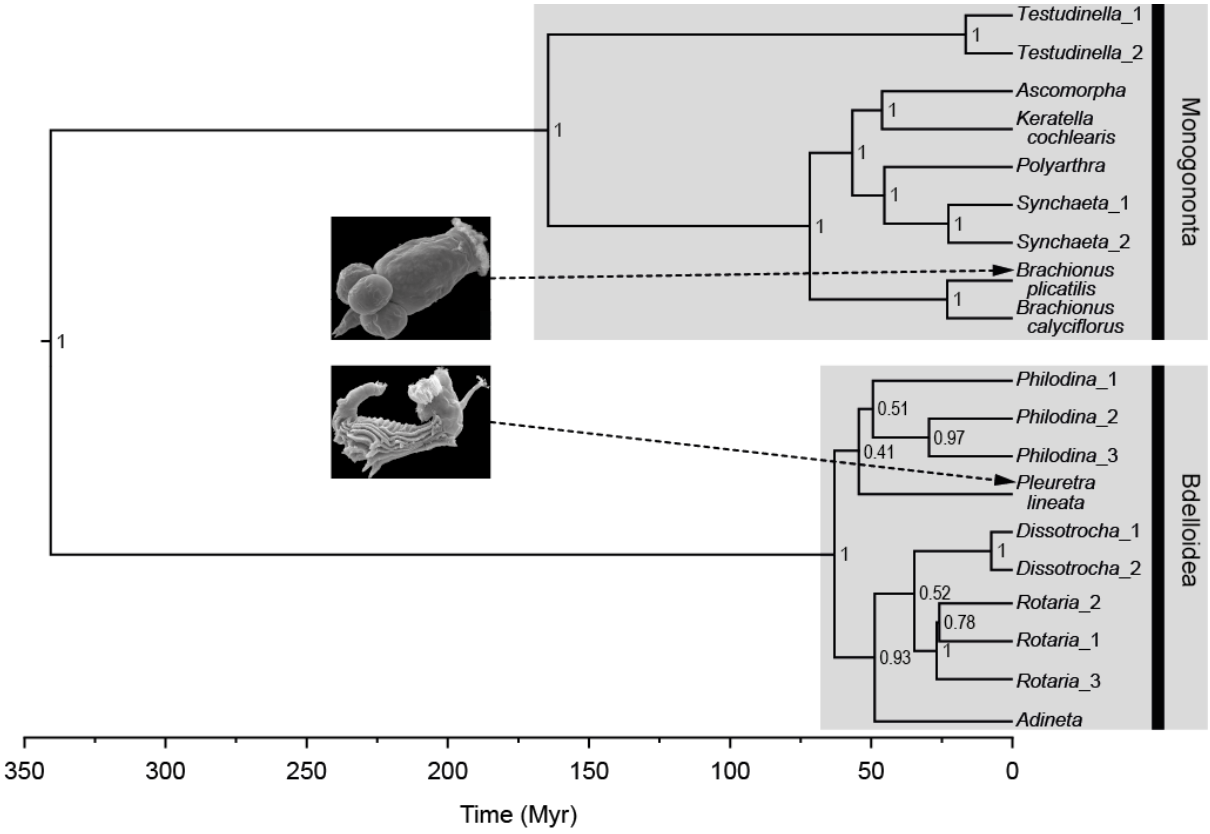

Figure 5.2 BEAST chronogram for a subset of Bdelloidea and Monogononta inferred using a concatenated alignment of both COI mtDNA and 18S rDNA.
The substitution model GTR+Γ+I was found to be the best fit for both COI and 18S. A lognormal relaxed clock with separate substitution rates for COI (1.76% MYR^{-1}) and 18S (0.02% MYR^{-1}) were used. The posterior probability values are shown as clade support at the nodes. Images of *Brachionus manjavacas* (of the *Brachionus plicatilis* species complex) and *Adineta tuberculosa* were taken by Diego Fontaneto and Giulio Melone.

Phylogenetic analyses

Phylogenetic methods are visualised in Figure S5.1. For the backbone phylogeny, all of the 19 COI and 18S sequences were aligned using MAFFT v7.017 (Katoh et al. 2009) within Geneious Pro v5.4.2 (Drummond et al. 2006) and checked by eye. A concatenated alignment of 18S and COI was used to reconstruct a time-calibrated phylogeny with BEAST v1.7.5 (Drummond and Rambaut 2007). The parameters comprised a GTR+Γ+I substitution model (defined using Akaike information criteria in jModelTest 2 - Darriba et al. 2012), a relaxed lognormal clock, a birth-death prior (Gernhard 2008), a random starting tree, 100,000,000 generations, and sampling every 1,000 generations. Separate calibration clocks for COI (1.76% MYR^{-1}; tested for the GTR+Γ+I model in aquatic invertebrates - Wilke et al. 2009) and 18S (0.02% MYR^{-1}; as suggested by Ochman and Wilson 1987 and Bargues et al. 2000) were used. These calibrations were used in the absence of published Rotifera specific rates; however, we acknowledge that this external rate may lead to the underestimation of intraspecific rates (Ho et al. 2008). The Markov chain Monte Carlo (MCMC) sample was checked for convergence in Tracer v1.5 (Rambaut and Drummond 2009), and the trees were combined into a maximum

credibility tree while keeping the target node heights with a 10% burnin in TreeAnnotator v1.7.5 (Fig. 5.2).

To reduce the impact of clade-specific rate heterogeneity, the large COI alignment was analysed in two combined analyses (instead of 13 individual ones) using the node ages (including the 95% highest posterior densities [HPD] confidence intervals) and sequences from the backbone tree. As dichotomy is a prerequisite for the downstream processes, alignments were collapsed into unique haplotypes using DnaSP v5 (Librado and Rozas 2009). The COI haplotype alignment was split into two by separating out sister clades (see Supplementary Materials). Ultrametric trees were generated from these two alignments using the protocol outlined above for the backbone phylogeny except that the node ages of each divergence were specified with soft boundaries corresponding to the 95% HPD confidence intervals. Three independent runs were performed and combined using LogCombiner v1.7.5 and subsequently summed using TreeAnnotator. These two large combined gene trees were then separated into the 13 individual species complexes and genera gene trees. For each tree, the effect of rate heterogeneity on branch lengths (Supplementary File S5.1) and the effect of a combined analysis on diversity estimation were validated (Supplementary File S5.2). All phylogenetic analyses were performed on the CIPRES Science Gateway (Miller et al. 2010).

Generalised Mixed Yule Coalescent model (GMYC)

The GMYC was used to delimit genetic clusters indicative of independently evolving groups akin to species (Pons et al. 2006; Fujisawa and Barraclough 2013). The GMYC tests for significant shifts in branching rate in an ultrametric tree, which represents a switch from interspecific evolutionary processes to intraspecific population level processes. This is expected if the dataset comprises multiple individuals from a set of independently evolving entities (Birky and Barraclough 2009). A model encompassing two different branching rates is fitted and assessed against the data, and a X^2 test is performed to gauge the significance of the GMYC model fit against the null hypothesis (i.e. a single coalescent with one branching rate). If the X^2 test is significant, the threshold is used to delimit species on the gene tree. This method has been used to identify independently evolving bdelloid (e.g. Fontaneto et al. 2007b, 2012; Birky and Barraclough 2009) and monogonont rotifers (e.g. Obertegger et al. 2012; Leasi et al. 2013; Malekzadeh-Viayeh et al. 2014), and produces clusters that are congruent with other species delimitation methods (Tang et al. 2012). The analysis was performed with the *splits* 1.0–11 package (Ezard et al. 2009 - available from https://r-forge.r-project.org/projects/splits) in R 2.15.2 (R Core Team 2012). The effect of sample size on GMYC support values and how that differs between bdelloid and monogonont datasets was assessed (Supplementary File S5.3).

Patterns of genetic discreteness

Discreteness measures

The discreteness of the genetic clusters was assessed in terms of intra- and interspecific phylogenetic distances (branch lengths equivalent to age on a time calibrated tree) and raw genetic distances (Fig. 5.1). Two alternative metrics of intraspecific variation were calculated: the Time to the Most Recent Common Ancestor (TMRCA) and the average raw nucleotide diversity within a cluster (π; Nei and Li 1979). These two measures are concerned with different aspects of the data and are affected differently by variable sample sizes: TMRCA is more directly relevant for species clustering but is strongly affected by small sample sizes leading to underestimation, while π accounts for sample size. TMRCA was measured using the basal node age of each GMYC species on the ultrametric tree using the *ape* 3.0.5 package (Paradis et al. 2004) in R. Interspecific genetic divergence was calculated as the minimum phylogenetic distance (divergence time) and the minimum raw genetic distance to a heterospecific. Minimum phylogenetic distance between GMYC species was obtained from edge lengths on the trees, and this total branch length was halved to obtain divergence time. Raw intra- and interspecific pairwise distances were calculated in MEGA v5 (Tamura et al. 2011).

Population genetic signatures

Neutrality tests were conducted for each GMYC species in DnaSP, and their signatures compared between bdelloids and monogononts to test whether differences in the frequency of demographic and selection processes affect intraspecific variation. It is important to note that we cannot firmly distinguish selection and demographic processes from single locus data alone, but we can test whether there is a systematic difference in the pattern of genetic variation consistent with our predictions based on selection and demography. Five related population genetic neutrality signatures were estimated: D^* (Fu and Li 1993), F^* (Fu and Li 1993), F_S (Fu 1997), Tajima's D (Tajima 1989), and R_2 (Ramos-Onsins and Rozas 2002). These tests are closely related but differ in their ability to detect shifts from neutrality, namely bottlenecks, selective sweeps, hitchhiking, and opposing signatures of selection (Ramos-Onsins and Rozas 2002). For each of the test statistics, a value close to zero indicates neutrality, a positive value indicates either balancing selection at the locus or a recent population decrease, while a negative value indicates population expansion, genetic hitchhiking, or purifying selection at the locus.

Patterns of net diversification

Investigating the net diversification rate (i.e. speciation rate [λ] minus extinction rate [μ]) and the constancy of net diversification over time (i.e. departure from a constant diversification rate model) requires ultrametric trees with branch lengths and tips corresponding to time and species, respectively. Therefore, for each dataset the ultrametric tree was pruned so that each tip represented a GMYC species. The retained tip was the one with the longest sequence length.

Net diversification rate

Net diversification rate was independently estimated for bdelloids and monogononts using a modified version of the *ape birthdeath* function; with the modified version, the λ and μ of pooled data (e.g. bdelloids, monogononts, or Rotifera) can be assessed simultaneously (Supplementary Materials). A log likelihood statistic was used to validate the separate parameterisation of λ and μ for bdelloids and monogononts (4 parameters) over a "global" model with a single λ and μ estimated across all of the data (2 parameters).

Constancy of net diversification

The constancy of net diversification of each dataset was tested using the γ statistic of Pybus and Harvey (2000) within the *laser* 2.3 package (Rabosky 2006) in R. The analysis followed Fontaneto et al. (2012) but includes additional rotifer taxa. The γ statistic tests the constancy of per-lineage net diversification rates over time by comparing relative positions of internal nodes within a phylogeny to expected positions generated by a constant-rate model. Positive γ values signify either recent increases in net diversification rate or high background extinction rates (Barraclough and Nee 2001). Negative γ values indicate either early net diversification followed by deceleration (expected with density-dependent net diversification such as ecological niche filling - McPeek 2008) or incomplete species sampling (Barraclough and Nee 2001; Rabosky and Lovette 2008). We account for the effect of incomplete sampling in two ways: (1) an *a priori* correction was performed using a missing species simulator (CorSiM - Cusimano et al. 2012) based on a constant rate birth-death model (within *TreePar* 2.5 - Stadler 2011) and (2) a *post hoc* correction performed using a Monte Carlo constant rates test (MCCR within *laser* - Pybus and Harvey 2000). Further details can be found in the Supplementary Materials.

Data analysis

Statistical analyses were performed in R to identify whether reproductive mode explains differences in species discreteness, sample sizes per species, and patterns of net diversification. To identify whether species discreteness measures are affected by reproductive mode (asexuality vs. sexuality) or habitat type (limnoterrestrial vs. aquatic), general linear mixed effects models (LMEMs) with a Gaussian error structure and an identity link function were implemented in the *lme4* 0.999999.0 package (Bates and Sarkar 2007). Response variables included (i) π, (ii) TMRCA, the nearest heterospecific neighbour in terms of (iii) genetic distance and (iv) phylogenetic distance, and (v) various population genetic signatures (D^*, F^*, F_S, Tajima's D, and R_2). Reproductive mode and habitat type were included into the model as fixed effects. To account for potential disproportionate influence of few taxa (i.e. taxonomic pseudoreplication), morphospecies nested within genus and number of sequences per GMYC species were blocked out as random effects. The nested random effects (i.e. morphospecies within genus) made LMEMs appropriate. Markov chain Monte Carlo *P*

values (pMCMC) with HPD confidence intervals for the parameters of each model were estimated using 10,000 samples within the *languageR* 1.4 package (Baayen et al. 2008).

The difference in the number of sequences and unique haplotypes per GMYC cluster, the proportion of singleton taxa per dataset, and the constancy of net diversification between bdelloids and monogononts, estimated independently for γ corrected *a priori* and *post hoc*, were assessed using Wilcoxon Rank Sum tests. This test was appropriate due to the lack of random effects and because each dataset has a single measure for each of those variables.

Retrospective power analyses were performed to determine whether any lack of significance was due to inadequate sample size or insufficient power. Power is the proportion of times the null hypothesis is rejected when it is false; this was calculated from sample sizes, significance level (α), and effect sizes (Cohen's d) using the *pwr* 1.1.1 package (Champely and Champely 2007). Cohen's d effect size provides an indication of the strength of the focal relationship, with higher values indicative of a stronger relationship; these were calculated by dividing the group means (i.e. asexual or sexual) by the pooled standard deviation (Cohen 1992).

Results

The 13 datasets contained between 38 and 1,541 sequences and yielded 5 to 120 GMYC species. The ratio of species estimated using the GMYC compared to traditional taxonomy ranged from 2:1 to 77:1 (on average 16 times higher; Table S5.2). On average, bdelloid species had fewer sequences (5.63±1.56 and 16.4±3.32, bdelloid and monogonont, respectively) and unique haplotypes per GMYC cluster (1.75±0.18 and 4.42±1.1, respectively) than the monogonont species ($Wilcox_{sequences}$: W=3, *P*=0.0082; $Wilcox_{haplotypes}$: W=1, *P*=0.0053, respectively). As a result, the transition from inter- to intraspecific branching used by the GMYC to detect clusters was qualitatively steeper in monogononts than in bdelloids (average GMYC *P* values: 0.0081 vs. 0.014; Table S5.2) and indicative of a more saturated sample of haplotypes (Supplementary File S5.3). Furthermore, the proportion of singletons was higher in the bdelloid clades (63.4±4.05% in bdelloids; 40.97±5.17% in monogononts; $Wilcox_{singletons}$: W=144, *P*=0.0022). Singletons can either consist of multiple clonal samples (collapsed into a single haplotype) or a single-sample specimen; the proportion of single-sample specimens was similar between bdelloids (37%) and monogononts (39%).

Discreteness measures

Interspecific divergence (raw and phylogenetic distance) was significantly greater in monogononts than in bdelloids (Table 5.1; Fig. 5.3; Fig. 5.4); in contrast, intraspecific variation (π or TMRCA) was similar between the two classes. The pattern of clustering was consequently more discrete in monogonont rotifers. These differences in discreteness were not attributed to habitat type (aquatic vs. limnoterrestrial; Table 5.1) and remained significant when the number of haplotypes per GMYC species, dataset, and morphospecies were blocked out as random effects.

Table 5.1 Results of general linear mixed effects models (LMEMs) for the discreteness of species (intraspecific variation [π: pDist], time to most recent common ancestor [TMRCA: MYR], nearest neighbour [pDist], and nearest neighbour [MYR], analysed separately). Reproductive mode and habitat type were included as fixed effects (**bold**), while morphospecies identity, sample size (# of haplotypes per GMYC species), and the focal dataset were included as random effects (*italics*). *P* values of fixed effects on the HPD intervals obtained from Markov Chain Monte Carlo (MCMC) sampling and *P* values of random effects are based on likelihood ratio tests (LR X^2).

Response	**Explanatory (fixed/*random*)**	**$MCMC_{mean}$ /*Variance***	**HPD(-/+) /*SD***	**LR X^2**	***P***
Intraspecific variation (pDist)	**Asexual aquatic (Intercept)**	**0.013**	**0.0057, 0.022**	-	**0.0016**
	Sexual	**0.0012**	**-0.0089, 0.01**	-	**0.79**
	Limnoterrestrial	**-0.0004**	**-0.0095, 0.0082**	-	**0.95**
	Morphospecies identity	*0*	*0*	*0*	*0*
	Sample size	*$6.26e^{-6}$*	*0.0025*	*-1.18*	*0*
	Dataset	*$3.16e^{-5}$*	*0.0056*	*-4*	*0*
	Residual	*0.0002*	*0.014*		
TMRCA (patristic)	**Asexual aquatic (Intercept)**	**1.13**	**0.61, 1.64**	-	**0.0001**
	Sexual	**0.16**	**-0.41, 0.71**	-	**0.56**
	Limnoterrestrial	**0.33**	**-0.15, 0.76**	-	**0.16**
	Morphospecies identity	*$4.21e^{-17}$*	*$6.49e^{-9}$*	*0*	*0*
	Sample size	*0.15*	*0.39*	*-18.12*	*0*
	Dataset	*0.23*	*0.48*	*-2.16*	*0*
	Residual	*0.38*	*0.62*		
Nearest neighbour (pDist)	**Asexual aquatic (Intercept)**	**0.076**	**0.048, 0.1**	**-**	**0.0001**
	Sexual	**0.069**	**0.033, 0.1**	**-**	**0.0001**
	Limnoterrestrial	**-0.0031**	**-0.024, 0.016**	**-**	**0.76**
	Morphospecies identity	*0.00065*	*0.026*	*-26.48*	*0*
	Sample size	*0*	*0*	*0*	*0*
	Dataset	*0.0015*	*0.038*	*-1.42*	*0*
	Residual	*0.0012*	*0.035*		
Nearest neighbour (patristic)	**Asexual aquatic (Intercept)**	**8.27**	**3.94, 11.94**	**-**	**0.001**
	Sexual	**5.86**	**0.72, 11.02**	**-**	**0.023**
	Limnoterrestrial	**0.32**	**-2.77, 3.4**	**-**	**0.83**
	Morphospecies identity	*17.83*	*4.22*	*-16.4*	*0*
	Sample size	*0*	*0*	*0*	*0*
	Dataset	*22.36*	*4.73*	*-1.2*	*0*
	Residual	*34.24*	*5.85*		

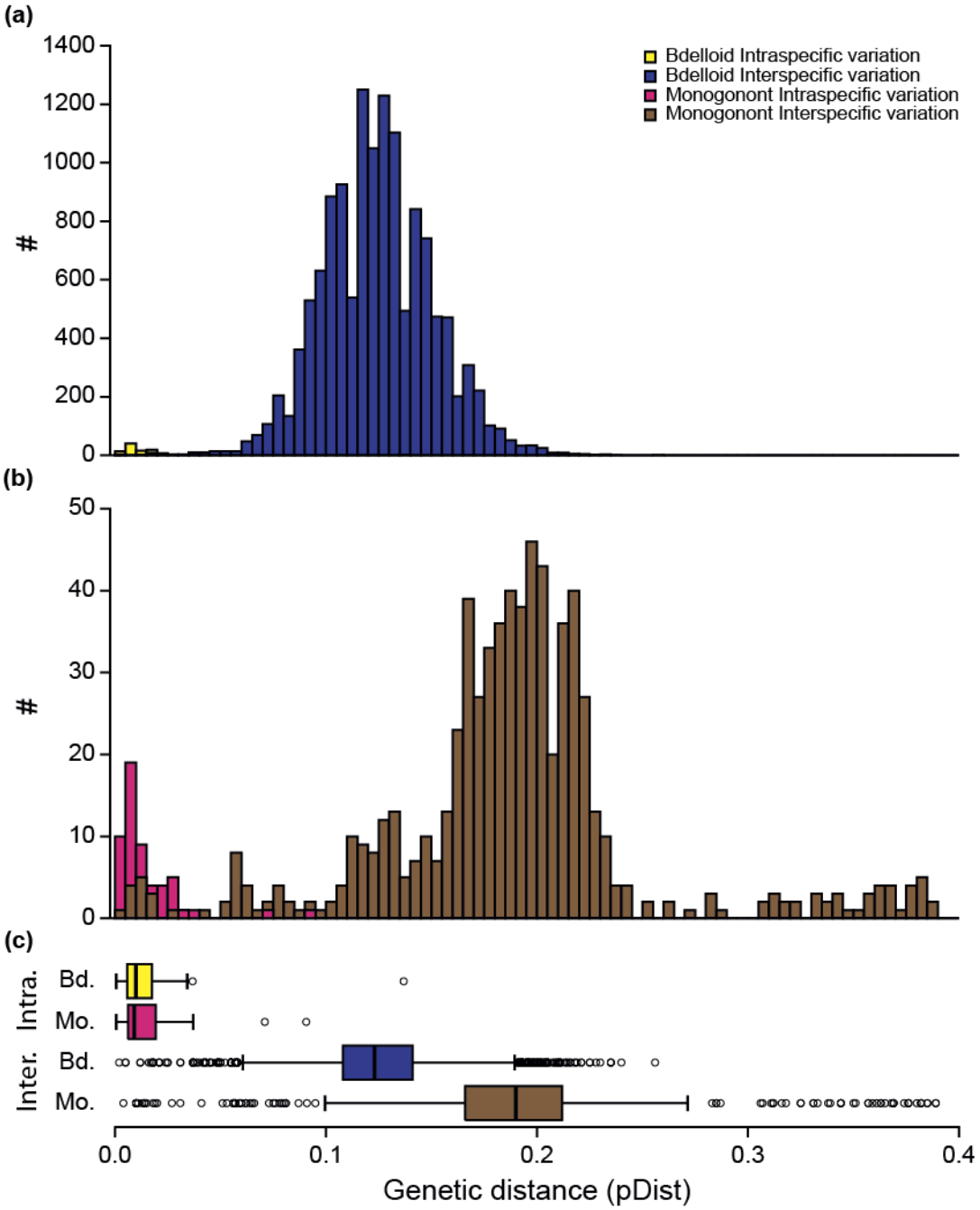

Figure 5.3 Distribution of all the intra- and interspecific raw pairwise genetic distances for bdelloid and monogonont rotifers and the differences in the two groups for intra- and interspecific genetic distance.

The distribution of genetic distances for bdelloid (**a**) and monogonont (**b**) GMYC species delimited using Bayesian gene trees is shown. The boxplots highlight the differences between bdelloid and monogonont rotifers for intra-and interspecific genetic distance (**c**). The small open circles indicate data points outside of the 75% quartile.

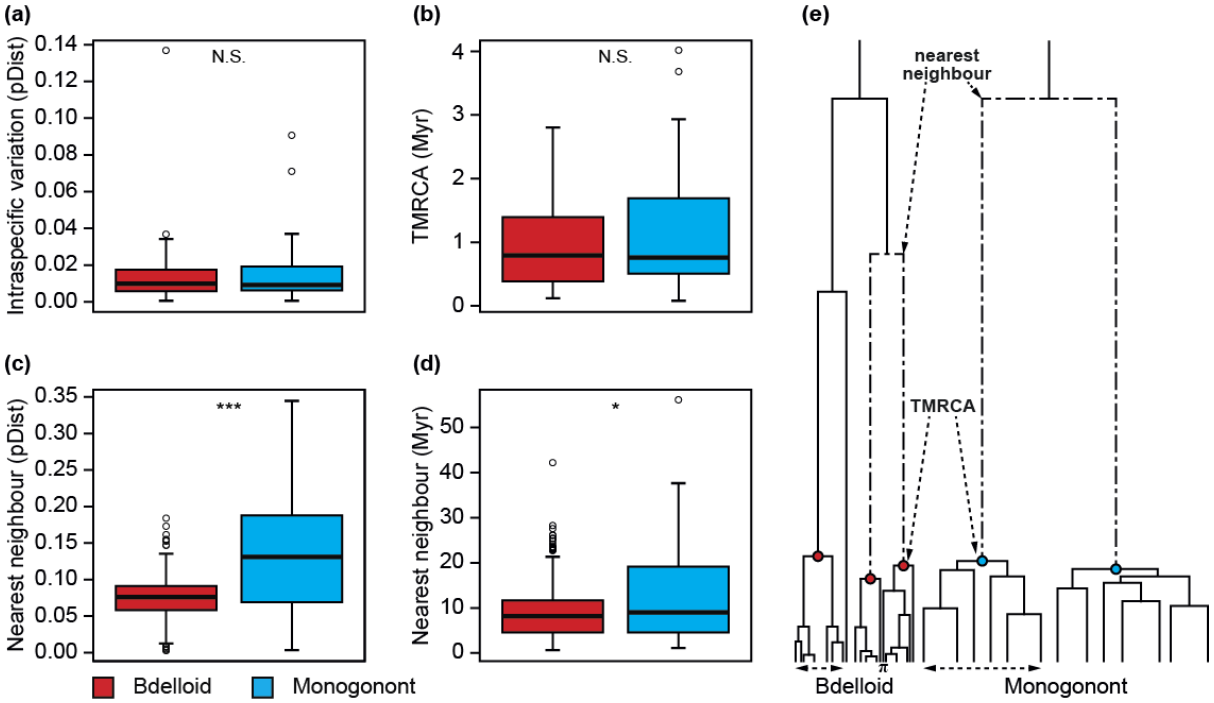

Figure 5.4 Boxplots representing the discreteness of bdelloid (red) and monogonont (blue) rotifer GMYC species in relation to intraspecific genetic distance (π [pDist]; **a**), time to the most recent common ancestor (TMRCA [MYR]; **b**), genetic distance to the nearest heterospecific neighbour (pDist; **c**), and phylogenetic distance to the nearest heterospecific neighbour (MYR; **d**). (**e**) Schematic of the typical bdelloid and monogonont gene trees; species are represented by nodes at the point of coalescence.
The dashed arrows highlight aspects of the phylogeny used to measure nearest neighbour (**d**), TMRCA (**b**) and Pi (π) (**a**). For the box plots, measurements were averaged across bdelloid and monogonont Bayesian datasets. Open circles represent outlier values. The significance of the difference between bdelloid and monogonont datasets for the various measures is shown at the top of each box (N.S. = $P > 0.05$; * = $P < 0.05$; ** = $P < 0.01$; *** = $P < 0.001$).

Population genetic signatures

None of the five population genetic signatures differed significantly between bdelloid and monogonont rotifers or habitat types (Table 5.2; Fig. 5.5), although monogononts exhibited qualitatively more negative estimates for each of the population genetic signatures (Table 5.2).

Table 5.2 Results of general linear mixed effects models (LMEMs) assessing whether results of the neutrality tests (D^*, F^*, F_S, D, and R_2, analysed separately) were explained by reproductive mode and/or habitat type.
Reproductive mode and habitat type were included as fixed effects (**bold**), while morphospecies identity, sample size (# of haplotypes per GMYC species), and the focal dataset were included as random effects (*italics*). *P* values of fixed effects on the HPD intervals obtained from Markov Chain Monte Carlo (MCMC) sampling and *P* values of random effects are based on likelihood ratio tests (LR X^2).

Response	Explanatory (fixed/*random*)	$MCMC_{mean}$ /*Variance*	HPD(-/+) /*SD*	LR X^2	*P*
D^*	**Asexual aquatic (Intercept)**	**-0.27**	**-1.41, 0.95**	**-**	**0.63**
	Sexual	**-0.64**	**-1.75, 0.51**	**-**	**0.25**
	Limnoterrestrial	**-0.63**	**-1.86, 0.52**	**-**	**0.28**
	Morphospecies identity	*0*	*$7.13e^{-7}$*	*0*	*0*
	Sample size	*1.68*	*1.3*	*-13.05*	*0*
	Dataset	*0.12*	*0.35*	*-0.084*	*0*
	Residual	*0.48*	*0.69*		
F^*	**Asexual aquatic (Intercept)**	**-0.27**	**-1.47, 0.96**	**-**	**0.65**
	Sexual	**-0.68**	**-1.86, 0.48**	**-**	**0.24**
	Limnoterrestrial	**-0.64**	**-1.87, 0.62**	**-**	**0.3**
	Morphospecies identity	*$2.80e^{-11}$*	*$5.29e^{-6}$*	*0*	*0*
	Sample size	*1.68*	*1.3*	*-11.68*	*0*
	Dataset	*0.14*	*0.37*	*-0.056*	*0*
	Residual	*0.54*	*0.74*		
F_S	**Asexual aquatic (Intercept)**	**-6.66**	**-14.09, 0.8**	**-**	**0.088**
	Sexual	**-2.94**	**-9.96, 3.65**	**-**	**0.39**
	Limnoterrestrial	**-0.41**	**-8.23, 6.65**	**-**	**0.91**
	Morphospecies identity	*0*	*0*	*0*	*0*
	Sample size	*228.38*	*15.11*	*-158.42*	*0*
	Dataset	*0.48*	*0.69*	*-2.58*	*0*
	Residual	*0.72*	*0.85*		
D	**Asexual aquatic (Intercept)**	**0.011**	**-0.9, 0.84**	**-**	**0.97**
	Sexual	**-0.59**	**-1.47, 0.35**	**-**	**0.19**
	Limnoterrestrial	**-0.66**	**-1.64, 0.3**	**-**	**0.16**
	Morphospecies identity	*$3.21e^{-28}$*	*$1.79e^{-14}$*	*0*	*0*
	Sample size	*0*	*0*	*0*	*0*
	Dataset	*0.24*	*0.49*	*-0.22*	*0*
	Residual	*0.56*	*0.75*		
R_2	**Asexual aquatic (Intercept)**	**0.37**	**0.18, 0.56**	**-**	**0.001**
	Sexual	**-0.17**	**-0.36, 0.029**	**-**	**0.089**
	Limnoterrestrial	**-0.1**	**-0.27, 0.069**	**-**	**0.25**
	Morphospecies identity	*0*	*0*	*0*	*0*
	Sample size	*0.015*	*0.12*	*-8.27*	*0*
	Dataset	*$2.22e^{-12}$*	*$1.49e^{-6}$*	*0*	*0*
	Residual	*0.14*	*0.38*		

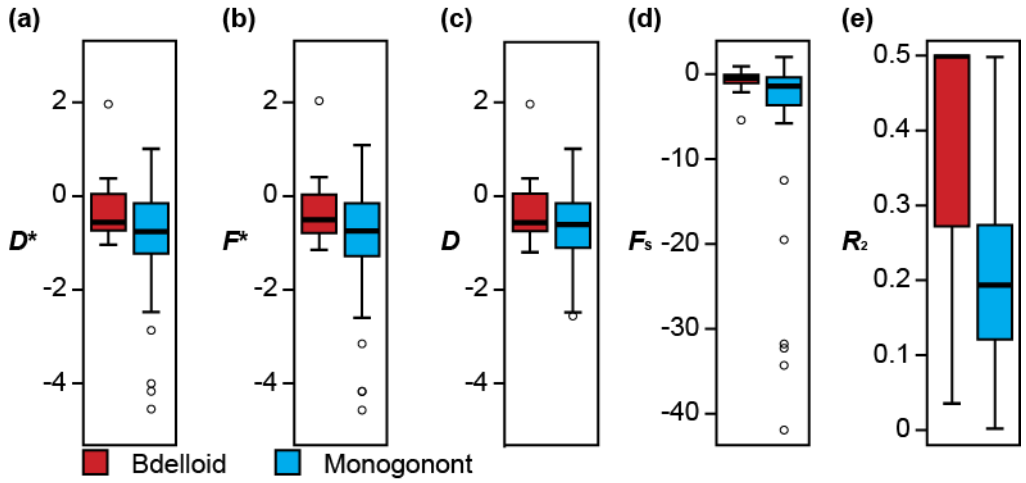

Figure 5.5 Boxplots showing the distribution of five population genetics signatures across clusters within both bdelloid (red) and monogonont (blue) rotifers.
Boxes indicate the extent of the first and third quartiles. Whiskers indicate the most extreme data points within 1.5 times the inter-quartile distance from the box and open circles represent outlier values. (**a**) *D**; (**b**) *F**; (**c**) F_S; (**d**) Tajima's *D*; (**e**) R_2.

Patterns of net diversification

Phylogenetic analyses of this sample indicated that bdelloids and monogononts are both monophyletic. The crown age of the bdelloids was found to be 58.16 MYR (HPD 95% - 34.84-99.99; Fig. 5.2), a finding congruent with the available fossil evidence. Bdelloids had a significantly faster net diversification rate (0.072±0.003) than monogononts (0.048±0.004; Table 5.3). Separate parameterisation for both bdelloid and monogonont clades produced a better model fit than modelling all the data together (X^2=11.26, *P*=0.018; Table 5.3). All the bdelloid clades (except *Pleuretra*) exhibited decelerating net diversification rates with negative values for the γ statistic; these γ values remained significantly negative despite incomplete sampling (corrected for using either CorSiM or the MCCR test; Fig. 5.6; Table S5.2). In contrast, only one monogonont dataset (*Brachionus plicatilis*) remained significantly negative when sampling biases were corrected for (Table S5.2). Monogonont clades typically exhibited more constant net diversification rates compared to bdelloid clades, this was indicated by more positive γ values (-1.13±0.55 vs. -3.63±1.22; Table 5.4; Fig. 5.6). The difference in rate slowdowns between monogononts and bdelloids was not significant, this is likely due to the insufficient power at this significance level (0.05), effect size (determined by Cohen's d: 0.98), and sample size (Power analysis: effect size=1.58, power=0.36).

Table 5.3 Estimation of net diversification rates (speciation [λ] minus extinction [μ]) from separately parameterised pooled bdelloid, monogonont, and total datasets.

Phylogenetic method	Dataset	Diversification rate (λ-μ)	Standard error	# tips	Deviance	Log likelihood	*P* compared to "All"
BEAST	Bdelloid	0.072	0.003	334	168.70	-84.35	0
BEAST	Monogonont	0.048	0.004	93	329.06	-164.53	0
BEAST	All rotifers	0.066	0.002	427	509.02	-254.51	NA

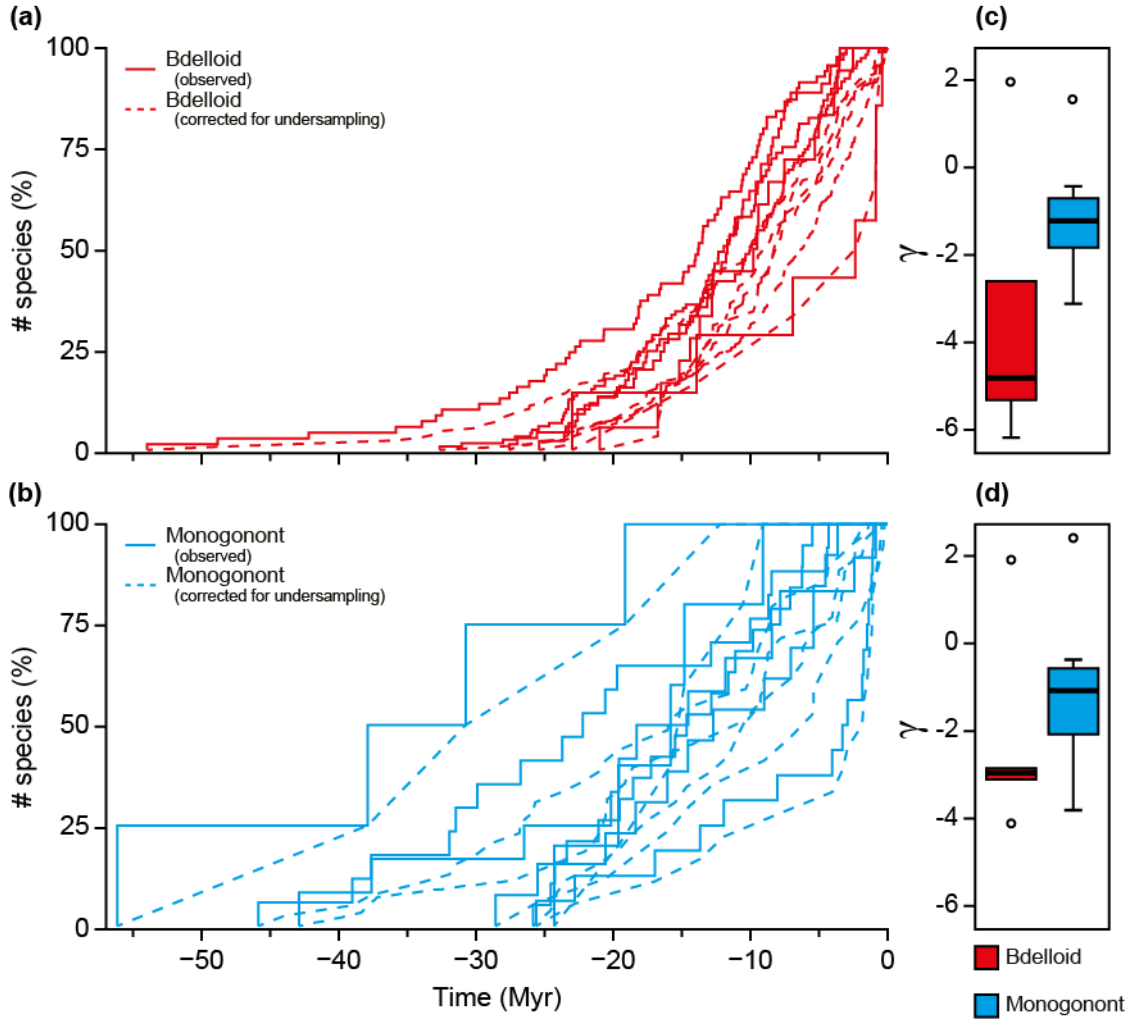

Figure 5.6 Lineage through time plots of bdelloid (red) and monogonont rotifers (blue) on absolute time scales with differences in shifts in diversification rate (γ) shown.
Lineage through time plots (bdelloid [**a**] and monogonont [**b**]) are based on pruned Bayesian trees, each tip represents only one terminal per species as identified by the GMYC. Lineage through time plots of phylogenies corrected for undersampling using CorSiM are also shown (dotted lines). Differences between bdelloids and monogononts in the distribution of the raw (**c**) and corrected values for the γ statistic (**d**) are shown. Open circles represent outlier values.

Table 5.4 γ statistic for both bdelloid and monogonont rotifers and significance of their comparison. Incomplete sampling was addressed using MCCR tests and CorSiM.

	Bdelloid γ_{mean}	Bdelloid $\gamma_{S.E.}$	Monogonont γ_{mean}	Monogonont $\gamma_{S.E.}$	W	*P*
γ (MCCR)	-3.63	1.22	-1.13	0.55	8	0.073
γ (CorSiM)	-2.22	0.86	-1.01	0.72	10	0.14

Discussion

Both bdelloid and monogonont rotifers display significant clustering of mitochondrial DNA variation, as expected if both groups had diversified into multiple, independently evolving species. The shift from slow to fast branching rates used to delimit GMYC genetic clusters, however, is steeper in monogononts than in bdelloids. Monogonont clusters are separated by significantly larger distances than bdelloid clusters, and tend to contain more sequences per cluster for equivalently sampled clades: a higher proportion of the sampled sequences group together into clusters. We discuss how this observed difference in discreteness could be ascribed to differences in reproductive mode, ecology, or sampling, and formulate a framework with which these hypotheses could be separated.

The higher discreteness observed in monogononts relative to bdelloids is not due to differences in intraspecific variation. Although there were several theoretical reasons to predict systematic differences (for example because bdelloids might have double the effective population size of mtDNA or stronger effects of recurring selective sweeps), average measures of intraspecific variation and neutrality were similar in bdelloids and monogononts. Strong differences in population genetic signatures between the clades might have been obscured by the opposing effects of alternative mechanisms. Future surveys with additional markers would help to investigate these effects further.

Instead, the greater discreteness of monogonont species, compared to bdelloid species, was due to wider genetic gaps between clusters. This pattern is associated with faster net diversification rates in bdelloids than in monogononts, because faster rates lead to species that tend to be more closely related to their nearest relatives. One possible explanation is that, as predicted in the Introduction, bdelloids are better able to take advantage of ecological opportunities for speciation because their diversification does not depend on the evolution of reproductive isolation that would otherwise breakdown the early stages of speciation (Barraclough et al. 2003). Conversely, slower diversification rates in monogononts would be expected if the need to evolve reproductive isolation limits speciation in sexuals (Felsenstein 1985).

There could be other confounding differences between bdelloids and monogononts that explain the observed patterns. One is that greater interspecific distances might be an artefact of differences in sampling. The monogonont sample might have more missing species, which would lead to artificially larger interspecific distances. For example, if monogonont species are more locally endemic than bdelloid species, then geographically restricted sampling might miss more species. We used three different approaches to assess the effect of sampling as a confounding factor: factoring out habitat type, constancy of net diversification rate, and jack-knife analyses of GMYC entities. Both bdelloid and monogonont rotifers can disperse by water, wind, or as commensals, and thus have a high dispersal capacity (Wilson and Sherman 2013; Walsh et al. 2014) and broad distributions (Gómez et

al. 2002; Segers 2007; Fontaneto et al. 2008; Malekzadeh-Viayeh et al. 2014). Monogonont rotifers, however, exhibit geographical structuring owing to strong founder effects, locally adapted genotypes, and large resting egg banks that buffer against subsequent invasion (Monopolization hypothesis - De Meester et al. 2002). Bdelloids do not have large resting egg banks and might therefore have lower endemism owing to their ability to survive desiccation as adults (Ricci 2001) and thus colonise a wide distribution of habitats. However, aquatic bdelloids are much less capable of surviving desiccation (Ricci 1998) and therefore should exhibit similar dispersal patterns to the monogononts they cohabit with. We used habitat type as a proxy for dispersal and colonisation capability to address this possibility, reasoning that species of deeper water bodies are less prone to passive dispersal via wind dispersal and have lower desiccation tolerance (as shown for certain bdelloid species - Ricci 1998). Interspecific variation was explained by reproductive mode rather than habitat type indicating that differences in clustering between bdelloids and monogononts are not explained by differences in habitat type. It remains possible, however, that other facets of rotifer biology, which affect either true diversification patterns or species sampling, cannot be accounted for by this coarse measure.

As an independent assessment of species sampling, we compared the shapes of species trees. Undersampling of species tends to lead to an apparent slowdown in the net diversification rate towards the present in species trees (Barraclough and Nee 2001) and lower observed net diversification rate (Pybus and Harvey 2000; Ricklefs 2007). In fact, bdelloid but not monogonont trees exhibited deceleration in net diversification rate, which is indicative of either actual diversity dependent diversification or incompleteness of sampling (Pybus and Harvey 2000; Rabosky and Lovette 2008). If our bdelloid dataset contained a smaller species sample than the monogonont one, then supplementary sampling would further increase bdelloids' net diversification rates and strengthen our findings.

The final feature relevant to sampling is that there are fewer monogonont clusters but they contain on average three times as many sampled individuals than in bdelloid clusters. This difference indicates that there is a tendency for total genetic diversity to quickly saturate in monogonont samples (as shown by Swanstrom et al. 2011): additional sequences supplement closely related genotypes within species clusters, while maintaining the interspecific gaps. In contrast, further sampling of bdelloids is more likely to continue the discovery of additional divergent haplotypes, acting to fill interspecific gaps. The jack-knifing of the bdelloid and monogonont datasets (Supplementary File S5.3) resulted in a steeper deterioration in GMYC model fits for bdelloids than for monogononts. This indicates that removing bdelloid sequences tends to underrepresent the coalescent part of the tree and thus reduce the GMYC model fit. In contrast, removal of 50% of the monogonont sequences has less effect on the model fits. Monogonont diversity in these samples was therefore more saturated than the bdelloids, the corollary being that increased monogonont sampling will tend to supplement existing haplotypes and therefore not affect the interspecific gaps or overall diversification rate.

Although we believe that sampling does not explain the observed differences between bdelloids and monogononts, we cannot firmly rule out that possibility. For example, our analyses could not assess whether potential incomplete sampling was randomly dispersed with respect to species. The lack of geographically restricted clades for focused sampling and current underestimation of diversity levels in both clades (e.g. Tang et al. 2012) means that it is hard to envisage a targeted sampling scheme that could improve greatly on our opportunistic one. One alternative would be to focus on co-occurring species in local habitat patches (e.g. ponds) to compare patterns of discreteness of sympatric forms. For example, using environmental metabarcode approaches could allow surveys across multiple habitat patches (e.g. Robeson et al. 2011). Furthermore, our study looks at a single measure of genetic variation, namely variation in one mitochondrial marker. A single marker meta-survey was necessary to encompass the breadth of individual and taxon sampling needed for this study, but cannot capture the entire speciation process and changes in biologically interesting traits (Rokas et al. 2003). For this, an integrative, multi-locus, or candidate gene approach is necessary (see Blair and Murphy 2011). Variation among rotifer species for jaw morphology, for example, has been attributed to food particle size preference (monogononts - Ciros-Perez 2001; hypothesised in bdelloids - Melone and Fontaneto 2005). However, even with recent technological advances in sequencing, identifying the genes underlying these traits would remain a challenging task across the scale of samples included here.

Returning to the original question of whether asexual species are as discrete as sexual species: if discrete niches in the environment explained species, we would expect the same level of discreteness in both sexuals and asexuals assuming both were able to adapt to those niches (Barraclough et al. 2003), and this is not observed. Hypothetically, if the environment were continuous and there was no geographical isolation, selection would not create genetic gaps in asexuals, rather there would be increasing divergence as lineages adapted to increasingly divided partitioning of resources (Roughgarden 1979). In sexuals, however, recombination would act as a cohesive force: organisms with similar genotypes are reproductively compatible and only rarely do mechanisms arise to permit reproductive isolation. Of course isolation by distance cannot be ignored and might well be different between bdelloids and monogononts. However, the ubiquity and inter-continental dispersal of both monogonont (Malekzadeh-Viayeh et al. 2014) and bdelloid (Fontaneto et al. 2008) haplotypes makes isolation by distance an unlikely primarily mechanism for the difference in discreteness observed between bdelloid and monogonont species (Mills et al. 2007).

Our analysis provides the first genetic evidence that monogonont rotifer species are more discrete than bdelloid rotifer species. Multilocus sequencing of cohabiting bdelloid and monogonont specimens would enable one to narrow down this pattern to either differences in reproductive mode or ecology. Additional targeted sequencing of bdelloid specimens would also help in identifying whether or not the perceived patterns are due to a lower representativeness of the bdelloid datasets. We posit that difference in sampling is an unlikely explanation given the global sample of bdelloid taxa present

here but this needs to be explicitly tested. If we can confirm that the difference in reproductive mode is key to species discreteness, then the results will indicate that while asexuals do speciate into distinct clusters, potentially mediated by adaptation to distinct niches and/or geographical isolation, reproductive isolation is a stronger driver for species discreteness.

Chapter 6: Dated, multilocus, molecular phylogeny of bdelloid rotifers

Abstract

Phylogenies are needed to determine the timing and pattern of radiations; for Bdelloidea, an ecologically and evolutionarily unique clade of microinvertebrates, there is no widely accepted multilocus phylogeny. Here we present the most up to date molecular phylogeny of Bdelloidea (Rotifera); it has representatives from 16 of the 19 genera, all four families, and all three orders, and was reconstructed using maximum likelihood and Bayesian inference methods, and includes data from five loci. Phylogenetic reconstruction without topological constraints serves as the best fitting model for these data, indicating that recognised bdelloid higher taxa are polyphyletic and have much more nebulous boundaries than previously assumed. This conclusion leads us to believe that morphological differences between the higher taxa in Bdelloidea, a mainstay for their traditional taxonomy, are labile and plastic. Model derived estimates for the crown age of Bdelloidea show that they have been evolving for at least 51.8 MYR, making them truly ancient asexuals. Furthermore, amplification of the non-Metazoan gene indicates that it was horizontally transferred before the radiation of bdelloid crown group. Further analyses including additional taxa (ingroup and outgroup) and more sequences are still required to confirm or refute these findings, but as it stands, these data lay the foundations with which bdelloid taxonomy can be tested within an evolutionary framework.

Introduction

Bdelloidea is a class of Rotifera containing at least 470 recognised morphological species (Segers 2007), although this is widely regarded as a vast underestimate of their true diversity given that cryptic species are particular prevalent (e.g. Fontaneto et al. 2009; Tang et al. 2012; Fontaneto 2014). Despite being the most well studied ancient asexual model system (e.g. Flot et al. 2013) and rotifers being among the "most important soft-bodied invertebrates in the fresh-water plankton" (Hutchinson 1967), their systematics is a glaring gap in our knowledge of the group (Sørensen and Giribet 2006). Phylogeneties can be used to test the evolutionary relationships within and between taxa; knowledge of this would aid in better understanding the rate, composition, distribution, and ancestry of bdelloid biodiversity evolution. Identifying monophyletic groups in an anciently asexual taxon would add weight to the argument that asexual taxa can diversify into discrete groups at higher taxonomic ranks as well as at the species level (e.g. Fontaneto et al. 2007d). As yet, a robust Bdelloidea phylogeny does not exist, and this impinges on how much we can extrapolate from other bdelloid studies.

The unusual evolutionary life span, tolerances to stresses, genomic structure, and ubiquity, among other aspects, make bdelloid rotifers an interesting study system. For example, bdelloid rotifers, among Metazoa, have the highest proportion of horizontally transferred genes (Boschetti et al. 2012), are the best supported case of ancient asexuality (Birky 2010; Danchin et al. 2011; Flot et al. 2013), and are able to resist extreme levels of ionising radiation (Gladyshev 2008; Krisko et al. 2012) and desiccation by undergoing anhydrobiosis (Ricci et al. 2007). Furthermore, they have a wide distribution (Segers 2007; Fontaneto et al. 2008a) owing to the their propensity for passive dispersal and colonisation (Wilson and Sherman 2010). The increasing prevalence of evolutionary studies of this study system warrants a deeper evaluation of how the taxa are related so that observed novelties within Bdelloidea can be put within an evolutionary framework and extrapolated across the clade with more support. Outside of taxonomic surveys (e.g. Iakovenko 2000; Fontaneto et al. 2007b; Kaya et al. 2010; Iakovenko et al. 2013), most bdelloid studies have used four model "*species*": *Adineta vaga*, *A. ricciae*, *Macrotrachela quadricornifera*, and *Philodina roseola*. What we know about bdelloid genomic structure (Mark Welch et al. 2008; Boschetti et al. 2012; Eyres et al. 2012; Flot et al. 2013), anhydrobiosis (Ricci et al. 2003; Pouchkina-Stantcheva et al. 2007; Boschetti et al. 2011), and stress tolerances (Ricci et al. 2007; Gladyshev 2008) is based on studies concentrating nearly exclusively on these lab strains, which are easily culturable (Table S6.1). The phylogenetic analyses that we generate will provide a baseline with which future comparative tests of bdelloid biology can be used to justify their extrapolations.

The current state of bdelloid taxonomy is unstable and this is most apparent at the lower taxonomic scale (i.e. species) where morphological stasis and cryptic diversity are very common (Fontaneto et al. 2009; Kaya et al. 2009). This taxonomic instability is driven by plastic and convergently evolved

morphological characters, and exacerbated by the astonishing dearth of expert "rotiferologists" (Wallace 2002; Fontaneto et al. 2012a) and lack of an overarching modern key (Donner 1965 is the most widely used key and is yet to be translated from German). What we know about bdelloid rotifers is heavily influenced by where the few rotiferologists are or were (Fontaneto et al. 2012a), while much of the world (especially the tropics) remain *aqua incognita* (Wallace 2002).

Bdelloidea is a class belonging to the Rotifera phylum, which includes three other classes (Monogononta, Seisonacea, and Acanthocephela). It comprises three orders (Adinetida, Philodinavida, and Philodinida), four families (Adinetidae, Habrotrochidae, Philodinidae, and Philodinividae) and 19 genera, which have not been subjected to taxonomic revisions since their descriptions (e.g. Melone and Ricci 1995). Bdelloids are mostly bottom dwelling animals that crawl using their rasping head and feet in a leech-like (Greek for leech = *bdella*) motion. All bdelloid rotifers share the same basic body plan (Fig. 6.1): elongated body, ciliated apical region (trochi), telescopically retractable foot and head, paired gonads (leading to their previous synonym Digononta), single dorsal antenna, apical rostrum, ramate mastax, foot ending with toes and spurs, and adhesive pedal glands (Melone and Ricci 1995). The three orders are morphologically recognised by the position of their ramate mastax and by characteristics of their trochi (the rotary apparatus used to generate vortex water currents into their mouths for filter feeding): Philodinida have a deep mastax and developed trochi, Philodinavida have a superficial mastax and reduced trochi, and Adinetida have a deep mastax and a ventralised trochal field. At the family level, Philodinida is split into Habrotrochidae and Philodinidae based on the presence of observable spherical pellets (food vacuoles) and lack of visible stomach lumen in well fed individuals as opposed to unpacked faeces and clearly distinguishable stomach lumen, respectively. Each of the 19 genera can be differentiated by specific morphological traits such as the number of toes and spurs, the texture of the outer integument, length of the foot, and teeth morphology (Ricci and Melone 2000). These characters are often difficult to discern under microscopy and require an expert eye and patience to fully observe. Whether these diagnostic characters are homologous or homoplasic is unknown.

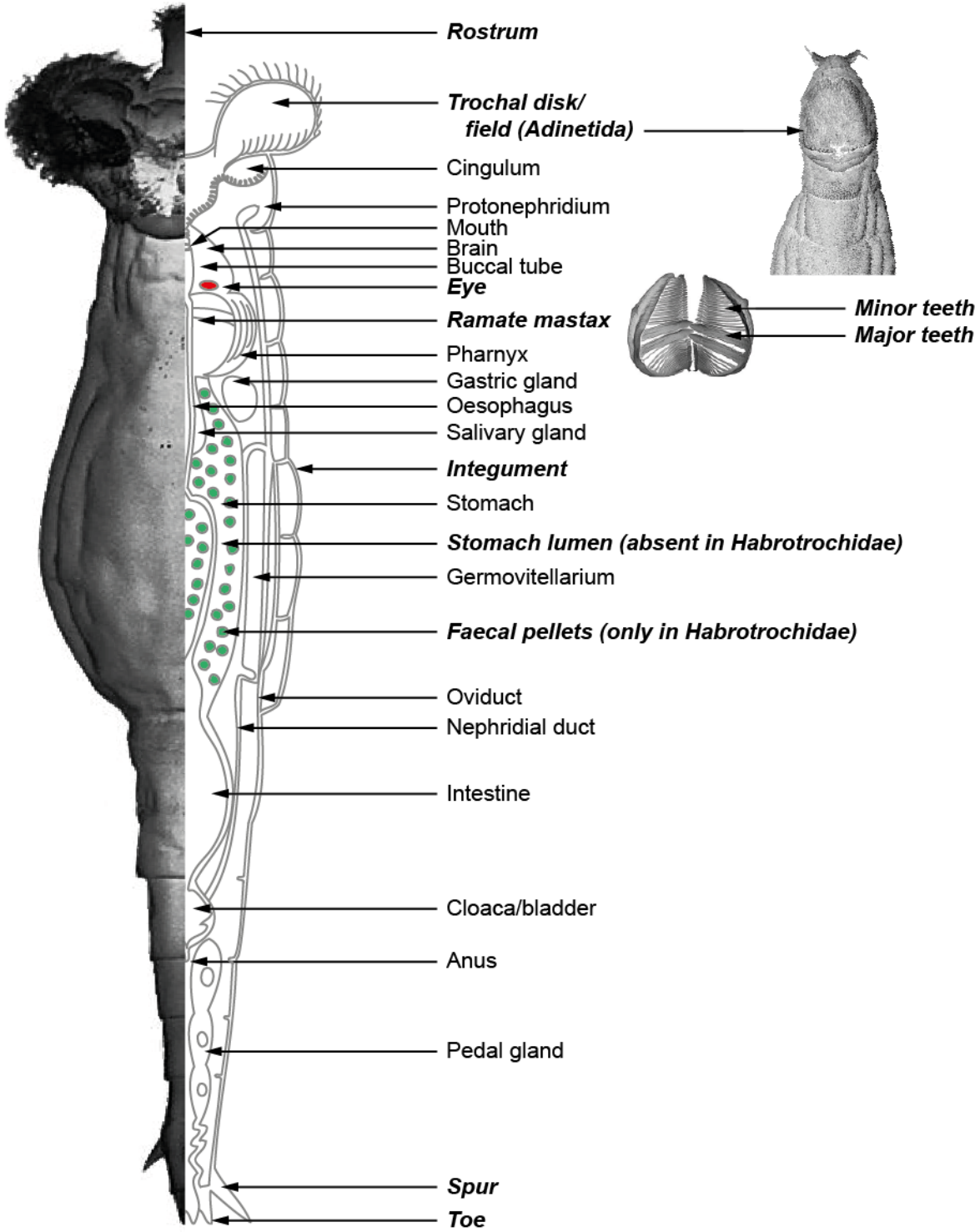

Figure 6.1 Schematic drawing of a typical bdelloid body plan.
Bold and italicised labels are characteristics that are used to delineate bdelloid higher taxa. For *Philodina* species, the eye is on the brain, but for *Rotaria* species, the eye is on the rostrum. The figure is adapted from an image by Richard Fox with additional images taken by *Rotaria macrura* (left) and the trophi of *R. tardigrada* taken by Diego Fontaneto and *Adineta tuberculosa* taken by Giulio Melone.

While the relationships between the Rotifera classes (Bdelloidea, Mongononta, Seisonida, and Acanthocephela) have received attention (Wallace 2002; García-Varela and Nadler 2006; Sørensen

and Giribet 2006; Fontaneto and Jondelius 2011; Lasek-Nesselquist 2012), the systematic relationships at the lower taxonomic levels are understudied. Birky et al. (2005) used COI mtDNA with multiple samples from *Adineta*, *Habrotrocha*, *Macrotrachela*, *Philodina*, and *Rotaria*, to reconstruct a gene tree with which to delimit cryptic species clusters. The tree had no backbone support (i.e. >70% bootstrap support) between the species clusters and so it was not possible to determine whether the higher taxa shown even some level of support for monophyly. In a previous phylogenetic assessment of the group, Tang et al. (2014b; Chapter 5) used a concatenated alignment of COI mtDNA and 18S rDNA to show that bdelloid rotifers are monophyletic when assessed with monogononts, and that all of the three genera with multiple samples (*Philodina*, *Rotaria*, and *Dissotrocha*) were monophyletic. The paraphyletic placement of *Adineta* within the other Philodindae samples) provided the first clue that bdelloid higher taxa might not be monophyletic.

At present, bdelloids have received more attention for their novel physiological (anhydrobiosis; e.g. Gladyshev 2008; Hespeels et al. 2014) and evolutionary characteristics (ancient asexuality; e.g. Mark Welch and Meselson 2000; Flot et al. 2013) than for their systematics. At present, little is known about the relationships among the higher taxa or even if these entities represent evolutionary clades. We present the most robust dated molecular phylogeny of Bdelloidea with representatives from 16 of the 19 described genera, all four families and all three orders, using a concatenated alignment of five genes.

Materials and Methods

Biological samples

Samples were collected by CQT, CGW, DF, NI and CWB from various locations (Table 6.1). Upon collection these animals were sorted and identified to the species level using Donner (1965), Birky et al. (2011), and Iakovenko et al. (2013) as guides. Of the collectors, DF, NI, and CWB have all described bdelloid species and are considered among the most reliable taxonomists for bdelloids; the taxonomic identity of samples collected by CQT and CGW were confirmed by DF. In total, forty two bdelloid samples were collected.

DNA extraction and PCR amplification

For each individual specimen, DNA was extracted using 30µL of 6% Chelex 100 resin (Bio-Rad, Hemel Hempstead, UK) and 2µL proteinase K. The mixture was heated at 56°C for an hour followed by 96°C for 10 min. For a few samples, namely *Adineta vaga*, *Adineta ricciae*, *Habrotrocha bidens*, *Habrotrocha constricta*, *Habrotrocha elliptica*, *Habrotrocha elusa*, and *Abrochtha meselsoni*, colonies were cultured prior to DNA extraction. For each sample, COI mtDNA, 18S rDNA, 28SrDNA, and two genomic loci (fragment 686 and 1054 - designed from transcriptomic alignments generated by Eyres, 2013; Supplementary Materials) were PCR amplified using RedTaq and the primers and cycle conditions outlined in Table 6.2 and described in more detail in the Supplementary Materials. Primers for the amplification of 18S, 28S, and the two genomic regions (fragments 686 and 1054) were designed as outlined in the Supplementary Materials. Amplicons were checked on a 1.5% agarose gel prior to purification and sequenced in both directions by Macrogen Europe (Amsterdam, The Netherlands) on an ABI3730XL sequencer. Chromatograms were checked by eye and assembled in Geneious v5.4.6 (Drummond et al. 2006). For the nested fragments (18S and 28S), several fragments were joined by overlapping regions into a single sequence. As an additional fidelity check, the protein coding loci (COI, 686, and 1054) were translated into amino acids and checked for stop codons. The final sequences were aligned using the MAFFT plugin (Katoh et al. 2009) with Geneious with additional sequences downloaded from GenBank (Table 6.1). The substitution model of each locus was assessed from a subset of 88 possible models using jModelTest 2 (Darriba et al. 2012; Table S6.3). For the protein coding regions, we used the alignment of translated amino acids and the appropriate protein model was determined using ProtTest 2.4 (Abascal et al. 2005; Table S6.4) by Akaike Information Criterion (AIC) from a potential 112 different models and optimised for branch lengths, model, and topology using PhyML and nearest neighbour interchange (NNI) tree rearrangement.

Table 6.1 Taxa sampled. Unique identifier, collection information, and GenBank accession numbers of shown.

Order	Family	Genus	Species	ID	Coll.	Date	Location	Habitat	COI	18S	28S	686	1054
Adinetida	Adinetidae (Hudson & Goose, 1886)	*Adineta* Hudson, 1886	*ricciae* Segers & Shiel, 2005	AD001	CGW†	26/06/1998	Victoria, Australia	Dried mud	KM043179	KM043251	KM043216	KM043132	KM043154
		Adineta Hudson, 1887	*vaga* Bryce, 1893	AD002	CGW	12/04/2007	New York, USA	Moss on oak	KF582480*	KF561095*	KM043217	KM043133	KM043155
		Adineta Hudson, 1888	*vaga* Bryce, 1893	AD003	CGW	27/05/2009	Tochigi prefecture, Japan	Moss and soil	KM043180	JX494733*	KM043218	NA	NA
		Adineta Hudson, 1889	*vaga* Bryce, 1893	AD004	CGW	05/11/2009	Tokyo, Japan	Moss and soil	KM043181	JX494739*	KM043219	KM043134	KM043156
		Adineta Hudson, 1890	*vaga* Bryce, 1893	AD005	CGW	25/03/2011	Ascot, UK	Moss	KM043182	KM043252	KM043220	NA	KM043157
		Adineta Hudson, 1891	*vaga* Bryce, 1893	AD006	CGW	09/01/2012	Ascot, UK	Moss on oak	KM043183	KM043253	KM043221	NA	NA
		Adineta Hudson, 1892	*vaga* Bryce, 1893	AD007	CGW	09/01/2012	Ascot, UK	Moss on oak	KM043184	KM043254	KM043222	NA	NA
		Adineta Hudson, 1893	*vaga* Bryce, 1893	AD008	CGW†	1984	Italy	Moss	DQ089725*	DQ089733*	DQ089739*	KM043135	KM043158
		Bradyscela Bryce, 1910	*clauda* Bryce, 1893	A953 BC	DF	08/04/2014	Brittany, France	Moss	NA	KM043255	KM043223	NA	KM043159
Philodinavida	Philodinavidae (Harring, 1913)	*Abrochta* Bryce, 1910	*meselsoni* Birky, Ricci, Melone & Fontaneto, 2011	Angl.1.1	CWB	2011	Colorado and Wyoming, USA	Temporary rock pools	KM043177	KM043249	KM043214	NA	KM043153
		Abrochta Bryce, 1910	*sonneborni* Birky, Ricci, Melone & Fontaneto, 2011	Bird.3.2	CWB	2011	Arizona, USA	Bird bath	KM043178	KM043250	KM043215	KM043131	NA
		Philoadinavus Harring, 1913	*paradoxus* Murray, 1905	A533 PP	DF	23/06/2009	Lapland, Finland	Moss	KM043203	JX494731*	KM043240	KM043146	NA
Philodinida	Habrotrochidae (Harring, 1913)	*Habrotrocha* Bryce, 1910	*bidens* Gosse, 1851	HB002	CGW	01/06/2006	New York, USA	Soil	KM043191	KM043258	KM043230	KM043140	KM043162
		Habrotrocha Bryce, 1910	*constricta* Dujardin, 1841	HB005	CGW	05/11/2009	Tokyo, Japan	Moss and soil	KM043192	KM043259	KM043231	NA	KM043163
		Habrotrocha Bryce, 1910	*elusa elusa* Milne, 1916	HB001	CGW	01/06/2006	New York, USA	Soil	KM043193	KM043260	KM043232	KM043141	KM043164
		Habrotrocha Bryce, 1910	*ligula* Bryce, 1913	HB003	CGW	05/04/2006	New York, USA	Rabbit dung	KM043194	KM043261	KM043233	KM043142	KM043165
		Otostephanos Milne, 1916	*jolantae* Iakovenko, Kasparova, Plewka & Janko, 2013	NI	NI		Borkovice vilage, Czech Republic	Sphgnum bog	KM043199	KM043265	KM043236	NA	KM043169
	Philodinidae (Ehrenberg, 1838)	*Anomopus* Piovanelli, 1903	*telphusae* Piovanelli, 1903	X3878	DF	Gen Bank	Italy	epibiont on freshwater crab	DQ089727*	DQ089732*	DQ089741*	NA	NA
		Didymodactylus Milne, 1916	*carnosus* Milne, 1916	A550 DC	DF	30/06/2009	Sweden	*Parmelia saxatilus* lichen	KM043185	JX494735*	KM043224	NA	NA
		Didymodactylus Milne, 1916	*carnosus* Milne, 1916	A953 DC	DF	09/04/2014	Brittany, France	Moss	KM043186	KM043256	KM043225	KM043136	NA
		Dissotrocha Bryce, 1910	*aculeata* Ehrenberg, 1830	A745 DA	DF	26/07/2010	Svalbard	Moss in a bog	KM043187	JX494743*	KM043226	KM043137	NA
		Dissotrocha Bryce, 1910	*macrostyla* Ehrenberg, 1838	A726 DM	DF	17/07/2010	Svalbard	Submerged moss	KM043188	KF582497*	KM043227	KM043138	KM043160
		Embata Bryce, 1910	*commensalis* Western, 1893	A956	DF	11/04/	Brittany, France	epibiont on	KM043	KM043	KM043	KM043	KM043

			EC		2014		waterlouse	3189	3257	3228	3139	3161
	Embata Bryce, 1910	*laticornis* Murray, 1905	A538 EL	DF	22/06/ 2009	Lappland, Sweden	Submerged moss	KM04 3190	JX49 4742*	KM04 3229	NA	NA
	Macrotrachela Milne, 1886	*habita* Bryce, 1894	A953 MH	DF	09/04/ 2014	Brittany, France	Moss	KM04 3195	NA	NA	KM04 3143	NA
	Macrotrachela Milne, 1886	*papillosa* Thompson, 1892	A953 MP	DF	08/04/ 2014	Brittany, France	Moss	KM04 3196	KM04 3262	KM04 3234	KM04 3144	KM04 3166
	Mniobia Bryce, 1910	*magna* Plate, 1889	645a MM	NI		Crimea, Ukraine	Lichen on rocks	KM04 3197	KM04 3263	KM04 3235	NA	KM04 3167
	Mniobia Bryce, 1910	*russeola* Zelinka, 1891	A953 MR	DF	08/04/ 2014	Brittany, France	Moss	KM04 3198	KM04 3264	NA	NA	KM04 3168
	Philodina Ehrenberg, 1830	*citrina* Ehrenberg, 1830	A739 PC	DF	22/07/ 2010	Svalbard	Moss in a bog	KM04 3200	KF561 100*	KM04 3237	NA	NA
	Philodina Ehrenberg, 1830	*gregaria* Murray, 1910	656 PHG	NI		Victoria Land, Antarctica	Algal mat	KM04 3201	KM04 3266	KM04 3238	NA	NA
	Philodina Ehrenberg, 1830	*megalotrocha* Ehrenberg, 1832	A754 PM	DF	11/09/ 2010	Sardinia, Italy	Moss	KM04 3202	JX494 737*	KM04 3239	KM04 3145	NA
	Pleuretra Bryce, 1910	*hystrix* Bartoš, 1950	A732 PH	DF	19/07/ 2010	Svalbard	Moss	KM04 3204	JX494 746*	KM04 3241	NA	KM04 3170
	Pleuretra Bryce, 1910	*lineata* Donner, 1962	654a PL	NI		Crimea, Ukraine	Moss on rocks	KM04 3205	NA	KM04 3242	NA	NA
	Rotaria Scopoli, 1777	*macrura* Ehrenberg, 1832	A539 RM	DF	22/06/ 2009	Lappland, Sweden	Moss submerged in a lake	KM04 3206	JX494 738*	KM04 3243	NA	KM04 3171
	Rotaria Scopoli, 1777	*magnacalcarata* Parsons, 1892	A952 RM	DF	07/04/ 2014	Brittany, France	Pond	KM04 3207	KM04 3267	NA	KM04 3147	KM04 3172
	Rotaria Scopoli, 1777	*magnacalcarata* Parsons, 1892	C008 RM	CQT	24/03/ 2014	London, UK	Pond	KM04 3208	KM04 3268	KM04 3244	KM04 3148	KM04 3173
	Rotaria Scopoli, 1777	*rotatoria* Pallas, 1766	A691 RR	DF	05/06/ 2010	Fulufjället National Park, Sweden	Sphgnum bog	KM04 3209	JX494 744*	KM04 3245	KM04 3149	NA
	Rotaria Scopoli, 1777	*rotatoria* Pallas, 1766	X3888		Gen Bank			DQ08 9729*	DQ08 9736*	DQ08 9743*	NA	NA
	Rotaria Scopoli, 1777	*sordida* Western, 1893	A955 RS	DF	08/04/ 2014	Brittany, France	Moss	KM04 3210	KM04 3269	KM04 3246	KM04 3150	KM04 3174
	Rotaria Scopoli, 1777	*tardigrada* Ehrenberg, 1830	A603 RT	DF	27/09/ 2009	Råstasjön, Sweden	Lake among algae	KM04 3211	NA	KM04 3247	NA	KM04 3175
	Rotaria Scopoli, 1777	*tardigrada* Ehrenberg, 1830	A717 RT	DF	06/07/ 2010	Abisko National Park, Sweden	Submerged moss	KM04 3212	KM04 3270	NA	KM04 3151	KM04 3176
	Zelinkiella Harring, 1913	*synaptae* Zelinka, 1887	A957 ZS	DF	14/04/ 2014	Brittany, France	Epizoic on a sea cucumber	KM04 3213	KM04 3271	KM04 3248	KM04 3152	NA

*** = Sequences supplemented from GenBank, † = culture strain**

Table 6.2 Primers used in this study. The substitution model, alignment length, sample coverage, and PCR cycle conditions are also shown.

Marker	Primer	Oligonucleotide Sequence (5'-3')	T_m	Cycle conditions	Nucleotide/ Protein model	Alignment length (bp)	GC content (%) overall; GC3	Coverage (X/42); (%)
18S rDNA[1]	18SFnew*	AGATTAAGCCATGCATGTCT	48.0	Whole fragment: 95°C for 5 min, 38 cycles of 95°C for 1 min, 60°C for 1 min, 72 °C for 1.5 min, followed by 72°C for 10 min.	GTR+G/ NA	1790	42.8; NA	39; 85.7
	4R	GAATTACCGCGGCTGCTGG	55.4					
	18SFnew*	AGATTAAGCCATGCATGTCT	48.0					
	18SCT1*	TGGAGGGCAAGTCTGGTGCCAGC	62.4					
	18Sbi	GAGTCTCGTTCGTTATCGGA	51.8	Internal fragments: 95°C for 5 min, 25 cycles of 95°C for 1 min, 60°C for 1 min, 72 °C for 1 min, followed by 72°C for 10 min.				
	18Sa2.0	ATGGTTGCAAAGCTGAAAC	46.8					
	9R	GATCCTTCCGCAGGTTCACCTAC	58.8					
28S rDNA[2]	28S1FCT*	CGAGACCGATAGCGAACAAGTACCGTG	62.8	Whole fragment: 95°C for 5 min, 38 cycles of 95°C for 1 min, 60°C for 1 min, 72 °C for 4 min, followed by 72°C for 10 min.	GTR+I+G/ NA	2356	43.5; NA	38; 88.1
	28S0FCT*	ACGAATGGCCGCATTCATCAGAT	55.3					
	28S1RCT*	GTTTGACGATCGATTTGCACGTC	55.3					
	28S2FCT*	GACCCGAAAGATGGTGAACT	51.8					
	28S2RCT*	CGTCAGTCTTCAAAGTTCTCATTTGA	54.8	Internal fragments: 95°C for 5 min, 25 cycles of 95°C for 1 min, 60°C for 1 min, 72 °C for 1 min, followed by 72°C for 10 min.				
	28S3FCT*	GCGTCGAAGGCTAACACGTGA	56.3					
	28S3RCT*	TGTTTTAATTAGACAGTCGGATTCC	52.8					
	28S4FCT*	CTTCGGGATAACGATTGGCTCTAAG	57.7					
	28S4RCT*	GGCTCTTCCTATCATTGCGAAGCAGACT	61.4					
	28S5RCT*	GAGTCAAGCTCAACAGGGTCTTCTT	57.7					
COI mtDNA	HCOI	TAAACTTCAGGGTGACCAAAAAATCA	53.2	95°C for 5 min, 30 cycles of 95°C for 1 min, 40°C for 1 min, 72 °C for 1 min, followed by 72°C for 10 min.	GTR+I+G/ MtREV+G+F	722	30.4; 13.3	41; 97.6
	LCOI	GGTCAACAAATCATAAAGATATTGG	51.1					
686 HTG nuDNA	686CTF*†	GGTTGGACACAACGAGCATTTGA	55.3	95°C for 5 min, 12 cycles of 95°C for 1 min, 60°C for 1 min (-1°C every cycle), 72 °C for 1 min, 23 cycles of 95°C for 1 min, 50°C for 1 min, 72 °C for 1 min, followed by 72°C for 5 min.	GTR+I+G/ HIVb+I+G	268	39.1; 48.6	22; 52.4
	686CTR*†	TGTCCTTTTCGACCCATGCCT	54.4					
1054 nuDNA[4]	1054CTF*†	AGTACGTGGACCTATGGGTATTGG	57.4	95°C for 5 min, 12 cycles of 95°C for 1 min, 60°C for 1 min (-1°C every cycle), 72 °C for 1 min, 23 cycles of 95°C for 1 min, 50°C for 1 min, 72 °C for 1 min, followed by 72°C for 5 min.	GTR+I+G/ JTT+G	429	40.2; 57.0	24; 57.1
	1054CTR*†	CCTGGTGGAGTATCATCTACTTTGACA	58.2					

†Designed using Primer3; [1] = Giribet et al., 1996, Whiting et al., 1997; [2] = Whiting et al., 1997, Crandall et al., 2000, Park and O´ Foighil, 2000, [3] = Folmer et al., 1994; * = this study.

Phylogenetic analyses

Nucleotide sequences were used for 18S rDNA, 28S rDNA, and COI mtDNA, and were concatenated with amino acid sequences for the protein coding 686 nuDNA, and 1054 nuDNA. This partition combination of nucleotide and amino acid alignments was justified by various other iterations described in more detail in the Supplementary File S6.1 and S6.2. For example, high GC_3 content for 686 and 1054 (indicate of gene saturation; Table 6.2) and incongruence of these gene trees (the reconstruction of which is described in detail below) with the other gene trees indicated that these rapidly evolving gene regions (BEAST analyses indicate that they evolve faster than COI) were saturated and so were best analysed as amino acids, which are less affected by saturated codon positions (typically the third). This partitioning is particularly appropriate for 1054 nuDNA because the gene is putatively non-Metazoan in origin (Eyres 2013), which is a likely explanation as to why it has the highest codon bias among the five loci. COI nucleotide trees were congruent with the gene trees produced by 18S and 28S (Supplementary File S6.1), therefore COI sequences were not translated into amino acids. Concatenated analyses of COI, 18S, and 28S are typical of phylogenetic analyses for meiofauna (e.g. Jørgensen et al. 2011; Todaro et al. 2011).

A time calibrated phylogeny was reconstructed using BEAST v1.7.5 (Drummond and Rambaut 2007). The priors for the analyses were set using BEAuti v 1.7.5. Evolutionary rates along the branches were independent for each of the loci. The evolutionary rate for each locus followed a lognormal relaxed clock. The evolutionary rate for COI (1.76% MYR^{-1} [0.66% MYR^{-1} – 95% confidence interval]) and 18S (0.02% MYR^{-1} [no published confidence interval]), were selected based on Wilke et al. (2009), and Ochman (1987) and Bargues et al. (2000), respectively, and estimated for 28S, 686, and 1054 with a normally distributed sampling regime. The appropriate substitution models defined using jModelTest and ProtTest (Table S6.3; Table S6.4) were applied. A birth-death speciation process with a random start tree was used for each tree. Four independent runs were conducted with the MCMC samples every 1,000 generations for 100,000,000 generations run on the CIPRES Science Gateway (Miller et al. 2010). After checking the convergence of these runs using Tracer v1.5.0 (Rambaut and Drummond 2009), 10% of each run was removed as burnin, amalgamated using LogCombiner v1.7.5, and resampled to provide a total of 40,000 trees (quadruple the recommended minimum). TreeAnnotator v1.7.5 was used to summarise a maximum credibility tree with tree node heights kept.

Monophyly of higher taxa

To test the monophyly of the higher taxa, we performed four separate BEAST analyses with varying levels of topological constraints based on the taxonomy of higher taxa: 1) no taxonomic constraints, or 2) sequences belonging to polytypic genera, 3) families, or 4) orders were constrained to be monophyletic. The likelihood outputs of each of the four models were compared using Bayes factors (Kass and Raftery 1995; Suchard et al. 2005) with the expectation being that if the bdelloid higher

taxa were real entities with greater variation among them compared to within them, then the constrained tree should not be significantly less likely than the unconstrained tree. Bayes factors are the harmonic mean of the likelihood of the posterior, differences among the models are deemed strong, very strong, and decisive if the difference between the logarithms of the Bayes factors are 2.3-3.4, 3.4-4.6, and >4.6, respectively (Kass and Raftery 1995). Bayes factors were computed for every pairwise combination of the four models with 1,000 bootstrap replicates within Tracer.

While model selection with marginal likelihood estimated using harmonic means is known to underestimate the marginal posterior probability of the model (Baele et al. 2013), it is computational inexpensive. Other methods are available for model comparison (i.e. path sampling or stepping-stone sampling) but these are typically prohibitively computationally demanding (Baele et al. 2012) for the factorial and inter-model (e.g. unconstrained vs. order-constrained) comparisons performed here.

Variation among loci

Various measures were used to compare topological congruency between trees generated using the five different loci. The pairwise global topological similarity of each of the 52 trees (2,652 pairwise tree combinations) were calculated using Compare2Trees (Nye et al. 2006). Symmetric difference (Robinson and Foulds 1981) and branch length distance (Kuhner and Felsenstein 1994) among the pairwise tree combinations were computed using the *phangorn* v1.99-7 (Schliep 2011) package in R v2.15.1 (R Core Team 2014). Symmetric distance (or the Robinson-Foulds metric) is the sum of the number of internal partitions that exist in one tree but not the other and is negatively related to the topological similarity of the two trees. Kuhner and Felsenstein's branch score is the sum of squares of the differences between the branch lengths between the two trees, where an increased score is indicative of increasingly incongruent trees.

Variation among the groups

To further investigate the reality of the higher taxonomic groupings of the bdelloids, genetic distances within and among the groups (genus, family, and order) were compared. The raw genetic distances within and among the different taxonomic ranks (genus, family and order) were computed using MEGA6 (Tamura et al. 2013) and compared against the average variation across the entire sample. Wilcoxon signed-rank tests were used to compare the distribution of raw genetic distances within and between the groups.

Results

DNA sequence data were obtained for five loci, which ranged in size from 206bp to 2,356bp (Table 6.1). The final concatenated alignment was 4,886 characters in length. In total 141 new sequences were generated for this study, and assembled together with 23 sequences downloaded from GenBank (Table 6.1). All of the new sequences were deposited on GenBank (KM043131 - KM043271). The coverage of 686 (52.4%) and 1054 (57.1%) is lower than that of COI (97.6%), 18S (92.9%), and 28S (90.5%). The average coverage is 78.1% with missing sequence data (in terms of 'N's in the alignment) averaging 16.9%. Fifteen specimens had complete coverage for all five loci, and missing data was typically either 686 or 1054. The final dataset included 42 taxa representing 16 of the 19 known bdelloid genera, and multiple specimens within each genus for 11 of those.

Congruence among the phylogenetic methods

All of these phylogenetic analyses (Fig. 6.2; Fig. S6.2; Fig. S6.3) produce trees with typically high support at the tips but lower backbone support; this is particularly true of the maximum likelihood analysis (Fig. S6.3), which, outside of placing *Mniobia* and *Didymoactylos* as being sister to all other bdelloids, had very little backbone support and long branches associated with missing sequence data. The most likely Bayesian inferred tree had no topological constraints (Supplementary File S6.1) and included nucleotide alignments for noncoding 18S and 28S rDNA, and amino acid alignments for the three protein coding loci (COI mtDNA, 686 nuDNA, and 1054 nuDNA). The topological similarity of the RAxML and best BEAST tree was 75.5%.

Figure 6.2 Phylogenetic tree inferred by Bayesian inference with the most likely substitution model for each of the five loci and no topological constrains imposed on the model.
Nodes with a posterior probability value or more than 0.95 are denoted by black circles, nodes with more than 0.8 support are denoted with white diamonds, and nodes with more than 0.7 support are denoted with white squares. Node support less than 0.7 are not shown. The scale bar represents the age (MYR) of the clade. Pictures were adapted from Donner (1965), Segers and Shiel (2005), Birky et al. (2011), and Iakovenko et al. (2013).

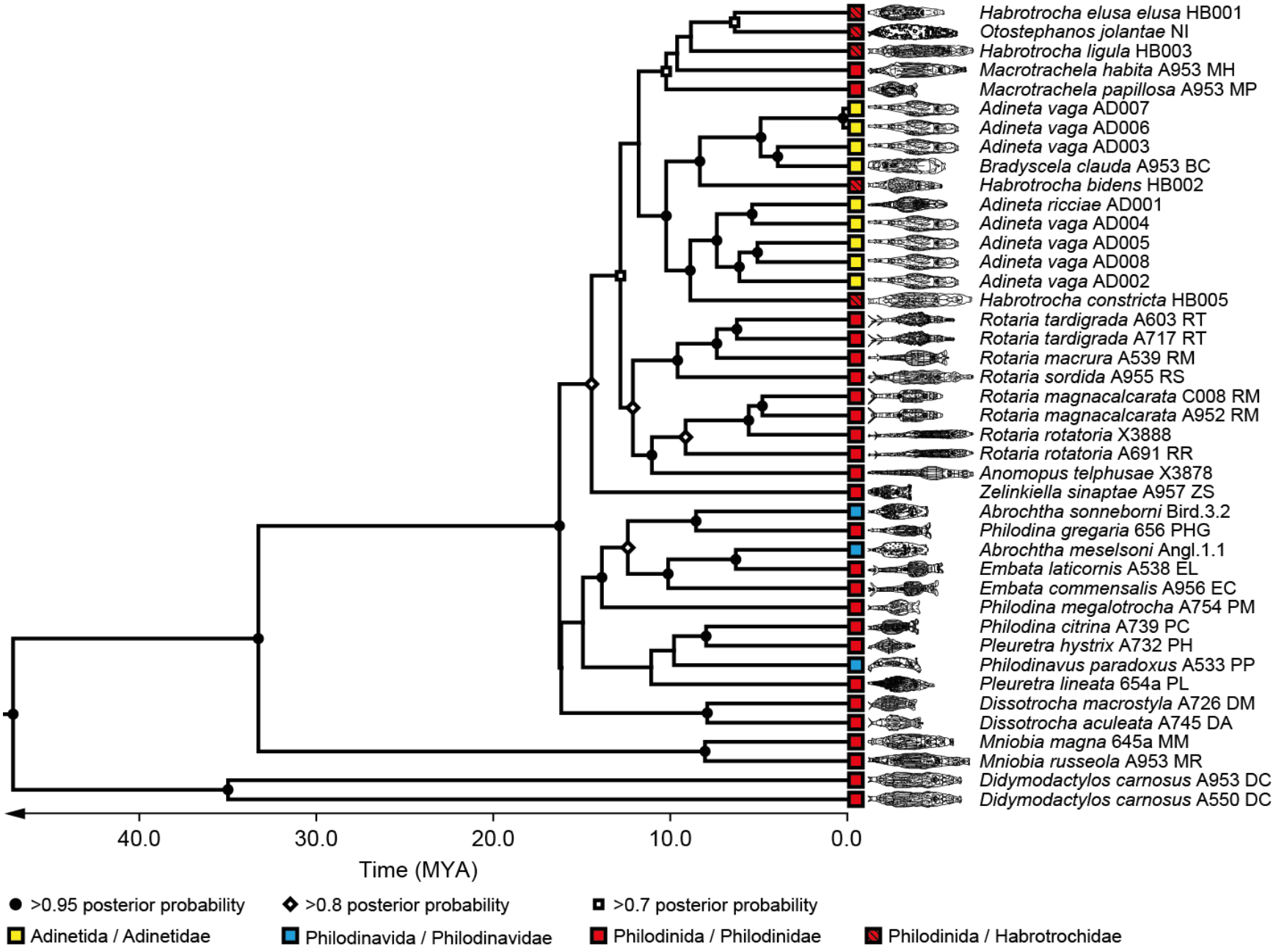
Habrotrocha elusa elusa HB001
Otostephanos jolantae NI
Habrotrocha ligula HB003
Macrotrachela habita A953 MH
Macrotrachela papillosa A953 MP
Adineta vaga AD007
Adineta vaga AD006
Adineta vaga AD003
Bradyscela clauda A953 BC
Habrotrocha bidens HB002
Adineta ricciae AD001
Adineta vaga AD004
Adineta vaga AD005
Adineta vaga AD008
Adineta vaga AD002
Habrotrocha constricta HB005
Rotaria tardigrada A603 RT
Rotaria tardigrada A717 RT
Rotaria macrura A539 RM
Rotaria sordida A955 RS
Rotaria magnacalcarata C008 RM
Rotaria magnacalcarata A952 RM
Rotaria rotatoria X3888
Rotaria rotatoria A691 RR
Anomopus telphusae X3878
Zelinkiella sinaptae A957 ZS
Abrochtha sonneborni Bird.3.2
Philodina gregaria 656 PHG
Abrochtha meselsoni Angl.1.1
Embata laticornis A538 EL
Embata commensalis A956 EC
Philodina megalotrocha A754 PM
Philodina citrina A739 PC
Pleuretra hystrix A732 PH
Philodinavus paradoxus A533 PP
Pleuretra lineata 654a PL
Dissotrocha macrostyla A726 DM
Dissotrocha aculeata A745 DA
Mniobia magna 645a MM
Mniobia russeola A953 MR
Didymodactylos carnosus A953 DC
Didymodactylos carnosus A550 DC
40.0
30.0
20.0
10.0
0.0
Time (MYA)
>0.95 posterior probability
>0.8 posterior probability
>0.7 posterior probability
Adinetida / Adinetidae
Philodinavida / Philodinavidae
Philodinida / Philodinidae
Philodinida / Habrotrochidae

Monophyly of bdelloid higher taxa

Separate BEAST analyses, partitioning the sequences *a priori* by genus, family, and order were less likely than the unconstrained model (Bayes factors: -172.373, -185.138, and -179.304, respectively; Table 6.3). The lower likelihood of the constrained phylogenetic analyses indicates that the majority of the sampled bdelloid higher taxa are not monophyletic. High likelihood of genus constrained models indicates that genus is a more plausible rank than order, which in turn had more support than the family rank (Table 6.3). Analysis of the intra- and interclade raw genetic distances for all the loci and for the concatenated alignment revealed large overlaps (Table 6.4; Fig. 6.3), although separate analyses revealed that COI and 18S genetic distances within genera are smaller than distances between genera (Table 6.4). Separate independent analyses of each locus with missing taxa pruned out confirmed much of the taxonomic polyphyly (Supplementary File S6.1), and show that these patterns are not an artefact of undersampling.

Table 6.3 Bayes factor analysis used to compare the likelihood of different phylogenetic analyses with four levels of topological constraint based on traditional taxonomic ranks (none, genus, family, order).

Constraint	Crown age	Height	Lower 95% HPD	Upper 95% HPD	ln P	S.E	None	Genus	Family	Order
None	47.13	51.77	42.49	61.08	-28595	± 0.051	-	127.16	290.86	289.80
Genus	56.68	53.36	43.93	64.44	-28887	± 0.155	-127.16	-	163.70	162.64
Family	27.22	26.75	22.86	30.70	-29264	± 0.1	-290.86	-163.70	-	-1.06
Order	23.07	26.77	22.93	30.97	-29262	± 0.099	-289.80	-162.64	1.06	-

Adineta and *Rotaria* were the two most densely sampled genera in these analyses (eight samples each), both of which did not form monophyletic clades. *Adineta* was forms a paraphyletic clade with *Bradyscela clauda* (the only other representative of the Adinetida order) and *Habrotrocha bidens* nested within it. These analyses confirmed that *Adineta vaga*, a dustbin taxa, is a polyphyletic clade (Fontaneto et al. 2011). The *Rotaria* samples formed a paraphyletic clade with the *Anomopus telphusae* sample nested within it. The two samples each of *Didymodactylos*, *Dissotrocha*, and *Mniobia* grouped together (1, 0.99, and 0.99 posterior probability, respectively), but the remaining genera with multiple samples (*Abrochtha*, *Embata*, *Habrotrocha*, *Macrotrachela*, *Philodina*, and *Pleuretra*) did not form monophyletic clades and were typically separated by nodes of strong support (Fig. 6.2). The deep divergence between the *Didymodactylos carnosus* samples warrants further investigation. None of the bdelloid orders (Adinetida, Philodinavida, and Philodinida) or families (Adinetidae, Philodinavidae, Habrotrochidae, and Philodinidae) were monophyletic in any of the unconstrained analyses (Fig. 6.2; Fig. S6.2; Fig. S6.3).

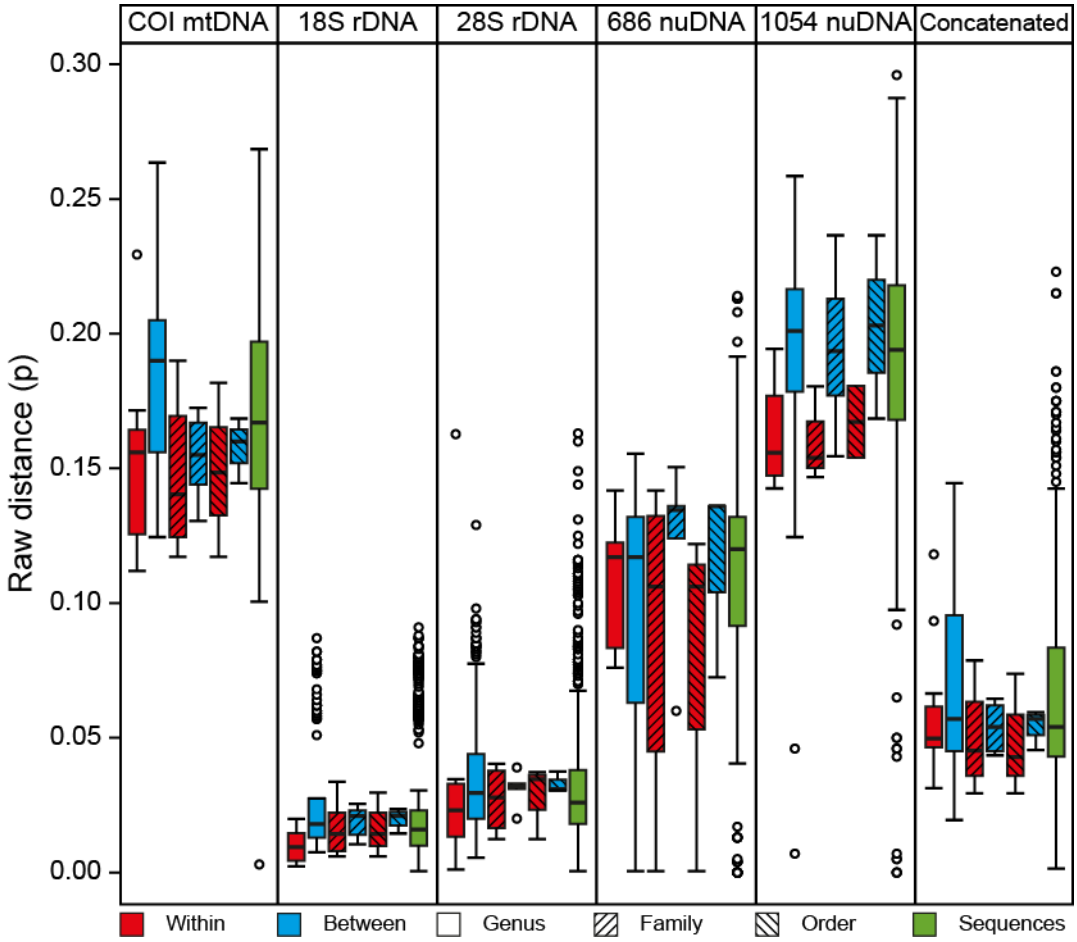

Figure 6.3 Raw genetic distances within and between genus (no hatch), family (up hatch) and order (down hatch) level groups, and among the sequences with no grouping (green).
The five loci (COI, 18S, 28S, 686, and 1054) and the concatenated alignments were analysed separately. Each box represents the distribution of raw genetic distances; median (thick black lines), first and third quartiles (box), 1.5 times the interquartile range (whiskers), and outliers (circles) are shown.

Age estimation

The reduced variation, and potentially saturation (Supplementary File S6.1), from using amino acid alignments for the protein coding genes (COI, 686, and 1054) instead of nucleotide alignments, resulted in much younger crown age estimates for Bdelloidea (Table S6.8). The overall best supported tree (i.e. no constraints and amino acid alignments for the 686 and 1054 amino acid alignments) suggested that the bdelloid crown age is 51.8 MYR (95% HPD = 42.5-61.1). Phylogenetic analyses of different partitions and analyses with different levels of constraint produced different age estimates (Table S6.8).

Table 6.4 Wilcoxon's signed rank test used to identify differences in raw genetic distance within and between taxonomic ranks (genus, family, and order). The five different loci and the concatenated alignment were analysed separately.

Gene	**Comparison**	**W**	***P***
Concatenated (nucleotide)	Genus	15307	0.31
	Family	605	0.19
	Order	184	0.31
COI mtDNA	Genus	868	0.01
	Family	14	0.76
	Order	5	1.00
18S rDNA	Genus	885	0.00
	Family	36	0.67
	Order	5	1.00
28S rDNA	Genus	696	0.15
	Family	12	1.00
	Order	5	1.00
686 nuDNA	Genus	135	0.96
	Family	17	0.34
	Order	7	0.38
1054 nuDNA	Genus	175	0.05
	Family	16	0.10
	Order	5	0.40

Discussion

These are the first multilocus, genus-level molecular phylogenetic analyses for Bdelloidea. The analyses included a multilocus sampling regime incorporating five genetic loci, representatives of 16 of the 19 bdelloid genera, all four families, and all three of the orders. Results from these analyses suggest that not all of the bdelloid higher taxa, historically delimited as early as 1777 (Scopoli, 1777 – *Rotaria*) and as recent as 1916 (Milne, 1916 – *Didymodactylos*, *Henoceros*, *Otostephanos*), are monophyletic groups. Dating of the phylogeny using evolutionary rates estimated by the best supported multilocus BEAST analysis suggests that the bdelloid crown age is 51.8 MYR old (with a wide range of 32-98 MYR depending on the phylogenetic analyses), this estimate is older than that of the limited fossil record (Poinar and Ricci 1992) and of our previous analysis (where we included fewer taxa and only two of the five genes used here – Tang et al. 2014). Combined, these results indicate the anciently asexual bdelloids (Flot et al. 2013) have not only persisted for millions of years despite tremendous evolutionary pressures (Bell 1982; Butlin 2002; Coyne and Orr 2004), but have also diversified, albeit not into higher taxonomic groups recognised consistently with respect to morphology.

Even with low backbone support in the tree, well supported sister taxa relationships (e.g. *Abrochtha meseloni* being sister to *Embata laticornis* and not *Abrochtha sonneborni*) indicate that bdelloid higher taxa are not monophyletic. The phylogenetic analyses presented here and in the Supplementary Files include different phylogenetic methods, different combinations of nucleotide and amino acid alignments, various topological constraints and separate loci, indicate that bdelloid higher taxa are not evolutionary entities.

Assuming our data and analyses are correct, we envisage two non-mutually exclusive reasons as to why these analyses do not support bdelloid higher taxa: either (1) bdelloid higher taxa, in their current form, do not reflect monophyletic clades, and/or (2) the phylogenetic signal among the five loci is incongruent and collectively inconclusive.

(1) The traditional taxonomic groupings were formed by extensive morphological analyses (e.g. Donner 1965; Melone and Ricci 1995; Birky et al. 2011), which constitute a difficult undertaking confounded by the malleability and plasticity of the telescopic bodies of bdelloid rotifers (Fontaneto et al. 2007d). Bdelloid morphological assessments have been based primarily on discrete characteristics: orders are historically defined based on mastax and trochi morphology, families are defined by a combination of trochi and gut morphology, and genera are defined based of various aspects of their foot, integument, teeth, and egg morphologies.

It remains plausible that aspects of their morphologies are plastic and potentially convergent for particular niches. In principle, convergent evolution of different trochi, teeth, and mastax

characteristics might result from divergent selection associated with feeding. For example, food particle size has been hypothesised as the driving force behind mastax shape and size variation in *Rotaria* (Fontaneto et al. 2007d), while the macrophage *Abrochtha carnivora* (Ricci et al. 2001) has unique trochi characteristics (more minor teeth, more widely separated major teeth, larger trophi, but similar body plans) that suit its predatory behaviour. Although, the homogeneity of Philodinida and Adinetida trophi structure, despite their different corona shape (fan versus field) and feeding patterns (filter versus scraping), and the taxonomic irrelevance of certain trophi characteristics (i.e. the number of uncus teeth), is surprising (Melone et al. 1998a). Detailed ultrastructure morphometric analyses of bdelloid jaws (e.g. Melone et al. 1998a; Fontaneto et al. 2007c) needs to be combined with meticulous observations of their feeding ecology to test whether, across the entirety of Bdelloidea, the evolution of the masticatory apparatus is related to their diet.

Similarly foot morphology might evolve under selection for specific locomotion plans in specific habitats. In principle habitation of ephemeral environments might drive the evolution of more powerful foot morphologies. This expectation is contradicted by the fact that most genera live in most habitats (Fontaneto et al. 2008a), seemingly unassociated with their morphologies.

It is likely that there is some degree of unresolved higher taxonomy of bdelloids is associated with the use of taxonomically uninformative characteristics, but the convergent evolution of complex multifaceted morphologies and ecologies seems unlikely given that phylogenetic constraints are likely more stringent in ameiotic asexual organisms. Overarching claims of convergent evolution are difficult to test in a group of detritivorous, ubiquitous species, which are seemingly indifferent to habitat type, although a thorough, class-wide examination of morphology with ecology is lacking.

(2) The observed patterns are driven heavily by some of the genes and so the concatenation of all of these partitions and their combined analysis might not be representative of the true phylogeny (although other studies have argued that congruence among genes is not a requirement for combining different partitions - Zanol et al. 2010). Theoretically in asexuals, the entire genome is linked and should be inherited as a single unit (Barraclough et al. 2003), but different genomic regions (i.e. mitochondria, ribosomes, and the nucleus) are likely under different evolutionary pressures. For example, high metabolic rates in the mitochondria could be invoked to explain the faster rate of evolution in the COI (Castellana et al. 2011), or the relaxed selection and redundancy of 1054 might be a product of its non-Metazoan origin (Eyres 2013). The rapidly evolving genes sampled here (particularly 1054 and 686, which had the highest evolutionary rates of 2.36% MYR^{-1} and 6.54% MYR^{-1}, respectively) might have a higher degree of saturation leading to discordance with the other loci. Even still, phylogenetic analyses of each of the different loci (nucleotide or amino acid), with varying levels of support, indicate that higher taxa are not monophyletic.

For the second explanation additional taxonomic sampling and the addition of more nuclear loci under putatively varying levels of selection will aid in confirming or refuting the patterns observed here. The primary issue with the phylogeny is the lower support in the backbone. The first half of the tree (from the root) has an average node support of 0.88 compared to the second half, which has an average node support of 0.97. While ML analyses of the nuclear loci on their own with no missing taxa pull out similar sister taxa topologies to the unconstrained concatenated tree, filling in these sampling gaps will be necessary to evaluate their effect on the concatenated analysis. The level of intrageneric sampling is relatively low and only with the collection of additional species for each of the genera will we be able to fully evaluate the monophyly of these taxa. However, *Rotaria* and *Adineta*, which both have eight representatives, are not monophyletic in any of the six unconstrained trees and typically split with strongly supported nodes. It remains to be seen whether the genera *Ceratotrocha*, *Henoceros*, and *Scepanotrocha* are monophyletic.

In explaining the high levels of polyphyly reported here, it might be difficult for phylogenetic analyses to pull out monophyletic clades in animals with small body sizes, where there are few dedicated taxonomists and the characteristics used to define them might be less informative or misleading. Phylogenetic analyses of other meiofaunal animals using similar loci (typically 18S, 28S, and COI) have produced mixed results, some are congruent with traditional higher taxa (e.g. annelids - Struck and Purschke 2005; gnathostomulids - Sørensen and Giribet 2006), while others have split up previously known higher taxa (e.g. gastrotrichs - Littlewood et al. 2000; annelids - Zrzavý et al. 2009; tardigrades - Jørgensen et al. 2010; gastrotrichs - Kånneby et al. 2011, Chaetonotidae - 2013; gastrotrichs - Todaro et al. 2011; kinorhynchs - Yamasaki et al. 2013).

Throughout this study we have use point estimates for the substitution rates for both COI and 18S instead of a more nebulous estimate incorporating the entire confidence limits surrounding those estimates. Here we have used two substitution rate estimates (COI – 1.76% MYR^{-1} and 18S – 0.02% MYR^{-1}) and estimated the rates of the other genes from the posterior distribution; each undoubtedly has a lot of uncertainty surrounding these estimates. While the Wilke et al. (2009) substitution rate estimate of COI evolving under a GTR+I+Γ model has a 95% confidence interval of 0.66% MYR^{-1} based on a mean of five Gastropoda (Hellberg and Vacquier 1999; Wilke 2003), Annelida (Chevaldonné et al. 2002), and Decapoda datasets (Knowlton and Weigt 1998; Schubart et al. 1998), the Ochman and Wilson (1987) 18S estimate has no published error rate. The choice of using point estimates of these rates was based on the practicality of simultaneously estimating the phylogeny and the rates. Clearly, the age estimates of these phylogenies is inherently affected by the rates that we define, and while the error margin of these dates is large, we do not envisage the ancientness of bdelloid asexuality being refuted by even the lower estimated substitution rates of these genes. Indeed, the youngest age estimate of the bdelloid crown age, including all the various combinations of genes and the lower bounds of their 95% highest posterior probabilities, returned a date that is

undeniably ancient (7.15 MYR - lower 95% posterior probability of a concatenated dataset with three out of five amino acid partitions). Nevertheless, future iterations of this phylogeny will encompass broader, more encompassing estimates of the rates at which these genes evolve.

Additional independent nuclear loci will potentially help resolve the backbone and add further weight on to the more recent relationships. We are currently trialling whole genome amplification kits and the sequencing of an additional 50 nuclear primer pairs designed from the transcriptomic alignments generated by Eyres (2013). Soon we will be able to generate a larger number of independent, orthologous reads for each specimen and use these to build upon these foundations. A combined molecular morphological approach could improve cohesiveness within higher taxa. These additional steps will be necessary to confirm or refute the findings presented here, namely, that bdelloid higher taxa are not monophyletic.

Chapter 7: Discussion

In this thesis, I have investigated biodiversity patterns in rotifers and what role reproductive mode has played in shaping it. Specifically, the thesis has provided more substantiated empirical evidence to answer: (1) how can molecular techniques be adopted to better assess rotifer biodiversity, (2) why do species exist as discrete entities as opposed to a continuum of forms, and (3) are named bdelloid higher taxa monophyletic? Here I will summarise the main findings of the chapters with respect to these three questions, explain how they fit in with the current state of scientific theory, and discuss the avenues of research they opened up.

(1) How can molecular techniques be adopted to better assess bdelloid biodiversity?

The first section of this thesis (Chapters 2-4) examined different aspects of the DNA taxonomy process and indicates that changing the parameters (i.e. different genes, species delimitation metrics, and phylogenetic reconstruction methods) has a significant impact on the final biodiversity estimation. These chapters are the largest comparisons for their respective purposes and conclusions drawn therein can be used for any DNA taxonomy study, including single-locus and next generation species delimitation studies.

Chapter 2

The massive underestimation of biodiversity using 18S rDNA in meiofauna morphological species estimates diminish its potential for species-level delimitation (Tang et al. 2012). In contrast, species delimitation with COI oversplits diversity relative to the, likely conservative, morphospecies estimate. The conservativeness of these morphological estimates for meiofauna was already known (Ciros-Perez 2001; Westheide and Hass-Cordes 2001; Gómez et al. 2002; Blaxter et al. 2004; Suatoni et al. 2006; Fontaneto et al. 2009; Kaya et al. 2009; Kieneke et al. 2012), so their splitting using COI mtDNA was encouraging. Furthermore, this splitting of morphospecies was true irrespective of the various species delimitation metrics (nucleotide similarity - Hebert et al. 2003a; K/θ - Birky et al. 2005; GMYC - Pons et al. 2006; ABGD - Puillandre et al. 2012a) and is congruent with conclusions drawn from crossing experiments (Schröder and Walsh 2007). Although the investigation focussed on meiofaunal lineages, 5 of the 10 phyla include large-bodied representatives. Conclusions drawn from the Chapter 2 are broad and applicable to larger organisms, indeed Tang et al (2012) has helped studies of taxa ranging from amphipods (Weiss et al. 2014) to Collembola (Cicconardi et al. 2013).

The investigation promotes COI, over 18S, for use with next generation sequencing (NGS) biosurveys, which are growing in popularity (Creer et al. 2010; Fonseca et al. 2010; Bik et al. 2012a). What NGS technology can do for biodiversity research is equivalent to what microscopes did for

microbiology. The smaller scale fauna that are so quintessential for much of the Earth's natural processes, which have been relatively neglected due to a technological bottleneck associated with their size, are now accessible via their molecules (Taberlet et al. 2012; Yoccoz 2012). So far, most NGS studies have used 18S to assess species-level diversity (Creer et al. 2010; Fonseca et al. 2010; Bik et al. 2012c; Creer and Sinniger 2012; Chariton et al. 2014) owing to the fact that 18S has a longer history of use with whole community surveys, has highly conserved regions with which primers can be designed across a wide range of taxa, and variable regions with which to delineate taxa. An independent performance comparison of 18S rDNA, 16S mtDNA, and COI mtDNA, using actual NGS technologies instead of the Sanger technologies used in this thesis, is congruent with the conclusion that 18S has low resolution at lower taxonomic scales (Zhan et al. 2014). Given that biotic interactions act at or below the species-level, the underestimation of species level diversity using this gene will likely limit what we can conclude about the composition and evolution of communities and how these taxa interact ecologically. To date, the study has been cited 33 times and used to justify gene (e.g. Cicconardi et al. 2013; Casu et al. 2014; Chariton et al. 2014; Weiss et al. 2014) and species delimitation method choice (e.g. Birky 2013; Fujisawa and Barraclough 2013; Leasi et al. 2013) in DNA taxonomy studies, or used for particular methods used in the paper (e.g. Fontaneto 2014; Tang et al. 2014b). Of these investigations most have been traditional, targeted DNA taxonomy studies or have adopted NGS technology.

What is the future of COI and metabarcoding?

There is already a huge foundation for COI-based taxonomy (i.e. BOLD - Ratnasingham and Hebert 2007) as COI is the most widely used marker for first generation DNA taxonomy. If species-level, and not higher taxa, biodiversity is the primary goal of metabarcoding surveys, then a broader evaluation of COI primer sets is required, perhaps redesigned primers (e.g. Geller et al. 2013; Leray et al. 2013), primer cocktails (e.g. Prosser et al. 2013b), or lineage specific primers (e.g. Robeson et al. 2009; Prosser et al. 2013a). Approaches such as those adopted by Yu et al. (2012), where communities of known composition and abundances are used to evaluate primers, would be a good start. As yet the efficacy of robust COI primer sets for metabarcoding surveys is unknown, but the potential benefits of this combined approach are huge.

Two alternatives to this pipeline include the design of case-specific primers for PCR-based NGS using aligned genomes (ecoPrimers - Riaz et al. 2011), or PCR-free methods (Fig. 7.1; Zhou et al. 2013). The future of NGS metabarcoding of bulk samples is likely a PCR-free pipeline (Zhou et al. 2013). Instead of the bulk pyrosequencing and OTU clustering of PCR amplified markers, the PCR-free method consists of mitochondrial enrichment followed by Illumina shotgun sequencing and gene annotation. This provides an abundance of longer COI barcodes, proportional to the biomass of the constituents of the bulk sample (allowing for rough abundance measures), with a vastly reduced false positive rate, and which can be used for DNA barcoding or DNA taxonomy. Moreover, the longer

spans of mtDNA can be used to design more robust and effective COI primers. However, this PCR-free pipeline is still in its infancy and requires the methodological improvements for the assessing of more diverse communities (Zhou et al. 2013).

Assessing biodiversity using single locus approaches does have its limitations (as discussed in the Chapter 1), for example, results based on a single locus (e.g. COI) will not be representative of the evolution of those species if the focal gene is incongruent with other loci and the species phylogeny (Sota and Vogler 2001; Rubinoff 2006; Rubinoff et al. 2006) - the likelihood is that one gene does not fit all (Moritz and Cicero 2004). Species delimitation, using targeted sampling approaches or bulk sampling regimes, is going to adopt multiple loci from different genomic backgrounds (different organelles such as nuclear, mitochondrial, chloroplast, ribosomal genes) or whole genomes. The amalgamation of data from different sources, by dampening the potential biases inherent in few, will lead to more reliable and accurate definitions of the species boundary. Progress towards these multigene approaches are currently limited by the current technologies and theoretical models, although advances in both are ongoing (e.g. Cummings et al. 2008; Yang and Rannala 2010; Zhou et al. 2013). Until these systems are in place, choosing which genetic markers to use for biosurveys will be an important decision that needs to be justified.

Chapter 3

Chapter 3 was an investigation of how robust two coalescent-based (phylogenetic) species delimitation metrics (GMYC - Pons et al. 2006; PTP - Zhang et al. 2013) were to different phylogenetic reconstruction methods, and thus provided recommendations for which phylogenetic methods to use for each metric. Combined, these methods have been used to delimit species in over 150 studies, but rarely are the phylogenetic reconstruction methods justified (although see Talavera et al. 2013). I found that the choice in phylogenetic method as well as the species delimitation metric strongly affected the observed diversity but that diversity estimated using the GMYC and BEAST trees, or the PTP with RAxML trees were robust relative to morphological species estimates and the average molecular estimates.

This is one of two investigations into the effect of phylogenetic reconstruction methods on species delimitation (the other being an assessment of phylogenetic method choice on the GMYC model - Talavera et al. 2013), and is by far the most comprehensive in terms of phylogenetic methods, species delimitation metrics, and taxonomic groups used. It provides strong justification for choice in phylogenetic methods used for these types of studies and is timely given the recent release of the PTP method.

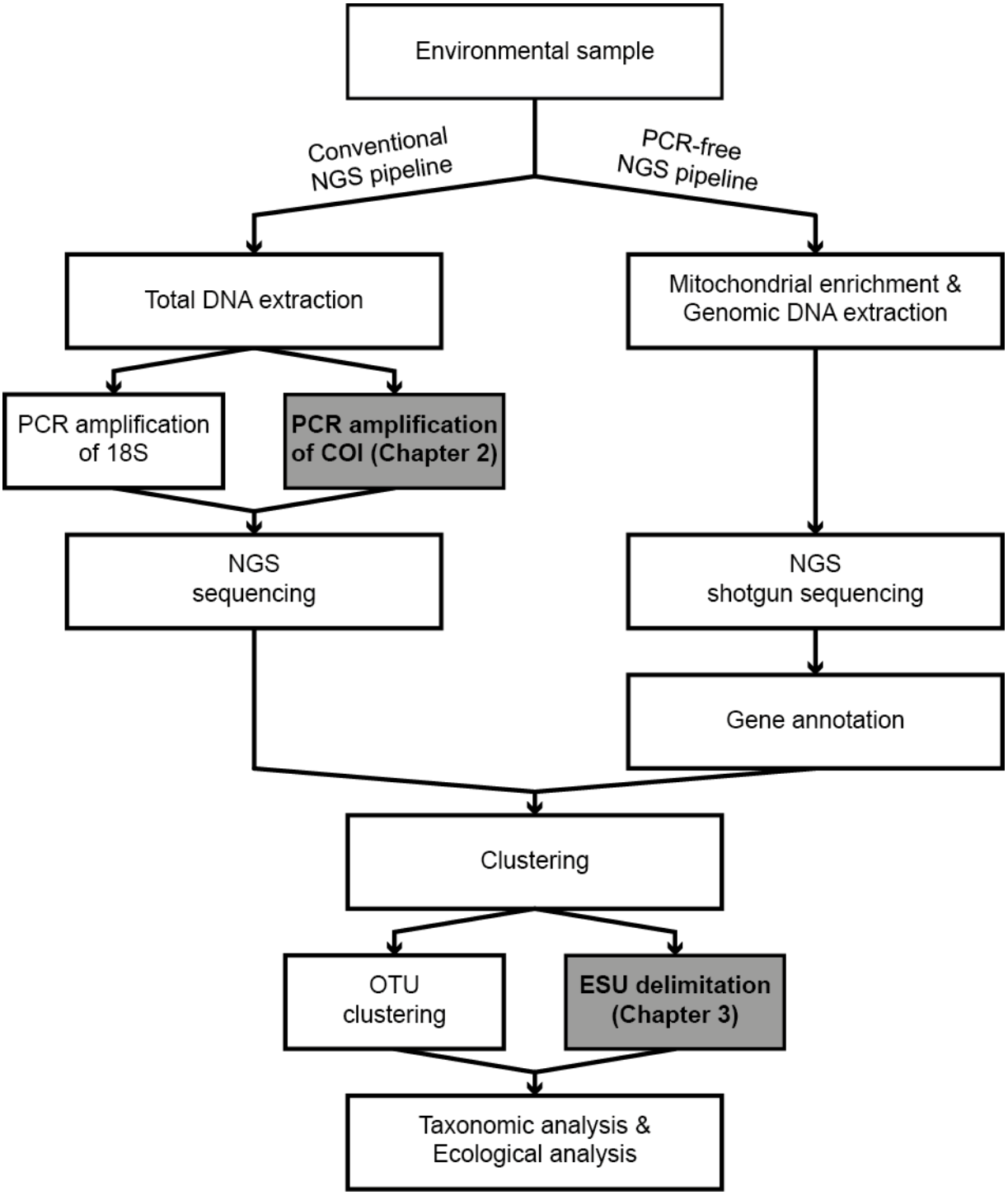

Figure 7.1 Schematic pipelines for both conventional PCR-based and PCR-free NGS metabarcoding.
Grey boxes indicate novel findings/suggestions from this thesis. Adapted from Zhou et al. (2013).

Can coalescent-based species delimitation be used for metabarcoding?

Metabarcoding approaches produce so much data that the bottleneck in biodiversity surveys is in the bioinformatics rather than the sequencing, as such species are typically clustered by relatively computationally inexpensive methods such as nucleotide similarity (QIIME - Caporaso et al. 2010; OCTUPUS – available from http://octupus.sourceforge.net/; AmpliconNoise - Quince et al. 2011) or phylogenetic placement (pplacer - Matsen et al. 2010). Despite showing that nucleotide similarity producing similar levels of diversity compared to more evolutionary robust methods (e.g. GMYC, K/θ - Tang et al. 2012), the thresholds used are arbitrary and without evolutionary grounding. The adoption of coalescent-based species delimitation methods (e.g. GMYC - Pons et al. 2006; PTP - Zhang et al. 2013; Fig. 7.1) for larger scale analyses has huge potential (Barraclough et al. 2009). Still, the computational expense of this process (either building phylogenies or delimiting clusters) is the main reason as to why these methods are not more widely used (Zhang et al. 2013). A collaborative effort is currently underway to find a means to delimit coalescent groups from NGS derived datasets (i.e. a pipeline that delimits GMYC or PTP ESUs from NGS data). The aim is to provide an automated pipeline that takes sequences (NGS or Sanger) and provides units of diversity grounded in evolutionary theory.

Chapter 4

Chapter 4 is an investigation into how successfully rotifers, delimited by traditional or molecular means, can be identified by DNA barcoding. The greater identification success of dustbin taxa so prevalent in Rotifera and of sexual monogonont rotifers compared to the asexual bdelloid rotifers suggests two things: (1) poor taxonomy can artificially inflate the success of DNA barcoding studies, and (2) the properties of sexual taxa might make them more amenable to DNA barcoding (investigated further in Chapter 5). Furthermore, no study has looked at identification success of DNA barcoding with ESUs as the base unit of diversity, which might become more prevalent given the taxonomic crisis (i.e. the paucity of traditional taxonomists and the prevalence of inaccessible, cryptic diversity).

These three chapters culminate in guidelines that could be used to obtain better species hypotheses in the absence of or in addition to other informative morphological, ecological, and behavioural characteristics. In summary, the use of either the GMYC model with BEAST trees or the PTP with RAxML trees reconstructed using cytochrome oxidase *c* subunit 1 (COI) mtDNA will provide putative species estimates that are better than traditional estimates based on rotifer morphology, grounded in evolutionary theory, and under a single species concept. We are in the midst of a taxonomic crisis (Blaxter 2003); while the number of taxonomists and species descriptions may be on the rise in more charismatic groups (Joppa et al. 2011), for poorly known groups the pattern is reversed (Gaston and May 1992; Godfray 2002). The promise of DNA taxonomy, particularly with

NGS, yields an opportunity to build an extensive foundation with which a broad taxonomic assessment can be made for lesser studied groups (e.g. Blaxter et al. 2004).

The immediate impact of Chapters 2-4 was the justification of DNA taxonomy methods necessary for delimiting comparable units of diversity for use in Chapter 5. The taxonomy of rotifers is poorly known, and the different reproductive modes of bdelloid and monogonont rotifers make them incomparable under the biological species concept (Mayr 1942; de Queiroz 2005b). Using robust DNA taxonomy methods outlined and tested in Chapters 2-4, both bdelloid and monogononts evolutionary significant units of biodiversity can be compared under the same evolutionary genetic species concept (Simpson 1951; Birky et al. 2005; De Queiroz 2007), while also circumventing the unresolved taxonomy of both groups.

(2) Why do species exist as discrete entities as opposed to a continuum of forms?

Chapter 5

Chapter 5 provides empirical evidence to answer one of the most neglected and important questions about speciation: "Why are there species?" (Coyne and Orr 2004), specifically, why do species exist as discrete clusters rather than a continuum of morphological, ecological, and genetic forms? By comparing sexual and asexual rotifers, one can tease apart sex-centric and ecological theories (Maynard Smith and Száthmary 1995; Coyne and Orr 2004). The previous assessments of this question using rotifers (Holman 1987; Fontaneto et al. 2007c) lacked sampling regimes that could adequately address this question (Coyne and Orr 2004), used diversity estimates that were not comparable between asexual bdelloid and sexual monogonont rotifers (De Queiroz 2007), and were confounded by different degrees of taxonomic effort between the groups (Fontaneto et al. 2007c). Our analysis follows a method proposed by Barraclough and Herniou (2003), and provides the best empirical evidence to date in answering this conundrum, that sex is a predominant driver of species discreteness.

I assessed the degree of discreteness in asexual bdelloid and sexual monogonont rotifers, and analysed how differences related to their reproductive mode, degree of sampling, and their ecology. The results suggest that sexual species are separated by larger gaps than in asexual species in rotifers (Tang et al. 2014b), a conclusion preferred over the sampling or ecological explanations. Analysis of their diversification rates indicate that asexual bdelloids have speciated at a faster rate than the sexual monogononts (Felsenstein 1981) and not an age artefact (Neiman et al. 2009). Combined, I proposed that the faster diversification in asexual bdelloid rotifers results in the smaller observed genetic gaps. This study provides the best evidence for a long standing question in speciation biology: "why are there species?" (Maynard Smith and Száthmary 1995; Coyne and Orr 2004).

Does a targeted sampling regime, rather than an opportunistic one, confirm sex as a primary driver for discreteness of species clusters?

While the observed differences in genetic and phylogenetic clustering are striking, they are conclusions drawn from a single locus (Tang et al. 2014b). COI was chosen opportunistically given the breadth and depth of sampling available on GenBank but it remains to be seen whether these patterns are congruent with other loci and morphologies. Furthermore, despite efforts to disentangle the effects of sampling, ecology, and reproductive mode on species discreteness, the findings are still confounded by alternative hypotheses that are only resolvable with a carefully designed sampling regime. It would be an enormous undertaking to produce a level of taxonomic sampling similar to those reported in Chapter 5, but might be feasible with NGS. Metabarcoding bulk samples of sympatric bdelloid and monogonont species using specific primers might alleviate the confounding issues regarding ecological differences. The claim that sex is the predominant driver of species discreteness can only really be fully justified once the confounding factors are ruled out, but until then this chapter provides the most substantiated answer as to why species are discrete.

(3) Are named bdelloid higher taxa monophyletic?

Chapter 6

Chapter 6 is the first multilocus phylogeny for the group and indicates that bdelloid higher taxa (genera, families, and orders) are rife with polyphyly and that traditional taxonomic relationships (e.g. Melone et al. 1998b) are not supported. Furthermore, an up to date age estimate for bdelloid rotifers, combined with the monophyly concluded from Chapter 5 (Tang et al. 2014b), suggests that bdelloids have been anciently asexual for 51.8 MYR (95% HPD = 42.5-61.1). This age varies with phylogenetic methods, but the range is mostly consistent with the minimum age estimated from the fossil record (Waggoner and Poinar 1993). This investigation is the foundation for a larger scale investigation of the taxonomic relationships within Bdelloidea.

Will additional loci and samples provide better backbone support and more agreement with traditional taxonomy?

This phylogeny is confounded by incomplete sampling for the nuclear loci, and perhaps by incongruences between loci. Currently, the limit for phylogenetic analyses with rotifers, or indeed meiofauna, is the sequencing of multiple independent nuclear loci. However, more than 350 primer pairs have been designed using transcriptomic data from Eyres (2013), of these, only two were used for the phylogeny. The sequencing of additional loci was limited by the amount of starting template available for each individual rotifer. Rotifers are eutelic, and thus the number of cells (900-1,000) remains constant throughout the life cycle of the rotifer (Gilbert 1983), and so the amplification of specific loci is often difficult. Preliminary results suggest whole amplification kits can be used to produce copious amount of genomic DNA with which to PCR. The next stage of this phylogenetic

project would be to sequence many more loci for each individual, but also to add more samples (bdelloid and monogonont). To this end, there exists a network of bdelloid taxonomists (i.e. Carl William Birky Jr., Diego Fontaneto, Nataliia Iakovenko, and Chris Wilson) who can provide genetic material for a much greater sample of rotifer diversity.

Overall conclusion

This thesis provides a robust analysis of factors that affect species delimitation and as such provides recommendations for the practise. I also suggest that sex is the predominant driver of species discreteness, at least in rotifers. Lastly, the phylogeny is the broadest sample ever used for a bdelloid phylogeny. Together these chapters show how molecular approaches can transform understanding of diversity and evolution in a challenging study clade.

References

Abascal, F., R. Zardoya, and D. Posada. 2005. ProtTest: selection of best-fit models of protein evolution. Bioinformatics 21:2104–5.

Agnarsson, I., and M. Kuntner. 2007. Taxonomy in a changing world: seeking solutions for a science in crisis. Syst. Biol. 56:531–9.

Arkhipova, I. R., and M. Meselson. 2005. Deleterious transposable elements and the extinction of asexuals. BioEssays 27:76–85.

Arkhipova, I. R., and M. Meselson. 2000. Transposable elements in sexual and ancient asexual taxa. Proc. Natl. Acad. Sci. U. S. A. 97:14473–7.

Ashman, T.-L., D. Bachtrog, H. Blackmon, E. E. Goldberg, M. W. Hahn, M. Kirkpatrick, J. Kitano, J. E. Mank, I. Mayrose, R. Ming, S. P. Otto, C. L. Peichel, M. W. Pennell, N. Perrin, L. Ross, N. Valenzuela, and J. C. Vamosi. 2014. Tree of Sex: A database of sexual systems. Sci. Data 1:1–8.

Astrin, J. J., P. E. Stüben, B. Misof, J. W. Wägele, F. Gimnich, M. J. Raupach, and D. Ahrens. 2012. Exploring diversity in cryptorhynchine weevils (Coleoptera) using distance, character and tree based species delineation. Mol. Phylogenet. Evol. 63:1–14.

Baele, G., P. Lemey, T. Bedford, A. Rambaut, M. A. Suchard, and A. V Alekseyenko. 2012. Improving the accuracy of demographic and molecular clock model comparison while accommodating phylogenetic uncertainty. Mol. Biol. Evol. 29:2157–67.

Baele, G., P. Lemey, and S. Vansteelandt. 2013. Make the most of your samples: Bayes factor estimators for high-dimensional models of sequence evolution. BMC Bioinformatics 14:85.

Baer, A., C. Langdon, S. Mills, C. Schulz, and K. Hamre. 2008. Particle size preference, gut filling and evacuation rates of the rotifer *Brachionus* "Cayman" using polystyrene latex beads. Aquaculture 282:75–82.

Baker, C., and S. Palumbi. 1994. Which whales are hunted? A molecular genetic approach to monitoring whaling. Science 265:1538–1539.

Bargues, M. D., A. Marcilla, J. M. Ramsey, J. P. Dujardin, C. J. Schofield, and S. Mas-Coma. 2000. Nuclear rDNA-based molecular clock of the evolution of triatominae (Hemiptera: reduviidae), vectors of Chagas disease. Mem. Inst. Oswaldo Cruz 95:567–73.

Barraclough, T. G., C. W. Birky, and A. Burt. 2003. Diversification in sexual and asexual organisms. Evolution 57:2166–2172.

Barraclough, T. G., D. Fontaneto, C. Ricci, and E. A. Herniou. 2007. Evidence for inefficient selection against deleterious mutations in cytochrome oxidase I of asexual bdelloid rotifers. Mol. Biol. Evol. 24:1952–62.

Barraclough, T. G., and E. A. Herniou. 2003. Why do species exist? Insights from sexuals and asexuals. Zoology 106:275–82.

Barraclough, T. G., M. Hughes, N. Ashford-Hodges, and T. Fujisawa. 2009. Inferring evolutionarily significant units of bacterial diversity from broad environmental surveys of single-locus data. Biol. Lett. 5:425–8.

Barraclough, T. G., and S. Nee. 2001. Phylogenetics and speciation. Trends Ecol. Evol. 16:391–399.

Bates, D. M., M. Maechler, B. M. Bolker, and S. Walker. 2014. lme4: Linear mixed-effects models using Eigen and S4. R package version 1.1-7.

Bell, G. 1982. The Masterpiece of Nature. University of California Press, Berkeley, CA.

Bergsten, J., D. T. Bilton, T. Fujisawa, M. Elliot, M. T. Monaghan, M. Balke, L. Hendrich, J. Geijer, J. Herrmann, G. N. Foster, I. Ribera, A. N. Nilsson, T. G. Barraclough, and A. P. Vogler. 2012. The effect of geographical scale of sampling on DNA barcoding. Syst. Biol. 61:851–869.

Bhadury, P., M. C. Austen, D. T. Bilton, P. J. D. Lambshead, A. D. Rogers, and G. Smerdon. 2006. Development and evaluation of a DNA-barcoding approach for the rapid identification of nematodes. Mar. Ecol. Prog. Ser. 320:1–9.

Bik, H. M., K. M. Halanych, J. Sharma, and W. K. Thomas. 2012a. Dramatic shifts in benthic microbial eukaryote communities following the Deepwater Horizon oil spill. PLoS One 7:e38550.

Bik, H. M., D. L. Porazinska, S. Creer, J. G. Caporaso, R. Knight, and W. K. Thomas. 2012b. Sequencing our way towards understanding global eukaryotic biodiversity. Trends Ecol. Evol. 27:233–243.

Bik, H. M., W. Sung, P. De Ley, J. G. Baldwin, J. Sharma, A. Rocha-Olivares, and W. K. Thomas. 2012c. Metagenetic community analysis of microbial eukaryotes illuminates biogeographic patterns in deep-sea and shallow water sediments. Mol. Ecol. 21:1048–1059.

Birky, C. W. 2010. Positively negative evidence for asexuality. J. Hered. 101:S42–5.

Birky, C. W. 2013. Species detection and identification in sexual organisms using population genetic theory and DNA sequences. PLoS One 8:e52544.

Birky, C. W. 2007. Workshop on barcoded DNA: application to rotifer phylogeny, evolution, and systematics. Hydrobiologia 593:175–183.

Birky, C. W., J. Adams, M. Gemmel, and J. Perry. 2010. Using population genetic theory and DNA sequences for species detection and identification in asexual organisms. PLoS One 5:e10609.

Birky, C. W., and T. G. Barraclough. 2009. Asexual speciation. Pp. 201–216 *in* I. Schön, K. Martens, and P. van Dijk, eds. Lost Sex - The Evolutionary Biology of Parthenogenesis. Springer, Dordrecht.

Birky, C. W., C. Ricci, G. Melone, and D. Fontaneto. 2011. Integrating DNA and morphological taxonomy to describe diversity in poorly studied microscopic animals: new species of the genus *Abrochtha* Bryce, 1910 (Rotifera: Bdelloidea: Philodinavidae). Zool. J. Linn. Soc. 161:723–734.

Birky, C. W., C. Wolf, H. Maughan, L. Herbertson, and E. Henry. 2005. Speciation and selection without sex. Hydrobiologia 546:29–45.

Blaalid, R., T. Carlsen, S. Kumar, R. Halvorsen, K. I. Ugland, G. Fontana, and H. Kauserud. 2012. Changes in the root-associated fungal communities along a primary succession gradient analysed by 454 pyrosequencing. Mol. Ecol. 21:1897–1908.

Blaxter, M. L. 2003. Counting angels with DNA. Nature 421:122–124.

Blaxter, M. L. 2004. The promise of a DNA taxonomy. Philos. Trans. R. Soc. Lond. B. Biol. Sci. 359:669–79.

Blaxter, M. L., B. Elsworth, and J. Daub. 2004. DNA taxonomy of a neglected animal phylum: an unexpected diversity of tardigrades. Proc. R. Soc. London B 271 Suppl:S189–92.

Blaxter, M. L., J. Mann, T. Chapman, F. Thomas, C. Whitton, R. M. Floyd, and E. Abebe. 2005. Defining operational taxonomic units using DNA barcode data. Philos. Trans. R. Soc. Lond. B. Biol. Sci. 360:1935–43.

Bode, S. N. S., S. Adolfsson, D. K. Lamatsch, M. J. F. Martins, O. Schmit, J. Vandekerkhove, F. Mezquita, T. Namiotko, G. Rossetti, I. Schön, R. K. Butlin, and K. Martens. 2010. Exceptional cryptic diversity and multiple origins of parthenogenesis in a freshwater ostracod. Mol. Phylogenet. Evol. 54:542–52.

Boschetti, C., A. Carr, A. Crisp, I. Eyres, Y. Wang-Koh, E. Lubzens, T. G. Barraclough, G. Micklem, and A. Tunnacliffe. 2012. Biochemical diversification through foreign gene expression in bdelloid botifers. PLoS Genet. 8:e1003035.

Boschetti, C., N. N. Pouchkina-Stantcheva, P. Hoffmann, and A. Tunnacliffe. 2011. Foreign genes and novel hydrophilic protein genes participate in the desiccation response of the bdelloid rotifer *Adineta ricciae*. J. Exp. Biol. 214:59–68.

Brady, G. S., and D. Robertson. 1870. The Ostracoda and Foraminifera of tidal rivers. Ann. Mag. Nat. Hist. Ser. 4 6:1–31.

Britton, T., C. L. Anderson, D. Jacquet, S. Lundqvist, and K. Bremer. 2007. Estimating divergence times in large phylogenetic trees. Syst. Biol. 56:741–52.

Brown, S. D. J., R. A. Collins, S. Boyer, M.-C. Lefort, J. Malumbres-Olarte, C. J. Vink, and R. H. Cruickshank. 2012. SPIDER: an R package for the analysis of species identity and evolution, with particular reference to DNA barcoding. Mol. Ecol. Resour. 12:562–5.

Burt, A. 2000. Perspective: Sex, recombination, and the efficacy of selection - was Weismann right? Evolution 54:337–351.

Butlin, R. K. 2002. The costs and benefits of sex: new insights from old asexual lineages. Nat. Rev. Genet. 3:311–317.

Camargo, A., and J. W. Sites. 2013. Species delimitation: a decade after the renaissance. *in* I. Pavlinov, ed. The Species Problem - Ongoing Issues.

Caporaso, J. G., J. Kuczynski, and J. Stombaugh. 2010. QIIME allows analysis of high-throughput community sequencing data. Nature 7:335–336.

Carbayo, F., and A. C. Marques. 2011. The costs of describing the entire animal kingdom. Trends Ecol. Evol. 26:154–5.

Castagnone-Sereno, P. 2006. Genetic variability and adaptive evolution in parthenogenetic root-knot nematodes. Heredity 96:282–9.

Castellana, S., S. Vicario, and C. Saccone. 2011. Evolutionary patterns of the mitochondrial genome in Metazoa: exploring the role of mutation and selection in mitochondrial protein coding genes. Genome Biol. Evol. 3:1067–1079.

Casu, M., F. Scarpa, V. Delogu, P. Cossu, T. Lai, D. Sanna, and M. Curini-Galletti. 2014. Biodiversity patterns in interstitial marine microturbellaria: a case study within the genus *Parotoplana* (Platyhelminthes: Rhabditophora) with the description of four new species. J. Zool. Syst. Evol. Res. 52:190–202.

CBOL Plant Working Group. 2009. A DNA barcode for land plants. Proc. Natl. Acad. Sci. U. S. A. 106:12794–7.

Chao, A. 1984. Nonparametric estimation of the number of classes in a population. Scand. J. Stat. 11:265–270.

Chaplin, J. A., J. E. Havel, and P. D. N. Hebert. 1994. Sex and ostracods. Trends Ecol. Evol. 9:435–439.

Chariton, A. A., L. N. Court, D. M. Hartley, M. J. Colloff, and C. M. Hardy. 2010. Ecological assessment of estuarine sediments by pyrosequencing eukaryotic ribosomal DNA. Front. Ecol. Environ. 8:233–238.

Chariton, A. A., K. T. Ho, D. Proestou, H. M. Bik, S. L. Simpson, L. M. Portis, M. G. Cantwell, J. G. Baguley, R. M. Burgess, M. M. Pelletier, M. Perron, C. Gunsch, and R. A. Matthews. 2014. A molecular-based approach for examining responses of eukaryotes in microcosms to contaminant-spiked estuarine sediments. Environ. Toxicol. 33:359–369.

Chase, M. W., N. Salamin, M. J. Wilkinson, J. M. Dunwell, R. P. Kesanakurthi, N. Haidar, and V. Savolainen. 2005. Land plants and DNA barcodes: short-term and long-term goals. Philos. Trans. R. Soc. Lond. B. Biol. Sci. 360:1889–95.

Chevaldonné, P., D. Jollivet, D. Desbruyères, R. A. Lutz, and R. C. Vrijenhoek. 2002. Sister-species of eastern Pacific hydrothermal vent worms (Ampharetidae, Alvinellidae, Vestimentifera) provide new mitochondrial COI clock calibration. Cah. Biol. Mar. 43:367–370.

Cicconardi, F., P. P. Fanciulli, and B. C. Emerson. 2013. Collembola, the biological species concept and the underestimation of global species richness. Mol. Ecol. 22:5382–96.

Ciros-Perez, J. 2001. On the taxonomy of three sympatric sibling species of the *Brachionus plicatilis* (Rotifera) complex from Spain, with the description of *B. ibericus* n. sp. J. Plankton Res. 23:1311–1328.

Collins, R. A., and R. H. Cruickshank. 2012. The seven deadly sins of DNA barcoding. Mol. Ecol. Resour. 13:969–975.

Coyne, J. A., and H. A. Orr. 2004. Species: Reality and Concepts. Pp. 1–54 *in* Speciation. Sinauer Associates, Inc., Sunderland, Massachusetts.

Crawley, M. J. 2007. The R Book. John Wiley & Sons Ltd, Chichester.

Creer, S., V. G. Fonseca, D. L. Porazinska, R. M. Giblin-Davis, W. Sung, D. M. Power, M. Packer, G. R. Carvalho, M. L. Blaxter, P. J. D. Lambshead, and W. K. Thomas. 2010. Ultrasequencing of the meiofaunal biosphere: practice, pitfalls and promises. Mol. Ecol. 19:4–20.

Creer, S., and F. Sinniger. 2012. Cosmopolitanism of microbial eukaryotes in the global deep seas. Mol. Ecol. 21:1033–1035.

Cummings, M. P., M. C. Neel, and K. L. Shaw. 2008. A genealogical approach to quantifying lineage divergence. Evolution 62:2411–22.

Curini-Galletti, M., T. J. Artois, V. Delogu, W. H. De Smet, D. Fontaneto, U. Jondelius, F. Leasi, A. Martínez, I. Meyer-Wachsmuth, K. S. Nilsson, P. Tongiorgi, K. Worsaae, and M. A. Todaro. 2012. Patterns of diversity in soft-bodied meiofauna: dispersal ability and body size matter. PLoS One 7:e33801.

Cusimano, N., T. Stadler, and S. S. Renner. 2012. A new method for handling missing species in diversification analysis applicable to randomly or nonrandomly sampled phylogenies. Syst. Biol. 61:785–92.

Danchin, E. G. J., J.-F. Flot, L. Perfus-Barbeoch, and K. Van Doninck. 2011. Genomic Perspectives on the Long-Term Absence of Sexual Reproduction in Animals. Pp. 223–242 *in* P. Pontarotti, ed. Evolutionary Biology. Springer, Berlin, Heidelberg.

Darriba, D., G. L. Taboada, R. Doallo, and D. Posada. 2012. jModelTest 2: more models, new heuristics and parallel computing. Nat. Methods 9:772.

Dawnay, N., R. Ogden, R. McEwing, G. R. Carvalho, and R. S. Thorpe. 2007. Validation of the barcoding gene COI for use in forensic genetic species identification. Forensic Sci. Int. 173:1–6.

De Queiroz, K. 2005a. Different species problems and their resolution. BioEssays 27:1263–9.

De Queiroz, K. 2005b. Ernst Mayr and the modern concept of species. Proc. Natl. Acad. Sci. U. S. A. 102:6600–7.

De Queiroz, K. 2007. Species concepts and species delimitation. Syst. Biol. 56:879–86.

Derycke, S., T. Remerie, A. Vierstraete, T. Backeljau, J. R. Vanfleteren, M. Vincx, and T. Moens. 2005. Mitochondrial DNA variation and cryptic speciation within the free-living marine nematode *Pellioditis marina*. Mar. Ecol. Prog. Ser. 300:91–103.

Desalle, R. 2006. Species discovery versus species identification in DNA barcoding efforts: response to Rubinoff. Conserv. Biol. 20:1545–7.

DeSalle, R., M. G. Egan, and M. Siddall. 2005. The unholy trinity: taxonomy, species delimitation and DNA barcoding. Philos. Trans. R. Soc. Lond. B. Biol. Sci. 360:1905–16.

Dinca, V., E. V Zakharov, P. D. N. Hebert, and R. Vila. 2011. Complete DNA barcode reference library for a country's butterfly fauna reveals high performance for temperate Europe. Proc. R. Soc. London B 278:347–55.

Dobzhansky, T. 1950. Mendelian populations and their evolution. Am. Nat. 84:401–418.

Dobzhansky, T., and T. G. Dobzhansky. 1937. Genetics and the Origin of Species. Columbia University Press, New York.

Domes, K., R. A. Norton, M. Maraun, and S. Scheu. 2007. Reevolution of sexuality breaks Dollo's law. Proc. Natl. Acad. Sci. U. S. A. 104:7139–44.

Donner, J. 1965. Ordnung Bdelloidea (Rotifera, Rädertiere). Akademie Verlag, Berlin.

Drummond, A. J., M. Kearse, J. Heled, R. Moir, T. Thierer, B. Ashton, A. Wilson, and S. Stones-Havas. 2006. Geneious v5.4.2.

Drummond, A. J., and A. Rambaut. 2007. BEAST: Bayesian evolutionary analysis by sampling trees. BMC Evol. Biol. 7:214.

Drummond, A. J., and M. A. Suchard. 2010. Bayesian random local clocks, or one rate to rule them all. BMC Biol. 8:114.

Ebach, M. C., and C. Holdrege. 2005. DNA barcoding is no substitute for taxonomy. Nature 434:697.

Esselstyn, J. A., B. J. Evans, J. L. Sedlock, F. Ali, A. Khan, R. Lawrence, and L. R. Heaney. 2012. Single-locus species delimitation : a test of the mixed Yule − coalescent model , with an empirical application to Philippine round-leaf bats. Proc. R. Soc. London B 279:3678–3686.

Eyres, I. 2013. Horizontal gene transfer and the unusual genomic architecture of bdelloid rotifers. Imperial College London.

Eyres, I., E. Frangedakis, D. Fontaneto, E. A. Herniou, C. Boschetti, A. Carr, G. Micklem, A. Tunnacliffe, and T. G. Barraclough. 2012. Multiple functionally divergent and conserved copies of alpha tubulin in bdelloid rotifers. BMC Evol. Biol. 12:148. BMC Evolutionary Biology.

Ezard, T. H. G., T. Fujisawa, and T. G. Barraclough. 2009. splits: SPecies' LImits by Threshold Statistics.

Felsenstein, J. 1981. Skepticism towards Santa Rosalia, or why are there so few kinds of animals? Evolution 35:124–138.

Ficetola, G. F., C. Miaud, F. Pompanon, and P. Taberlet. 2008. Species detection using environmental DNA from water samples. Biol. Lett. 4:423–5.

Fisher, R. A. 1930. The genetical theory of natural selection. Oxford University Press, Oxford.

Flot, J.-F., A. Couloux, and S. Tillier. 2010. Haplowebs as a graphical tool for delimiting species: a revival of Doyle's "field for recombination" approach and its application to the coral genus *Pocillopora* in Clipperton. BMC Evol. Biol. 10:372. BioMed Central Ltd.

Flot, J.-F., B. Hespeels, X. Li, B. Noel, I. R. Arkhipova, E. G. J. Danchin, A. Hejnol, B. Henrissat, R. Koszul, J.-M. Aury, V. Barbe, R.-M. Barthélémy, J. Bast, G. A. Bazykin, O. Chabrol, A. Couloux, M. Da Rocha, C. Da Silva, E. A. Gladyshev, P. Gouret, O. Hallatschek, B. Hecox-Lea, K. Labadie, B. Lejeune, O. Piskurek, J. Poulain, F. Rodriguez, J. F. Ryan, O. A. Vakhrusheva, E. Wajnberg, B. Wirth, I. Yushenova, M. Kellis, A. S. Kondrashov, D. B. Mark Welch, P. Pontarotti, J. Weissenbach, P. Wincker, O. Jaillon, and K. Van Doninck. 2013. Genomic evidence for ameiotic evolution in the bdelloid rotifer *Adineta vaga*. Nature 500:453–457.

Floyd, R. M., E. Abebe, A. Papert, and M. L. Blaxter. 2002. Molecular barcodes for soil nematode identification. Mol. Ecol. 11:839–50.

Folmer, O., M. Black, W. Hoeh, R. Lutz, and R. Vrijenhoek. 1994. DNA primers for amplification of mitochondrial cytochrome *c* oxidase subunit I from diverse metazoan invertebrates. Mol. Mar. Biol. Biotechnol. 3:294–9.

Fonseca, G., S. Derycke, and T. Moens. 2008. Integrative taxonomy in two free-living nematode species complexes. Biol. J. Linn. Soc. 94:737–753.

Fonseca, V. G., G. R. Carvalho, W. Sung, H. F. Johnson, D. M. Power, S. P. Neill, M. Packer, M. L. Blaxter, P. J. D. Lambshead, W. K. Thomas, and S. Creer. 2010. Second-generation environmental sequencing unmasks marine metazoan biodiversity. Nat. Commun. 1:98.

Fontaneto, D. 2014. Molecular phylogenies as a tool to understand diversity in rotifers. Int. Rev. Hydrobiol. 99:1–10.

Fontaneto, D., A. M. Barbosa, H. Segers, and M. Pautasso. 2012a. The "rotiferologist" effect and other global correlates of species richness in monogonont rotifers. Ecography 35:174–182.

Fontaneto, D., T. G. Barraclough, K. Chen, C. Ricci, and E. A. Herniou. 2008a. Molecular evidence for broad-scale distributions in bdelloid rotifers: everything is not everywhere but most things are very widespread. Mol. Ecol. 17:3136–46.

Fontaneto, D., C. Boschetti, and C. Ricci. 2008b. Cryptic diversification in ancient asexuals: evidence from the bdelloid rotifer *Philodina flaviceps*. J. Evol. Biol. 21:580–587.

Fontaneto, D., I. Giordani, G. Melone, and M. Serra. 2007a. Disentangling the morphological stasis in two rotifer species of the *Brachionus plicatilis* species complex. Hydrobiologia 583:297–307.

Fontaneto, D., E. A. Herniou, T. G. Barraclough, and C. Ricci. 2007b. On the Global Distribution of Microscopic Animals : New Worldwide Data on Bdelloid Rotifers. Zool. Stud. 46:336–346.

Fontaneto, D., E. A. Herniou, T. G. Barraclough, C. Ricci, and G. Melone. 2007c. On the reality and recognisability of asexual organisms: morphological analysis of the masticatory apparatus of bdelloid rotifers. Zool. Scr. 36:361–370.

Fontaneto, D., E. A. Herniou, C. Boschetti, M. Caprioli, G. Melone, C. Ricci, and T. G. Barraclough. 2007d. Independently evolving species in asexual bdelloid rotifers. PLoS Biol. 5:e87.

Fontaneto, D., N. S. Iakovenko, I. Eyres, M. Kaya, M. Wyman, and T. G. Barraclough. 2011. Cryptic diversity in the genus *Adineta* Hudson & Gosse, 1886 (Rotifera: Bdelloidea: Adinetidae): a DNA taxonomy approach. Hydrobiologia 662:27–33.

Fontaneto, D., and U. Jondelius. 2011. Broad taxonomic sampling of mitochondrial cytochrome c oxidase subunit I does not solve the relationships between Rotifera and Acanthocephala. Zool. Anz. 250:80–85.

Fontaneto, D., M. Kaya, E. A. Herniou, and T. G. Barraclough. 2009. Extreme levels of hidden diversity in microscopic animals (Rotifera) revealed by DNA taxonomy. Mol. Phylogenet. Evol. 53:182–9.

Fontaneto, D., C. Q. Tang, U. Obertegger, F. Leasi, and T. G. Barraclough. 2012b. Different diversification rates between sexual and asexual organisms. Evol. Biol. 39:262–270.

Fujisawa, T., and T. G. Barraclough. 2013. Delimiting species using single-locus data and the Generalized Mixed Yule Coalescent (GMYC) approach: A revised method and evaluation on simulated datasets. Syst. Biol. 62:707–724.

Funk, D. J., and K. E. Omland. 2003. Species-level paraphyly and polyphyly: Frequency, causes, and consequences, with insights from animal mitochondrial DNA. Annu. Rev. Ecol. Evol. Syst. 34:397–423.

García-Morales, A. E., and M. Elías-Gutiérrez. 2013. DNA barcoding of freshwater Rotifera in Mexico: Evidence of cryptic speciation in common rotifers. Mol. Ecol. Resour. 13:1097–1107.

García-Varela, M., and G. de León. 2000. Phylogenetic relationships of Acanthocephala based on analysis of 18S ribosomal RNA gene sequences. J. Mol. Evol. 50:532–540.

García-Varela, M., and S. A. Nadler. 2006. Phylogenetic relationships among Syndermata inferred from nuclear and mitochondrial gene sequences. Mol. Phylogenet. Evol. 40:61–72.

Garey, J., and T. J. Near. 1996. Molecular evidence for Acanthocephala as a subtaxon of Rotifera. J. Mol. Evol. 43:287–292.

Garey, J. R., A. Schmidt-rhaesa, T. J. Near, and S. A. Nadler. 1998. The evolutionary relationships of rotifers and acanthocephalans. Nat. Hist. 83–91.

Gascuel, O., and M. Steel. 2006. Neighbor-joining revealed. Mol. Biol. Evol. 23:1997–2000.

Gaston, K., and R. M. May. 1992. Taxonomy of taxonomists. Nature 356:281–282.

Geller, J., C. P. Meyer, M. Parker, and H. Hawk. 2013. Redesign of PCR primers for mitochondrial cytochrome *c* oxidase subunit I for marine invertebrates and application in all-taxa biotic surveys. Mol. Ecol. Resour. 13:851–61.

Gernhard, T. 2008. The conditioned reconstructed process. J. Theor. Biol. 253:769–78.

Giere, O. 2009. Meiobenthology the microscopic motile fauna of aquatic sediments. Springer-Verlag, Heidelberg.

Gilbert, J. J. 1988. Rotifera. Pp. 73–80 *in* K. G. Adiyodi and R. G. Adiyodi, eds. Reproductive Biology of Invertebrates, Vol. 5, Accessory Sex Glands. John Wiley and Sons, Ltd, New York.

Gilbert, J. J. 1993. Rotifera. Pp. 231–263 *in* K. G. Adiyodi and R. G. Adiyodi, eds. Reproductive Biology of Invertebrates, Vol. 6A. Asexual Propagation and Reproductive Strategies. Oxford & IBH Publishing Co., New Delhi.

Gilbert, J. J. 1983. Rotifera. Pp. 181–209 *in* K. G. Adiyodi and R. G. Adiyodi, eds. Reproductive Biology of Invertebrates, Vol. 1, Oogenesis, oviposition, and oosorption. John Wiley & Sons Ltd, Chichester.

Giribet, G., S. Carracnza, J. Baguñà, M. Riutort, and C. Ribera. 1996. First molecular evidence Arthropoda clade for the existence of a Tardigrada. Mol. Biol. Evol. 13:76–84.

Gladyshev, E. A. 2008. Extreme resistance of bdelloid rotifers to ionizing radiation. Proc. Natl. Acad. Sci. U. S. A. 105:5139.

Gladyshev, E. A., M. Meselson, and I. R. Arkhipova. 2008. Massive horizontal gene transfer in bdelloid rotifers. Science 320:1210–1213.

Goddard, M. R., H. C. J. Godfray, and A. Burt. 2005. Sex increases the efficacy of natural selection in experimental yeast populations. Nature 434:636–640.

Godfray, H. C. J. 2002. Challenges for taxonomy. Nature 417:17–9.

Goldberg, E. E., and B. Igić. 2008. On phylogenetic tests of irreversible evolution. Evolution 62:2727–41.

Gómez, A. 2005. Molecular ecology of rotifers: from population differentiation to speciation. Hydrobiologia 546:83–99.

Gómez, A., M. Serra, G. R. Carvalho, and D. H. Lunt. 2002. Speciation in ancient cryptic species complexes: evidence from the molecular phylogeny of *Brachionus plicatilis* (Rotifera). Evolution 56:1431–44.

Grabherr, M. G., B. J. Haas, M. Yassour, J. Z. Levin, D. A. Thompson, I. Amit, X. Adiconis, L. Fan, R. Raychowdhury, Q. Zeng, Z. Chen, E. Mauceli, N. Hacohen, A. Gnirke, N. Rhind, F. di Palma, B. W. Birren, C. Nusbaum, K. Lindblad-Toh, N. Friedman, and A. Regev. 2011. Full-length transcriptome assembly from RNA-Seq data without a reference genome. Nat. Biotechnol. 29:644–52.

Gregory, T. R. 2005. DNA barcoding does not compete with taxonomy. Nature 434:1067.

Guindon, S., J.-F. Dufayard, V. Lefort, M. Anisimova, W. Hordijk, and O. Gascuel. 2010. New algorithms and methods to estimate maximum-likelihood phylogenies: assessing the performance of PhyML 3.0. Syst. Biol. 59:307–21.

Hamilton, W. D., R. Axelrod, and R. Tanese. 1990. Sexual reproduction as an adaptation to resist parasites (a review). Proc. Natl. Acad. Sci. U. S. A. 87:3566–73.

Hammer, M., and J. A. Wallwork. 1979. A review of the world distribution of oribatid mites (Acari: Cryptostigmata) in relation to continental drift. Biol. Skr. K. Danske Vidensk. Selsk. 22:1–31.

Hebert, P. D. N., A. Cywinska, S. L. Ball, and J. R. DeWaard. 2003a. Biological identifications through DNA barcodes. Proc. R. Soc. London B 270:313–21.

Hebert, P. D. N., S. Ratnasingham, and J. R. DeWaard. 2003b. Barcoding animal life: cytochrome *c* oxidase subunit 1 divergences among closely related species. Proc. R. Soc. London B 270 Suppl:S96–9.

Heethoff, M., K. Domes, M. Laumann, M. Maraun, R. A. Norton, and S. Scheu. 2007. High genetic divergences indicate ancient separation of parthenogenetic lineages of the oribatid mite *Platynothrus peltifer* (Acari, Oribatida). J. Evol. Biol. 20:392–402.

Heethoff, M., R. A. Norton, S. Scheu, and M. Maraun. 2009. Parthenogenesis in oribatid mites (Acari, Oribatida): Evolution without sex. Pp. 241–258 *in* I. Schön, K. Martens, and P. van Dijk, eds. Lost Sex - The Evolutionary Biology of Parthenogenesis. Springer, Dordrecht.

Hellberg, M. E., and V. D. Vacquier. 1999. Rapid evolution of fertilization selectivity and lysin cDNA sequences in teguline gastropods. Mol. Biol. Evol. 16:839–848.

Henry, L., T. Schwander, and B. J. Crespi. 2012. Deleterious mutation accumulation in asexual Timema stick insects. Mol. Biol. Evol. 29:401–8.

Hespeels, B., M. Knapen, D. Hanot-Mambres, A.-C. Heuskin, F. Pineux, S. Lucas, R. Koszul, and K. Van Doninck. 2014. Gateway to genetic exchange? DNA double-strand breaks in the bdelloid rotifer *Adineta vaga* submitted to desiccation. J. Evol. Biol. In Press.

Higuchi, R., C. von Beroldingen, G. F. Sensabaugh, and H. A. Erlich. 1988. DNA typing from single hairs. Nature 332:543–546.

Holman, E. 1987. Recognizability of sexual and asexual species of rotifers. Syst. Biol. 36:381–386.

Holterman, M., G. Karssen, S. van den Elsen, H. van Megen, J. Bakker, and J. Helder. 2009. Small subunit rDNA-based phylogeny of the Tylenchida sheds light on relationships among some high-impact plant-parasitic nematodes and the evolution of plant feeding. Phytopathology 99:227–35.

Hothorn, T., F. Bretz, and P. Westfall. 2008. Simultaneous inference in general parametric models. Biometrical J. 50:346–63.

Hsu, W. S. 1956. Oogenesis in *Habrotrocha tridens* (Milne). Biol. Bull. 111:364.

Hudson, R. R. 1990. Gene genealogies and the coalescent process. Oxford Surv. Evol. Biol. 7:1–44.

Huelsenbeck, J. P., and F. Ronquist. 2001. MRBAYES: Bayesian inference of phylogenetic trees. Bioinformatics 17:754–7.

Hugall, A., J. Stanton, and C. Moritz. 1997. Evolution of the AT-rich mitochondrial DNA of the root knot nematode, *Meloidogyne hapla*. Mol. Biol. Evol. 14:40–48.

Hull, D. L. 1980. Individuality and Selection. Annu. Rev. Ecol. Syst. 11:311–332.

Hunt, D. J., and Z. A. Handoo. 2009. Taxonomy, identification and principal species. Pp. 55–97 *in* R. N. Perry, M. Moens, and J. L. Starr, eds. Root-know nematodes. CABI Publishing, Wallingford.

Hurst, L. D., and J. R. Peck. 1996. Recent advances in understanding of the evolution and maintenance of sex. Trends Ecol. Evol. 11:46–52.

Hutchinson, G. E. 1967. A treatise on limnology, Vol II. John Wiley & Sons, Inc., New York.

Iakovenko, N. S. 2000. New for the fauna of Ukraine rotifers (Rotifera, Bdelloidea) of Adinetidae and Habrotrochidae families. Vestn. Zool. 34:11–19.

Iakovenko, N. S., E. KaŠparová, M. Plewka, and K. Janko. 2013. *Otostephanos* (Rotifera, Bdelloidea, Habrotrochidae) with the description of two new species. Syst. Biodivers. 11:477–494.

Jaenike, J. 1978. An hypothesis to account for the maintenance of sex within populations. Evol. Theory 3:191–194.

Jeffroy, O., H. Brinkmann, F. Delsuc, and H. Philippe. 2006. Phylogenomics: the beginning of incongruence? Trends Genet. 22:225–31.

Joppa, L. N., D. L. Roberts, and S. L. Pimm. 2011. The population ecology and social behaviour of taxonomists. Trends Ecol. Evol. 26:551–3. Elsevier Ltd.

Jørgensen, A., S. Faurby, J. G. Hansen, N. Møbjerg, and R. M. Kristensen. 2010. Molecular phylogeny of Arthrotardigrada (Tardigrada). Mol. Phylogenet. Evol. 54:1006–15.

Jørgensen, A., N. Møbjerg, and R. M. Kristensen. 2011. Phylogeny and evolution of the Echiniscidae (Echiniscoidea, Tardigrada)–an investigation of the congruence between molecules and morphology. J. Zool. Syst. Evol. Res. 49:6–16.

Judson, O. P., and B. B. Normark. 1996. Ancient asexual scandals. Trends Ecol. Evol. 11:41–46.

Kånneby, T., M. A. Todaro, and U. Jondelius. 2011. A phylogenetic approach to species delimitation in freshwater Gastrotricha from Sweden. Hydrobiologia 683:185–202.

Kånneby, T., M. A. Todaro, and U. Jondelius. 2013. Phylogeny of Chaetonotidae and other Paucitubulatina (Gastrotricha: Chaetonotida) and the colonization of aquatic ecosystems. Zool. Scr. 42:88–105.

Kass, R. E., and A. E. Raftery. 1995. Bayes Factors. J. Am. Stat. Assoc. 90:773–795.

Katoh, K., G. Asimenos, and H. Toh. 2009. Multiple alignment of DNA sequences with MAFFT. Methods Mol. Biol. 537:39–64.

Kaya, M., E. A. Herniou, T. G. Barraclough, and D. Fontaneto. 2009. Inconsistent estimates of diversity between traditional and DNA taxonomy in bdelloid rotifers. Org. Divers. Evol. 9:3–12.

Kaya, M., W. H. Smet, and D. Fontaneto. 2010. Survey of moss-dwelling bdelloid rotifers from middle Arctic Spitsbergen (Svalbard). Polar Biol. 33:833–842.

Kennedy, A., and C. Jacoby. 1999. Biological indicators of marine environmental health: meiofauna–a neglected benthic component? Environ. Monit. Assess. 54:47–68.

Kieneke, A., P. M. Martínez Arbizu, and D. Fontaneto. 2012. Spatially structured populations with a low level of cryptic diversity in European marine Gastrotricha. Mol. Ecol. 21:1239–1254.

Kimura, M. 1980. A simple method for estimating evolutionary rates of base substitutions through comparative studies of nucleotide sequences. J. Mol. Evol. 16:111–120.

Knowlton, N., and L. A. Weigt. 1998. New dates and new rates for divergence across the Isthmus of Panama. Proc. R. Soc. B Biol. Sci. 265:2257.

Kondrashov, A. S. 1993. Classification of hypotheses on the advantage of amphimixis. J. Hered. 84:372–87.

Koste, W. 1978. Rotatoria. Die Rädertiere Mitteleuropas. 2 volumes. Gebrüder Borntraeger, Berlin.

Krell, F. 2002. Why impact factors don't work for taxonomy. Nature 415:1211.

Krisko, A., M. Leroy, M. Radman, and M. Meselson. 2012. Extreme anti-oxidant protection against ionizing radiation in bdelloid rotifers. Proc. Natl. Acad. Sci. U. S. A. 109:2354–7.

Kuhner, M. K., and J. Felsenstein. 1994. A simulation comparison of phylogeny algorithms under equal and unequal evolutionary rates. Mol. Biol. Evol. 11:459–68.

Kurtzman, C. P. 1994. Molecular taxonomy of the yeasts. Yeast 10:1727–1740.

Lasek-Nesselquist, E. 2012. A mitogenomic re-evaluation of the bdelloid phylogeny and relationships among the Syndermata. PLoS One 7:e43554.

Leasi, F., C. Q. Tang, W. H. De Smet, and D. Fontaneto. 2013. Cryptic diversity with wide salinity tolerance in the putative euryhaline *Testudinella clypeata* (Rotifera, Monogononta). Zool. J. Linn. Soc. 168:17–28.

Leray, M., J. Y. Yang, C. P. Meyer, S. C. Mills, N. Agudelo, V. Ranwez, J. T. Boehm, and R. J. Machida. 2013. A new versatile primer set targeting a short fragment of the mitochondrial COI region for metabarcoding metazoan diversity: application for characterizing coral reef fish gut contents. Front. Zool. 10:34.

Librado, P., and J. Rozas. 2009. DnaSP v5: A software for comprehensive analysis of DNA polymorphism data. Bioinformatics 25:1451–1452.

Lim, G. S., M. Balke, and R. Meier. 2012. Determining species boundaries in a world full of rarity: singletons, species delimitation methods. Syst. Biol. 61:165–9.

Littlewood, D. T. J., M. Curini-Galletti, and E. A. Herniou. 2000. The interrelationships of proseriata (Platyhelminthes: seriata) tested with molecules and morphology. Mol. Phylogenet. Evol. 16:449–66.

Lohse, K. 2009. Can mtDNA barcodes be used to delimit species? A response to Pons et al. (2006). Syst. Biol. 58:439–42.

Lunt, D. H. 2008. Genetic tests of ancient asexuality in root knot nematodes reveal recent hybrid origins. BMC Evol. Biol. 8:194.

Malekzadeh-Viayeh, R., R. Pak-Tarmani, N. Rostamkhani, and D. Fontaneto. 2014. Diversity of the rotifer *Brachionus plicatilis* species complex (Rotifera: Monogononta) in Iran through integrative taxonomy. Zool. J. Linn. Soc. 170:233–244.

Maraun, M., M. Heethoff, S. Scheu, R. A. Norton, G. Weigmann, and R. H. Thomas. 2003. Radiation in sexual and parthenogenetic oribatid mites (Oribatida, Acari) as indicated by genetic divergence of closely related species. Exp. Appl. Acarol. 29:265–77.

Mark Welch, D. B., J. L. Mark Welch, and M. Meselson. 2008. Evidence for degenerate tetraploidy in bdelloid rotifers. Proc. Natl. Acad. Sci. U. S. A. 105:5145.

Mark Welch, D. B., and M. Meselson. 2000. Evidence for the evolution of bdelloid rotifers without sexual reproduction or genetic exchange. Science 288:1211–1215.

Mark Welch, D. B., and M. Meselson. 2001. Rates of nucleotide substitution in sexual and anciently asexual rotifers. Proc. Natl. Acad. Sci. U. S. A. 98:6720–4.

Martens, K., and I. Schön. 2008. Ancient asexuals: darwinulids not exposed. Nature 453:8600.

Matsen, F. A., R. B. Kodner, and E. V. Armbrust. 2010. pplacer: linear time maximum-likelihood and Bayesian phylogenetic placement of sequences onto a fixed reference tree. BMC Bioinformatics 11:538.

Matz, M. V, and R. Nielsen. 2005. A likelihood ratio test for species membership based on DNA sequence data. Philos. Trans. R. Soc. Lond. B. Biol. Sci. 360:1969–74.

Maynard Smith, J. 1986. Contemplating life without sex. Nature 324:300–301.

Maynard Smith, J. 1978. The Evolution of Sex. Cambridge University Press, Cambridge.

Maynard Smith, J., and E. Száthmary. 1995. The major transitions in evolution. W.H. Freeman, Oxford.

Mayr, E. 1942. Systematics and the origin of species, from the viewpoint of a zoologist. Harvard University Press.

Meier, R., K. Shiyang, G. Vaidya, and P. K. L. Ng. 2006. DNA barcoding and taxonomy in Diptera: a tale of high intraspecific variability and low identification success. Syst. Biol. 55:715–28.

Meier, R., G. Zhang, and F. Ali. 2008. The use of mean instead of smallest interspecific distances exaggerates the size of the "barcoding gap" and leads to misidentification. Syst. Biol. 57:809–13.

Melone, G., and C. Ricci. 1995. Rotatory apparatus in Bdelloids. Hydrobiologia 313/314:91–98.

Melone, G., C. Ricci, and H. Segers. 1998a. The trophi of Bdelloidea (Rotifera): a comparative study across the class. Can. J. Zool. 1755–1765.

Melone, G., C. Ricci, H. Segers, and R. L. Wallace. 1998b. Phylogenetic relationships of phylum Rotifera with emphasis on the families of Bdelloidea. Hydrobiologia 387/388:101–107.

Meusnier, I., G. A. C. Singer, J.-F. Landry, D. A. Hickey, P. D. N. Hebert, and M. Hajibabaei. 2008. A universal DNA mini-barcode for biodiversity analysis. BMC Genomics 9.

Meyer, C. P. 2003. Molecular systematics of cowries (Gastropoda: Cypraeidae) and diversification patterns in the tropics. Biol. J. Linn. Soc. 79:401–459.

Meyer, C. P., and G. Paulay. 2005. DNA barcoding: error rates based on comprehensive sampling. PLoS Biol. 3:e422.

Michod, R. E., and B. R. Levin (eds). 1988. The Evolution of Sex. Sinauer Associates, Sunderland, MA.

Miller, M. A., W. Pfeiffer, and T. Schwartz. 2010. Creating the CIPRES Science Gateway for inference of large phylogenetic trees. Pp. 45–52 *in* 2010 Gateway Computing Environments Workshop. Institute of Electrical and Electronics Engineers (IEEE), New Orleans, Louisiana, USA.

Mills, S., D. H. Lunt, and A. Gómez. 2007. Global isolation by distance despite strong regional phylogeography in a small metazoan. BMC Evol. Biol. 7:225.

Min, G.-S., and J.-K. Park. 2009. Eurotatorian paraphyly: Revisiting phylogenetic relationships based on the complete mitochondrial genome sequence of *Rotaria rotatoria* (Bdelloidea: Rotifera: Syndermata). BMC Genomics 10:533.

Monaghan, M. T., R. Wild, M. Elliot, T. Fujisawa, M. Balke, D. J. G. Inward, D. C. Lees, R. Ranaivosolo, P. Eggleton, T. G. Barraclough, and A. P. Vogler. 2009. Accelerated species inventory on Madagascar using coalescent-based models of species delineation. Syst. Biol. 58:298–311.

Moore, R. C. (ed). 1961. Treatise on invertebrate paleontology, part Q; Arthropoda 3, Crustacea, Ostracoda. Geological Society of America.

Moritz, C., and C. Cicero. 2004. DNA barcoding: promise and pitfalls. PLoS Biol. 2:e354.

Morlon, H., B. D. Kemps, J. B. Plotkin, and D. Brisson. 2012. Explosive radiation of a bacterial species group. Evolution 66:2577–86.

Muller, H. J. 1932. Some genetic aspects of sex. Am. Nat. 66:118–138.

Nee, S., R. M. May, and P. H. Harvey. 1994. The reconstructed evolutionary process. Philos. Trans. R. Soc. Lond. B. Biol. Sci. 344:305–11.

Neiman, M., S. Meirmans, and P. G. Meirmans. 2009. What can asexual lineage age tell us about the maintenance of sex? Ann. N. Y. Acad. Sci. 1168:185–200.

Normark, B. B., O. P. Judson, and N. A. Moran. 2003. Genomic signatures of ancient asexual lineages. Biol. J. Linn. Soc. 79:69–84.

Nye, T. M. W., P. Liò, and W. R. Gilks. 2006. A novel algorithm and web-based tool for comparing two alternative phylogenetic trees. Bioinformatics 22:117–9.

O'Grady, P. M., and T. A. Markow. 2009. Phylogenetic taxonomy in *Drosophila*. Fly 3:10–14.

O'Meara, B. C. 2010. New heuristic methods for joint species delimitation and species tree inference. Syst. Biol. 59:59–73.

Ochman, H., and A. Wilson. 1987. Evolution in bacteria: evidence for a universal substitution rate in cellular genomes. J. Mol. Evol. 26:74–86.

Otto, S. P., and T. Lenormand. 2002. Resolving the paradox of sex and recombination. Nat. Rev. Genet. 3:252–61.

Pace, N. R. 1997. A Molecular View of Microbial Diversity and the Biosphere. Science 276:734–740.

Packer, L., J. Gibbs, C. Sheffield, and R. Hanner. 2009. DNA barcoding and the mediocrity of morphology. Mol. Ecol. Resour. 9 Suppl s1:42–50.

Palmer, S. C., and R. A. Norton. 1992. Genetic diversity in thelytokous oribatid mites (Acari; Acariformes: Desmonomata). Biochem. Syst. Ecol. 20:219–231.

Palmer, S. C., and R. A. Norton. 1991. Taxonomic, geographic and seasonal distribution of thelytokous parthenogenesis in the Desmonomata (Acari: Oribatida). Exp. Appl. Acarol. 12:67–81.

Papadopoulou, A., J. Bergsten, T. Fujisawa, M. T. Monaghan, T. G. Barraclough, and A. P. Vogler. 2008. Speciation and DNA barcodes: testing the effects of dispersal on the formation of discrete sequence clusters. Philos. Trans. R. Soc. Lond. B. Biol. Sci. 363:2987–96.

Paradis, E., J. Claude, and K. Strimmer. 2004. APE: Analyses of Phylogenetics and Evolution in R language. Bioinformatics 20:289–290.

Pawlowski, J., S. Audic, S. Adl, D. Bass, L. Belbahri, C. Berney, S. S. Bowser, I. Cepicka, J. Decelle, M. Dunthorn, A. M. Fiore-Donno, G. H. Gile, M. Holzmann, R. Jahn, M. Jirků, P. J. Keeling, M. Kostka, A. Kudryavtsev, E. Lara, J. Lukeš, D. G. Mann, E. a D. Mitchell, F. Nitsche, M. Romeralo, G. W. Saunders, A. G. B. Simpson, A. V Smirnov, J. L. Spouge, R. F. Stern, T. Stoeck, J. Zimmermann, D. Schindel, and C. de Vargas. 2012. CBOL protist working group: barcoding eukaryotic richness beyond the animal, plant, and fungal kingdoms. PLoS Biol. 10:e1001419.

Pinheiro, J., D. M. Bates, S. DebRoy, D. Sarkar, and T. R. D. C. Team. 2013. nlme: Linear and Nonlinear Mixed Effects Models.

Poinar, G. O., and C. Ricci. 1992. Bdelloid rotifers in Dominican amber: Evidence for parthenogenetic continuity. Experientia 48:408–410.

Pons, J., T. G. Barraclough, J. Gomez-Zurita, A. Cardoso, D. Duran, S. Hazell, S. Kamoun, W. Sumlin, and A. P. Vogler. 2006. Sequence-based species delimitation for the DNA taxonomy of undescribed insects. Syst. Biol. 55:595–609.

Posada, D. 2009. Selection of models of DNA evolution with jModelTest. Methods Mol. Biol. 537:93–112.

Pouchkina-Stantcheva, N. N., B. M. McGee, C. Boschetti, D. Tolleter, S. Chakrabortee, A. V. Popova, F. Meersman, D. Macherel, D. K. Hincha, and A. Tunnacliffe. 2007. Functional divergence of former alleles in an ancient asexual invertebrate. Science 268:268–271.

Powell, J. R. 2012. Accounting for uncertainty in species delineation during the analysis of environmental DNA sequence data. Methods Ecol. Evol. 3:1–11.

Powell, J. R., M. T. Monaghan, M. Opik, and M. C. Rillig. 2011. Evolutionary criteria outperform operational approaches in producing ecologically relevant fungal species inventories. Mol. Ecol. 20:655–66.

Prosser, S. W. J., A. Martínez-Arce, and M. Elías-Gutiérrez. 2013a. A new set of primers for COI amplification from freshwater microcrustaceans. Mol. Ecol. Resour. 13:1151–5.

Prosser, S. W. J., M. G. Velarde-Aguilar, V. León-Règagnon, and P. D. N. Hebert. 2013b. Advancing nematode barcoding: A primer cocktail for the cytochrome *c* oxidase subunit I gene from vertebrate parasitic nematodes. Mol. Ecol. Resour.

Puillandre, N., A. Lambert, S. Brouillet, and G. Achaz. 2012a. ABGD, Automatic Barcode Gap Discovery for primary species delimitation. Mol. Ecol. 21:1864–1877.

Puillandre, N., M. V. Modica, Y. Zhang, L. Sirovich, M.-C. Boisselier, C. Cruaud, M. Holford, and S. Samadi. 2012b. Large-scale species delimitation method for hyperdiverse groups. Mol. Ecol. 21:2671–91.

Pybus, O. G., and P. H. Harvey. 2000. Testing macro-evolutionary models using incomplete molecular phylogenies. Proc. R. Soc. London B 267:2267–72.

Quince, C., A. Lanzen, R. J. Davenport, and P. J. Turnbaugh. 2011. Removing noise from pyrosequenced amplicons. BMC Bioinformatics 12:38. BioMed Central Ltd.

R Core Team. 2014. R: A language and environment for statistical computing. R Core Team. R Foundation for Statistical Computing, Vienna, Austria.

Rambaut, A., and A. J. Drummond. 2009. Tracer V1.5. Available from http//beast.bio.ed.ac.uk/Tracer.

Ratnasingham, S., and P. D. N. Hebert. 2007. BOLD : The Barcode of Life Data System (www.barcodinglife.org). Mol. Ecol. Notes 7:355–364.

Reid, N. M., and B. C. Carstens. 2012. Phylogenetic estimation error can decrease the accuracy of species delimitation: a Bayesian implementation of the general mixed Yule-coalescent model. BMC Evol. Biol. 12:196.

Riaz, T., W. Shehzad, A. Viari, F. Pompanon, P. Taberlet, and E. Coissac. 2011. ecoPrimers: inference of new DNA barcode markers from whole genome sequence analysis. Nucleic Acids Res. 39:e145.

Ricci, C. 1987. Ecology and bdelloids: how to be successful. Hydrobiologia 42:117–127.

Ricci, C., M. Caprioli, and D. Fontaneto. 2007. Stress and fitness in parthenogens: is dormancy a key feature for bdelloid rotifers? BMC Evol. Biol. 7 Suppl 2:S9.

Ricci, C., and G. Melone. 2000. Key to the identification of the genera of bdelloid rotifers. Hydrobiologia 73–80.

Ricci, C., G. Melone, N. Santo, and M. Caprioli. 2003. Morphological response of a bdelloid rotifer to desiccation. J. Morphol. 257:246–53.

Ricci, C., G. Melone, and E. J. Walsh. 2001. A carnivorous bdelloid rotifer, *Abrochtha carnivora* n. sp. Invertebr. Biol. 120:136–141.

Ritz, K., and D. Trudgill. 1999. Utility of nematode community analysis as an integrated measure of the functional state of soils: perspectives and challenges. Plant Soil 212:1–11.

Robeson, M. S., E. K. Costello, K. R. Freeman, J. Whiting, B. Adams, A. P. Martin, and S. K. Schmidt. 2009. Environmental DNA sequencing primers for eutardigrades and bdelloid rotifers. BMC Ecol. 9:25.

Robinson, D., and L. Foulds. 1981. Comparison of phylogenetic trees. Math. Biosci. 141:131–141.

Ronquist, F., M. Teslenko, P. van der Mark, D. L. Ayres, A. Darling, S. Höhna, B. Larget, L. Liu, M. a Suchard, and J. P. Huelsenbeck. 2012. MrBayes 3.2: efficient Bayesian phylogenetic inference and model choice across a large model space. Syst. Biol. 61:539–42.

Rosen, D. E. 1979. Fishes from the uplands and intermontane basins of Guatemala: revisionary studies and comparative geography. Bull. Am. Museum Nat. Hist. 162:267–376.

Rubinoff, D. 2006. Essays: Utility of Mitochondrial DNA Barcodes in Species Conservation. Conserv. Biol. 20:1026–1033.

Rubinoff, D., S. Cameron, and K. W. Will. 2006. A genomic perspective on the shortcomings of mitochondrial DNA for “barcoding” identification. J. Hered. 97:581–94.

Rutschmann, F. 2006. Molecular dating of phylogenetic trees: A brief review of current methods that estimate divergence times. Divers. Distrib. 12:35–48.

Saitou, N., and M. Nei. 1987. The neighbor-joining method: a new method for reconstructing phylogenetic trees. Mol. Biol. Evol. 4:406–25.

Sanderson, M. J. 2003. r8s: Inferring absolute rates of molecular evolution and divergence times in the absence of a molecular clock. Bioinformatics 19:301–302.

Sanna, D., T. Lai, P. Francalacci, M. Curini-Galletti, and M. Casu. 2009. Population structure of the *Monocelis lineata* (Proseriata, Monocelididae) species complex assessed by phylogenetic analysis of the mitochondrial cytochrome *c* oxidase subunit I (COI) gene. Genet. Mol. Biol. 32:864–7.

Sasser, J. N., and C. C. Carter. 1985. An advanced treatise on *Meloidogyne*. Vol. 1. North Earolina state University and USAID Lima Pune.

Schliep, K. P. 2011. phangorn: phylogenetic analysis in R. Bioinformatics 27:592–3.

Schoch, C. L., K. a Seifert, S. Huhndorf, V. Robert, J. L. Spouge, C. A. Levesque, and W. Chen. 2012. Nuclear ribosomal internal transcribed spacer (ITS) region as a universal DNA barcode marker for Fungi. Proc. Natl. Acad. Sci. U. S. A. 109:6241–6.

Schön, I., and K. Martens. 2003. No slave to sex. Proc. R. Soc. London B 270:827–33.

Schön, I., R. L. Pinto, S. Halse, A. J. Smith, K. Martens, and C. W. Birky. 2012. Cryptic species in putative ancient asexual Darwinulids (Crustacea, Ostracoda). PLoS One 7:e39844.

Schön, I., G. Rossetti, K. Martens, and P. Dijk. 2009. Darwinulid Ostracods: Ancient Asexual Scandals or Scandalous Gossip? Pp. 217–240 *in* I. Schön, K. Martens, and P. Dijk, eds. Lost Sex - The Evolutionary Biology of Parthenogenesis. Springer Netherlands, Dordrecht.

Schröder, T., and E. J. Walsh. 2007. Cryptic speciation in the cosmopolitan *Epiphanes senta* complex (Monogononta, Rotifera) with the description of new species. Hydrobiologia 593:129–140.

Schubart, C. D., R. Diesel, and S. B. Hedges. 1998. Rapid evolution to terrestrial life in Jamaican crabs. Nature 393:363–365.

Schurko, A. M., M. Neiman, and J. M. Logsdon. 2009. Signs of sex: what we know and how we know it. Trends Ecol. Evol. 24:208–17.

Schwander, T., L. Henry, and B. J. Crespi. 2011. Molecular evidence for ancient asexuality in *Timema* stick insects. Curr. Biol. 21:1129–34. Elsevier Ltd.

Segers, H. 2007. Annotated checklist of the rotifers (Phylum Rotifera), with notes on nomenclature, taxonomy and distribution. Magnolia Press, Auckland, New Zealand.

Segers, H. 2008. Global diversity of rotifers (Rotifera) in freshwater. Hydrobiologia 595:49–59.

Segers, H. 1995. Nomenclatural consequences of some recent studies on *Brachionus plicatilis* (Rotifera, Brachionidae). Hydrobiologia 313/314:121–122.

Segers, H., and R. J. Shiel. 2005. Tale of a Sleeping Beauty: A New and Easily Cultured Model Organism for Experimental Studies on Bdelloid Rotifers. Hydrobiologia 546:141–145.

Sepp, S., and J. Paal. 1998. Taxonomic continuum of *Alchemilla* (Rosaceae) in Estonia. Nord. J. Bot. 18:519–535.

Serra, M., and T. Snell. 2009. Sex loss in Monogonont rotifers. Pp. 280–294 *in* I. Schön, K. Martens, and P. van Dijk, eds. Lost Sex - The Evolutionary Biology of Parthenogenesis. Dordrecht.

Shiel, R. J., and W. Koste. 1993. Rotifera from Australian inland waters. IX. Gastropodidae, Synchaetidae, Asplanchnidae (Rotifera: Monogononta). Trans. R. Soc. South Aust. 113:111–139.

Silvestro, D., and I. Michalak. 2011. raxmlGUI: a graphical front-end for RAxML. Org. Divers. Evol. 12:335–337.

Simpson, G. G. 1951. The species concept. Evolution 5:285–298.

Sites, J. W., and J. C. Marshall. 2003. Delimiting species: a Renaissance issue in systematic biology. Trends Ecol. Evol. 18:462–470.

Smith, R. J., T. Kamiya, and D. J. Horne. 2006. Living males of the "ancient asexual" Darwinulidae (Ostracoda: Crustacea). Proc. R. Soc. London B 273:1569–78.

Snyder, D. W., C. H. Opperman, and D. M. Bird. 2006. A method for generating *Meloidogyne incognita* males. J. Nematol. 38:192–4.

Sokal, R., and C. Michener. 1958. A statistical method for evaluating systematic relationships. Univ. Kansas Sci. Bull. 38:1409–1438.

Sokal, R. R., and T. J. Crovello. 1970. The biological species concept: A critical evaluation. Am. Nat. 104:127–153.

Song, H., J. E. Buhay, M. F. Whiting, and K. A. Crandall. 2008. Many species in one: DNA barcoding overestimates the number of species when nuclear mitochondrial pseudogenes are coamplified. Proc. Natl. Acad. Sci. U. S. A. 105:13486–91.

Sørensen, M. V., and G. Giribet. 2006. A modern approach to rotiferan phylogeny: combining morphological and molecular data. Mol. Phylogenet. Evol. 40:585–608.

Sota, T., and A. P. Vogler. 2001. Incongruence of mitochondrial and nuclear gene trees in the carabid beetles *Ohomopterus*. Syst. Biol. 50:39–59.

Srivathsan, A., and R. Meier. 2012. On the inappropriate use of Kimura-2-parameter (K2P) divergences in the DNA-barcoding literature. Cladistics 28:190–194.

Stadler, T. 2011. TreePar in R - Estimating diversification rates in phylogenies.

Stamatakis, A. 2006. RAxML-VI-HPC: maximum likelihood-based phylogenetic analyses with thousands of taxa and mixed models. Bioinformatics 22:2688–90.

Stamatakis, A., P. Hoover, and J. Rougemont. 2008. A rapid bootstrap algorithm for the RAxML Web servers. Syst. Biol. 57:758–71.

Struck, T. H., and G. Purschke. 2005. The sister group relationship of Aeolosomatidae and Potamodrilidae (Annelida: "Polychaeta") — a molecular phylogenetic approach based on 18S rDNA and cytochrome oxidase I. Zool. Anz. 243:281–293.

Suatoni, E., S. Vicario, S. Rice, T. Snell, and A. Caccone. 2006. An analysis of species boundaries and biogeographic patterns in a cryptic species complex: the rotifer *Brachionus plicatilis*. Mol. Phylogenet. Evol. 41:86–98.

Suchard, M. a, R. E. Weiss, and J. S. Sinsheimer. 2005. Models for estimating bayes factors with applications to phylogeny and tests of monophyly. Biometrics 61:665–73.

Taberlet, P., E. Coissac, M. Hajibabaei, and L. H. Rieseberg. 2012. Environmental DNA. Mol. Ecol. 21:1789–93.

Talavera, G., V. Dinca, and R. Vila. 2013. Factors affecting species delimitations with the GMYC model: insights from a butterfly survey. Methods Ecol. Evol. 4:1101–1110.

Tamura, K., D. Peterson, N. Peterson, G. Stecher, M. Nei, and S. Kumar. 2011. MEGA5: molecular evolutionary genetics analysis using maximum likelihood, evolutionary distance, and maximum parsimony methods. Mol. Biol. Evol. 28:2731–9.

Tamura, K., G. Stecher, D. Peterson, A. Filipski, and S. Kumar. 2013. MEGA6: Molecular Evolutionary Genetics Analysis version 6.0. Mol. Biol. Evol. 30:2725–9.

Tang, C. Q., A. Humphreys, D. Fontaneto, and T. G. Barraclough. 2014a. Effects of phylogenetic reconstruction method on the robustness of species delimitation using single locus data. Methods Ecol. Evol. in press.

Tang, C. Q., F. Leasi, U. Obertegger, A. Kieneke, T. G. Barraclough, and D. Fontaneto. 2012. The widely used small subunit 18S rDNA molecule greatly underestimates true diversity in biodiversity surveys of the meiofauna. Proc. Natl. Acad. Sci. U. S. A. 109:16208–16212.

Tang, C. Q., U. Obertegger, D. Fontaneto, and T. G. Barraclough. 2014b. Sexual species are separated by larger genetic gaps than asexual species in rotifers. Evolution 68:2901–2916.

Tateno, Y., N. Takezaki, and M. Nei. 1994. Relative efficiencies of the maximum-likelihood, neighbor-joining, and maximum-parsimony methods when substitution rate varies with site. Mol. Biol. Evol. 11:261–77.

Tautz, D., P. Arctander, A. Minelli, R. H. Thomas, and A. P. Vogler. 2003. A plea for DNA taxonomy. Trends Ecol. Evol. 18:70–74.

Thalmann, O., J. Hebler, H. N. Poinar, S. Pääbo, and L. Vigilant. 2004. Unreliable mtDNA data due to nuclear insertions: a cautionary tale from analysis of humans and other great apes. Mol. Ecol. 13:321–335.

Todaro, M. A., T. Kånneby, M. Dal Zotto, and U. Jondelius. 2011. Phylogeny of Thaumastodermatidae (Gastrotricha: Macrodasyida) inferred from nuclear and mitochondrial sequence data. PLoS One 6:e17892.

Turner, C. H. 1895. Fresh-water Ostracoda of the United States. Pp. 277–337 *in* Minnesota Geological Natural History Survey, Zoological Series 2.

Untergasser, A., I. Cutcutache, T. Koressaar, J. Ye, B. C. Faircloth, M. Remm, and S. G. Rozen. 2012. Primer3--new capabilities and interfaces. Nucleic Acids Res. 40:e115.

Van Valen, L. 1976. Ecological species, multispecies, and oaks. Taxon 25:233–239.

Venables, W. N., and B. D. Ripley. 2002. Modern Applied Statistics with S. 4th ed. Springer, New York.

Vences, M., M. Thomas, R. M. Bonett, and D. R. Vieites. 2005. Deciphering amphibian diversity through DNA barcoding: chances and challenges. Philos. Trans. R. Soc. Lond. B. Biol. Sci. 360:1859–68.

Vogler, A. P., and M. T. Monaghan. 2007. Recent advances in DNA taxonomy. J. Zool. Syst. Evol. Res. 45:1–10.

Waggoner, B. M., and G. O. Poinar. 1993. Fossil habrotrochid rotifers in Dominican amber. Experientia 49:354–357.

Wallace, R. L. 2002. Rotifers: exquisite metazoans. Integr. Comp. Biol. 42:660–667.

Wallace, R. L., and H. A. Smith. 2013. Rotifera. Pp. 1–8 *in* eLS. John Wiley & Sons Ltd, Chichester.

Wallace, R. L., T. Snell, and C. Ricci. 2006. Rotifera part 1: biology, ecology and systematics. *in* H. J. F. Dumont, ed. Guides to the Identification of the Microinvertebrates of the Continental Waters of the World. Kenobi Production & Backhuys Publishers, The Netherlands.

Walsh, E. J., H. A. Smith, and R. L. Wallace. 2014. Rotifers of temporary waters. Int. Rev. Hydrobiol. 98:1–17.

Ward, R. D., T. S. Zemlak, B. H. Innes, P. R. Last, and P. D. N. Hebert. 2005. DNA barcoding Australia's fish species. Philos. Trans. R. Soc. Lond. B. Biol. Sci. 360:1847–57.

Webb, K. E., D. K. A. Barnes, M. S. Clark, and D. A. Bowden. 2006. DNA barcoding: A molecular tool to identify Antarctic marine larvae. Deep Sea Res. Part II Top. Stud. Oceanogr. 53:1053–1060.

Weismann, A. 1889. The significance of sexual reproduction in the theory of natural selection. Pp. 251–332 *in* E. B. Poulton, S. Schonland, and A. E. Shipley, eds. Essays upon heredity and kindred biological problems. Clarendon Press, Oxford.

Weiss, M., J. N. Macher, M. A. Seefeldt, and F. Leese. 2014. Molecular evidence for further overlooked species within the *Gammarus fossarum* complex (Crustacea: Amphipoda). Hydrobiologia 721:165–184.

West, S. A., C. M. Lively, and A. F. Read. 1999. A pluralist approach to sex and recombination. Science 12:1003–1012.

Westheide, W., and E. Hass-Cordes. 2001. Molecular taxonomy: description of a cryptic *Petitia* species (Polychaeta : Syllidae) from the island of Mahe (Seychelles, Indian Ocean) using RAPD markers and ITS2 sequences. J. Zool. Syst. Evol. Res. 39:103–111.

White, M. J. D. 1945. Animal cytology and evolution. CUP Archive, 1977.

White, M. J. D. 1978. Modes of speciation. WH Freeman, San Francisco.

Wiemers, M., and K. Fiedler. 2007. Does the DNA barcoding gap exist? - a case study in blue butterflies (Lepidoptera: Lycaenidae). Front. Zool. 4:8.

Wiens, J. J. 2007. Species delimitation: new approaches for discovering diversity. Syst. Biol. 56:875–8.

Wilke, T. 2003. Salenthydrobia gen. nov. (Rissooidea: Hydrobiidae): A potential relict of the Messinian salinity crisis. Zool. J. Linn. Soc. 137:319–336.

Wilke, T., R. Schultheiß, and C. Albrecht. 2009. As time goes by: A simple fool's guide to molecular clock approaches in invertebrates. Am. Malacol. Bull. 27:25–45.

Will, K. W., and D. Rubinoff. 2004. Myth of the molecule: DNA barcodes for species cannot replace morphology for identification and classification. Cladistics 20:47–55.

Williams, G. C. 1975. Sex and evolution. Princeton University Press, New Jersey.

Wilson, C. G., and P. W. Sherman. 2010. Anciently asexual bdelloid rotifers escape lethal fungal parasites by drying up and blowing away. Science 327:574–6.

Wilson, K. H. 1995. Molecular biology as a tool for taxonomy. Clin. Infect. Dis. 20:S117–S121.

Wu, T., E. Ayres, R. D. Bardgett, D. H. Wall, and J. R. Garey. 2011. Molecular study of worldwide distribution and diversity of soil animals. Proc. Natl. Acad. Sci. U. S. A. 108:17720–17725.

Yamasaki, H., S. F. Hiruta, and H. Kajihara. 2013. Molecular phylogeny of kinorhynchs. Mol. Phylogenet. Evol. 67:303–10.

Yang, Z., and B. Rannala. 2010. Bayesian species delimitation using multilocus sequence data. Proc. Natl. Acad. Sci. U. S. A. 107:9264–9.

Yoccoz, N. G. 2012. The future of environmental DNA in ecology. Mol. Ecol. 21:2031–8.

Yoccoz, N. G., K. A. Bråthen, L. Gielly, J. Haile, M. E. Edwards, T. Goslar, H. Von Stedingk, A. K. Brysting, E. Coissac, F. Pompanon, J. H. Sønstebø, C. Miquel, A. Valentini, F. De Bello, J. Chave, W. Thuiller, P. Wincker, C. Cruaud, F. Gavory, M. Rasmussen, M. T. P. Gilbert, L. Orlando, C. Brochmann, E. Willerslev, and P. Taberlet. 2012. DNA from soil mirrors plant taxonomic and growth form diversity. Mol. Ecol. 21:3647–3655.

Yu, D. W., Y. Ji, B. C. Emerson, X. Wang, C. Ye, C. Yang, and Z. Ding. 2012. Biodiversity soup: metabarcoding of arthropods for rapid biodiversity assessment and biomonitoring. Methods Ecol. Evol. 3:613–623.

Yule, G. U. 1925. A mathematical theory of evolution, based on the conclusions of Dr. JC Willis, FRS. Philos. Trans. R. Soc. Lond. B. Biol. Sci. 213:21–87.

Zanol, J., K. M. Halanych, T. H. Struck, and K. Fauchald. 2010. Phylogeny of the bristle worm family Eunicidae (Eunicida, Annelida) and the phylogenetic utility of noncongruent 16S, COI and 18S in combined analyses. Mol. Phylogenet. Evol. 55:660–76.

Zhan, A., S. A. Bailey, D. D. Heath, and H. J. Macisaac. 2014. Performance comparison of genetic markers for high-throughput sequencing-based biodiversity assessment in complex communities. Mol. Ecol. Resour. in press.

Zhang, J., P. Kapli, P. Pavlidis, and A. Stamatakis. 2013. A general species delimitation method with applications to phylogenetic placements. Bioinformatics 29:2869–76.

Zhang, J.-Y., Y. Xi, Q. Ma, and X.-L. Xiang. 2010. Taxonomical status of two *Brachionus calyciflorus* morphotypes in Lake Liantang based on ITS sequence. Acta Hydrobiol. Sin. 34:935–942.

Zhou, X., Y. Li, S. Liu, Q. Yang, X. Su, L. Zhou, M. Tang, R. Fu, J. Li, and Q. Huang. 2013. Ultra-deep sequencing enables high-fidelity recovery of biodiversity for bulk arthropod samples without PCR amplification. Gigascience 2:4.

Zrzavý, J., P. Říha, L. Piálek, and J. Janouskovec. 2009. Phylogeny of Annelida (Lophotrochozoa): total-evidence analysis of morphology and six genes. BMC Evol. Biol. 9:189.

Zwickl, D. J. 2006. GARLI: genetic algorithm for rapid likelihood inference. University Texas at Austin.

Supplementary Files

Chapter 2: Supplementary Materials and Methods

DNA extraction

DNA was extracted from individual animals; these were isolated into sterile tubes, and 40µl of Chelex (InstaGene Matrix; Bio-Rad, http://www.bio-rad.com) was added to each sample. Sample mixtures were vortexed for a minimum of 5 seconds each and heated as per the manufacturer's protocol (56°C for 20 minutes followed by 96°C for 20 minutes), but then stored at -20°C overnight and heated at 56°C for 20 minutes followed by 96°C for 20 minutes. The suspended DNA was directly used in subsequent PCR amplification.

DNA amplification

PCRs were performed in a total volume of 25µl using the illustra Ready-To-Go™ RT-PCR Beads (GE Healthcare); 2µl of each primer (10mM), 2µl of DNA (10-50ng) and ddH_20 up to 25µl.

COI was amplified using optimised Folmer primers Hcox1 (5'-GGT CAA CAA ATC ATA AAG ATA TTG G-3') and Lcox1 (5'-TAA ACT TCA GGG TGA CCA AAA AAT CA-3'). Cycle conditions comprised initial denaturing at 95°C for 5 minutes, followed by 35 cycles of 95°C for 1 minute, 46.4°C for 1 minute and 72°C for 90 seconds, and a final extension step of 72°C for 5 minutes. Nested PCRs were performed where necessary using the primers COIrot (5'-ATT ATT CGT ACT GAR TTA GG-3') and COICT1R (5'-TAM ACT TCY GGA TGM CCR AAR AAT CA-3') and the same cycle conditions but for only 25 cycles.

18S rRNA was amplified using a nested approach; the total fragment was amplified using 18SFnew (5'-AGA TTA AGC CAT GCA TGT CT-3') and 9R (5'-GAT CCT TCC GCA GGT TCA CCT AC-3'). Cycle conditions comprised initial denaturing at 95°C for 5 minutes, followed by 38 cycles of 95°C for 1 minute, 55°C for 1 minute and 72°C for 2 minutes and a final extension step of 72°C for 10 minutes. Three nested PCRs were performed using these primer pairs: 18SFnew (5'-AGA TTA AGC CAT GCA TGT CT-3') – 4R (5'-GAA TTA CCG CGG CTG CTG G-3'), 18SCT1 (5'-TGG AGG GCA AGT CTG GTG CCA GC-3') – 18Sbi (5'-GAG TCT CGT TCG TTA TCG GA-3'), and 18Sa2.0 (5'-ATG GTT GCA AAG CTG AAA C-3') – 9R (5'-GAT CCT TCC GCA GGT TCA CCT AC-3'). The nested PCR cycle conditions comprised of an initial denaturation step of 95°C for 5 minutes, followed by 25 cycles of 95°C for 1 minute, 55°C for 1 minute and 72°C for 1 minutes, and a final extension step of 72°C for 5 minutes.

All PCR amplicons were purified and concentrated using Illustra GFX™ PCR DNA and Gel band purification kit as per manufacturer's protocol with a final volume ranging from 10µl to 20µl depending on the concentration of the amplicon. Cycle sequencing reactions were set up using

purified amplicons, 1:10 of the PCR primers and the ABI Big Dye Terminator v1.1 kit and run on an ABI 3770 automated sequencer. The sequences were checked and assembled by eye using Geneious Pro 5.4.2 (Drummond et al. 2006).

Phylogenetic analysis

Sequences were collapsed into unique types using DnaSP (Librado and Rozas 2009) and aligned using MAFFT (Katoh et al. 2009) with the default settings, followed by checking and manual editing in Geneious Pro 5.4.2 (Drummond et al. 2006). A matrix of pairwise uncorrected distances was generated using the package *ape* 2.8 (Paradis et al. 2004) in R 2.14.0 (R Core Team 2014). Maximum likelihood trees were constructed using PhyML 3.0 (Guindon et al. 2010) using the default settings with the best evolutionary model as determined using jModeltest (Posada 2009) and a suitable outgroup (Table S2.1). Gene trees were made ultrametric using penalized likelihood in r8s 1.71 (Sanderson 2003), where cross-validation analysis was performed to identify the best level of smoothing.

Nucleotide divergence threshold script for delimiting species

```
align<-read.dna("alignment.phy")
seq.dist<-dist.dna(align,model="raw",as.matrix=TRUE)
#Set the nucleotide divergence threshold (97%=0.03, 99%=0.01,
#99.5%=0.005)
threshold<-0.03
num.tips<-length(seq.dist[1,])
groups<-array(NA,num.tips)
k<-1
for (i in (1:num.tips)){
  match<-which(seq.dist[i,]<=threshold)
  if(length(match)==1){
    groups[match]<-k
    k<-k+1
    next}
  x<-is.na(groups[match])
  if(prod(x)==0){
    groups[match]<-unique(groups[match[!x]])}
  else{
    groups[match]<-k
    k<-k+1}
}
#How many species?
max(groups)
```

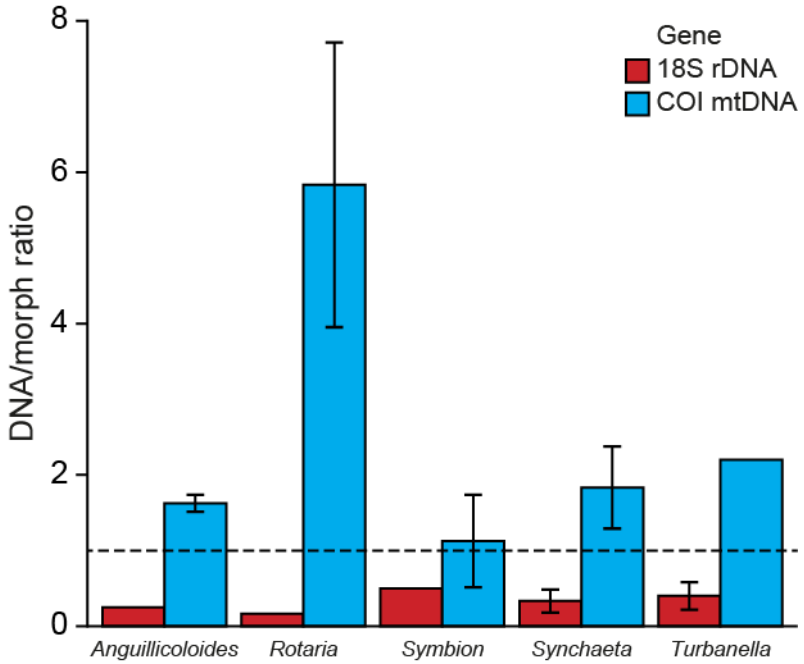

Figure S2.1 Species estimated from DNA taxonomy compared to morphological taxonomy (dotted line) for taxa where COI (blue) and 18S (red) were amplified from the same individuals. Estimates were averaged across the different delimitation metrics. Standard errors are given where there was variation among the different metric estimates.

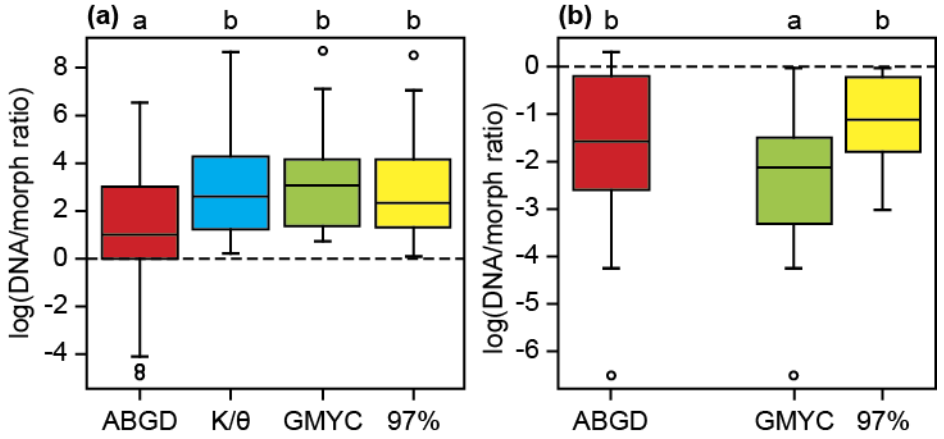

Figure S2.2 Equivalence of species estimates inferred using different delimitation metrics with either COI (**a**) or 18S (**b**).
All values are logged and relative to the morphological estimates (dotted line at y=0). Statistically significant differences are indicated by different letters above the bars (for details see Table S2.3). The K/θ method is not applicable for diploid 18S and is therefore not included.

Table S2.1 Results of species delimitation analyses.
Found on the attached CD, or available upon request.

Table S2.2 ANOVA output of a model explaining the congruence of species estimation among delimitation metrics (using coefficient of variance as a proxy for congruence), using a measure of sampling effort (number of countries), taxonomic rank, and their interaction.

Factor	D.F.	Sum Sq.	Mean Sq.	F value	*P*	% var.
All data						
Gene	1	23664	23664	14.79	0.00035	18.7
Sampling	1	14425	14424.9	9.02	0.0042	11.4
Tax.	2	9597	4798.4	3	0.059	7.6
Sampling x Tax.	2	2035	1017.3	0.64	0.53	1.6
Residuals	48	76778	1599.5			
COI mtDNA						
Sampling	1	74.3	74.3	0.086	0.77	0.3
Tax.	2	731.8	365.9	0.43	0.66	3.2
Sampling x Tax.	2	613.8	306.9	0.36	0.7	2.7
Residuals	25	21534	861.4			
18S rDNA						
Sampling	1	20475	20474.5	16.75	0.00068	25.6
Tax.	2	24488	12243.9	10.02	0.00121	30.7
Sampling x Tax.	2	12917	6458.4	5.28	0.016	16.2
Residuals	18	22001	1222.3			

% var. = amount of the variance explained by the factor, Tax. = taxonomic rank, Sampling = sampling (number of sequences).

Table S2.3 Tukey HSD comparisons of delimitation metric species estimates for COI and 18S.

Comparison	Diff. in means	Lower	Upper	*P*
COI mtDNA				
K/θ-ABGD	1.01	0.12	1.9	0.019
GMYC-ABGD	1.08	0.19	1.97	0.01
97%-ABGD	0.99	0.1	1.88	0.023
GMYC-K/θ	0.071	-0.82	0.96	1
97%-K/θ	-0.023	-0.91	0.87	1
97%-GMYC	-0.093	-0.98	0.8	0.99
18S rDNA				
GMYC-ABGD	-0.4	-1.33	0.53	0.56
97%-ABGD	0.59	-0.34	1.51	0.29
97%-GMYC	0.99	0.057	1.91	0.035

Table S2.4 ANOVA used to explain differences in DNA/morph ratios using a subset of taxonomically certified sequences.

Factor	Sum Sq.	D.F.	F value	*P*	% var.
Gene	290.0	1	311.70	$2.2e^{-16}$	53.1
Metric	12.6	3	4.51	0.0047	4.9
Tax.	63.1	2	33.91	$9.76e^{-13}$	25.9
Sampling	38.4	1	41.25	$1.95e^{-9}$	21.2
Metric x Tax.	2.8	6	0.51	0.8	2.0
Metric x Sampling	9.4	3	3.37	0.02	6.7
Residuals	130.3	140			

% var. = amount of the variance explained by the factor,
Tax. = taxonomic rank, Sampling = sampling (number of sequences).

Table S2.5 ANOVA used to explain DNA/morph ratio (COI and 18S analyzed separately, using a subset of taxonomically certified sequences).

	D.F.	Sum Sq.	Mean Sq.	F value	*P*	% var.
COI mtDNA						
Metric	3	27.0	9.0	10.44	$8.77e^{-6}$	15.4
Tax.	2	37.5	18.8	21.77	$4.03e^{-8}$	25.3
Country	1	15.5	15.5	17.94	$6.64e^{-5}$	13.3
Undersampling	1	0.1	0.1	0.07	0.79	0.0
Metric x Tax.	6	2.8	0.5	0.53	0.78	2.1
Tax. x Country	2	1.9	1.0	1.10	0.34	1.4
Metric x Undersampling	3	10.0	3.3	3.88	0.013	5.9
Tax. x Undersampling	2	1.8	0.9	1.05	0.36	1.1
Country x Undersampling	1	0.2	0.2	0.18	0.67	0.1
Metric x Tax. x Undersampling	4	10.8	2.7	3.12	0.020	6.8
Tax. x Country x Undersampling	1	5.6	5.6	6.47	0.013	3.8
Residuals	72	62.1	0.9			
18S rDNA						
Metric	2	5.8	2.9	4.16	0.021	7.3
Tax.	2	32.2	16.1	22.94	$9.29e^{-8}$	43.3
Country	1	0.8	0.8	1.19	0.28	2.0
Metric x Country	2	7.0	3.5	4.98	0.011	16.9
Residuals	49	34.4	0.7			

% var. = amount of the variance explained by the factor, Tax. = taxonomic rank.

Table S2.6 Differences between bdelloid and monogonont rotifers with respect to genetic distance assessed across all three taxonomic ranks (species complex, genus, higher taxon) using an unpaired Mann-Whitney U test.

Comparison	**W**	**Bdelloidea**			**Monogononta**			**Difference in mean**	***P***
		Mean	**S.E.**	**N**	**Mean**	**S.E.**	**N**		
Within species genetic distance*	32	0.0106	0.00102	9	0.0131	0.00172	11	0.0025	0.20
Between species genetic distance†	12	0.124	0.00825	NA	0.175	0.0275	NA	0.051	0.088

N = sample size, S.E. = standard error, *Genetic distances calculated as the mean of all the pairwise distance within a clade, †Genetic distances calculated as the mean of all the pairwise distance between pairs of clades.

Table S2.7 ANOVA used to explain differences in DNA/morph ratios with asexual taxa excluded.

Factor	**Sum Sq.**	**D.F.**	**F value**	***P***	**% var.**
Gene	195.1	1	100.89	$<2.2e^{-16}$	21.71
Metric	71.5	3	12.33	$2.32e^{-7}$	7.96
Tax.	289.9	2	74.95	$<2.2e^{-16}$	35.25
Residuals	342.3	177			

% var. = amount of the variance explained by the factor, Tax. = taxonomic rank.

Chapter 3: Supplementary Materials and Methods

Gene trees are required by both the GMYC and PTP models. Ultrametric trees are needed for the GMYC model (Pons et al. 2006; Fujisawa and Barraclough 2013) as it analyses branching rates, while the PTP delimits species from the number of substitutions inferred from "raw" (unsmoothed) or ultrametric trees (Zhang et al. 2013). Tree reconstruction followed these steps (outlined in Fig. S3.1): (1) align sequences, (2) remove non-unique haplotypes, (3) reconstruct gene trees, and (4) make ultrametric gene trees.

Obtaining gene trees

(1) Sequence alignment

Cytochrome oxidase *c* subunit 1 (COI) sequences were downloaded from GenBank (except for the cowrie dataset, which was provided by Christopher P. Meyer) and aligned with carefully selected outgroups (Table S3.3) using the MAFFT v6.814b plugin (Katoh et al. 2009) with the default settings within Geneious 5.4.6 (Drummond et al. 2006). Alignments were subsequently checked by eye and atypically short sequences (100bp shorter than all the others) were removed. Translation of the alignments (using the Invertebrate Mitochondrial Code) was used as an additional check of their validity. No indels, NUMTS or stop codons were found in any of the alignments. In total 10,244 sequences were obtained and aligned into 16 separate datasets representing different taxonomic ranks. The butterfly dataset was a comprehensive geographical sample (Romania) of an order (Lepidoptera; Dinca et al. 2011), the cowrie dataset was a comprehensive sample of a family (Cypraeidae; Meyer and Paulay 2005) and the remaining datasets were samples of genera with the exception of *Pleuretra lineata*, which is a species complex.

(2) Removal of non-unique haplotypes

The alignments were stripped of non-unique haplotypes using DnaSP 5.10.01 (Librado and Rozas 2009), resulting in 3,190 unique haplotypes. Non-unique haplotypes were removed as the GMYC model assumes a fully bifurcating tree and zero length terminal branches hamper the likelihood estimation (Fujisawa and Barraclough 2013). Collapsing datasets is typically the first step in tree based species delimitation analyses and does not significantly affect the outcome of the GMYC analysis (Talavera et al. 2013). Performing this step before both GMYC and PTP analyses allowed for direct comparisons between the methods at reduced computation expense.

(3) Reconstruction of gene trees

Haplotype alignments were used to generate gene trees using distance, maximum likelihood (ML) and Bayesian inference (BI) methods. For each haplotype alignment, 10 trees were reconstructed using different methods with the most commonly used software. Distance trees were reconstructed using Neighbour Joining (NJ; Saitou and Nei 1987) and UPGMA (Un-weighted Pair Group Method with

Arithmetic mean; Sokal and Michener 1958). NJ trees were generated using the *ape* 3.0.7 package (Paradis et al. 2004) in R 2.15.2 (R Core Team 2014) from sequence distance matrices computed by the Kimura (K80 or K2P) model (Kimura 1980). UPGMA distance trees were built with MEGA5 (Tamura et al. 2011) using p-distances instead of a model of evolution. For the ML and BI methods, gene trees were reconstructed using the best model of evolution as determined *a priori* using the lowest Akaike Information Criterion (AIC computed in jModelTest 2 - Darriba et al. 2012; Table S3.3). ML gene trees were reconstructed using GARLI 2.01 (Zwickl 2006), PhyML 3.0 (Guindon et al. 2010) and RAxML (Stamatakis 2006). GARLI trees were reconstructed with the evolutionary models with the lowest AIC score and 5,000,000 generations. All PhyML trees were generated using the ATGC online server. For each analysis, the appropriate evolutionary model was selected with optimised equilibrium frequencies and optimal trees were searched for using the combined nearest neighbour and subtree pruning and regrafting tree rearrangement option (available in PhyML 3.0), but otherwise default settings were used. RAxML trees were generated using either the RAxML BlackBox webserver (Stamatakis 2006; Stamatakis et al. 2008) or using the CIPRES Science Gateway server (Miller et al. 2010) with a Gamma model of rate heterogeneity, maximum likelihood model search and an estimated proportion of invariable sites.

BI trees were reconstructed using MrBayes 3.2.1 (Huelsenbeck and Ronquist 2001; Ronquist et al. 2012) and BEAST v1.7.5 (Drummond and Rambaut 2007). MrBayes analyses were run for 10,000,000 generations with four parallel searches sampling every 500 generations. Consensus trees were generated using the *sumt* command with a 10% burnin, but only if the average standard deviation of the chains was less than 0.01 (as recommended in the MrBayes documentation). Four separate BEAST runs, with different parameters, were performed for each clade. BEAST input files were generated using BEAUti v1.7.5, each search ran with a substitution rate of 1.76% per million years, the most accepted rate for most invertebrates (Wilke et al. 2009) under either an uncorrelated lognormal relaxed molecular clock or a strict molecular clock and either a 'Speciation: Birth-Death Process' (Gernhard 2008) or a 'Coalescent' tree prior. Each dataset was run for at least 30,000,000 generations sampling every 1,000 steps on the CIPRES Science Gateway server. All of the other options were kept as the BEAUti default settings. The effective sample size (ESS) of each run was determined using Tracer v1.5 (Rambaut and Drummond 2009) and only trees with an ESS of at least 200 were kept (as recommended in the BEAST manual). Initially low ESS scores for some runs were resolved by increasing the number of generations of MCMC sampling. The burnin was set to 10% and TreeAnnotator v1.6.1 was used to summarise the trees to give a maximum clade credibility tree with target node heights.

(4) Make ultrametric gene trees

Ultrametric trees are the required input for the GMYC model as branch lengths need to convey time; although not required by the PTP, ultrametric trees were also analysed using the PTP for a direct

comparison. Of the ten gene trees produced for each clade, five were ultrametric by default (the four BEAST combinations and UPGMA), while the remaining five (MrBayes, GARLI, PhyML, RAxML and NJ) were smoothed using four different methods (r8s - Sanderson 2003; the *ape* functions: *chronopl* and *chronos* - Paradis et al. 2004; and PATHd8 - Britton et al. 2007). These four branch smoothing methods were used independently on each raw gene tree to generate ultrametric input trees; this totalled 20 trees per clade. The r8s software was used to perform nonparametric branch smoothing (NPRS). This method smoothes rate changes among lineages while penalising fast rate changes from mother to daughter. The level of smoothing was optimised using a cross validation procedure. PATHd8 uses mean path length to smooth substitution rates between sister groups by sequentially averaging path lengths from an internode to all the descending terminals. The R package *ape* has two branch smoothing functions: *chronopl* (semi-parametric penalised likelihood) and *chronos* (an update of *chronopl*). For each of these functions a smoothing parameter, lambda (λ), needs to be set. Lambda controls the trade-off between branches having their own rate ($\lambda \rightarrow 0$) and minimising rate changes between connecting branches ($\lambda \rightarrow 1$). Rates vary more among branches as λ tends towards zero, while the variation among branches is more clock-like as λ tends towards one. For all analyses, λ was set to 1 as varying λ did not consistently affect the numbers of ESUs obtained (Supplementary File S2).

Species delimitation

Outgroup taxa were pruned from each tree before species delimitation analysis. For each dataset, the ten raw gene trees produced in (3) and the 20 additional smoothed trees produced in (4) were analysed with the PTP method ($n = 30$). The five ultrametric trees (BEAST and UPGMA) produced in (3) and the 20 additional smoothed trees produced in (4) were analysed with the GMYC method ($n = 25$). The GMYC and PTP methods delimit species defined as independently evolving, monophyletic units (an operational version of the Evolutionary Species Concept, Simpson 1951). Both methods model species- and population-level processes, separately, and identify a transition point between the two; this threshold is subsequently used to delimit ESUs.

Generalized Mixed Yule Coalescent model

The GMYC takes advantage of the pattern expected if species have been evolving independently for a sufficiently long period of time, namely distinct genetic clusters separated in genospace by long internal branches (Barraclough and Nee 2001). An ultrametric gene tree (where branch lengths are equivalent or relative to time) well-sampled for both intra- and interspecific variation will bifurcate in a predictable manner: species-level processes will lead to slower branching rates while population-level coalescent processes will exhibit accelerated branching patterns. It follows that there should be a transition in branching rate on a tree between species level processes (e.g. speciation and extinction) and population level processes (coalescence of alleles). The GMYC is a likelihood-based method that

models the branching rate of both diversification between species (Yule model - Yule 1925; Nee et al. 1994) and genealogical branching within populations (neutral coalescent - Hudson 1990) to identify from the data whether there is a significant shift (threshold) in branching rate. A X^2 test is performed to gauge the significance of the application of the GMYC against the null hypothesis of a single coalescent with one branching rate. If significant, the threshold is used to delimit species on the gene tree. The GMYC method allows for either a single or multiple thresholds at which branching rates shift. Multiple-threshold allows for depth of the transition from coalescent to speciation to vary among lineages (Monaghan et al. 2009; Fujisawa and Barraclough 2013), and so should better accommodate rate heterogeneity within datasets. The multiple-threshold algorithm assesses the likelihood of new clusters by either splitting or lumping existing clusters and identifying increases in likelihood improvement. Clusters that increase the likelihood of the model are chosen as new starting points for the next heuristic search.

Both single- and multiple-threshold GMYC methods search for the model with the highest likelihood score, however, the most likely solution may not be the only model with which the null model (single coalescent) can be rejected. Powell (2012) and Fujisawa and Barraclough (2013) implemented an alternative GMYC approach that assigns weights to and ranks all alternative models that reject the null model based on their fit to the data using AIC (Powell's GMYC multimodel script is available from http://dx.doi.org/10.1111/j.2024-210X.2011.00122.x). The Powell multimodel GMYC approach uses model averaging to infer parameters and species probabilities. Each ultrametric tree was analysed by the GMYC with three different approaches: single threshold (ST-GMYC), multiple thresholds (MT-GMYC), and multimodel (MM-GMYC). These analyses were performed with the *splits* 1.0–11 package (Ezard et al. 2009 - available from https://r-forge.r-project.org/ projects/splits) in R.

Poisson Tree Process (PTP)

The PTP method does not rely on ultrametric trees as input. Instead, the PTP model delimits species directly from the number of substitutions inferred by the branch lengths, which represent the mean expected number of substitutions per site between two branching events. The fundamental assumption is that the intraspecific number of substitutions will be significantly lower than the interspecific number of substitutions. It is assumed that a gene tree sampled both intra- and interspecifically will have been generated by two independent Poisson tree processes (species- and population-level). Support for only one PTP process could mean that only a single population exists or that each tip is a separate species. Note that this implicitly assumes that molecular substitution rates are constant across the tree: if they varied considerably then variation in substitution rates across the tree could impair correct identification of the transition from species- to population-level processes. A standard likelihood-ratio test with one degree of freedom is performed to test for multiple classes of branch length and, if present, a maximum likelihood search returns the most likely speciation rate, coalescent rate and the transition between them. The PTP model was used for each of the rooted trees (raw and

ultrametric), using the PTP web server (http://species.h-its.org/ptp/) and a mimimum *P*-value of 0.05. For the ultrametric trees, the PTP should still use the branch lengths to represent number of substitutions between branching events but if the branch lengths are not a good representation of the underlying substitution rates, then the PTP will be biased by that assumption.

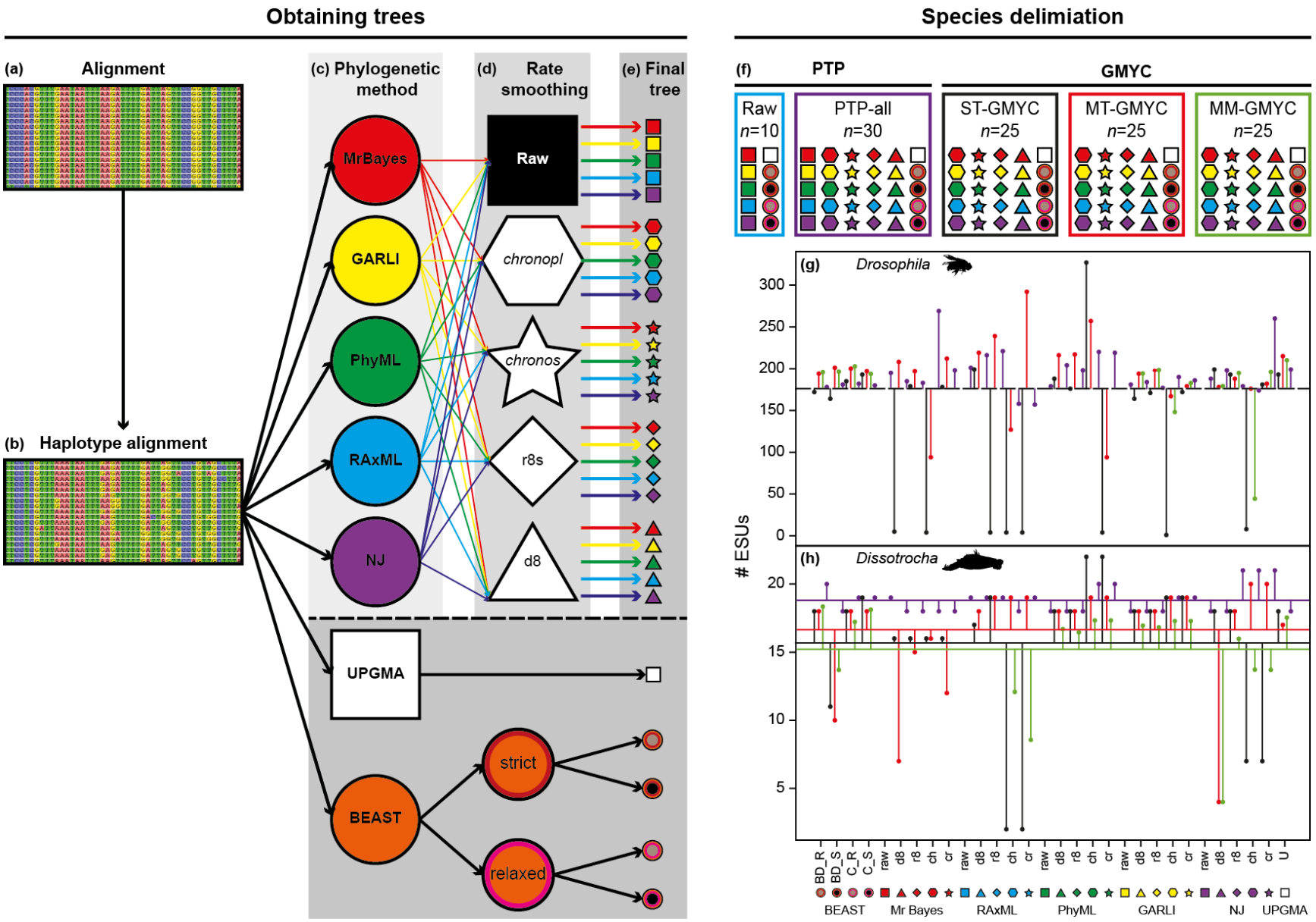
Obtaining trees
Species delimiation
(a) Alignment
(b) Haplotype alignment
(c) Phylogenetic method
(d) Rate smoothing
(e) Final tree
MrBayes
GARLI
PhyML
RAxML
NJ
UPGMA
BEAST
Raw
chronopl
chronos
r8s
d8
strict
relaxed
(f) PTP
GMYC
Raw n=10
PTP-all n=30
ST-GMYC n=25
MT-GMYC n=25
MM-GMYC n=25
(g) Drosophila
(h) Dissotrocha
ESUs
BD_R
BD_S
C_R
C_S
raw
d8
r8
ch
cr
U
BEAST
Mr Bayes
RAxML
PhyML
GARLI
NJ
UPGMA

Figure S3.1 Methods overview.
For each of the 16 datasets, an alignment with suitable outgroups is made (a) and collapsed into an alignment of unique haplotypes (b). This haplotype alignment is analysed with ten different phylogenetic methods (c). Of these, five produce ultrametric trees (UPGMA and BEAST), while the other five are either left "raw" or require smoothing with one of four smoothing methods (d). In total, 30 trees (e) are generated. These final trees are analysed using the PTP and GMYC species delimitation methods (f). Note that non-ultrametric trees can be analysed by the PTP but not the GMYC method. Species delimitation analyses are split into PTP using unsmoothed trees only (as intended by the authors [PTP-raw]), PTP with all trees [PTP-all], GMYC with a single (ST-GMYC) or multiple (MT-GMYC) thresholds and a multimodel approach (MM-GMYC), applied to n trees in total. The robustness of each delimitation method (using *Drosophila* [g] and Dissotrocha [a rotifer; h] as examples): the absolute distance of the ESU estimate (ESU_X) to the expected ESU count (either morphological species number, ESU_{morph}, [g] or the average ESU estimate for that particular delimitation method, ESU_{meanB}, [h]).

Table S3.1 Literature review of trees used as GMYC input (from 2006 to April 2014).
Found on the attached CD, or available upon request.

Table S3.2 Accession numbers and publication information
Found on the attached CD, or available upon request.

Table S3.3 Dataset information (# Seq., #Hap., outgroups, residual variation, etc.)
Found on the attached CD, or available upon request.

Table S3.4 Simultaneous pairwise Tukey HSD tests for General Linear Hypotheses using BEAST trees only. Differences in residual variation of ESU estimate between each delimitation method analysed separately for the non-Rotifera and Rotifera datasets.
ST-GMYC, MT-GMYC, and MM-GMYC refer to GMYC using a single-, multiple-threshold and multimodel approach. PTP-all refers to species delimitation analyses where all of the trees were used.

		non-Rotifera				Rotifera			
Comparison		**Estimate**	**Std. Error**	***Z***	***P***	**Estimate**	**Std. Error**	***Z***	***P***
ST-GMYC	MT-GMYC	-2.030	1.296	-1.567	0.385	0.216	0.633	0.341	0.986
ST-GMYC	MM-GMYC	-0.039	1.841	-0.021	1.000	0.591	0.708	0.835	0.837
ST-GMYC	PTP-all	0.661	1.911	-0.346	0.985	0.447	0.677	-0.661	0.911
MT-GMYC	MM-GMYC	1.991	1.500	-1.327	0.533	0.375	0.738	-0.509	0.957
MT-GMYC	PTP-all	2.691	1.686	-1.596	0.368	0.232	0.708	-0.327	0.988
MM-GMYC	PTP-all	0.700	2.134	-0.328	0.987	-0.144	0.776	0.185	0.998

Table S3.5 Simultaneous pairwise Tukey HSD tests for General Linear Hypotheses. Differences in residual variation of ESU estimate between each combination of phylogenetic and branch smoothing methods.
Asterisks correspond to significant differences at $P < 0.05$ (*), $P < 0.01$ (**) and $P < 0.001$ (***).
Found on the attached CD, or available upon request.

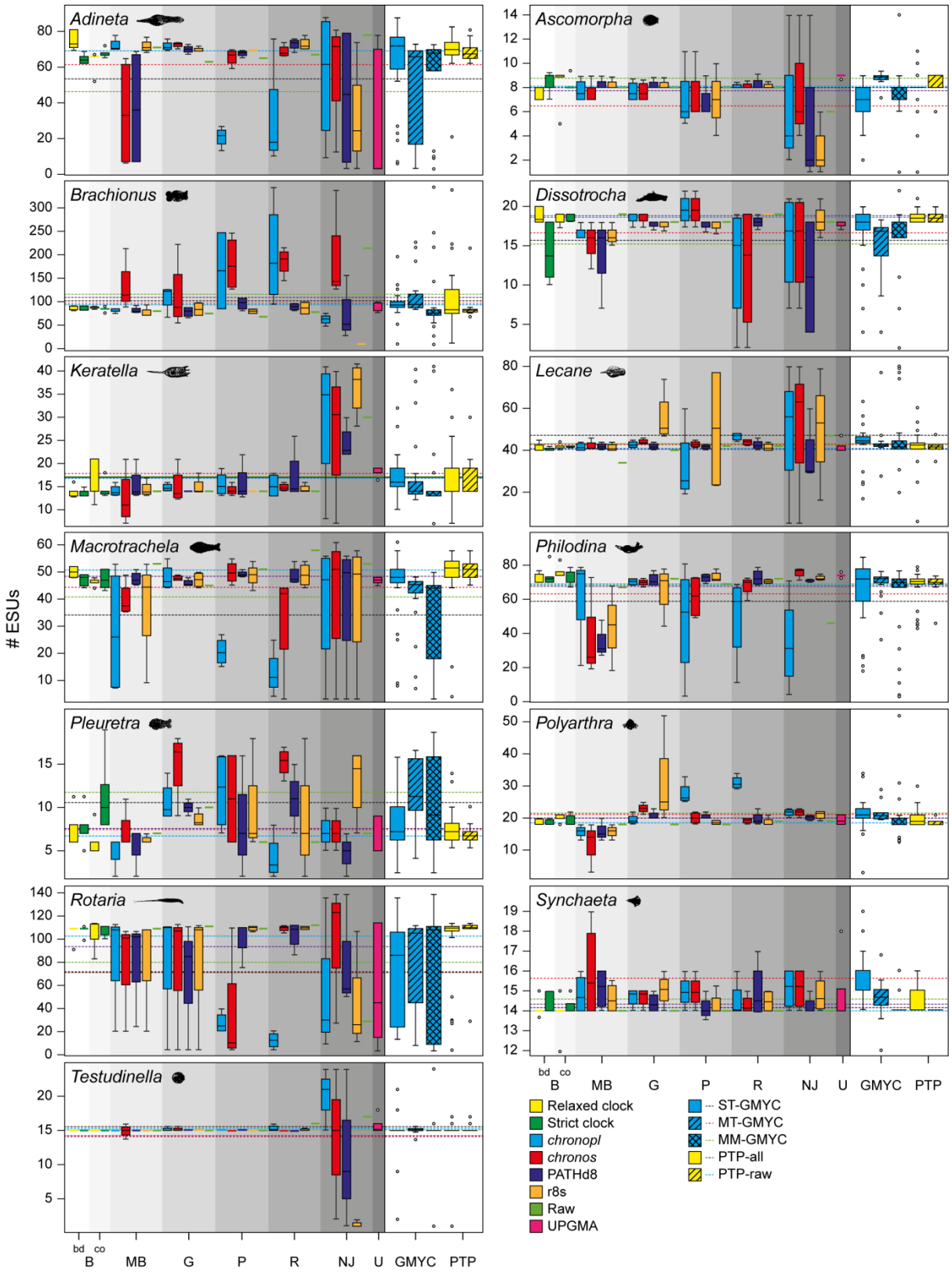

Figure S3.2 For each Rotifera clade separately, the number of ESUs delimited differs with respect to the combination of phylogenetic, smoothing, and species delimitation method (GMYC [blue] vs. PTP [yellow]).

Some combinations deviate more from the expected diversity (ESU_{meanB}) than others. The average for each species delimitation method (dotted lines) is shown: ST-GMYC (black), MT-GMYC (red), MM-GMYC (green), PTP-all (purple), and PTP-raw (blue). The grey shaded areas correspond to the different phylogenetic methods. Median (thick black lines), first and third quartiles (box), 1.5 times the interquartile range (whiskers), and outliers (circles) are shown. For results with no variation, a single line of the corresponding colour is used instead of a box. Abbreviations: bd = birthdeath, c = coalescent, B = BEAST, MB = MrBayes, G = GARLI, P = PhyML, R = RAxML, NJ = neighbour joining and U = UPGMA.

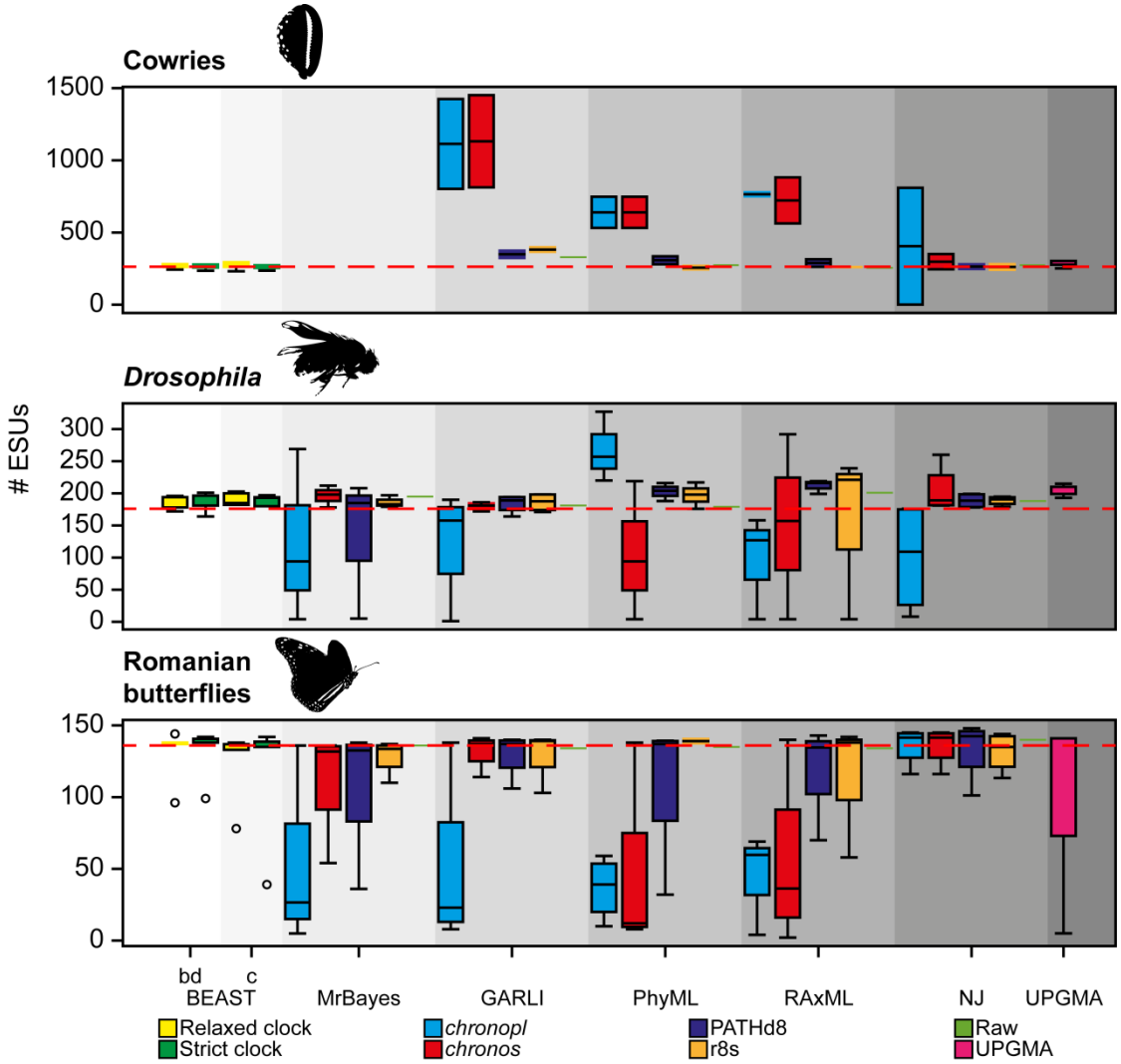

Figure S3.3 The relationship between the number of ESUs and different combinations of phylogenetic and smoothing method shown separately for cowries, *Drosophila* and Romanian butterflies.

Some combinations deviate more from the morphological species count (red, dashed line) than others. No data are available for the cowries dataset reconstructed with MrBayes. The grey shaded areas correspond to the different phylogenetic methods. Median (thick black lines), first and third quartiles (box), 1.5 times the interquartile range (whiskers), and outliers (circles) are shown. Abbreviations: bd = birthdeath, c = coalescent, NJ = neighbour joining.

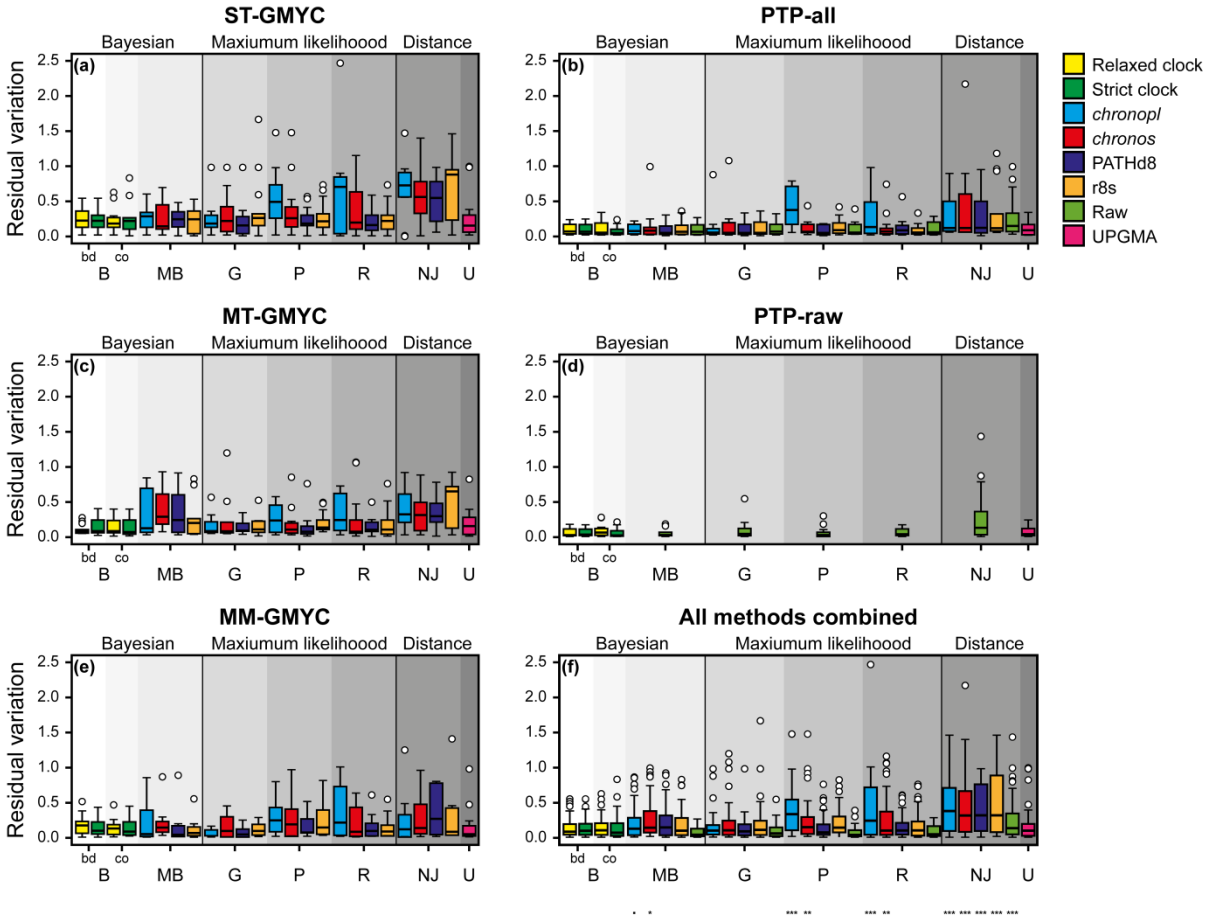

Figure S3.4 Residual variation of ESU estimates for all 16 datasets shown separately for each species delimitation method: ST-GMYC (**a**), MT-GMYC (**c**) MM-GMYC (**e**), PTP-all (**b**) PTP-raw (**d**) and all together (**f**).
Each dataset was analysed by Bayesian, maximum likelihood and distance methods using eight different phylogenetic methods (BEAST [B] with either a birthdeath [bd] or coalescent [co] tree prior, MrBayes [MB], GARLI [G], PhyML [P], RAxML [R], neighbour joining [NJ] and UPGMA [U]). The grey shaded areas correspond to the different phylogenetic methods. Median (thick, black lines), first and third quartiles (box), 1.5 times the interquartile range (whiskers), and outliers (circles) are shown.

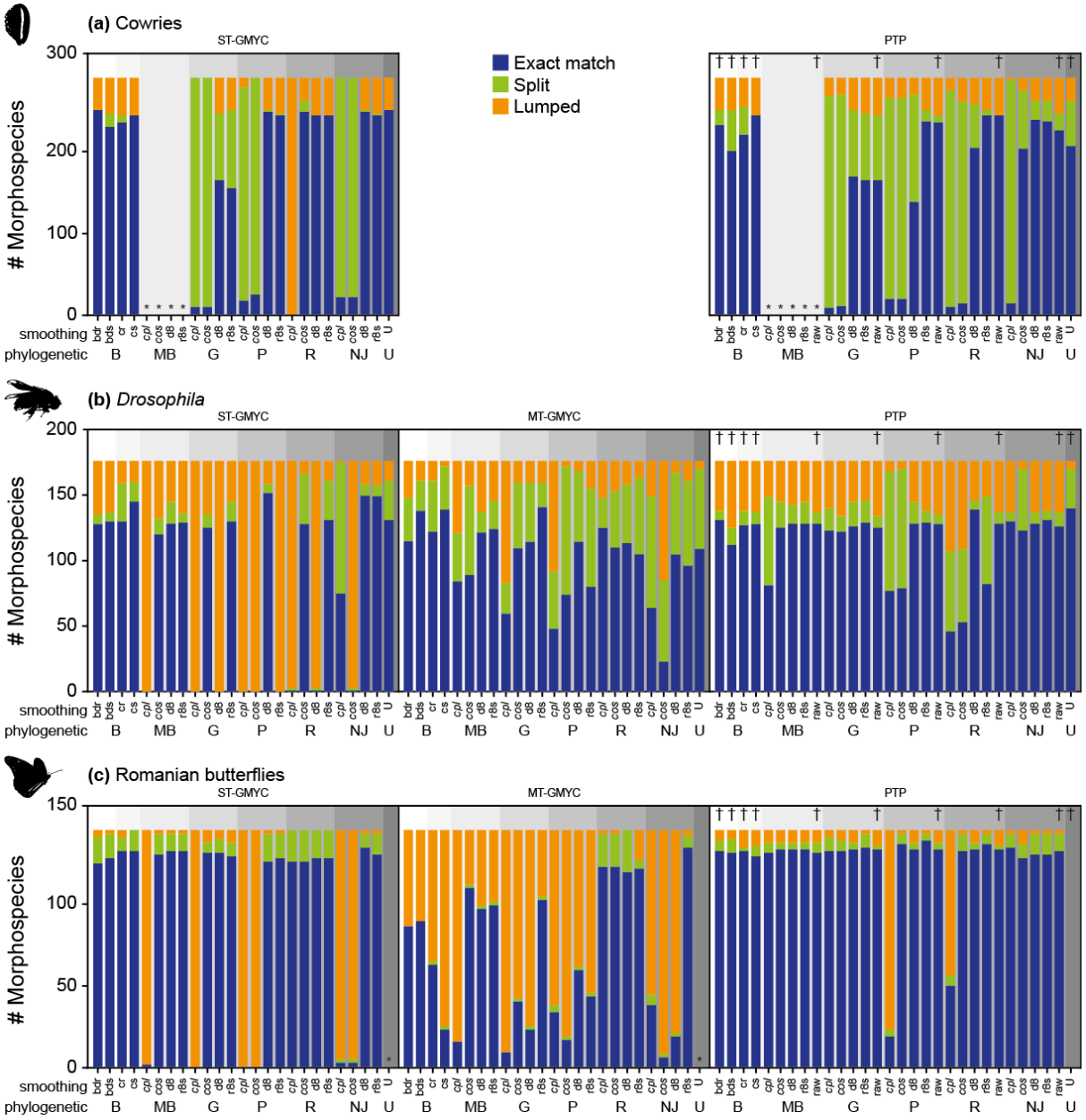

Figure S3.5 The number of morphospecies that are exact matches (purple), lumped (orange), or split (green) relative to the ESUs.

Species delimitation methods are shown separately (ST-GMYC with a single threshold, MT-GMYC with multiple thresholds, and PTP [PTP-raw are denoted with a † above the bar]). The MM-GMYC was not analysed as it averages ESU counts over multiple models and so does not return ESU counts as integers. Cowries (**a**; 263 morphospecies species), *Drosophila* spp. (**b**; 176 morphospecies species), and Romanian butterflies (**c**; 136 morphospecies species) are shown separately. Each dataset was analysed using eight different phylogenetic methods (grey shaded areas) and nine different rate smoothing methods; the specific combination of phylogenetic and rate smoothing methods is shown below each bar. Abbreviations: bdr = birthdeath with a relaxed molecular clock, bds = birthdeath with a strict molecular clock, cr = coalescent with a relaxed molecular clock, cs = coalescent with a strict molecular clock, *cpl* = *chronopl*, *cos* = *chronos*, d8 = PATHd8, r8s = r8s, B = BEAST, MB = MrBayes, G = GARLI, P = PhyML, R = RAxML, NJ = neighbour joining, U = UPGMA. Where species delimitation was not possible, no data are shown (*).

Supplementary File S3.1: Does ESU_{meanB} correspond to ESU_{morph}?

Residual variation is calculated as:

$$|ESU_{\chi}\text{-}ESU_{expected}| \div ESU_{meanA}$$

where $ESU_{expected}$ is either the morphological species count (ESU_{morph}) or the mean ESU estimate of the phylogenetic methods (ESU_{meanB}). The use of ESU_{meanB} as a proxy for ESU_{morph} was validated using the three datasets where residual variation could be calculated using both ESU_{morph} and ESU_{meanB} (cowries, *Drosophila* and Romanian butterflies). Residual variation using either ESU_{morph} and ESU_{meanB} never deviated by more than 8.5% and differences were on average 1.54± 0.78% within each other (Fig. S3.6).

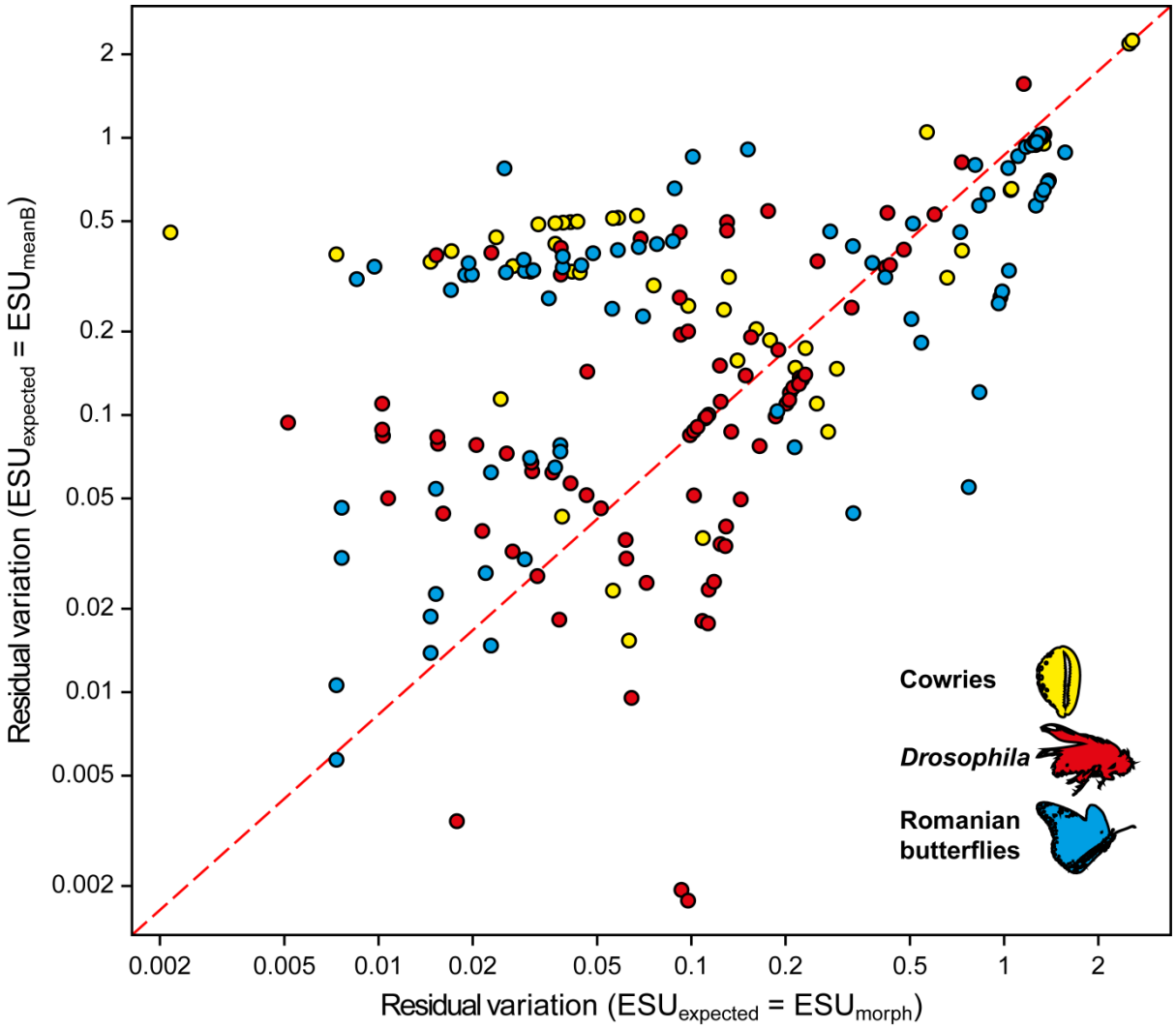

Figure S3.6 The relationship between the residual variation when the expected diversity ($ESU_{expected}$) is taken as either the morphological species estimate (ESU_{morph}) or the average of the delimitation methods (ESU_{meanB}).
The red dotted line represents where residual variation taken from these different expected diversities are equivalent (y = 1.08x - 0.05; LM: $t = 21.52$, $P < 0.0001$, $R^2 = 0.63$).

Supplementary File S3.2: Residual variation example calculation

Residual variation is calculated as:

$$|ESU_{X}\text{-}ESU_{expected}| \div ESU_{meanA}$$

For the cowries, *Drosophila*, and butterflies, the morphological species count (ESU_{morph}; as determined by GenBank species names) was used as the measure for expected diversity. As an example: the number of *Drosophila* ESUs identified using the PTP method using the RAxML tree smoothed using r8s (i.e. 221) was subtracted from the morphospecies count (i.e. 176) and divided by the average *Drosophila* ESU count for all of the PTP estimates (|221-176|÷194.66=0.23). Therefore, for this particular delimitation method and combination of phylogenetic reconstruction and branch smoothing method, the residual variation is 0.23.

For the Rotifera datasets, the mean species estimate from all of the methods excluding the focal estimate (ESU_{meanB}) was used as the measure of expected diversity. For example: for *Dissotrocha* (Bdelloidea: Rotifera), the number of ESUs identified using the PTP method on the RAxML tree smoothed using r8s (i.e. 19) was subtracted from the average PTP ESU estimate across the other 29 estimates (i.e. 18.79) and divided by the average *Dissotrocha* ESU count for all of the PTP estimates (|19-18.79|÷18.8=0.011). For this particular delimitation method and combination of phylogenetic reconstruction and branch smoothing method, the residual variation is 0.11.

This was repeated for each combination of species delimitation, phylogenetic reconstruction and branch smoothing method (Fig. S3.1g,h) and then for each dataset.

Supplementary File S3.3: Is λ a strong determinant of ESU estimation?

To ascertain the effect of changing the smoothing parameter, λ, on the ESU estimation of *chronopl* and *chronos* trees, we generated ten *chronopl* and ten *chronos* ultrametric trees per raw tree with λ values evenly distributed from 0.1 to 1.0 and estimated the diversity in each. This resulted in 1,560 ultrametric trees (minus the cowrie MrBayes and GARLI trees which did not converge and failed, respectively). For each one of these ultrametric trees, we delimited the number of ESUs using the ST-GMYC. We analysed the effect of λ on the estimated diversity using Generalized Linear Mixed Models via Penalised Quasi-Likelihood (Venables and Ripley 2002) with a quasiPoisson error structure to account for the overdispersed count data (ESU_X). The number of ESUs was used as the response variable and the branch smoothing method (*chronopl* or *chronos*), λ value and phylogenetic reconstruction method (five levels) as explanatory variables, while blocking out clades as a random effect. We found that there is substantial variation in ESU estimates for some datasets but not a consistent effect of λ on this variation. Phylogenetic reconstruction and branch smoothing method are much stronger determinants of ESU estimates (Table S3.6; Fig. S3.7).

Table S3.6 Summary of the Generalized Linear Mixed Model of the number of GMYC (single-threshold) ESUs estimated from gene trees smoothed with *chronopl* or *chronos* under varying smoothing parameters (λ).

	Value	**Std. Error**	**D.F.**	***t* value**	***P***
(Intercept) GARLI *chronopl*	3.13	0.26	1558	12.21	0.00
chronos	0.19	0.04	1558	4.49	0.00
lambda	0.00	0.07	1558	-0.01	1.00
MrBayes	0.19	0.08	1558	2.48	0.01
NJ	0.07	0.08	1558	0.91	0.37
PhyML	0.33	0.07	1558	4.55	0.00
RAxML	0.79	0.07	1558	11.59	0.00

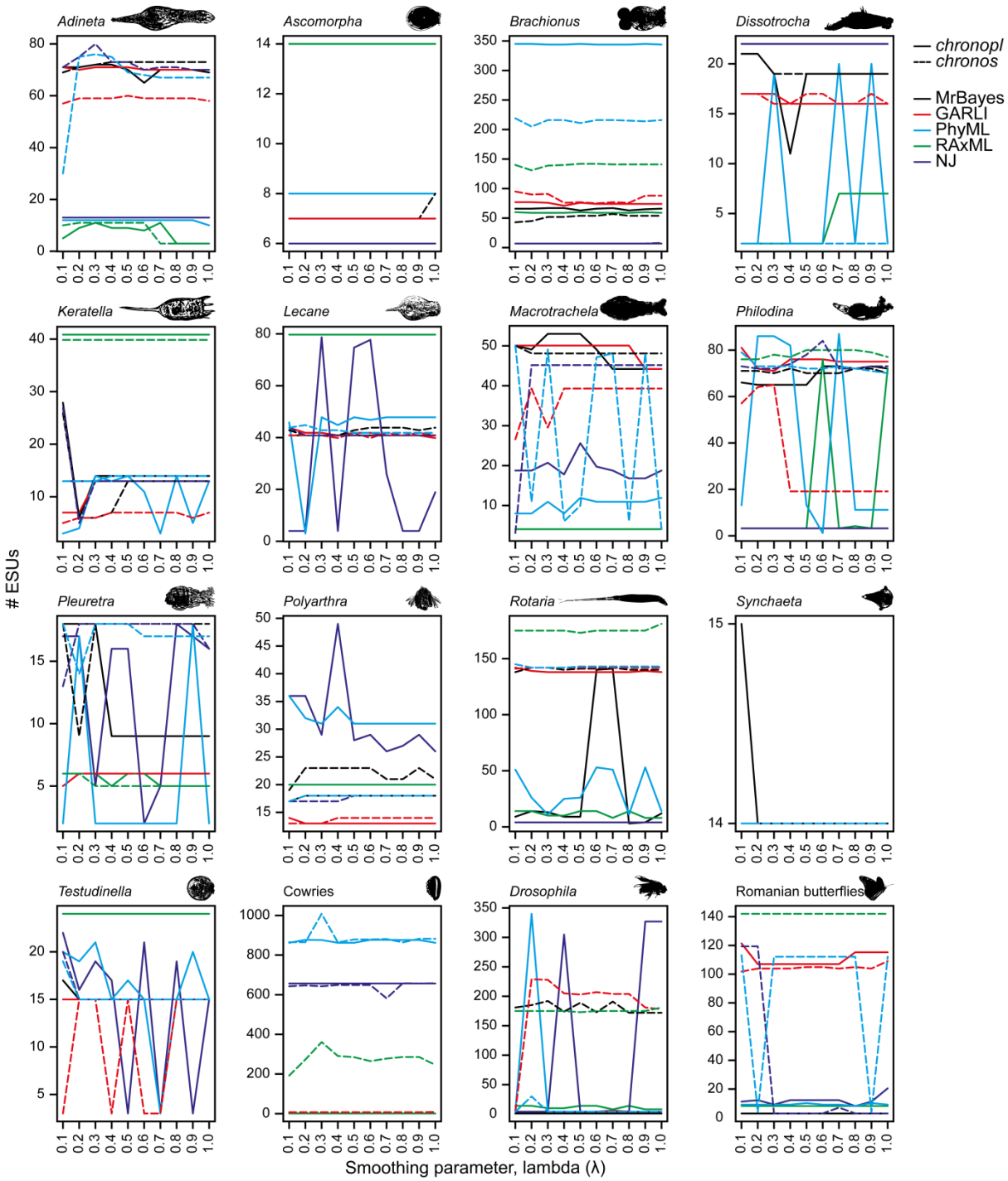

Figure S3.7 GMYC ESUs delimited from trees smoothed with *chronopl* (solid lines) and *chronos* (dotted lines) with different λ values using different phylogenetic methods (MrBayes [black], GARLI [red], PhyML [blue], RAxML [green], and NJ [purple])

Chapter 4: Supplementary Materials

Table S4.1 Sequence information and results from the GMYC analysis, and summary output of the intraspecific and interspecific variation.

Found on the attached CD, or available upon request.

Table S4.2 Barcode gap analyses using nearest neighbour, threshold ID, and best close match criteria analysed separately for morphospecies, and GMYC ESUs delimited using BEAST or RAxML trees. Separate analyses were also performed for datasets including and excluing unidentified species.

Found on the attached CD, or available upon request.

Table S4.3 GLMs used to explain that DNA barcoding identification success rates do not differ between GMYC ESUs delimited from BEAST or RAxML gene trees.
Metrics and the presence or absence of singletons are analysed separately.

DNA barcoding metric	**Singletons**		**Estimate**	**S.E.**	***t***	***P***
Nearest neighbour success (%)	Yes	BEAST	3.15	0.34	9.323	4.25E-09
		RAxML	0.08	0.48	0.17	0.87
	No	BEAST	5.03	0.46	10.96	2.22E-10
		RAxML	0.19	0.68	0.28	0.785
Threshold ID success (%)	Yes	BEAST	2.46	0.28	8.67	1.51E-08
		RAxML	0.28	0.42	0.65	0.522
	No	BEAST	3.04	0.32	9.36	3.96E-09
		RAxML	0.49	0.52	0.95	0.353
Best close match success (%)	Yes	BEAST	2.71	0.27	9.92	1.40E-09
		RAxML	0.27	0.41	0.66	0.515
	No	BEAST	3.54	0.30	11.79	5.55E-11
		RAxML	0.65	0.50	1.29	0.212

Table S4.4 GLMs used to explain that DNA barcoding identification success rates do not significantly differ between the metrics.

	Estimate	**S.E.**	***t***	***P***
BCM (intercept)	2.84	0.21	13.32	<2e-16
NN	0.34	0.33	1.05	0.3
TI	-0.26	0.29	-0.89	0.37

Chapter 5: Supplementary Materials and Methods

Figure S5.1 Phylogenetic methods workflow.
(a) Nineteen 18S and COI sequences, representing 12 of the 13 datasets were aligned separately and subsequently concatenated. (b) The concatenated alignment was used to construct a backbone phylogeny (c) with 15 calibration points (yellow nodes). The parameters of BEAST analysis comprised: a GTR+Γ+I model of evolution, a relaxed lognormal clock, a birth-death prior, a random starting tree, 100,000,000 generations, and sampling every 1,000 generations. Separate calibration clocks were used for COI (1.76% MYR^{-1}) and 18S (0.02% MYR^{-1}). (d) A more extensive sample of COI sequences were aligned and split by sister clades into two separate alignments. (e) Each of the two alignments were used to reconstruct large combined gene trees with the 15 calibration points set (as defined in [c]). (f) Thirteen datasets, representing species complexes and genera, were pulled out from these combined trees.

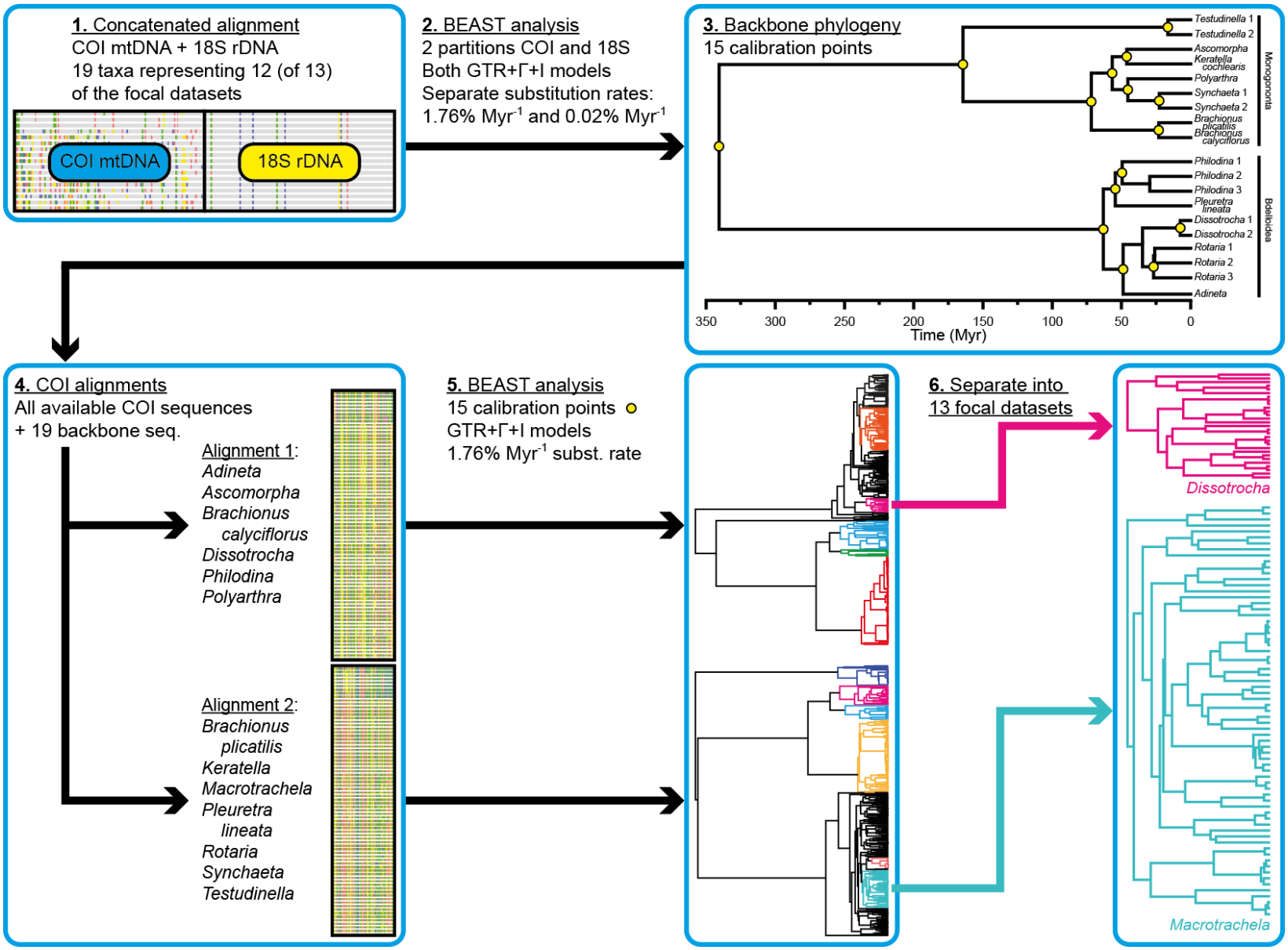
1. Concatenated alignment
COI mtDNA + 18S rDNA
19 taxa representing 12 (of 13)
of the focal datasets
COI mtDNA
18S rDNA
2. BEAST analysis
2 partitions COI and 18S
Both GTR+Γ+I models
Separate substitution rates:
1.76% Myr-1 and 0.02% Myr-1
3. Backbone phylogeny
15 calibration points
Testudinella 1
Testudinella 2
Ascomorpha
Keratella cochlearis
Polyarthra
Synchaeta 1
Synchaeta 2
Brachionus plicatilis
Brachionus calyciflorus
Monogononta
Philodina 1
Philodina 2
Philodina 3
Pleuretra lineata
Dissotrocha 1
Dissotrocha 2
Rotaria 1
Rotaria 2
Rotaria 3
Adineta
Bdelloidea
350
300
250
200
150
100
50
0
Time (Myr)
4. COI alignments
All available COI sequences
+ 19 backbone seq.
Alignment 1:
Adineta
Ascomorpha
Brachionus calyciflorus
Dissotrocha
Philodina
Polyarthra
Alignment 2:
Brachionus plicatilis
Keratella
Macrotrachela
Pleuretra lineata
Rotaria
Synchaeta
Testudinella
5. BEAST analysis
15 calibration points
GTR+Γ+I models
1.76% Myr-1 subst. rate
6. Separate into
13 focal datasets
Dissotrocha
Macrotrachela

Specimen collection, sequencing and concatenation

Collection of Ascomorpha, Keratella and Polyarthra specimens

Ascomorpha, *Keratella*, and *Polyarthra* populations were sampled between 2010 and 2012 from 42 water bodies using a 50µm mesh net. For each water body, specimens were isolated into a single sample and identified according to Koste (1978) and *Polyarthra* specific material from Shiel and Koste (1993). Full details of the sampling conditions (coordinates, depth, and date) and GenBank accession numbers are in Table S5.1.

COI sequencing of Ascomorpha, Keratella and Polyarthra specimens

DNA from each single animal was extracted in 35µL of Chelex (InstaGene Matrix; BioRad). Cytochrome *c* oxidase subunit I (COI) was PCR amplified using Folmer primers (Folmer et al. 1994) LCOI (5′-GGT CAA CAA ATC ATA AAG ATA TTGG-3′) and HCOI (5′-TAA ACT TCA GGG TGA CCA AAAAAT CA-3′). Cycle conditions comprised initial denaturation at 94°C for 3 min, followed by 40 cycles of 94°C for 30 sec, 48°C for 1 min, and 72°C for 1 min, and a final extension step of 72°C for 7 min. PCR amplicons were purified using ExoSAP-IT (USB Corporation) and were sequenced using the same PCR primers and ABI BigDye 3.1 chemistry on an ABI 3730XL sequencer (Applied Biosystems) at the Edmund Mach Foundation (Research and Innovation Centre). All sequences were deposited in GenBank (accessions numbers KC618769 - KC619309). These sequences were assembled, checked and edited by eye using Geneious Pro v5.4.2 (Drummond et al. 2006).

18S sequencing

Amplification of 18S rDNA was performed using a nested PCR approach as outlined by Tang et al. (2012). The total fragment was amplified using 18SFnew (5’-AGA TTA AGC CAT GCA TGT CT-3’) and 9R (5’-GAT CCT TCC GCA GGT TCA CCT AC-3’) using the following cycle conditions: initial denaturation at 95°C for 5 min, following by 38 cycles of 95°C for 1 min, 55°C for 1 min, and 72°C for 2 min, and a final extension at 72°C for 10 min. Three overlapping fragments of 18S were amplified using the previous amplicon as a template and the following primer pairs: 18SFnew (5’-AGA TTA AGC CAT GCA TGT CT-3’) – 4R (5’-GAA TTA CCG CGG CTG CTG G-3’), 18SCT1 (5’- TGG AGG GCA AGT CTG GTG CCA GC-3’) – 18Sbi (5’- GAG TCT CGT TCG TTA TCG GA-3’), and 18Sa2.0 (5’-ATG GTT GCA AAG CTG AAA C-3’) – 9R (5’-GAT CCT TCC GCA GGT TCA CCT AC-3’). Primers were either those of Giribet et al. (1996), or redesigned from five full length rotifer sequences (~1,800bp) obtained from GenBank (AF154566, AF154567, AY218118, AJ487049, DQ089733). These five sequences were aligned and priming sites were designed around regions that were conserved between bdelloid and monogonont sequences.

All PCR amplicons were purified and concentrated using Illustra GFX PCR DNA and Gel band purification kit as per the manufacturer's protocol with a final volume ranging from 10µl to 20µl depending on the concentration of the amplicons. Purified products were sequenced using purified amplicons, 1:10 of the PCR primers and the ABI Big Dye Terminator v1.1 kit and run on an ABI 3770 automated sequencer. Sequences were checked and edited using Geneious Pro. Direct sequencing of 18S yielded only single copies with no evidence of divergent ribosomal copies. The orthology of 18S was further validated by searching the *Adineta vaga* genome (Flot et al. 2013) for 18S copies. BLAT (*Adineta* genome equivalent to BLAST) was used to search for the *Adineta* 18S sequence (KF561095), the resulting scaffolds (>500bp) were less than 1% divergent from each other. Furthermore, searching the genome for the other eighteen 18S sequences (used for the backbone phylogeny) returned the same set of scaffolds as for the *Adineta* (KF561095) search. These lines of evidence indicate that 18S has a single copy in *Adineta vaga* and that this particular copy is orthologous across the samples (bdelloid and monogonont) used here.

18S and COI concatenation

A backbone phylogeny was generated using a concatenated alignment COI and 18S sequences (Table S5.2). Sequences were chosen to represent as much of our focal datasets as possible from the available resources (GenBank). For 18S, there was a limited collection of appropriately sized, annotated, and identified sequences available; therefore only 12 of the 13 datasets are represented and only 19 sequences in total were used (no 18S datum was available for *Macrotrachela*). The sequences used for the backbone phylogeny are shown in Table S5.2. Most of the COI and 18S sequences were concatenated from the same individuals (15 out of 19), but where this was not possible, sequences from the same morphospecies or genus were selected for concatenation. *Ascomorpha*, *Keratella*, and *Polyarthra* COI and 18S sequences belonged to specimens from the same morphospecies (Table S5.2), and for *Pleuretra*, a COI sequence from *P. lineata* (FJ426426) was concatenated with an 18S sequence from *P. hystrix* (JX494746). The COI and 18S sequences were aligned separately using MAFFT (Katoh et al. 2009) with the default settings and checked and edited in Geneious Pro. Non-alignable or substantially shorter sequences (<50% of the average alignment length) were discarded. These alignments had no indels or stop codons.

How are the two analyses split up?

The backbone phylogeny indicated that the following taxon pairs were sister clades: (*Ascomorpha*, *Keratella cochlearis*), (*Polyarthra*, *Synchaeta*), (*Brachionus calyciflorus*, *Brachionus plicatilis*), (*Philodina*, *Pleuretra lineata*), and (*Dissotrocha*, *Rotaria*). These lineages were split up into two alignments (Table S5.4) to maintain similar age distributions in each analysis. *Testudinella* and *Adineta* (which formed outgroups) and *Macrotrachela* (missing) were divided to maintain equivalent sequence numbers in each alignment.

The effect of incomplete sampling on constancy of net diversification rates

Incomplete sampling will result in γ becoming increasingly negative with more missing taxa because old nodes are disproportionately sampled over younger ones (Pybus and Harvey 2000). Incomplete sampling was corrected for both before and after the analyses. *A priori* correction was performed using a missing species simulator (by feeding in branches/splits, equivalent to species) based on a constant rate birth-death model (CorSiM - Cusimano et al. 2012). Missing species were simulated 1,000 times using the *TreePar* 2.5 package (Stadler 2011) in R, which requires estimates of net diversification rates under a constant birth-death model (estimated using ape) and a measure of expected diversity (estimated using the Chao estimator - Chao 1984). The *post hoc* correction was performed using a Monte Carlo constant rates test (MCCR within *laser* - Pybus and Harvey 2000). The MCCR test is based on a null distribution of γ using pruned trees simulated 1,000 times under a constant rate with the same number of tips corresponding to the expected diversity (also estimated by Chao).

Table S5.1 Specimen collection information and accessions numbers for the sequences generated for this study. Abbreviations: WC = water column

Found on the attached CD, or available upon request.

Table S5.2 Summary information for each of the 13 datasets, including number of sequences, number of unique haplotypes, estimated diversity, constancy of diversification statistics, estimated ages, and accessions.

Taxon	Group	Tax.	bp	N seq.	N hapl.	GMYC analyses		# GMYC entities				N singl.	N seq./ ESU	N hapl./ ESU	Estimated richness (chao)
						LR	*P* value	Bayesian			ML				
								1^{o}	relaxed	strict					
Adineta spp.	B	G	661	229	115	29.21	2.02E-06	70	71	64	70	44	3.3	1.6	119.8
Ascomorpha spp.	M	G	661	38	13	8.28	0.04	5	6	5	5	2	7.6	2.6	6
Brachionus calyciflorus	M	S	712	460	173	96.85	0	17	19	21	8	4	27.1	10.2	20
Brachionus plicatilis	M	S	729	460	129	32.61	3.89E-07	20	33	23	26	6	23.0	6.5	27.5
Dissotrocha spp.	B	G	661	38	27	10.21	0.017	19	18	11	19	12	2.0	1.4	31
Keratella cochlearis	M	S	661	59	23	12.38	0.0062	6	6	3	6	2	9.8	3.8	7
Macrotrachela spp.	B	G	661	194	80	17.19	0.00065	46	50	44	44	29	4.2	1.7	92.7
Philodina spp.	B	G	661	386	139	57.96	1.61E-12	71	74	72	72	43	5.4	2.0	128.8
Pleuretra lineata	B	S	661	48	20	7.29	0.063	8	5	5	18	4	6.0	2.5	14
Polyarthra spp.	M	G	661	462	53	37.49	3.63E-08	18	18	18	18	10	25.7	2.9	40.5
Rotaria spp.	B	G	698	1541	147	14.17	0.0027	120	119	116	117	97	12.8	1.2	344
Synchaeta spp.	M	G	678	210	32	11.40	0.0097	14	14	14	14	6	15.0	2.3	18.5
Testudinella spp.	M	G	661	86	34	38.01	2.82E-08	13	11	11	12	8	6.6	2.6	27

Abbreviations: Tax. – taxonomic scale; B – Bdelloidea; M – Monogononta; G – genus; S – species complex; bp - length of alignment; N seq. - Number of sequences; N hap. - Number of haplotypes; LR - Likelihood ratio; ML - Maximum likelihood; BI - Bayesian inference; N singl. - Number of singletons; MCCR crit. val. - Monte Carlo constant rates critical value.

Table S5.2 Summary information for each of the 13 datasets, including number of sequences, number of unique haplotypes, estimated diversity, constancy of diversification statistics, estimated ages, and accessions. Cont.

Taxon	Diversification rate					Age (MYR)	Backbone GenBank		TreeBASE
	γ	MCCR crit. val.	*P*	CorSiM γ	*P*		18S rDNA	COI mtDNA	
Adineta spp.	-6.21	-2.7	0.0001	-3.95	0.00004	27.58	KF561095	KF582480	66181
Ascomorpha spp.	-1.01	-1.15	0.06	-0.7	0.24	56.13	DQ297691	KC618773	66185
Brachionus calyciflorus	1.56	-1.37	0.92	2.45	0.99	25.61	KF561096	HQ444170	66189
Brachionus plicatilis	-3.15	-1.71	0.003	-3.68	0.00012	25.84	KF561097	HQ444171	66208
Dissotrocha spp.	-2.6	-1.97	0.011	-2.89	0.0019	20.99	KF561098-KF561099	KF582497, KJ913822	66212
Keratella cochlearis	-1.72	-1.01	0.011	-2.21	0.014	24.30	DQ297697	KC618852	66216
Macrotrachela spp.	-5.28	-2.68	0.0001	-2.96	0.0015	25.39	N/A	N/A	66220
Philodina spp.	-4.35	-2.84	0.0002	-2.71	0.0034	53.95	KF561100-KF561102	JQ309165, JQ309181, JQ309183	66224
Pleuretra lineata	1.96	-1.76	0.98	1.96	0.97	22.98	JX494746	FJ426426	66228
Polyarthra spp.	-1.93	-2.22	0.084	-1.69	0.046	45.85	DQ297716	DQ297789	66233
Rotaria spp.	-5.32	-4.68	0.009	-2.74	0.003	32.62	KF561103-KF561105	EU076828, JQ309460, JQ309578	66237
Synchaeta spp.	-1.22	-1.46	0.082	-0.97	0.17	28.57	KF561106-KF561107	JN936673, JN936516	66241
Testudinella spp.	-0.4	-2.14	0.57	-0.25	0.4	42.89	KF561108-KF561109	HQ444166, HQ444168	66245

Abbreviations: Tax. – taxonomic scale; B – Bdelloidea; M – Monogononta; G – genus; S – species complex; bp - length of alignment; N seq. - Number of sequences; N hap. - Number of haplotypes; LR - Likelihood ratio; ML - Maximum likelihood; BI - Bayesian inference; N singl. - Number of singletons; MCCR crit. val. - Monte Carlo constant rates critical value.

Table S5.3 Intra- and interspecific diversity measures (genetic and phylogenetic distances) for each of the delimited GMYC entities. The number of haplotypes per GMYC entity, morphospecies, habitat type (Aquatic or Limnoterrestrial), and population genetic measures are also shown. A minimum of four sequences was required for D^*, F^*, F_S, and D, and a minimum of two sequences was required for R_2.
Found on the attached CD, or available upon request.

Table S5.4 Datasets were split up by sister clades as determined using the backbone phylogeny (Fig. 5.2) and outgroup taxa were added to balance the sequence numbers for each alignment.

Sister clade	Group	Alignment 1	# Seq.	Group	Alignment 2	# Seq.
1	Monogononta	*Ascomorpha*	13	Monogononta	*Keratella cochlearis*	23
2	Monogononta	*Polyarthra*	53	Monogononta	*Synchaeta*	32
3	Monogononta	*Brachionus calyciflorus*	173	Monogononta	*Brachionus plicatilis*	129
4	Bdelloidea	*Philodina*	139	Bdelloidea	*Pleuretra lineata*	20
5	Bdelloidea	*Dissotrocha*	27	Bdelloidea	*Rotaria*	147
	Monogononta	*Testudinella*	34	Bdelloidea	*Adineta*	115
	Bdelloidea	*Macrotrachela*	80			
		Total	**519**			**466**

Table S5.5 Output from GLMM analysis of GMYC model fit (P value) differences between bdelloid and monogonont rotifers and varying degrees of jack-knifing.

Fixed effects	Value	Std. Error	D.F.	*t* value	*P*
Intercept (Bdelloid, jack-knifed: 20%)	-7.30	1.32	5181	-5.55	0.00
Monogonont	-2.08	1.83	11	-1.14	0.28
Jack-knife: 25%	0.20	0.05	5181	4.31	0.00
Jack-knife: 33%	0.26	0.05	5181	5.49	0.00
Jack-knife: 50%	0.50	0.05	5181	10.96	0.00
Monogonont, jack-knifed: 25%	0.07	0.15	5181	0.46	0.65
Monogonont, jack-knifed: 33%	0.28	0.14	5181	1.96	0.05
Monogonont, jack-knifed: 50%	0.46	0.14	5181	3.37	0.00
Random effect	(intercept)	Residual			
Dataset	3.15	0.11			

Script for multibirthdeath function

```
library(ape)
#multibirthdeath function
multi.birthdeath<-function(phy){
      if(!inherits(phy[[1]],"phylo"))
      stop("object\"phy\"isnotofclass\"phylo\"")
      dev<-function(a,r){
      if(r<0||a>1)
      return(1e+100)
      lik<-0
      N.sum<-0
      for(i in(1:length(phy))){
         N<-length(phy[[i]]$tip.label)
         N.sum<-N.sum+N
         x<-c(NA,branching.times(phy[[i]]))
         lik<-lik-2*(lfactorial(N-1)+(N-
            2)*log(r)+r*sum(x[3:N])+N*log(1-a)-
            2*sum(log(exp(r*x[2:N])-a)))}
      N.sum<<-N.sum
      return(lik)}
   out<-nlm(function(p)dev(p[1],p[2]),c(0.1,0.2),hessian=TRUE)
   if(out$estimate[1]<0){
      out<-nlm(function(p)dev(0,p),0.2,hessian=TRUE)
      para<-c(0,out$estimate)
      inv.hessian<-try(solve(out$hessian))
      se<-if(class(inv.hessian)=="try-error")
      NA
      elsesqrt(diag(inv.hessian))
      se<-c(0,se)}
   else{
      para<-out$estimate
      inv.hessian<-try(solve(out$hessian))
      se<-if(class(inv.hessian)=="try-error")
      c(NA,NA)
      elsesqrt(diag(inv.hessian))}
   Dev<-out$minimum
   foo<-function(which,s){
   i<-0.1
   if(which==1){
      p<-para[1]+s*i
      bar<-function()dev(p,para[2])}
   else{
      p<-para[2]+s*i
      bar<-function()dev(para[1],p)}
   while(i>1e-09){
      while(bar()<Dev+3.84)p<-p+s*i
      p<-p-s*i
      i<-i/10}
      p}
   CI<-mapply(foo,c(1,2,1,2),c(-1,-1,1,1))
   dim(CI)<-c(2,2)
   names(para)<-names(se)<-rownames(CI)<-c("d/b","b-d")
   colnames(CI)<-c("lo","up")
   obj<-list(tree=deparse(substitute(phy)),N=N.sum,dev=Dev,
      para=para,se=se,CI=CI)
```

```
   class(obj)<-"birthdeath"
   obj}
#Bdelloid, Monogonont and Rotifera trees were concatenated into a
#single multiphylo object
bdelloid.trees<-c(adin.prune,diss.prune,macr.prune,phil.prune)
monogonont.trees<-c(asco.prune,brac.prune,brap.prune,kera.prune)
all.trees<-c(bdelloid.trees,monogonont.trees)
#run code
multi.birthdeath(bdelloid.trees)
multi.birthdeath(monogonont.trees)
multi.birthdeath(all.trees)
#A likelihood ratio test was used to compare the fit of a nested
#model (bdelloids or monogononts) to the global model (Rotifera),
#where X is the log likelihood of the nested model and Y is the log
#likelihood of global model
1-pchisq(2*(X-(Y)),2)
```

Supplementary File S5.1 Are the ultrametric trees robust to rate heterogeneity?

Cladogenesis rates may be affected by differences in rate heterogeneity. Rate heterogeneity within a gene tree will result in branch length variation and potentially the artificial stretching of branches. Genetic distances among sequences should correlate strongly with branch lengths on a gene tree, but this relationship may be imperfect when trees are made ultrametric. Rate variation in one part of the dataset may lead to over-smoothing and stretching of other less diverse parts of the final gene tree; this stretching leads to biases in the GMYC analysis, which is concerned primarily with branching rates. Moreover, different clades may have different levels of rate heterogeneity, and strong departures from uniformity across the tree could result in artificially stretched branch lengths (i.e. artificially old tips). These artificially stretched tips may result in poor GMYC ESU estimation. We assessed the effect of rate heterogeneity on artificial branch stretching by comparing the raw minimum genetic distance and the minimum phylogenetic distance (on an ultrametric tree) between GMYC entities. A positive linear correlation between the two measures would indicate a clock-like rate, while a lack of correlation would indicate a departure from a molecular clock or artefacts from the method of phylogenetic reconstruction. This diagnostic was used iteratively to develop the phylogenetic analyses described above.

The main difference in discreteness between bdelloids and monogononts was not an artefact of the effect of smoothing on the greater substitution rate heterogeneity observed in bdelloids than monogononts, as the correlation between raw genetic and phylogenetic distance was equivalent between the two clades (LM: $F_{1,425}$=273.3, P<0.001; Fig. S5.2).

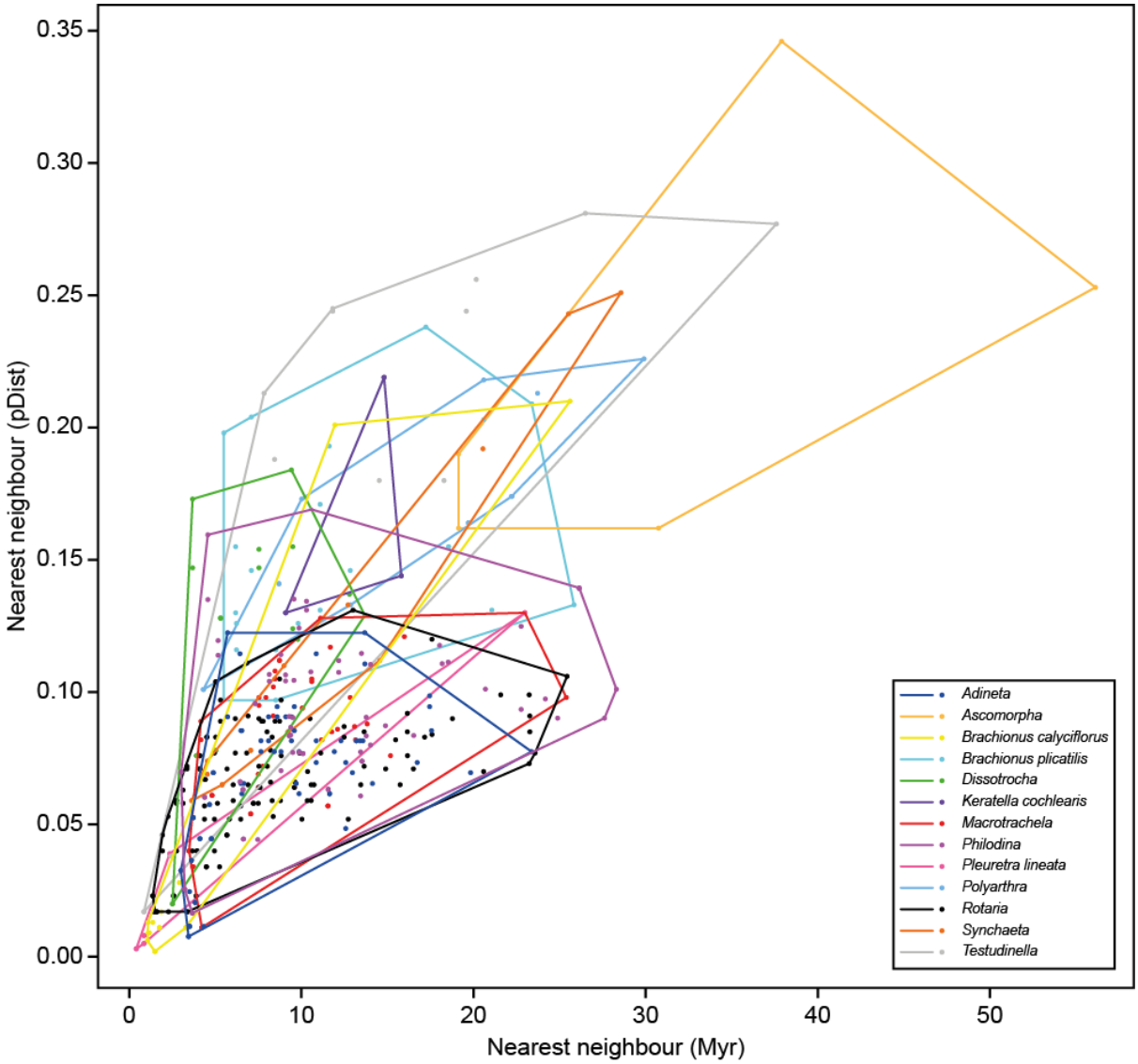

Figure S5.2 Minimum interspecific genetic distance (raw pDistance) against minimum phylogenetic distance to the nearest neighbour (MYR).
The strong relationship indicates that no bias from the phylogenetic reconstruction has been incorporated (LM: Y=0.0046x * 0.042, Adjusted R-square=0.39, P<0.001.

Supplementary File S5.2 How does phylogenetic reconstruction method affect s delimitation?

To assess the robustness of the trees reconstructed by two large combined analyses in terms of topology and rate smoothing, the number of GMYC clusters delimited from these trees was compared to ones reconstructed independently from the other datasets (i.e. 13 separate analyses instead of two) using both maximum likelihood (ML) and Bayesian inference (BI) techniques. ML trees were reconstructed using RAxML webservers (Stamatakis et al. 2008) with a Gamma model of rate heterogeneity, maximum likelihood model search, and an estimated proportion of invariable sites. The r8s software (Sanderson 2003) was used to perform nonparametric rate smoothing (NPRS). This method smooths rate changes among lineages while penalising fast rate changes from mother to daughter. The level of smoothing was optimised using a cross validation procedure.

Two separate BEAST runs, strict and relaxed clock models, were performed for each clade. BEAST input files were generated using BEAUti v1.7.5, each search ran with a substitution rate of 1.76% per million years (the most accepted rate for most invertebrates - Wilke et al. 2009) under either an uncorrelated lognormal relaxed molecular clock or a strict molecular clock and a birth-death (Gernhard 2008) tree prior. Each dataset was run for at least 30,000,000 generations sampling every 1,000 steps on the CIPRES Science Gateway server (Miller et al. 2010). All of the other options were kept as the BEAUti default settings. The effective sample size (ESS) of each run was determined using Tracer v1.5 (Rambaut and Drummond 2009) and only trees with an ESS of at least 200 were kept (as recommended in the BEAST documentation). TreeAnnotator v1.6.1 was used to summarise the trees with a 10% burnin to give a 50% majority-rule consensus ‘maximum clade credibility tree’ with target node heights.

The number of evolutionary significant units (GMYC s) was obtained from each tree using the GMYC (described in the main text) and compared to those produced using the larger analyses from the combined alignments (described in the main text).

There was no relationship between the method of phylogenetic tree inference (ML/BI) and the number of GMYC s delimited (t_{12}=-0.17, P=0.87; Fig. S5.3) and no significant difference between the three Bayesian methods (i.e. [1] analysed together in large matrices, [2] individually with a lognormal relaxed clock, and [3] with a strict clock; $F_{2,36}$=0.022, P=0.98; Fig. S5.2), therefore only the results from the larger primary analyses will be shown.

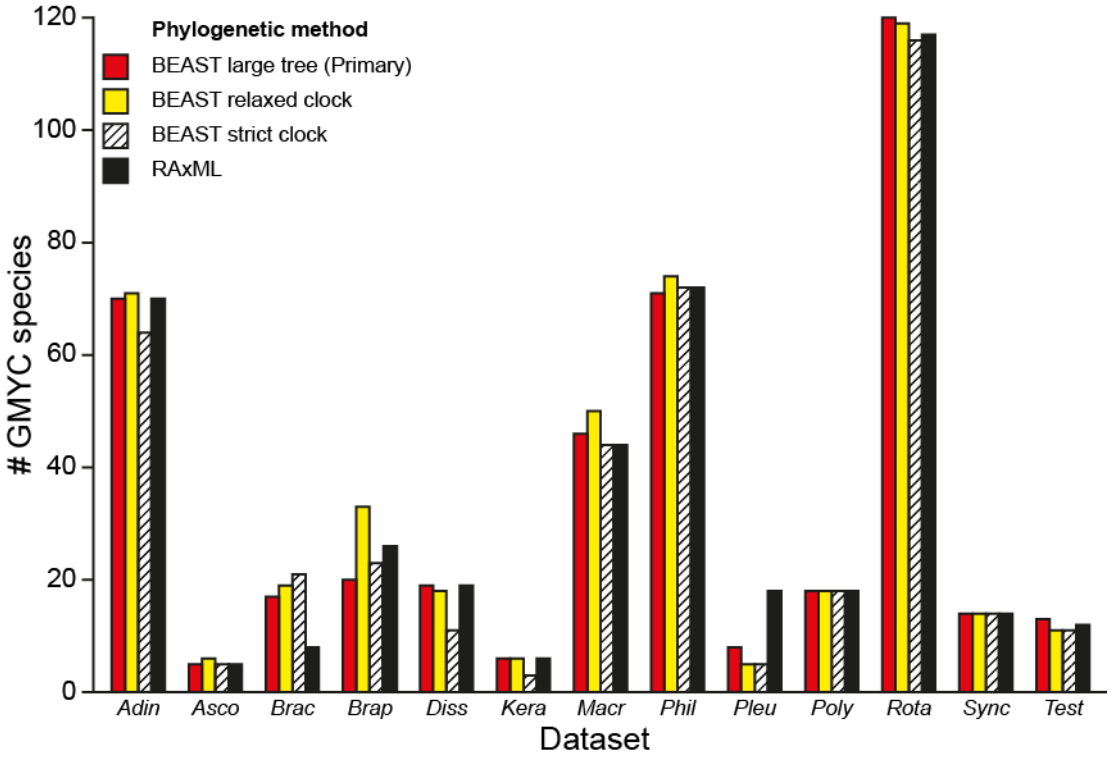

Figure S5.3 S richness of each of the 13 rotifer datasets analysed by GMYC but with different input ultrametric trees.
Four different means of generating ultrametric phylogenies: a single large Bayesian analysis simultaneously assessing the 13 datasets (red) with a lognormal relaxed molecular clock, or individual per dataset phylogenies generated by maximum likelihood and smoothed by nonparametric rate smoothing (black), Bayesian with a relaxed molecular clock (yellow) or Bayesian with a strict clock (white stripes).

Supplementary File S5.3 Is sampling effort differentially affecting bdelloid and monogonont diversity estimates?

The transition from Yule to Coalescent branching rates in the tree is used by the GMYC to detect s. Increased sampling can either supplement existing haplotypes or fill in gaps present in the sample; supplementation will increase the support for the coalescent part of the tree, while filling in the gaps will increase the representation of the Yule section. Higher support for the GMYC is indicative of a strong transition between the processes, this happens when the s richness in the sample is saturated (Yule process) and additional samples supplement the populations (Coalescent process). Adding new samples to a poorly sampled tree, with a low representation of the s richness, will tend to find more novelty and so will reduce the significance of a branching rate transition by supporting the Yule side of the tree. Supplementing pre-existing haplotypes is more likely than discovering novel haplotypes, and so increased sampling will tend to improve the support of GMYC units, but the slope of this improvement (associated with sampling effort) will indicate how well sampled the diversity in the dataset is.

The effect of sampling effort on how the GMYC model fits to the data and how this differs between bdelloid and monogonont rotifers was tested by jack-knifing gene trees and delimiting s from them using the GMYC model. Each tree was jack-knifed by a fifth, a quarter, a third and a half 100 times, and for each of these trees the GMYC model with a single threshold was performed. In total 5,200 GMYC analyses were performed (400 replicates for each clade). A generalised linear mixed effects model with a penalised quasi-likelihood and a quasibinomial error structure was used with GMYC model significance (using the *P* value of the likelihood ratio test) as the explanatory variable and group (bdelloid vs. monogonont) and proportion of pruned tips (20%, 25%, 33%, and 50%) as the response variables. Dataset was blocked out as a random variable.

The average GMYC model significance was qualitatively higher for 100% sampled (i.e. unpruned) monogonont datasets compared to bdelloid datasets (GMYC *P* values: 0.0081 vs. 0.014; Table S5.2), and this remained true for each of the jack-knifed proportions (Fig. S5.4). Jack-knife analyses indicate that the GMYC (*P* values) is more stable in monogonont samples than bdelloids. The slope of the decrease in the GMYC model fit with increasing levels of jack-knifing is steeper in bdelloids than it is for monogononts (Table S5.5; Fig. S5.4), which indicates that diversity in these monogonont samples is closer to saturation than in the bdelloids.

Sampling will be related to GMYC support, but the slope at which support improves with increased sampling will reflect the likelihood that increased sampling supplements existing haplotypes (Coalescent) as opposed to being novel (Yule). The slope at which monogonont GMYC support increases is shallower than that of the bdelloids, this indicates that additional samples are more likely

to supplement pre-existing haplotypes, thereby supporting the Coalescent side of the tree. This indicates that monogononts diversity in these datasets it more representative than the bdelloids, and that including additional sequences tends to supplement closely related genotypes to s clusters, while maintaining, rather than filling, interspecific gaps (as would be expected of the bdelloid datasets).

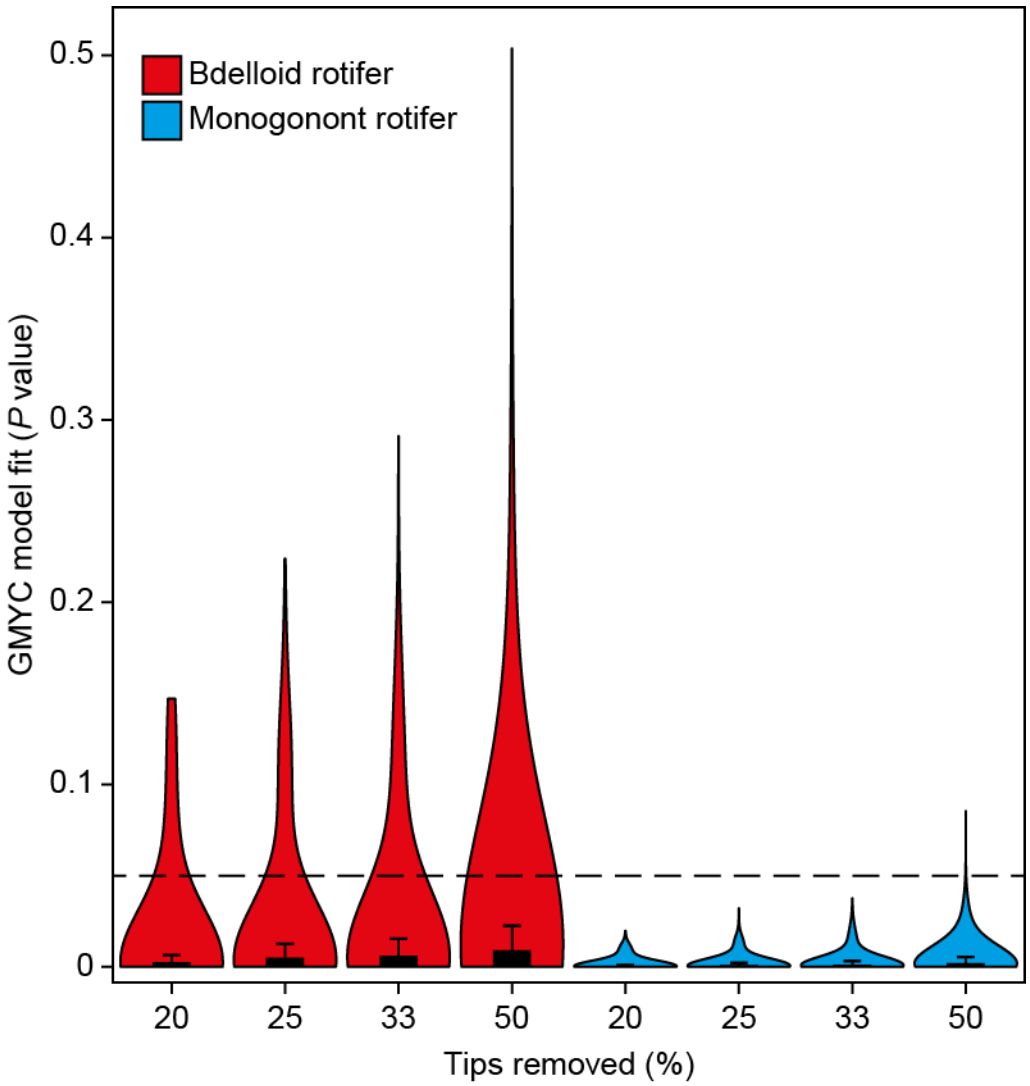

Figure S5.4 Significance of the GMYC model fit when bdelloid (red) and monogonont (blue) trees are jack-knifed by 20%, 25%, 33%, and 50%.
The dotted line represents the alpha value at which the GMYC model fit is considered significant ($\alpha = 0.05$). Boxes indicate the extent of the first and third quartiles. Whiskers indicate the most extreme data points within 1.5 times the inter-quartile distance from the box. Outliers are represented by the density plot, the width of the violin is indicative of the density of data.

Chapter 6: Supplementary Materials and Methods

Amplifying COI, 18S and 28S

COI mtDNA and 18S rDNA were amplified using previously reported protocols (Tang et al. 2012, 2014b). Similar to the method for 18S amplification, 28S rDNA was amplified using a nested PCR approach, of which all the primers used were redesigned from full length rotifer sequences (~2800bp) obtained from GenBank (Table S6.2). These sequences were aligned in Geneious 5.4.2 (Drummond et al. 2006) using the MAFFT (Katoh et al. 2009) plugin with the default settings. New external and internal primers were designed (Table 6.2) based on the 28S primers Sørensen and Giribet (2006). Two external and four internal primer pairs were designed to give wide amplification success across both bdelloid and monogonont rotifers, bind to conservative regions, and yield amplicon sizes of between 500-700bp.

PCRs were performed using 12.5µl of REDTaq ReadyMix PCR Reaction Mix (Sigma, Vienna, Austria), 2µl of each primer (10mM), 2µl of template DNA (or PCR amplicon: 10-50ng) and ddH_20 up to a total volume of 25µl. The total 28S rDNA fragment was amplified using 28SCT1F (5' - CGA GAC CGA TAG CGA ACA AGT ACC GTG – 3') and 28SCT4R (5' - GGC TCT TCC TAT CAT TGC GAA GCA GAC T -3'). Cycle conditions comprised initial denaturing at 95°C for 5 minutes, followed by 38 cycles of 95°C for 1 minute, 60°C for 1 minute and 72°C for 2 minutes, and a final extension step of 72°C for 10 minutes. Four nested PCRs were performed using these primer pairs: 28S0FCT (5'-ACG AAT GGC CGC ATT CAT CAG AT-3') – 28S1RCT (5'-GTT TGA CGA TCG ATT TGC ACG TC -3'), 28S2FCT (5'-GAC CCG AAA GAT GGT GAA CT-3') – 28S2RCT (5'-CGT CAG TCT TCA AAG TTC TCA TTT GA-3'), 28S3FCT.0 (5'-GCG TCG AAG GCT AAC ACG TGA-3') – 28S3RCT (5'-TGT TTT AAT TAG ACA GTC GGA TTC C-3'), and 28S4FCT (5'-CTT CGG GAT AAC GAT TGG CTC TAA G-3') – 28S5RCT (5'-GAG TCA AGC TCA ACA GGG TCT TCT T-3'). PCR amplicons were purified and sequenced bidirectionally by Macrogen Europe's EZ-seq direct service. The resulting sequences were checked by eye in Geneious and the overlapping sequences were stitched back together to produce partial sequences of ~2,300bp length.

Designing and amplifying the genomic primers

Transcriptomes sequenced for large clonal populations of *Rotaria socialis*, *R. magnacalcarata*, *R. sordida*, and *R. tardigrada* (Eyres 2013) were aligned by IE with orthologous regions present in the *Adineta ricciae* genome (Boschetti et al. 2012). Briefly, between 140 and 300 individuals of each s were collected by IE and DF from Silwood Park, Ascot, UK in 2012. RNA was extracted from these monospecific colonies using an RNeasy Mini kit (Qiagen) and purified by ethanol precipitation. cDNA libraries were prepared from the extracted RNA using the SMART PCR cDNA Synthesis kit and an Advantage 2 PCR Enzyme System (Clontech). These libraries were sequenced by The Eastern Sequence and Informatics Hub (University of Cambridge, http://www.easih.ac.uk). Illumina

sequencing was performed in a single HiSeq lane for one cDNA library per s and assembled with the Trinity assembler (Grabherr et al. 2011). Transcriptomes were compared to the *Adineta ricciae* transcriptome (Boschetti et al. 2012). In total, 799 different transcripts present in all five s were aligned. Each of the alignments was scored on an alien index (i.e. sequences that have non-Metazoan origins) and compared between each s for dN/dS ratios to identify the degree of selective pressure on each gene.

In this study, the alignments were sorted by percentage of identical sites and alignments under 65% were pruned to conservatively remove non-orthologous alignments. Each alignment was quality checked by eye in Geneious. Primers were designed for all of the alignments using the Primer3 (Untergasser et al. 2012) plugin with a minimum and optimal melting temperature of 45°C and 50°C, respectively, but otherwise default settings. Primers were successfully designed for 326/799 alignments, of these, 24 primer pairs with a range in dN/dS ratio and origin (16 native, 8 alien) were screened by PCR using four genomic DNA extracts from lab cultures provided by CGW (*Adineta riccae*, *Adineta vaga*, *Habrotrocha bidens*, and *Habrotrocha elusa elusa*). Each collection contained at least 100 individuals that were cleaned in ddH_2O and extracted using the modified Chelex protocol described in the main Methods section.

PCRs were performed using 12.5µl of REDTaq ReadyMix PCR Reaction Mix (Sigma, Vienna, Austria), 2µl of each primer (10mM), 2µl of template DNA (or PCR amplicon: 10-50ng) and ddH_20 up to a total volume of 25µl. A touchdown PCR was performed with the following cycle conditions: initial denaturation at 95°C for 5minutes, followed by 15 cycles of denaturation at 95°C for 1 minute, annealing at 60°C (dropping down 1°C per cycle down to 45°C) for 1 minute, and elongation at 72°C for 1 minute, and then 20 cycles of 95°C for 1 minute, 50°C for 1 minute, and 72°C for 1 minute, and lastly a final elongation at 72°C for 5 minutes. Of these 24 primer pairs, 686 and 1054 were most consistently amplified; these PCR amplicons were subsequently purified and sequenced by Macrogen. Fragment 1054 is non-Metazoan in origin and has a gene ontology matching to a phosphonoacetaldehyde hydrolase. Fragment 686 does not have a sufficiently similar match on GenBank, its top BLASTx hit is a ubiquitin-associated and sh3 domain-containing protein b.

Supplementary File S6.1: Arriving at the final phylogeny

Introduction

Phylogenetic analyses are affected by the input and the parameters of the model used to reconstruct the phylogeny. For this bdelloid phylogeny, given that bdelloid rotifers are ancient asexuals with no recombination by meiosis (Flot et al. 2013), it was assumed beforehand that the five different loci would be congruent with each other. Several phylogenetic analyses, described below, revealed incongruence among the different loci. Separate phylogenetic analyses were performed to gauge the effect of (1) using amino acid alignments instead of nucleotide alignments, and (2) separate analysis of the five loci.

(1) Different genetic loci are appropriate for different scale phylogenetic analyses. Analysis of higher taxa is confounded by rapidly evolving genes, while conserved genes like 18S and 28S rDNA are more suited for deeper scale phylogenies because they are less likely to become saturated. Protein coding genes have more redundancy in their sequences, and if they evolve rapidly then these will be particularly prone to genetic saturation. Saturated sequences are not representative of the mutational history of that gene, and ultimately lead to erroneous, nonphylogenetic signal (Jeffroy et al. 2006).

Sequence saturation can be observed by investigating biases at certain codon position for each protein coding loci, such that the prevalence of high GC at the third codon position (GC_3) will be indicative of either purifying selection for protein stability (due to the extra covalent bond between pyrimidines) or increased time for saturation. This is important to identify because if s independently acquire codon bias at certain codon positions (e.g. high GC_3) then these sequences would be attracted to each other in phylogenetic analyses irrespective of whether these reflationary have any evolutionary justification. Protein coding genes can be useful for deeper phylogenetic analyses because the amino acid sequence will be more conserved than the nucleotide sequence, and these amino acid sequences will be less biased by genetic saturation.

(2) Different loci might be under different evolutionary stresses and so may evolve along different trajectories. Congruency of the genes, while being more likely in a putatively linked genome, cannot be assumed. Comparison of phylogenies built separately for each locus is necessary to identify potential sources of bias.

Combining the results of these two lines of inquiry will allow for the justification of one tree over another.

Methods

Fifty two BEAST trees were generated with different combinations of alignments (i.e. five nucleotide alignments, three nucleotide and two amino acid alignments, or two nucleotide and three amino acid alignments), different topological constraints (none, genera, families, and orders), and separately for the unlinked loci. These different alignments suffer from different levels of saturation; this was ascertained by codon bias analyses. Separate gene trees were reconstructed for each of the five loci, and for three different concatenations of those loci. To judge the effect of topological constraints on the phylogenetic model, genera, families, and orders were constrained for each of the three different concatenated alignments and for each of the separate loci. Topologies were compared between each of the 52 trees using the Robinson-Fould symmetry metric (Robinson and Foulds 1981) and Compare2Trees (Nye et al. 2006). Branch lengths among the trees were compared using a branch length score metric (Kuhner and Felsenstein 1994). Bayes factor analyses (Kass and Raftery 1995; Suchard et al. 2005) were used to compare the likelihood of analyses with different topological constraints. Figure S1 depicts a schematic of this workflow.

Codon bias

To identify the level of genetic saturation for the three protein coding genes (COI, 686, and 1054), the GC content and GC_3 codon bias for the protein coding loci, were calculated from the alignments using DnaSP v5.10 (Librado and Rozas 2009). Using BEAST, three different concatenated alignments were used to reconstruct phylogenies (described below). Specifically, trees had either 1) nucleotide alignments for each of the five loci, or 2) nucleotide alignments for 18S, 28S, and COI, and amino acid alignments for 686 and 1054 (GC_3 rich nuclear protein coding genes), 3) nucleotide alignments for 18S and 28S, and amino acid alignments for 686, 1054, and COI (all protein coding genes).

Phylogenetic analyses

Time calibrated phylogenies were reconstructed using BEAST v1.7.5 (Drummond and Rambaut 2007). The priors for the analyses were set using BEAUti v 1.7.5. Trees were reconstructed using the best fitting substitution model (jModelTest) and protein evolution model (ProtTest). The evolutionary rate for each locus followed a lognormal relaxed clock. The evolutionary rate for the COI nucleotide alignment, 1.76% MYR^{-1}, was selected based on Wilke et al. (2009), and the evolutionary rate for 18S, 0.02% MYR^{-1}, was selected based on Ochman (1987) and Bargues et al. (2000). For 28S, COI (amino acid), 686 (amino acid and nucleotide), and 1054 (amino acid and nucleotide), BEAST was used to estimate the evolutionary rates with a normally distributed sampling regime. A birth-death speciation process with a random start tree was used for each tree. Four independent runs were conducted with the MCMC samples every 1,000 generations for 100,000,000 generations run on the CIPRES Science Gateway (Miller et al. 2010). After checking the convergence of these runs using Tracer v1.5.0 (Rambaut and Drummond 2009), a 10% burnin for each run was removed, the runs

were then amalgamated and resampled using LogCombiner v1.7.5 to provide a total of >40,000 trees. TreeAnnotator v1.7.5 was used to summarise a maximum credibility tree with tree node heights kept.

Given the results of the topological comparisons (described below), a maximum likelihood tree was built (described in the main Methods section) using the preferred concatenated alignment. An additional BEAST tree, was built excluding the nuclear loci.

To test the monophyly of the higher taxa, we performed four separate BEAST analyses with varying levels of topological constraints based on the taxonomy of higher taxa: 1) no taxonomic constraints (described above), or 2) sequences belonging to polytypic genus, 3) family, or 4) order were constrained to be monophyletic. The likelihood outputs of each of the four constrained models were compared to each other using Bayes factors. Bayes factors are the harmonic mean of the likelihood of the posterior, differences among the models are deemed strong, very strong and decisive if the difference between the logarithms of the Bayes factors are 2.3-3.4, 3.4-4.6, and >4.6, respectively (Kass and Raftery 1995). Bayes factors were computed for every pairwise combination of the four models with 10,000 bootstrap replicates within Tracer. While model selection with marginal likelihood estimated using harmonic means is known to underestimate the marginal posterior probability of the model, they are computational inexpensive. Other methods are available for model comparison (i.e. path sampling or stepping-stone sampling) but these are typically prohibitively computationally demanding (Baele et al. 2012) for the factorial inter-model (e.g. unconstrained vs. order-constrained) comparisons performed here.

Topological comparison

Various measures were used to compare topological congruency between 52 trees. First, unlinked trees were reconstructed for each of the loci and each of the topological constraints using BEAST and the same parameters as described above. The pairwise global topological similarity of each of the 52 pairwise tree combinations were calculated using Compare2Trees (Nye et al. 2006). Symmetric difference (Robinson-Foulds metric; Robinson and Foulds 1981) and branch length distance among the 2704 pairwise tree combinations were computed using the *phangorn* v1.99-7 (Schliep 2011) package in R v2.15.1 (R Core Team 2014). Symmetric distance is the sum of the number of internal partitions that exist in one tree but not the other and is negatively related to the topological similarity of the two trees. Kuhner and Felsenstein's branch score is the sum of squares of the differences between the branch lengths between the two trees, where an increased score is indicative of increasingly incongruent trees.

Statistics

The average node support for each of the trees was compared using generalised linear models (GLM) with node support values as the response variable, and locus, alignment type, and topological constraints as the explanatory variables. The overdispersed nature of the proportion data made the

quasibinomial error family appropriate. The minimum adequate model was simplified from the most complex model in a stepwise manner using X^2 tests. A Tukey *post hoc* test was performed using the *multcomp* package v1.3-1 (Hothorn et al. 2008) to compare factor levels. All analyses were performed in R.

Results

In total 52 different phylogenetic trees were reconstructed, these differed in the alignment, loci, and constraints used. Codon bias analyses of the three protein coding genes, specifically the high GC_3 content, indicates that the nuclear genes (686 and 1054) are saturated; lower GC_3 content for COI, however, indicates that this gene is not (Table 6.2). Topological comparisons (Table S6.5), but not branch length comparisons (Table S6.6), between each of the 52 trees indicate that, irrespective of topological constraint or whether they are nucleotide or amino acids, the genes 686 and 1054 are more incongruent to the other three genes.

Differences in node support values between each of the trees was explained by the different loci, rather than the different combinations of amino acid and nucleotide alignments or the topological constraint. Concatenated trees resulted in significantly higher average node support than any of their constituent loci, while the average support for trees based on 686 or 1054 alone were significantly lower than the other trees (Table S6.7; Fig. S6.2).

These differences however may be hampered by the lower level of sampling in 686 and 1054 (Table 6.2).

For each of the different concatenated alignments, unconstrained trees are most likely, followed, in order of likeliness, by trees constrained by genus, family and order (Table S6.8). Both unlinked and linked analyses indicate that bdelloid higher taxa are polyphyletic entities with hard incongruences with varying levels of support depending on the parameters of the analysis.

The concatenated alignment consisting three nucleotide alignments (for 18S, 28S, and COI) and two amino acid alignments (686 and 1054) was deemed the most plausible given the degree of genetic saturation for 686 and 1054, and the crown age of the clade. Given the incongruence of 686 and 1054, however, both this tree and a three gene tree (686 ad 1054 excluded) are presented in greater detail in the main manuscript. Concatenation of these loci provides enough variation to evaluate the deeper, higher taxonomic relationships of the group, while providing the highest average node support.

Figure S6.1 Workflow of the 29 phylogenies and their comparison.

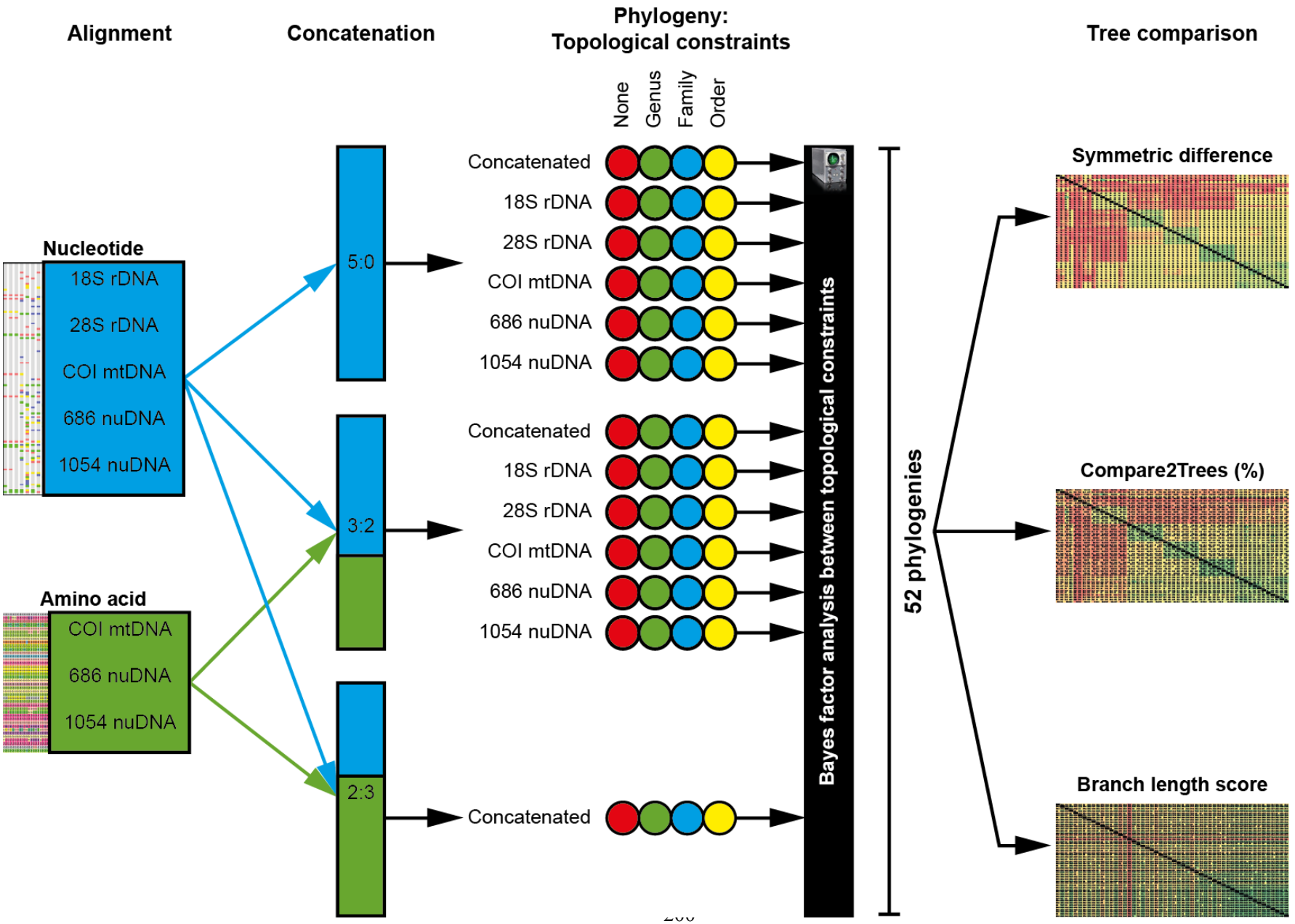
Alignment
Concatenation
Phylogeny:
Topological constraints
Tree comparison
None
Genus
Family
Order
Nucleotide
18S rDNA
28S rDNA
COI mtDNA
686 nuDNA
1054 nuDNA
Amino acid
COI mtDNA
686 nuDNA
1054 nuDNA
5:0
3:2
2:3
Concatenated
18S rDNA
28S rDNA
COI mtDNA
686 nuDNA
1054 nuDNA
Concatenated
18S rDNA
28S rDNA
COI mtDNA
686 nuDNA
1054 nuDNA
Concatenated
Bayes factor analysis between topological constraints
52 phylogenies
Symmetric difference
Compare2Trees (%)
Branch length score

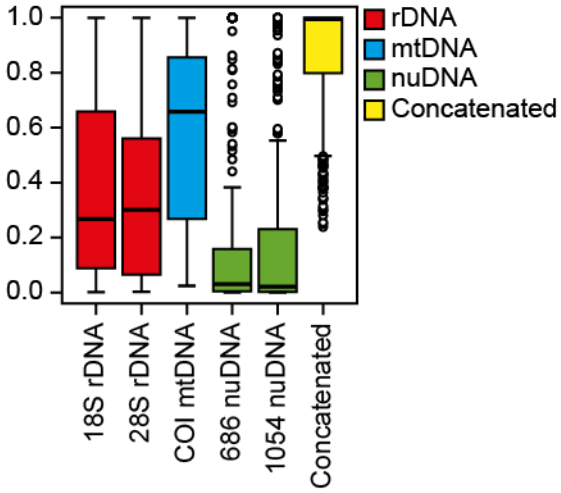

Figure S6.2 Node support value distributions obtained from phylogenetic reconstruction of loci (686, 1054, 18S, 28S, and COI) analysed separately and concatenated.

Supplementary File S6.2: Alternative phylogenies

Given the results of Supplementary File S6.1, namely that the trees generated using the genetic loci 686 and 1054 were less congruent with the other genes, the preferred tree was reconstructed using a concatenated alignment comprising: three nucleotide alignments (18S rDNA, 28S rDNA, and COI mtDNA) and two amino acid aligments (686 nuDNA and 1054 nuDNA). To identify whether this tree was biased by the method of phylogenetic reconstruction, the same concatenated alignment was used to reconstruct a maximum likelihood tree. Additionally, a BEAST analysis excluding the incongruent 686 and 1054 was performed using the protocol described in Supplementary File S6.1 (Fig. S6.3).

The maximum likelihood tree (Fig. S6.4) was reconstructed using Randomised Accelerated Maximum Likelihood (RAxML - Stamatakis 2006) through raxmlGUI (Silvestro and Michalak 2011). For the RAxML analysis, a gamma model of rate heterogeneity and a maximum likelihood search, with proportion of invariable sites estimated, was used for the nucleotide partitions (Table S6.3), and the appropriate protein evolution model for the amino acid partitions (Table S6.4).

The topology and level of support of each of these three trees were compared. The preferred tree was topologically similar to the ML (75.5%) and the alternative three gene tree (71.3%), but had higher average support (0.89 vs. 59% and 0.79, preferred, ML (bootstrap support), and alternative, respectively).

Figure S6.3 Phylogenetic trees inferred by Bayesian inference with the most likely substitution model for each of the three loci (18S rDNA, 28S rDNA, and COI mtDNA).
Posterior probability values are shown as clade support at the nodes. The scale bar represents the age (MYR) of the clade.
Figure S6.4 Phylogenetic tree inferred by maximum likelihood using RAxML.

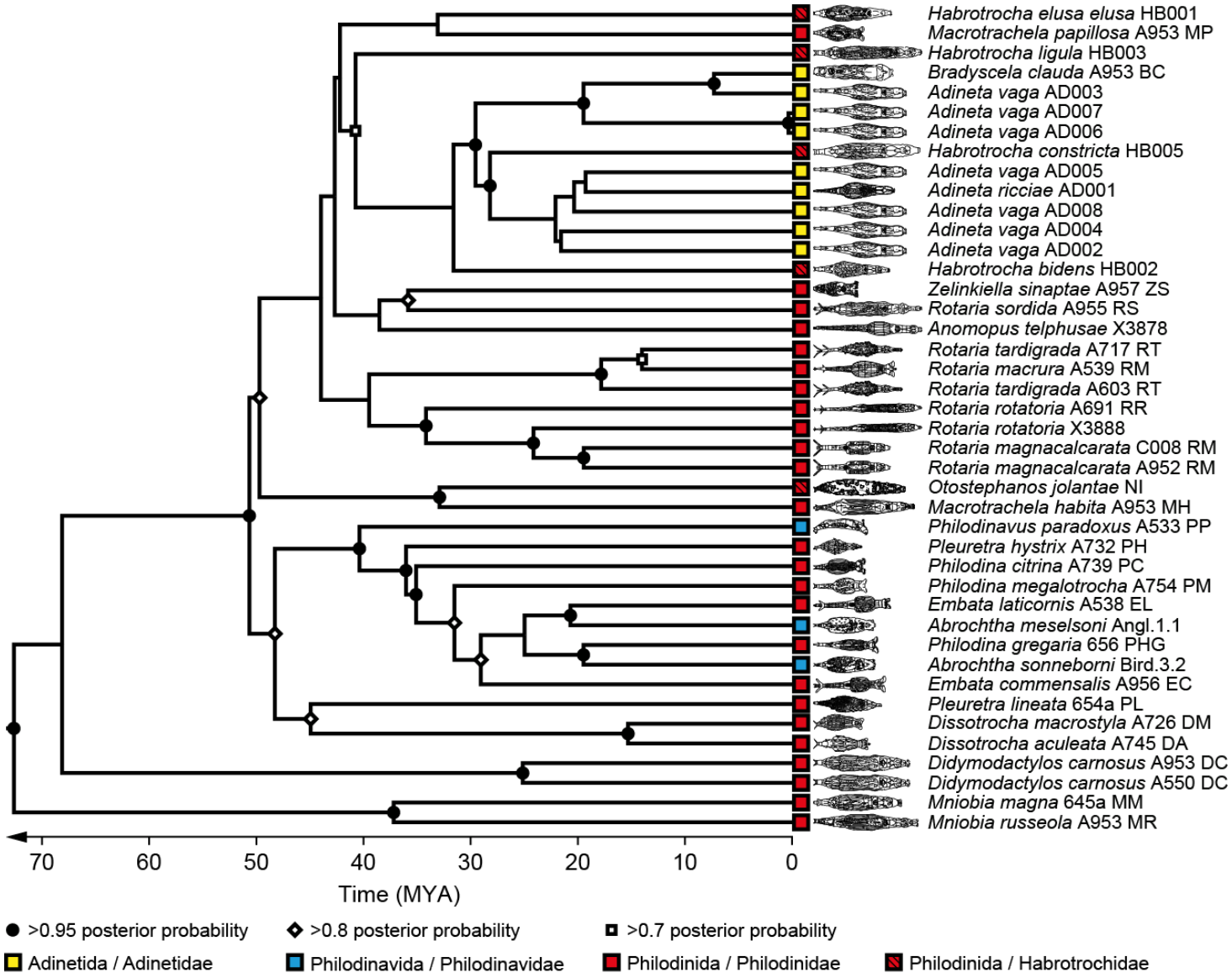
Habrotrocha elusa elusa HB001
Macrotrachela papillosa A953 MP
Habrotrocha ligula HB003
Bradyscela clauda A953 BC
Adineta vaga AD003
Adineta vaga AD007
Adineta vaga AD006
Habrotrocha constricta HB005
Adineta vaga AD005
Adineta ricciae AD001
Adineta vaga AD008
Adineta vaga AD004
Adineta vaga AD002
Habrotrocha bidens HB002
Zelinkiella sinaptae A957 ZS
Rotaria sordida A955 RS
Anomopus telphusae X3878
Rotaria tardigrada A717 RT
Rotaria macrura A539 RM
Rotaria tardigrada A603 RT
Rotaria rotatoria A691 RR
Rotaria rotatoria X3888
Rotaria magnacalcarata C008 RM
Rotaria magnacalcarata A952 RM
Otostephanos jolantae NI
Macrotrachela habita A953 MH
Philodinavus paradoxus A533 PP
Pleuretra hystrix A732 PH
Philodina citrina A739 PC
Philodina megalotrocha A754 PM
Embata laticornis A538 EL
Abrochtha meselsoni Angl.1.1
Philodina gregaria 656 PHG
Abrochtha sonneborni Bird.3.2
Embata commensalis A956 EC
Pleuretra lineata 654a PL
Dissotrocha macrostyla A726 DM
Dissotrocha aculeata A745 DA
Didymodactylos carnosus A953 DC
Didymodactylos carnosus A550 DC
Mniobia magna 645a MM
Mniobia russeola A953 MR
70
60
50
40
30
20
10
0
Time (MYA)
>0.95 posterior probability
>0.8 posterior probability
>0.7 posterior probability
Adinetida / Adinetidae
Philodinavida / Philodinavidae
Philodinida / Philodinidae
Philodinida / Habrotrochidae

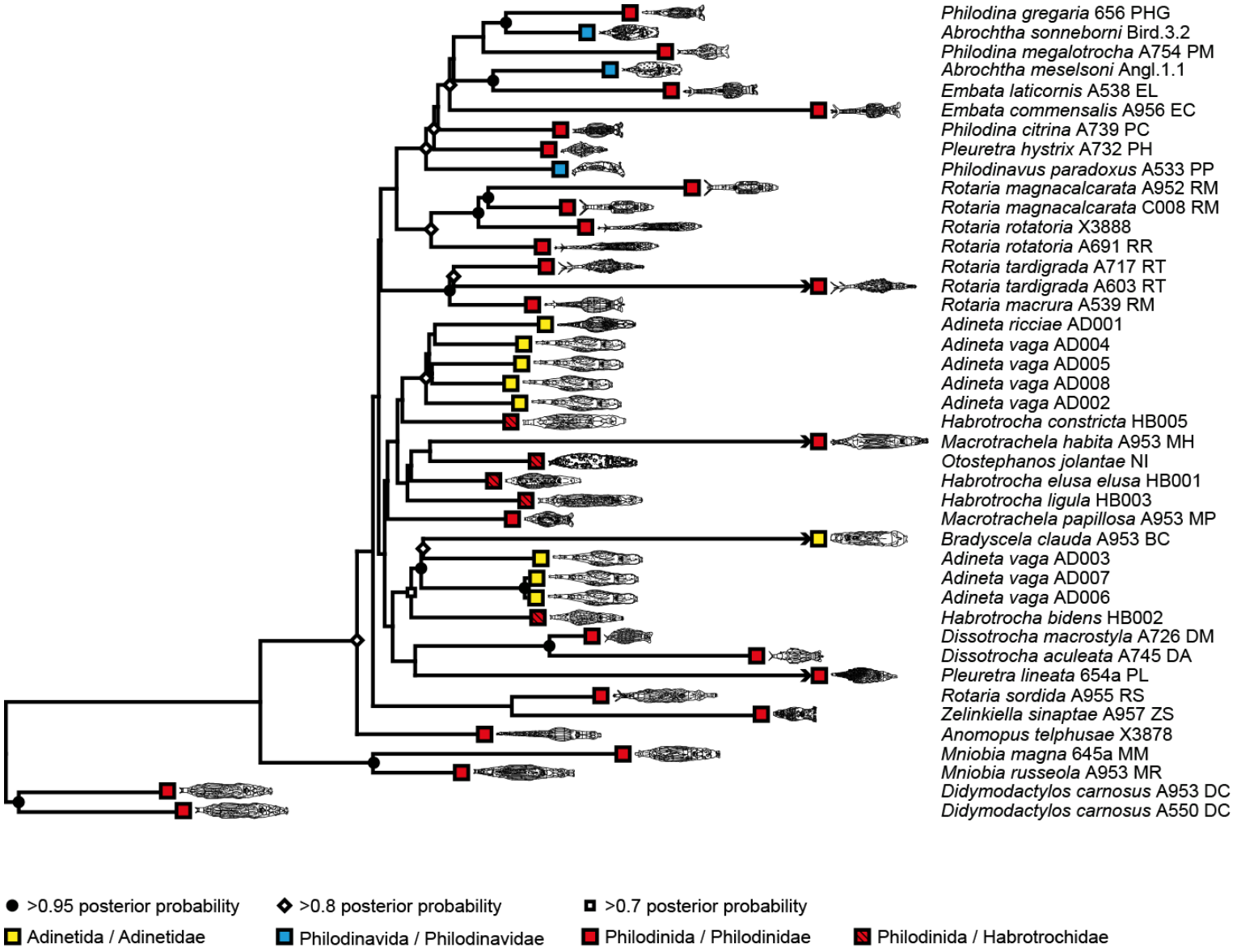
Philodina gregaria 656 PHG
Abrochtha sonneborni Bird.3.2
Philodina megalotrocha A754 PM
Abrochtha meselsoni Angl.1.1
Embata laticornis A538 EL
Embata commensalis A956 EC
Philodina citrina A739 PC
Pleuretra hystrix A732 PH
Philodinavus paradoxus A533 PP
Rotaria magnacalcarata A952 RM
Rotaria magnacalcarata C008 RM
Rotaria rotatoria X3888
Rotaria rotatoria A691 RR
Rotaria tardigrada A717 RT
Rotaria tardigrada A603 RT
Rotaria macrura A539 RM
Adineta ricciae AD001
Adineta vaga AD004
Adineta vaga AD005
Adineta vaga AD008
Adineta vaga AD002
Habrotrocha constricta HB005
Macrotrachela habita A953 MH
Otostephanos jolantae NI
Habrotrocha elusa elusa HB001
Habrotrocha ligula HB003
Macrotrachela papillosa A953 MP
Bradyscela clauda A953 BC
Adineta vaga AD003
Adineta vaga AD007
Adineta vaga AD006
Habrotrocha bidens HB002
Dissotrocha macrostyla A726 DM
Dissotrocha aculeata A745 DA
Pleuretra lineata 654a PL
Rotaria sordida A955 RS
Zelinkiella sinaptae A957 ZS
Anomopus telphusae X3878
Mniobia magna 645a MM
Mniobia russeola A953 MR
Didymodactylos carnosus A953 DC
Didymodactylos carnosus A550 DC
>0.95 posterior probability
>0.8 posterior probability
>0.7 posterior probability
Adinetida / Adinetidae
Philodinavida / Philodinavidae
Philodinida / Philodinidae
Philodinida / Habrotrochidae

Table S6.1 Literature review of studies using bdelloid s, and the type of investigation (experimental vs. survey).
Found on the attached CD, or available upon request.

Table S6.2 Sequences used to design new primers

Gene	Class	Genus	S	Accession
18S	Bdelloidea	*Adineta*	*vaga*	DQ089733
18S	Bdelloidea	*Anomopus*	*telphusae*	DQ089732
18S	Bdelloidea	*Mniobia*	*russeola*	AJ487049
18S	Bdelloidea	*Philodina*	*acuticornis*	U41281
18S	Bdelloidea	*Rotaria*	*rotatoria*	DQ089736
18S	Monogononta	*Brachionus*	*patulus*	AF154568
18S	Monogononta	*Brachionus*	*plicatilis*	U29235
18S	Monogononta	*Epiphanes*	*senta*	DQ089735
28S	Bdelloidea	*Adineta*	*vaga*	DQ089739
28S	Bdelloidea	*Anomopus*	*telphusae*	DQ089741
28S	Bdelloidea	*Philodina*	*roseola*	AY210469
28S	Bdelloidea	*Rotaria*	*rotatoria*	DQ089743
28S	Monogononta	*Asplanchna*	*sieboldi*	AY829085
28S	Monogononta	*Brachionus*	*patulus*	AY829084
28S	Monogononta	*Brachionus*	*urceolaris*	DQ089740
28S	Monogononta	*Epiphanes*	*senta*	DQ089742
28S	Monogononta	*Lecane*	*bulla*	AY829083

Table S6.3 Best evolutionary model from 88 evolutionary models tested for each of the five loci (686 nuDNA, 1054 nuDNA, 18S rDNA, 28S rDNA, and COI mtDNA).
For each locus, output from the other 87 models can be found on the attached CD, or is available upon request.

Locus	Model	-lnL	AIC	BIC	DT
686	GTR+I+G	1435.596	3055.1919	3385.9053	345.507
1054	GTR+I+G	3591.088	7366.1759	7742.7843	331.344
18S	GTR+G	7228.908	14639.815	15166.806	96.603
28S	GTR+I+G	12454.36	25092.716	25645.852	30.4897
COI	GTR+I+G	9815.58	19815.16	20236.706	1.6575

Table S6.4 Best protein model from 112 protein models tested for each of the protein coding loci (686 nuDNA, 1054 nuDNA, and COI mtDNA).
For each locus, output from the other 87 models can be found on the attached CD, or is available upon request.

Locus	Model	AIC	-lnL
686	HIVb+I+G	1444.63	-679.32
1054	JTT+G	3777.92	-1842.96
COI	MtREV+G+F	5348.04	-2575.02

Table S6.5 Pairwise symmetry metric topological comparisons values (Robinson-Fould metric; upper triangle) and topological comparisons percentages (Compare2Trees metric; lower triangle) between each of the 52 different phylogenies.
The average node support and the number of nodes with more than 0.9 Bayesian probability support for each tree are shown. In the alignment column, 5 corresponds to a phylogenetic analysis with five nucleotide alignments, 3 corresponds to three nucleotide alignments and two amino acid alignments, and 2 corresponds to two nucleotide alignments and three amino acid alignments.
Found on the attached CD, or available upon request.

Table S6.6 Pairwise branch length score comparisons values between each of the 52 different phylogenies.
The average node support and the number of nodes with more than 0.9 Bayesian probability support for each tree are shown. In the alignment column, 5 corresponds to a phylogenetic analysis with five nucleotide alignments, 3 corresponds to three nucleotide alignments and two amino acid alignments, and 2 corresponds to two nucleotide alignments and three amino acid alignments.
Found on the attached CD, or available upon request.

Table S6.7 Tukey comparison explaining differences between the phylogenetic node support values reconstructed using different genetic loci.

Comparison	**Estimate**	**Std. Error**	***Z***	***P***
18S - 1054	1.05	0.13	8.32	<1e-04
28S - 1054	0.91	0.13	7.13	<1e-04
28S - 18S	-0.14	0.11	-1.28	0.79
686 - 1054	-0.02	0.14	-0.16	1
686 - 18S	-1.07	0.13	-8.46	<1e-04
686 - 28S	-0.93	0.13	-7.27	<1e-04
COI - 1054	1.80	0.13	14.32	<1e-04
COI - 18S	0.75	0.11	6.79	<1e-04
COI - 28S	0.89	0.11	8.01	<1e-04
COI - 686	1.82	0.13	14.43	<1e-04
concatenated - 1054	3.38	0.14	24.87	<1e-04
concatenated - 18S	2.33	0.12	19.09	<1e-04
concatenated - 28S	2.47	0.12	20.12	<1e-04
concatenated - 686	3.40	0.14	24.94	<1e-04
concatenated - COI	1.58	0.12	12.99	<1e-04

Chapter 6: Supplementary Materials

Table S6.8 Bayes factor analysis used to compare the likelihood of different phylogenetic models with different levels of taxonomic constraint (none, genera, families, and orders).

Different alignments, linked and unlinked by loci, were analysed separately. The best model by topological constraint is emboldened.

Nulceotide: Protein	Gene	Constraint	Crown age (MYR)	Height (MYR)	Lower 95% HPD	Upper 95% HPD	ln P	S.E	None	Genus	Family	Order
5:0	18S rDNA	**None**	66.19	56.96	50.00	65.07	-29381.91	± 1.105	-	30.43	47.23	51.51
	28S rDNA		45.85	58.12	37.85	83.95						
	COI mtDNA		80.80	52.65	32.78	77.81						
	686 nuDNA		49.25	56.01	35.47	81.06						
	1054 nuDNA		76.03	64.51	44.43	88.23						
5:0	18S rDNA	Genus	47.25	56.53	36.29	80.51	-29451.98	± 0.968	-30.43	-	16.79	21.08
	28S rDNA		64.82	55.52	37.06	77.23						
	COI mtDNA		53.43	50.72	32.42	71.67						
	686 nuDNA		44.47	53.52	35.16	74.88						
	1054 nuDNA		57.34	61.62	42.58	82.61						
5:0	18S rDNA	Family	52.60	56.76	36.58	80.94	-29490.65	± 0.632	-47.23	-16.79	-	4.29
	28S rDNA		52.18	55.94	37.22	77.78						
	COI mtDNA		42.07	51.23	32.96	72.18						
	686 nuDNA		60.09	53.66	35.68	75.38						
	1054 nuDNA		63.52	62.28	43.74	83.86						
5:0	18S rDNA	Order	69.49	56.06	35.91	80.55	-29501	± 1.331	-52	-21	-4	-
	28S rDNA		59.10	55.73	36.61	77.59						
	COI mtDNA		61.00	50.88	32.03	72.67						
	686 nuDNA		52.92	53.79	35.64	75.53						
	1054 nuDNA		54.54	61.91	43.10	83.99						
5:0	Concatenated	**None**	71.67	61.90	38.46	91.23	-30008	± 0.275	-	229	245	218
5:0	Concatenated	Genus	102.50	70.79	45.31	97.70	-30535	± 0.267	-229	-	16	-11
5:0	Concatenated	Family	50.11	46.13	36.09	57.55	-30572	± 0.262	-245	-16	-	-28
5:0	Concatenated	Order	41.10	47.07	36.19	58.91	-30509	± 0.305	-218	11	28	-
3:2	18S rDNA	**None**	207.64	394.72	69.23	1016.62	-26890	± 0.345	-	15	24	22
	28S rDNA		293.18	360.57	56.42	902.39						
	COI mtDNA		141.32	122.86	59.67	189.47						
	686 nuDNA		268.59	315.93	78.02	771.18						
	1054 nuDNA		164.85	281.33	49.82	906.91						
3:2	18S rDNA	Genus	91.19	342.12	60.32	812.12	-26925	± 0.384	-15	-	9	7
	28S rDNA		192.30	255.78	59.70	524.10						
	COI mtDNA		150.24	127.67	60.64	195.82						
	686 nuDNA		177.87	575.41	116.87	1270.14						
	1054 nuDNA		413.79	270.99	59.50	861.11						
3:2	18S rDNA	Family	985.13	256.95	60.58	608.88	-26945	± 0.409	-24	-9	-	-2
	28S rDNA		203.16	260.47	50.42	844.82						
	COI mtDNA		117.49	493.53	98.19	1095.14						
	686 nuDNA		191.29	275.39	64.50	725.20						
	1054 nuDNA		189.92	109.98	61.34	169.33						
3:2	18S rDNA	Order	407.37	359.14	61.64	909.81	-26941	± 0.401	-22	-7	2	-
	28S rDNA		819.27	332.35	74.04	750.14						
	COI mtDNA		78.48	120.01	59.90	185.23						
	686 nuDNA		183.48	225.72	57.96	503.83						
	1054 nuDNA		540.28	302.92	52.95	970.16						
3:2	Concatenated	**None**	47.13	51.77	42.49	61.08	-28595	± 0.051	-	127	291	290
3:2	Concatenated	Genus	56.68	53.36	43.93	64.44	-28887	± 0.155	-127	-	164	163
3:2	Concatenated	Family	27.22	26.75	22.86	30.70	-29264	± 0.1	-291	-164	-	-1
3:2	Concatenated	Order	23.07	26.77	22.93	30.97	-29262	± 0.099	-290	-163	1	-
2:3	Concatenated	**None**	9.72	13.16	7.80	19.26	-20208	± 0.288	-	172	185	179
2:3	Concatenated	Genus	10.94	11.39	7.15	16.46	-20605	± 0.21	-172	-	13	7
2:3	Concatenated	Family	10.72	10.45	7.22	14.25	-20635	± 0.42	-185	-13	-	-6
2:3	Concatenated	Order	14.29	10.54	7.36	14.36	-20621	± 0.218	-179	-7	6	-

Permission to reprint chapters

Chapter 2

Dear Proceedings of the National Academy of Sciences,

I have completed my PhD thesis at Imperial College London entitled "*The Consequences of Life without Sex: An Examination into Taxonomy and Evolution of the Anciently Asexual Bdelloid Rotifers*".

I seek your permission to reprint, in my thesis, the published version of a paper I published in: "*Tang, C. Q., Leasi, F., Obertegger, U., Kieneke, A., Barraclough, T. G., & Fontaneto, D. (2012). The widely used small subunit 18S rDNA molecule greatly underestimates true diversity in biodiversity surveys of the meiofauna. Proceedings of the National Academy of Sciences of the United States of America, 109, 16208–16212.*"

I would like to include the paper in the electronic version which will be added to Spiral, Imperial's online repository http://spiral.imperial.ac.uk/ and made available to the public under a Creative Commons Attribution-NonCommercial-NoDerivs licence.

If you are happy to grant me all the permissions requested, please return a signed copy of this letter. If you wish to grant only some of the permissions requested, please list these and then sign.

Yours sincerely,

Cuong Q. Tang

Chapter 3

JOHN WILEY AND SONS LICENSE TERMS AND CONDITIONS

Oct 20, 2014

This is a License Agreement between Cuong Q Tang ("You") and John Wiley and Sons ("John Wiley and Sons") provided by Copyright Clearance Center ("CCC"). The license consists of your order details, the terms and conditions provided by John Wiley and Sons, and the payment terms and conditions.

All payments must be made in full to CCC. For payment instructions, please see information listed at the bottom of this form.

License Number	3493121002657
License date	Oct 20, 2014
Licensed content publisher	John Wiley and Sons
Licensed content publication	Methods in Ecology & Evolution
Licensed content title	Effects of phylogenetic reconstruction method on the robustness of species delimitation using single-locus data
Licensed copyright line	This article is protected by copyright. All rights reserved.
Licensed content author	Cuong Q. Tang,Aelys M. Humphreys,Diego Fontaneto,Timothy G. Barraclough
Licensed content date	Aug 13, 2014
Start page	n/a
End page	n/a
Type of use	Dissertation/Thesis
Requestor type	Author of this Wiley article
Format	Print and electronic
Portion	Full article
Will you be translating?	No
Title of your thesis / dissertation	The Consequences of Life without Sex: An Examination into Taxonomy and Evolution of the Anciently Asexual Bdelloid Rotifers
Expected completion date	Oct 2014
Expected size (number of pages)	207
Total	0.00 USD

Chapter 5

JOHN WILEY AND SONS LICENSE TERMS AND CONDITIONS

Oct 20, 2014

This is a License Agreement between Cuong Q Tang ("You") and John Wiley and Sons ("John Wiley and Sons") provided by Copyright Clearance Center ("CCC"). The license consists of your order details, the terms and conditions provided by John Wiley and Sons, and the payment terms and conditions.

All payments must be made in full to CCC. For payment instructions, please see information listed at the bottom of this form.

License Number	3423581220922
License date	Jul 07, 2014
Licensed content publisher	John Wiley and Sons
Licensed content publication	Evolution
Licensed content title	SEXUAL SPECIES ARE SEPARATED BY LARGER GENETIC GAPS THAN ASEXUAL SPECIES IN ROTIFERS
Licensed copyright line	This article is protected by copyright. All rights reserved
Licensed content author	Cuong Q. Tang,Ulrike Obertegger,Diego Fontaneto,Timothy G. Barraclough
Licensed content date	Jun 26, 2014
Start page	n/a
End page	n/a
Type of use	Dissertation/Thesis
Requestor type	Author of this Wiley article
Format	Print and electronic
Portion	Full article
Will you be translating?	No
Title of your thesis / dissertation	The Consequences of Life without Sex: An Examination into Taxonomy and Evolution of the Anciently Asexual Bdelloid Rotifers
Expected completion date	Aug 2014
Expected size (number of pages)	200
Total	0.00 USD